January 2014

Genetic basis for the virulence of enterohemorrhagic Escherichia coli strain TW14359

Jason Kyle Morgan
University of South Florida, jkmorgan@mail.usf.edu

Genetic basis for the virulence of enterohemorrhagic *Escherichia coli* strain TW14359

by

Jason K. Morgan

A dissertation submitted in partial fulfillment
of the requirements for the degree of
Doctor of Philosophy
Department of Cell Biology, Microbiology & Molecular Biology
College of Arts and Sciences
University of South Florida

Major Professor: James Riordan, Ph.D.
Lindsey Shaw, Ph.D.
Burt Anderson, Ph.D.
Stanley Stevens, Ph.D.

Date of Approval:
May 2, 2014

Keywords: Bacterial Pathogenesis, Gene Regulation, Bicarbonate, EHEC, RcsB

Table of Contents

List of Tables

List of Figures

Abstract

Enterohemorrhagic *Escherichia coli* (EHEC) is a virulent pathotype of *E. coli* that is associated with major outbreaks of hemorrhagic colitis and the life-threatening kidney disease hemolytic uremic syndrome. For successful host colonization and attachment to the intestinal mucosa, EHEC requires the locus of enterocyte effacement (LEE) pathogenicity island, which encodes a type III secretion system (TTSS) responsible for secreting and translocating effector proteins into host colonocytes. Regulation of the LEE is primarily directed through the first operon, *LEE1*, encoding the locus encoded regulator (Ler), and occurs through the direct and indirect action of several regulators. The 2006 U.S. spinach outbreak of *E. coli* O157:H7, characterized by unusually severe disease, has been attributed to a strain (TW14359) with enhanced pathogenic potential including elevated virulence gene expression, robust adherence, and the presence of novel virulence factors.

Aim 1 of this dissertation proposes a mechanism for the unique virulence expression and adherence phenotype of this strain, and further expands the role for regulator RcsB in control of the *E. coli* locus of enterocyte effacement (LEE) pathogenicity island. Proteomic analysis of TW14359 revealed a virulence proteome consistent with previous transcriptome studies that included elevated levels of the LEE regulatory protein Ler and type III secretion system (T3SS) proteins, secreted T3SS effectors, and Shiga toxin 2. Basal levels of the LEE activator and Rcs phosphorelay response regulator, RcsB, were increased in strain TW14359 relative to O157:H7 strain Sakai. Deletion of *rcsB* eliminated inherent differences between these strains in *ler* expression, and in T3SS-dependent adherence. A reciprocating regulatory pathway involving RcsB and LEE-encoded activator GrlA was identified and predicted to coordinate LEE activation

with repression of the *flhDC* flagellar regulator and motility. Overexpression of *grlA* was shown to increase RcsB levels, but did not alter expression from promoters driving *rcsB* transcription. Expression of *rcsDB* and RcsB was determined to increase in response to physiologic levels of bicarbonate, and bicarbonate-dependent stimulation of the LEE was shown to be dependent on an intact Rcs system and *ler* activator *grvA*. The results of this aim significantly broaden the role for RcsB in EHEC virulence regulation.

The bicarbonate ion (HCO_3^-) has been shown to stimulate LEE gene transcription through the *LEE1* promoter, and is predicted to serve as a physiologic signal for EHEC colonization. Results from the previous aim demonstrated that bicarbonate induction of the LEE is mediated through the Rcs phosphorelay, and is dependent upon an intact global regulator of virulence *grvA* gene. However, the direct mechanism through which RcsB-GrvA regulates *ler*, and the contribution of GrvA to the virulence of EHEC is unknown. In Aim 2, the RcsB-GrvA regulon of EHEC was determined by RNA sequencing, and the contributions of each to virulence and stress fitness was explored. A significant increase in transcription of the *gad* genes for extreme acid resistance was observed for both EHEC strains TW14359Δ*grvA* and TW14359Δ*rcsB*Δ*grvA* compared to TW14359, and corresponded with a significant increase in acid survival for TW14359Δ*grvA* during exponential growth. Therefore, a model by which RcsB-GrvA coordinate LEE expression with acid resistance through GadE was proposed. Finally, the temporal regulation of both *rcsDB* and *grvAB* operons in response to bicarbonate was defined using single copy *luxE* chromosomal reporter fusions. Taken together, these results demonstrate the role of RcsB and GrvA to EHEC virulence, and reveal a novel role for GrvA in of extreme acid resistance and LEE gene expression and in EHEC.

Finally, production of the ECP pilus has been demonstrated in enterohemorrhagic *Escherichia coli* O157:H7 (EHEC), and has been shown to be required for efficient adherence to epithelial cells during colonization. The first gene of the *ecpRABCDE* operon encodes a transcriptional regulator (EcpR) that positively regulates its own transcription, and promotes transcription and production of the downstream gene, *ecpA*, encoding the major ECP subunit EcpA. However, the distance between the *ecpR* and *ecpA* genes suggests the presence of regulatory elements that control *ecpA* directly. Therefore, it was hypothesized that an additional promoter was able to direct transcription of *ecpA*, independent of the promoter upstream of *ecpR*. To test this, promoter-*lacZ* transcriptional reporter fusions were created using the regions upstream of *ecpR* and *ecpA* to test for promoter activity, coupled with western blot analysis to detect EcpA in both wild-type and *ecpR* promoter mutant strains. In Aim 3, we showed that an additional promotable element, downstream of the EHEC O157:H7 strain TW14359 *ecpR* translational start site, is capable of driving transcription of *ecpA*, and that its activity is independent of an intact *ecpR* promoter. In addition, site-directed mutagenesis was used to characterize a TW14359 specific single nucleotide polymorphism within the predicted *ecpA* promoter region. Overproduction of EcpR was observed to increase cytosolic RcsB and Tir, indicating that *ecp* production is able to stimulate the *LEE*, and that the *ecpA* promoter polymorphism may contribute to intrinsically increased *rcsB* transcription in TW14359. Taken together, the results, and those obtained in Aims 1 and 2, expand the model for regulation of the *ecp* operon in EHEC O157:H7 strain TW14359, and broaden the model for EcpR and RcsB in the coordinate regulation of *E. coli* common pilus and type III secretion.

Chapter 1: Introduction

1.1 Enterohemorrhagic *Escherichia coli* (EHEC)

Escherichia coli is a facultatively anaerobic gram negative bacteria of the family Enterobacteriaceae, and is commonly found as a component of the normal mammalian lower intestinal flora (Giangrossi et al., 2005). And though it is found in the gut, *E. coli* can survive for extended periods of time in terrestrial and aquatic habitats (van Elsas et al., 2011). Since its discovery, *E. coli* has become an integral part of modern molecular biology as a model organism and has been intensively studied. Though the average genome size of *E. coli* is roughly 4.7 Megabases (Mb), there exists a highly diverse subset of *E. coli* strains and pathotypes with unique properties and ecological niches (Touchon et al., 2009). The core genome of *E. coli* is composed of roughly 2,000 genes, while the pan genome contains roughly 18,000 orthologous genes (Touchon et al., 2009). This extensive repertoire of genes provides *E. coli* with an enormous set of tools to adapt and respond to various environments, including those found in the human host. While some *E. coli* strains are non-pathogenic, a subset of important *E. coli* pathotypes exist which can cause overt disease in humans. These include enteropathogenic *E. coli* (EPEC), enteroinvasive *E. coli* (EIEC), enteroaggregative *E. coli* (EAEC), enterotoxigenic *E. coli* (ETEC), extra-intestinal pathogenic *E. coli* (ExPEC), uropathogenic *E. coli* (UPEC), and enterohemorrhagic *E. coli* (EHEC) (Lim et al., 2011; Nataro and Kaper, 1998).

Enterohemorrhagic *Escherichia coli* is a zoonotic pathogen capable of causing severe diarrheagenic illness, as well as life-threatening kidney disease, in humans. There are an

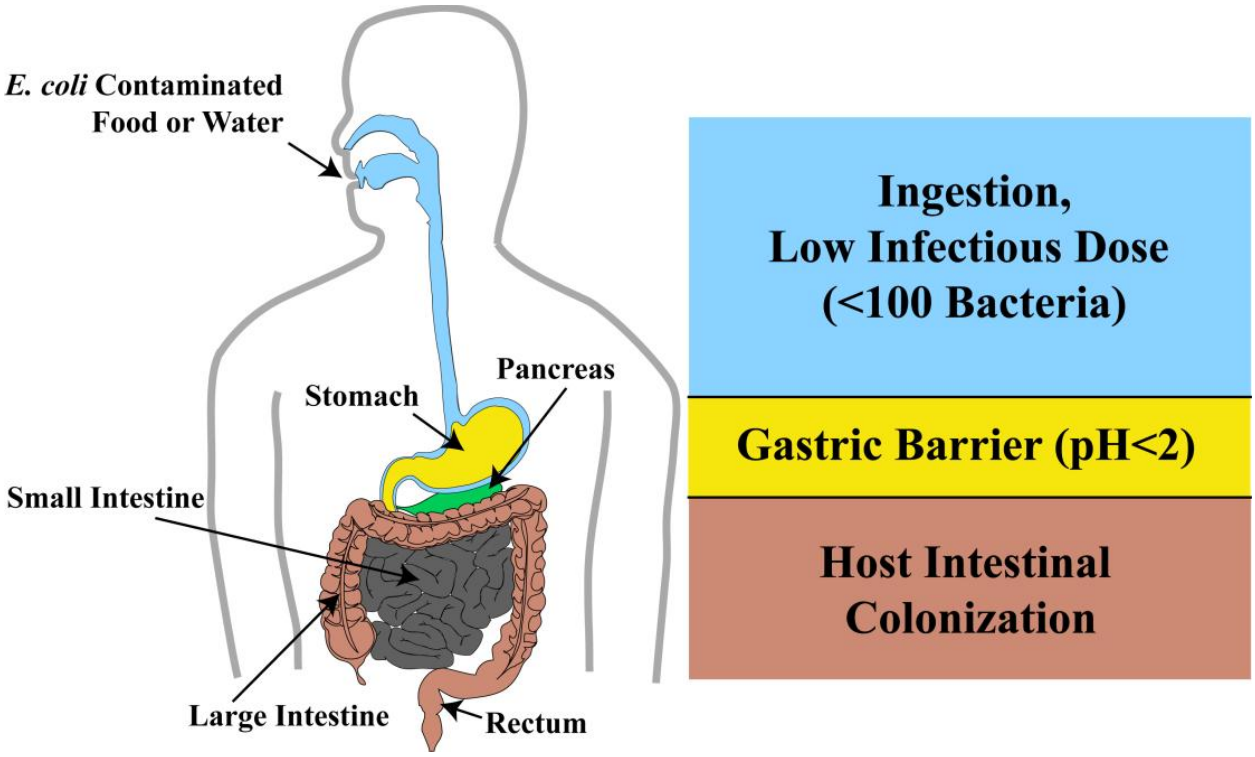

Figure 1 - Model depicting the pathway for enterohemorrhagic *E. coli* host colonization
The model for *E. coli* colonization of the human host, following ingestion of bacteria in contaminated water or food, involves passage through the gastric barrier and successful competitive colonization of the intestinal mucosa.

estimated 77,000 EHEC infections each year, resulting in 2,000 hospitalizations and 60 deaths, with an estimated annual cost of $405 million (Frenzen et al., 2005). An infection caused by EHEC typically presents with frankly bloody diarrhea (hemorrhagic colitis), and may progress to a toxin-associated illness known as hemolytic uremic syndrome, which is characterized by thrombocytopenia, and microangiopathic hemolytic anemia (Nataro and Kaper, 1998).

The primary reservoir of EHEC is domestic and wild ungulates, however colonized calves and adult cattle typically remain asymptomatic (Cray and Moon, 1995). Transmission generally occurs indirectly through the fecal-oral route (**Fig. 1**), with outbreaks originating from contaminated food (Nataro and Kaper, 1998). Other sources of infection include direct contact with infected persons or domestic animals, and tainted water (drinking and recreational) (Rangel et al., 2005). The low oral infectious dose of EHEC (<100 bacteria) is determined by its ability to successfully survive passage through the stomachs gastric acid barrier, and by competitive colonization of the host intestine (Kaper et al., 2004). As antibiotic use is contraindicated for EHEC infections, due to complications associated with Shiga toxin production and HUS, there are very few strategies in use for infection treatment and prevention (Jaeger and Acheson, 2000). This fact underscores the importance of further understanding the mechanisms which determine the virulence of this pathogen.

1.2 Virulence determinants of EHEC and the mechanisms by which they cause disease

1.2.1 Shiga Toxin

The virulence of EHEC is largely dictated by production of Shiga toxin 2 (Stx2) (Boerlin et al., 1999; O'Brien et al., 1983). Stx2 is an AB_5 toxin, comprised of Stx2A and five Stx2B subunits. The genes which encode the toxin (*stx2AB*) are contained within a temperate lambdoid

prophage (Johannes and Romer, 2010; Unkmeir and Schmidt, 2000). The toxin can enter the host cell through binding of cell surface expressed glycolipids, specifically globotriaosylceramide (Gb3), leading to clathrin mediated endocytosis and retrograde transport of the toxin through the endoplasmic reticulum (Johannes and Romer, 2010). There, the A-subunit is released into the cytoplasm where it cleaves a single adenine base from the eurkaryotic 28S ribosomal RNA leading to an inhibition of protein synthesis, and cell death (Endo et al., 1988). It has been shown that cattle lack the vascular receptors for Stx2 binding, which can explain why they are asymptomatic carriers for *stx2* positive EHEC serotypes (Pruimboom-Brees et al., 2000). Recently, it was shown that EHEC strain EDL933 carrying a non-inducible variant of Stx2 was able to colonize a mouse host, but was not able to produce any pathological changes without Stx2 production, underscoring the significant role of Stx2 in EHEC pathogenesis following colonization (Tyler et al., 2013).

1.2.2 The Locus of Enterocyte Effacement (LEE)

Successful competitive colonization of the host intestine requires a 36 kb pathogenicity island termed the locus of enterocyte effacement (LEE), which contains five operons encoding structural, auxiliary and regulatory components of a contact-dependent type III secretion system (T3SS) (McDaniel et al., 1995; Moon et al., 1983) (**Fig. 3A**). The LEE contains genes necessary for production of the T3SS, regulation of the LEE, and effectors required for intimate attachment to host cells (Deng et al., 2004; McDaniel et al., 1995; Perna et al., 1998). Intimate attachment is dependent on the interaction of the TTSS translocated effector Tir, localized to the apical region of the host intestinal cell, with the EHEC-encoded adhesin, intimin (Kenny et al., 1997b).

Pedestal structures (attaching and effacing lesions) are a consequence of actin condensation below the attached bacterium (Campellone, 2010; Cheng et al., 2008; Garmendia et al., 2004; Knutton et al., 1989). Previous studies have identified the conditions which stimulate T3SS production and subsequently enhance EHEC gut adherence, this includes growth at 37°C, physiologic osmolarity, and the presence of sodium bicarbonate (Kenny et al., 1997a; Rosenshine et al., 1996). Abe *et al*. observed maximum expression of LEE genes in EHEC when grown in the presence of 44 mM sodium bicarbonate under nutrient-rich conditions, which has been proposed to be a similar environment to that of the intestinal ileum (Abe et al., 2002; Fordtran and Locklear, 1966). Currently, no mechanism for bicarbonate stimulation of the LEE has been identified in EHEC or EPEC (Yang et al., 2008).

The ATPase EscN is localized to the base of the inner membrane T3SS ring and hydrolyzes ATP to provide the energy for effector translocation (Sorg et al., 2005; Tree et al., 2009; Winnen et al., 2008; Yip et al., 2005; Zarivach et al., 2007). The type III secretion process in EHEC can be divided into two general modes of activity, (i) production and secretion of the filamentous translocon apparatus prior to contact and (ii) reduced secretion of translocon proteins following contact and intimate adherence with increased secretion of effector proteins (Tree et al., 2009) (**Fig. 2**). The T3SS itself is composed of a multi-ring basal apparatus spanning the inner and outer membranes, composed of EscD, EscQ, EscR, EscS, EscT, EscU, and EscV (Efromovich et al., 2008; Gauthier et al., 2003; Ogino et al., 2006; Partridge et al., 2009). The protein EscF forms the needle complex, a structure which spans the inner and outer membranes, onto which the EHEC translocon apparatus assembles. In this regard, the T3SS of EHEC and EPEC is different from that of *Yesinia pestis*, where type III secretion is independent of a filament structure and relies solely on the needle complex for secretion (composed of YscF)

(Torruellas et al., 2005). The translocon apparatus is composed of three proteins to form a filament and pore complex. The filament structure is composed of multimeric EspA subunits extending outward from the needle complex, with a diameter of 120 Å and central channel diameter of 25 Å (Keller et al., 2002). Each EspA filament is capped with a complex composed of two proteins, EspB and EspD, which serves to form a pore roughly 3-5 nm in diameter within the membrane of the host cell (Kresse et al., 1999; Mitra et al., 2012). Together, the T3SS filament and pore complex, formed by EspA and EspB/D, function to create a hollow conduit between the bacterial and host cell cytosol through which effector proteins are translocated.

Effector proteins that are encoded within the LEE, and those that are non-LEE-encoded, serve diverse functions in the infection process. The effector protein Tir (translocated intimin receptor) is preferentially secreted into the host cytoplasm, where it localizes to the host cell cytoplasmic membrane (DeVinney et al., 1999). There, it serves as a receptor for the EHEC outer membrane protein intimin. Binding of the host cell localized Tir with intimin facilitates intimate attachment of the bacterium, and is followed by the production of a pedestal structure formed by the condensation of actin below the bacterium (Garmendia et al., 2004; Kaper et al., 2004; Knutton et al., 1989; Knutton et al., 1987). Some effectors, such as NleE, NleC, and NleH, have been shown to modulate the host cell immune response (Hemrajani et al., 2008; Yen et al., 2010). Others, such as Map and EspF, are able to disrupt tight-junctions and promote apoptosis, respectively (Crane et al., 2001; Dean and Kenny, 2009). The switch between secretion of translocators (i.e. structural proteins which constitute the filament and pore complex) and effectors is complex, and the proper timing/regulation of their secretion is vital for successful attachment. It has been shown that the LEE-encoded chaperone CesT serves to

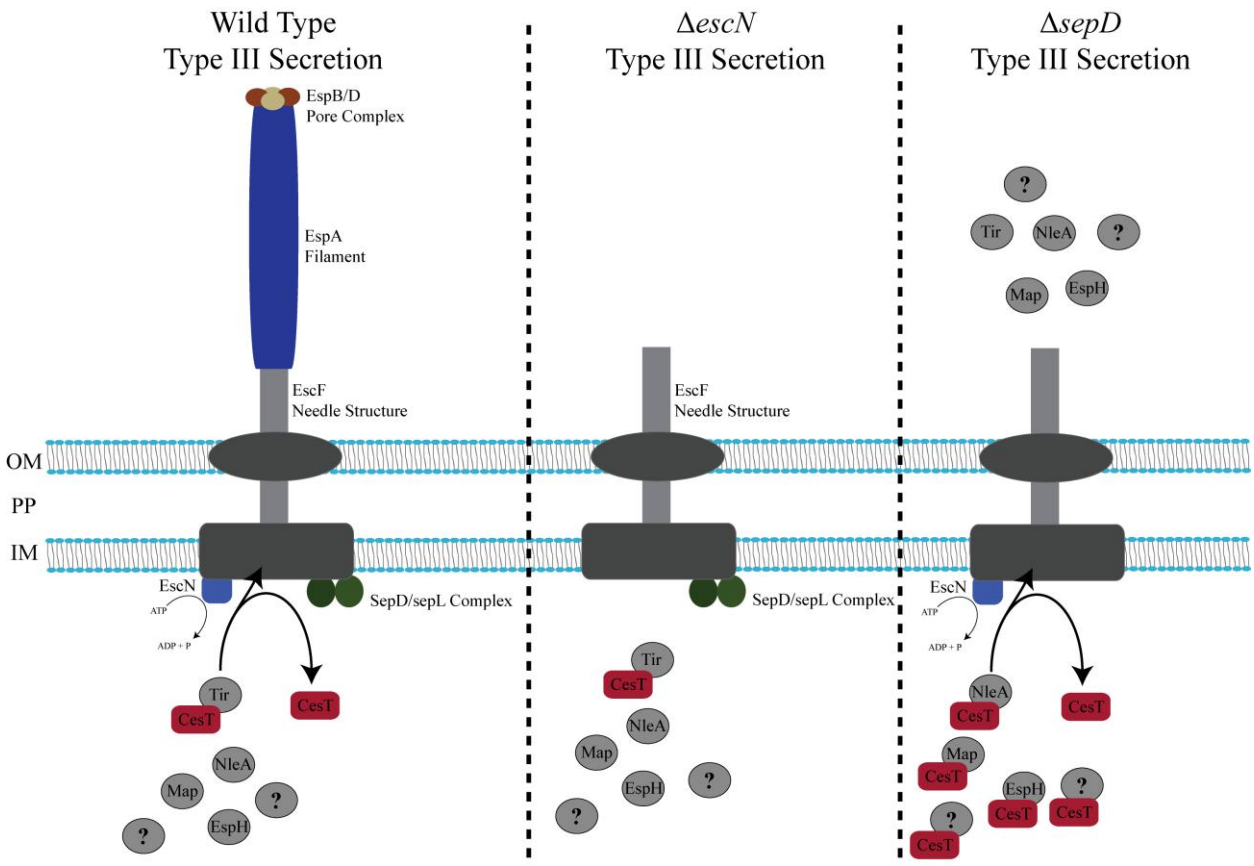

Figure 2 - Model for type III secretion in hemorrhagic *Escherichia coli* (EHEC)
(Left)The type III secretion system (T3SS) of EHEC is composed of the needle complex (Esc proteins) and the secreted translocon apparatus (Esp proteins). The EscF protein forms the minimal structure through which proteins can be secreted in a type III dependent manner. However the translocon apparatus proteins EspA, EspB, and EspD are required for pore complex formation and intimate adherence. (Middle) Loss of the ATPase EscN results in loss of ATP hydrolysis required for protein translocation through the T3SS. (Right) Secretion hierarchy of the T3SS is dictated by the SepD/SepL complex, and mutation of either results in hypersecretion of non-translocon effector proteins into the extracellular milieu.

localize effectors to the TTSS by association with the SepL/SepD complex, and that Tir is preferentially localized to the complex for secretion (Deng et al., 2005; Thomas et al., 2005; Yip et al., 2005). Secretion of both LEE- and non-LEE-encoded effectors is thought to occur in a rank order manner (Mills et al., 2008). Due to preferential binding of Tir-bound-CesT to the SepD/L complex, other effectors are effectively blocked from being secreted (Thomas et al., 2005). Prior to attachment to a host cell, the proteins composing the translocon filament (EspA, EspB, and EspD) are preferentially secreted, along with Tir. Following attachment and translocation of Tir, CesT is able to stabilize other effectors prior to proteolytic degradation and direct them to be secreted (Leverton and Kaper, 2005; Mills et al., 2008; Winnen et al., 2008).

1.2.3 Regulation of type III secretion in EHEC

The control and expression of the TTSS is tightly controlled and coordinated by factors which are both LEE- and non-LEE encoded (**Fig. 3B**). All of the genes required for formation of the TTSS are encoded within the 5 major operons of the LEE, *LEE1-LEE5* (Elliott et al., 1999). The master LEE regulator Ler, encoded as the first gene of the *LEE1* operon, positively stimulates LEE gene transcription by relieving H-NS mediated repression while negatively regulating its own transcription (Bingle et al., 2014; Elliott et al., 2000). It has been proposed that the antagonistic effect on H-NS repression by Ler is due to the formation of toroidal-protein DNA complexes, wherein Ler has a higher affinity for host DNA (Mellies et al., 2011). However, the precise mechanism of binding specificity remains unclear. Ler is also able to stimulate production of other LEE encoded regulators including GrlA and GrlR, which activate and repress *ler* transcription, respectively (Berdichevsky et al., 2005; Deng et al., 2004; Elliott et al., 2000; Haack et al., 2003; Islam et al., 2011; Sperandio et al., 2000). The genes *grlA* and *grlR*

are encoded as a discistron from an H-NS/Ler regulated promoter (Barba et al., 2005), and GrlA binds directly to the *LEE1* promoter region (Huang and Syu, 2008). Activation of *LEE1* transcription by GrlA, through the specific interaction with a region between the -10 and -35 sites of the *LEE1* P1 promoter, is dependent on its helix-turn-helix (HTH) motif, and is not required following deletion of H-NS, supporting its role in anti-silencing the *ler* promoter (Islam et al., 2011; Jimenez et al., 2010). The regulator GrlA has two functional domains, including a transcriptional domain and a domain involved in specific interaction with GrlR (Jimenez et al., 2010), a protein that binds directly with GrlA to inhibit its anti-silencing activity at the *LEE1* promoter (Iyoda et al., 2006). It was recently shown that the specific interaction of GrlR with GrlA inhibits the activity of GrlA by out-competing target DNA for its helix-turn-helix motif (Padavannil et al., 2013).

Further regulation of LEE gene transcription is mediated through numerous factors encoded outside of the LEE including RpoS, RpoN, EivF, EtrA, PchC, GrvA, Hfq, RgdR, QseA, and RcsB (Dong et al., 2009; Flockhart et al., 2012; Hansen and Kaper, 2009; Hengge, 2009; Iyoda and Watanabe, 2004; Kendall et al., 2010; Laaberki et al., 2006; Navarro Llorens et al., 2010; Riordan et al., 2010; Russell et al., 2007; Sharp and Sperandio, 2007; Tobe et al., 2005; Zhang et al., 2004). Transcription of LEE genes in EHEC, and subsequent type III secretion, is maximal during exponential growth, with LEE gene transcription collapsing during stationary phase (Bergholz et al., 2007b; Mitra et al., 2012). Stationary phase regulation by sigma factor RpoS is partially dependent on the protease ClpXP, which is also able to promote the stability of the LEE gene repressor GrlR, and the accumulation of RpoS leads to activation of the LEE repressing acid resistance regulators (Dong and Schellhorn, 2009; Iyoda and Watanabe, 2005). The regulators EivF and EtrA are two LEE regulatory proteins encoded within a defunct type III

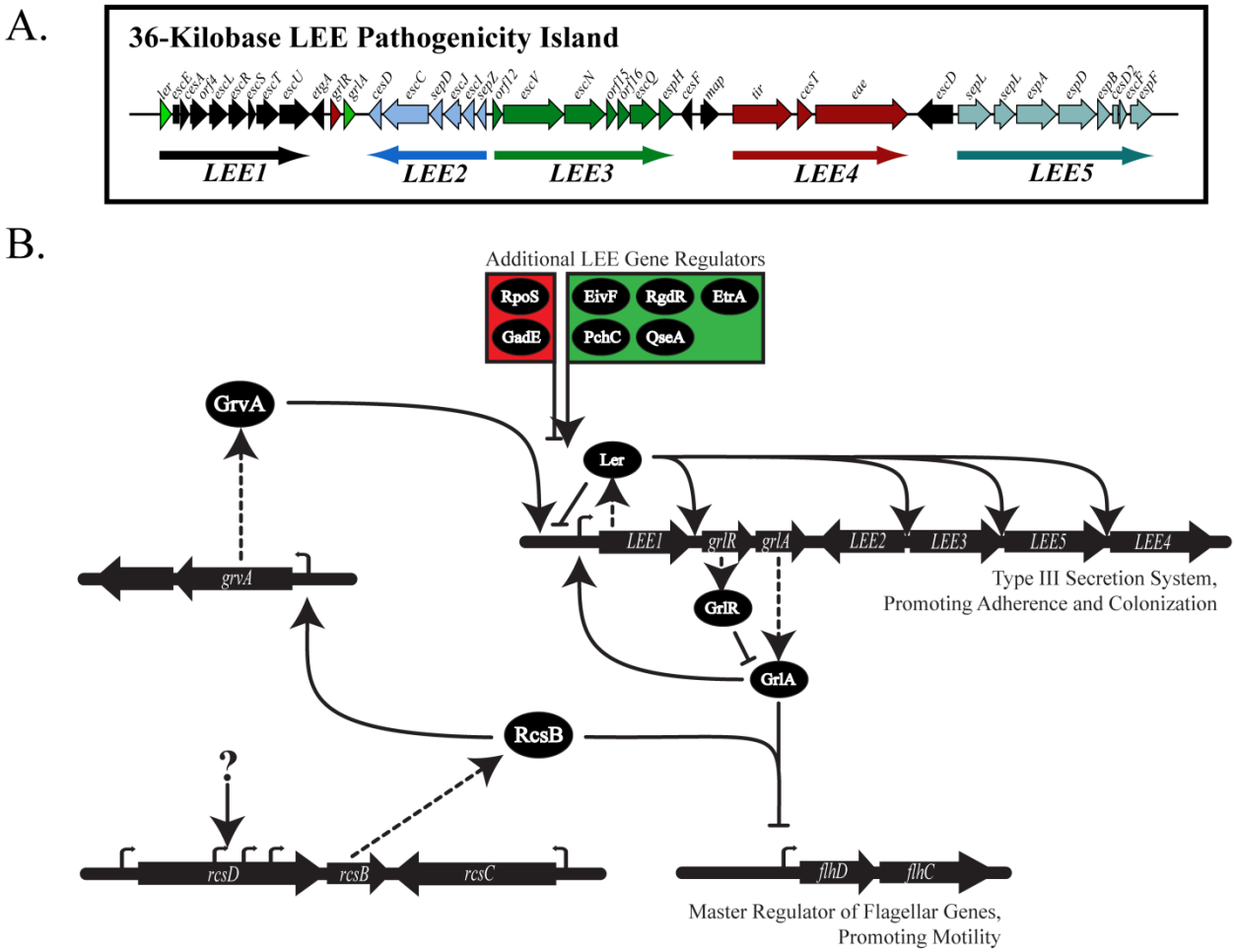

Figure 3 - Model for LEE gene regulation in EHEC
Shown above is (A) the schematic organization of the 36-kb LEE pathogenicity island, and (B) a regulatory model for LEE gene regulation through the known RcsB-GrvA pathway, including the master motility regulatory *flhDC*. The *LEE1* operon encodes Ler, a positive regulator of the remaining *LEE2-LEE5* operons. Ler is also able to stimulate transcription of the LEE encoded *grlRA* operon, producing the *LEE1* activator GrlA and the GrlA inhibiting protein GrlR. The Rcs phosphorelay response regulator RcsB directly represses motility, a phenotype also observed for GrlA, and stimulates transcription of the *grvAB* operon. Finally, in a direct or indirect manner, the GrvA transcriptional regulator positively affects LEE gene transcription through the *LEE1* promoter.

secretion system, termed ETT2, found in both pathogenic and non-pathogenic strains of *E. coli* (Zhang et al., 2004). The cross-talk between the LEE and EivF/EtrA has not yet been shown to be direct, since only repression of LEE gene transcription was demonstrated following their overproduction. These regulators are particularly notable in that they are the regulatory remnants of a defunct T3SS exerting influence over an extant PAI (the LEE), a phenomena that has been described as the "Cheshire cat effect" (Zhang et al., 2004). Another notable non-LEE encoded regulator of the LEE is actually a class of regulators, termed PerC homologs (Pch), which is derived from their homology to the EPEC specific LEE regulator, PerC (Iyoda and Watanabe, 2004). In some EPEC strains, the pEAF plasmid contains the *perC* gene which encodes a direct transcriptional activator of the *LEE1* operon (Mellies et al., 1999). However, as this plasmid is not found in EHEC, a search for other prophage encoded LEE regulators revealed a number of PerC homologs. These included PchA, PchB, PchC, PchD, and PchD; however, only PchA, PchB, and PchC had measurable effects on *LEE1* promoter activity in EHEC and EPEC strains (Iyoda and Watanabe, 2004; Porter et al., 2005). The Per and Pch regulators likely function in concert with other nucleoid associated proteins, such as IHF, to de-repress the *LEE1* promoter (Porter et al., 2005).

EHEC contains a number of horizontally acquired, multi-genic, elements termed O-islands that contribute roughly 1.3 Mb of genomic content that is not present in K-12 (Hayashi et al., 2001). The genes contained within O-islands are diverse in function, and play a significant role in EHEC virulence and pathogenesis. Adherence modulation, specifically through regulation of the LEE, has been demonstrated through mutational analysis of O-islands in EDL933. For example, the transcriptional regulator RgdR, located within O-island 51, was shown to activate transcription of *LEE1*, and promote type III secretion in a Ler dependent manner (Flockhart et

al., 2012). Moreover, two other transcriptional regulators were identified within O-islands 50 and 57, termed PsrA and PsrB, respectively (Tree et al., 2011). These regulators are of particular interest as their LEE regulatory effects are directed through the *gadE* P3 promoter, increasing production of the acid fitness regulator GadE, a direct repressor at the *LEE1* promoter (Kailasan Vanaja et al., 2009; Tree et al., 2011). Indeed, the acid fitness island (AFI) of *E. coli* contains numerous regulators which coordinate transcription of *gadE,* along with RcsB, to properly time its production. Loss of the Psr regulators was shown to significantly activate T3S during stationary growth, and they are believed to be involved in fine-tuning the activation of glutamate dependent acid resistance genes, and subsequently repress transcription of the LEE, to promote survival during gastric passage prior to colonization (Tree et al., 2011). Likewise, an additional prophage island encoded AraC type regulator, termed PatE, was shown to stimulate acid resistance through transcriptional regulation of the acid stress chaperone *hdeA*, and repress LEE gene transcription, which was hypothesized to occur through a pathway similar to that of PsrA/B (Bender et al., 2012).

Various host derived factors have been shown to directly and indirectly influence expression of EHEC virulence genes, and LEE gene transcription is enhanced during growth in media and conditions which are similar to those found in the gastrointestinal tract (Kenny et al., 1997a). Following gastric passage, LEE gene transcription is stimulated by the bicarbonate ion (Abe et al., 2002) produced by the pancreas to neutralize the stomachs acid (Feldman, 1983; Fordtran and Locklear, 1966). Further, the QseBC two-component system is directly involved in sensing host derived epinephrine, norepinephrine and AI-3 (Alam et al., 2010; Russell et al., 2007; Sharp and Sperandio, 2007; Sperandio et al., 2002). Phosphorylated QseB promotes transcription of the QseEFG phosphorelay system that senses epinephrine, sulfate, and phosphate

to activate transcription of LEE genes (Njoroge and Sperandio, 2012; Reading et al., 2010). Importantly, the regulator QseE has been shown to indirectly regulate the LEE through direct transcriptional repression of *rcsB* (Njoroge and Sperandio, 2012). The QseBC and QseEFG mutli-component phosphorelay systems provide a great example of the complex nature of bacterial interkingdom virulence gene regulation. Furthermore, EHEC has recently been shown to respond to host derived ethanolamine (EA) through the metabolic sensing of EA and production of the *eut* operon regulator EutR; direct transcriptional regulation of the *LEE1* operon by EutR occurs through direct binding at the *ler* promoter (Kendall et al., 2012; Luzader et al., 2013). Beyond factors which are produced directly by the host, products of native microflora are capable of modulating LEE gene transcription and type III secretion mediated adherence. For example, fucose is released from host intestinal mucin in the gut by *Bacteroides thetaiotaomicron* produced fucosidases (Xu et al., 2003), and its FusSK dependent metabolism by EHEC leads to repression of the LEE (Pacheco et al., 2012). Likewise, the products of fermentative metabolic processes (such as acetate, propionate, and butyrate) from native bacteria can stimulate LEE gene transcription through activation of the leucine-responsive regulatory protein (Lrp) and the *LEE1* transcriptional activator PchA (Nakanishi et al., 2009; Tobe et al., 2011).

1.2.4 The *E. coli* common pilus (ECP)

EHEC adherence to epithelial cells, and subsequent host colonization, is enhanced by a common pilus structure seen almost ubiquitously across *E. coli* strains, termed the *E. coli* common pilus (ECP) (Rendon et al., 2007). The *E. coli* common pilus is a chaperone-usher fimbrial adhesin, composed of a 21-kDa subunit encoded by the gene *ecpA*, and its production

plays a role in early-stage biofilm development for commensal and pathogenic *E. coli* and *Klebsiella pneumonia* strains (Alcantar-Curiel et al., 2013; Garnett et al., 2012; Lehti et al., 2010; Wurpel et al., 2013).

1.3 Variation in virulence among EHEC O157:H7 strains

Although there are hundreds of O:H serotypes of EHEC, the O157:H7 serotype is most frequently associated with humans disease (Nataro and Kaper, 1998). Strains of O157:H7 belong to a clonal complex which has been recently organized by phylogenetic analysis into eight discrete clades (Manning et al., 2008). Belonging to clade 8, strain TW14359 has been associated with high incidents of HUS (15%) and hospitalization (51%), as compared to strain Sakai HUS (~1.5%) and hospitalization (~4%) (Clade 1, 1996 Sakai city outbreak) (Manning et al., 2008). Clade 8 strains have demonstrated increased association with epithelial cells, along with increased expression of LEE and other virulence factors, including Shiga toxin 2 (Stx2) (Abu-Ali et al., 2010a; Manning et al., 2008; Neupane et al., 2011). A comparative analysis of O157:H7 strains Sakai and TW14359 revealed increased attachment to MAC-T epithelial cells corresponding to increased levels of LEE gene expression in TW14359, whereas Sakai showed higher expression levels for genes associated with motility (Abu-Ali et al., 2010b).

1.4 The RcsCDB phosphorelay system

Formation of extracellular capsular polysaccharide has been shown to have a role in bacterial adherence, protection from desiccation, and resistance to both specific and non-specific host immunity (Horwitz and Silverstein, 1980; Ophir and Gutnick, 1994; Roberts, 1996). The capsules of *E. coli* are surface enveloping structures composed of high-molecular weight

polysaccharides, and consist of 4 major groups, including colonic acid (Whitfield, 2006). While typical capsules produced by *E. coli* form a surface layer associated with the bacteria, a large quantity of colonic acid produced is ultimately secreted into the growth medium as expolysaccharide (Whitfield and Paiment, 2003), resulting in a mucoidy phenotype. Indeed, up to 30% of the total dry weight of some K-12 strains has been observed to be colonic acid and slime (Ophir and Gutnick, 1994). However, there can be substantial variation in the types and quantity of colonic acid produced among *E. coli* strains. The group 1 and 4 capsules are related to O-antigen LPS, and are found among EPEC, ETEC, and EHEC strains (Whitfield, 2006).

The regulation of capsular polysaccharide (CPS) was initially shown to be dependent on Lon, an ATP hydrolysis and temperature dependent protease (Chung and Goldberg, 1981), that is active at 37°C but not at 30°C (Phillips et al., 1984; Trisler and Gottesman, 1984). Identification of the three key regulatory elements (RcsB, RcsC, and RcsA) involved in colonic acid synthesis, using a *lon* mutant K-12 strain, suggested that one of the three genes was regulated indirectly by the Lon protease (Gottesman et al., 1985). RcsA was further shown to be a target of ATP-dependent Lon proteolysis, with a half-life of 5 minutes in wild type *E. coli* and 20 minutes in a *lon* defective *E. coli*. Temperature dependent CPS production is therefore dependent on the availability of RcsA for transcriptional activation of *cps* genes (Torres-Cabassa and Gottesman, 1987).

The components of the Rcs phosphorelay system include a membrane bound sensor histidine kinase, RcsC, that transfers a phosphate to the histidine phospho-transferase RcsD, which transfers the phosphate to the response regulator RcsB (**Fig. 4**) (Clarke, 2010). The *rcsB-rcsC* gene cluster was first identified as being required for CPS production. RcsC contains homology with known membrane bound sensor kinases, and was shown to act as a sensor

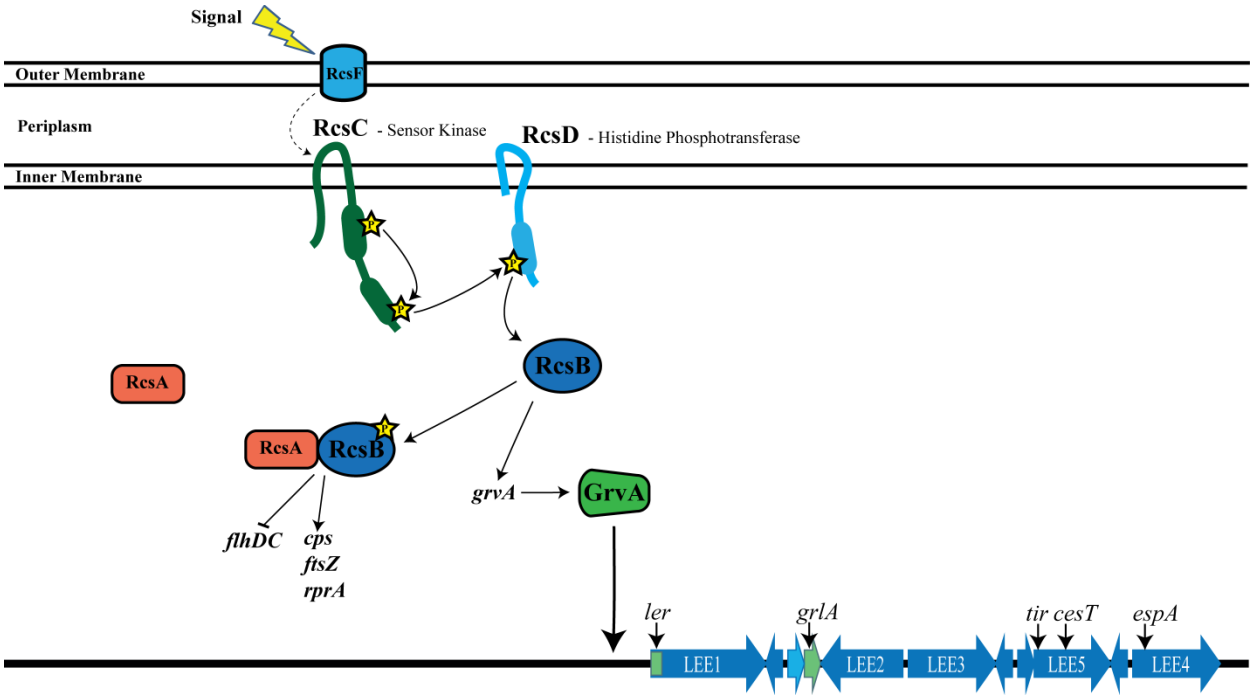

Figure 4 - The RcsCDB phosphorelay and regulation of type III secretion in EHEC
The Rcs phosphorelay system indirectly promotes transcription of the LEE PAI through the OI-47 encoded regulator GrvA. The Rcs relay is composed of 3 major components, including the sensory kinase (RcsC), the histidine phosphotransferase (RcsD), and the response regulator (RcsB). Signal transduction to RcsC occurs through different mechanisms, including activation by the outer-membrane lipoprotein RcsF.

activating the regulator RcsB (Brill et al., 1988; Stout and Gottesman, 1990). The sensor kinase RcsC is able to communicate membrane perturbations to RcsB caused by osmotic shock, membrane damaging agents, and growth on solid media; importantly, RcsC is required for normal biofilm formation (Ferrieres and Clarke, 2003). The response regulator RcsB binds to specific DNA sequences (RcsB box) at promoters to activate or repress transcription. In its phosphorylated state, RcsB can bind as a homodimer ($RcsB_2$) or as a heterodimer (RcsB/X) with other regulatory proteins, such as RcsA (Majdalani and Gottesman, 2005). In its activated state, RcsB/RcsA can repress transcription of flagellar genes (Francez-Charlot et al., 2003) and simultaneously activate genes involved in capsule synthesis during growth at low temperatures (Torres-Cabassa and Gottesman, 1987). While the regulatory capacity of RcsB is broadly dictated through activation by RcsC, binding with other non-RcsA regulatory proteins has been reported (Torres-Cabassa and Gottesman, 1987) (**Fig. 5**). For example, RcsB forms a heterodimer with BglJ relieving HN-S mediated repression of the *bgl* operon, and is thus involved in the uptake and utilization of beta-glucosides (Venkatesh et al., 2010). Finally, and importantly, RcsB can form a heterodimer with the central regulator of glutamate dependent acid resistance (GDAR), GadE, to facilitate transcription of acid fitness genes (Castanie-Cornet et al., 2010). As such, RcsB is required for wild-type levels of acid resistance, a factor that directly contributes to the low infectious dose of EHEC.

The RcsB response regulator is activated by the phosphorylation of an aspartic acid residue within the RcsB receiver domain through interaction with the membrane bound histidine phosphotransferase RcsD (Gupte et al., 1997), rather than by interaction with the cognate sensor kinase RcsC (Huang et al., 2006). In a typical two-component regulatory system, sensor kinase

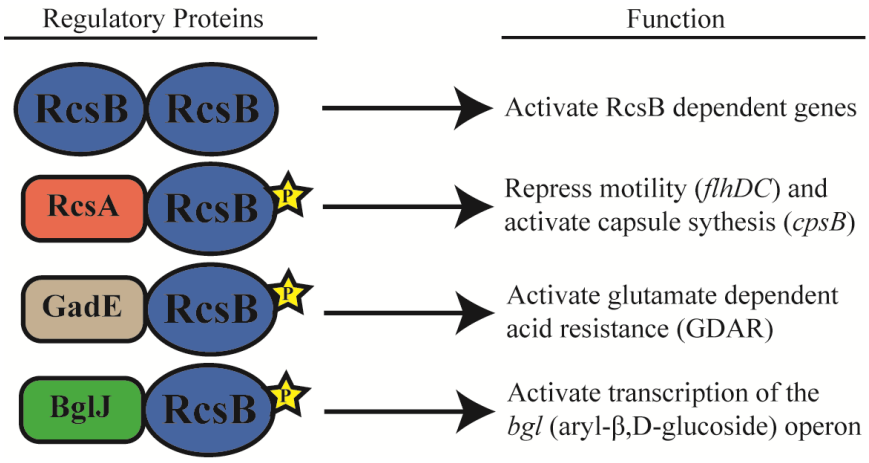

Figure 5 - Homo- and hetero-dimerization of RcsB in *E. coli*
The known heterodimerization proteins of RcsB in *E. coli* are listed with a brief description of their regulatory function. In *E. coli*, RcsB can form a homodimer with itself to regulate transcription at promoters containing an RcsB consensus sequence. Alternatively, RcsB can heterodimerize with RcsA, GadE, or BglJ to regulate transcription of motility, acid resistance, or the uptake and utilization of aryl beta-glucosides, respectively.

autophosphorylation is either enhanced or inhibited through the sensing of its specific signal, and the phosphate is typically transferred from a histidine residue on the sensor kinase to an aspartic acid residue within the cognate response regulator receiver domain (Stock et al., 1989). For example, this model of regulation is observed for a number of *E. coli* TCS, including CpxA/CpxR and EnvZ/OmpR (Danese and Silhavy, 1997; Egger et al., 1997), where the former is an example of a TCS sensor kinase that actively dephosphorylates its cognate response regulator in the absence of stimuli (Dorel et al., 2006). The multi-component RcsCDB phosphorelay utilizes a different method of activation, wherein the RcsD membrane bound histidine phospho-transferase acts as an adapter protein between RcsC and RcsB (Huang et al., 2006). Activated RcsC autophosphorylates at the His479 residue within its histidine-containing phosphotransmitter (Hpt) domain and transfers the phosphate to its phospho-acceping Asp875 residue within its receiver domain (**Fig. 6**). The phosphate is then transferred to the His842 residue on the RcsD Hpt domain (Takeda et al., 2001). Recent work has shown that the RcsD-ABL (α-β-Loop) domain interacts directly with RcsB effector domain, while the RcsD Hpt domain interacts with the phosphor-accepting receiver domain, suggesting that RcsD and RcsB function together in a very limited orientation (Schmoe et al., 2011). Interestingly, in *Salmonella enterica* serovar *Typhimurium*, overexpression of truncated RcsC or RcsD cytoplasmic domains results in phosphorylation of RcsB and subsequent activation of Rcs regulated genes, revealing a potentially complex activation pathway hitherto unknown (Pescaretti Mde et al., 2013). However, this finding has not yet been replicated in *E. coli*.

An additional, alternative, mechanism for Rcs activation exists in *E. coli* that couples carbon metabolism and the accumulation of acetyl phosphate with phosphorylation of the response regulator RcsB. In two specific signal transduction systems with sensor kinases that

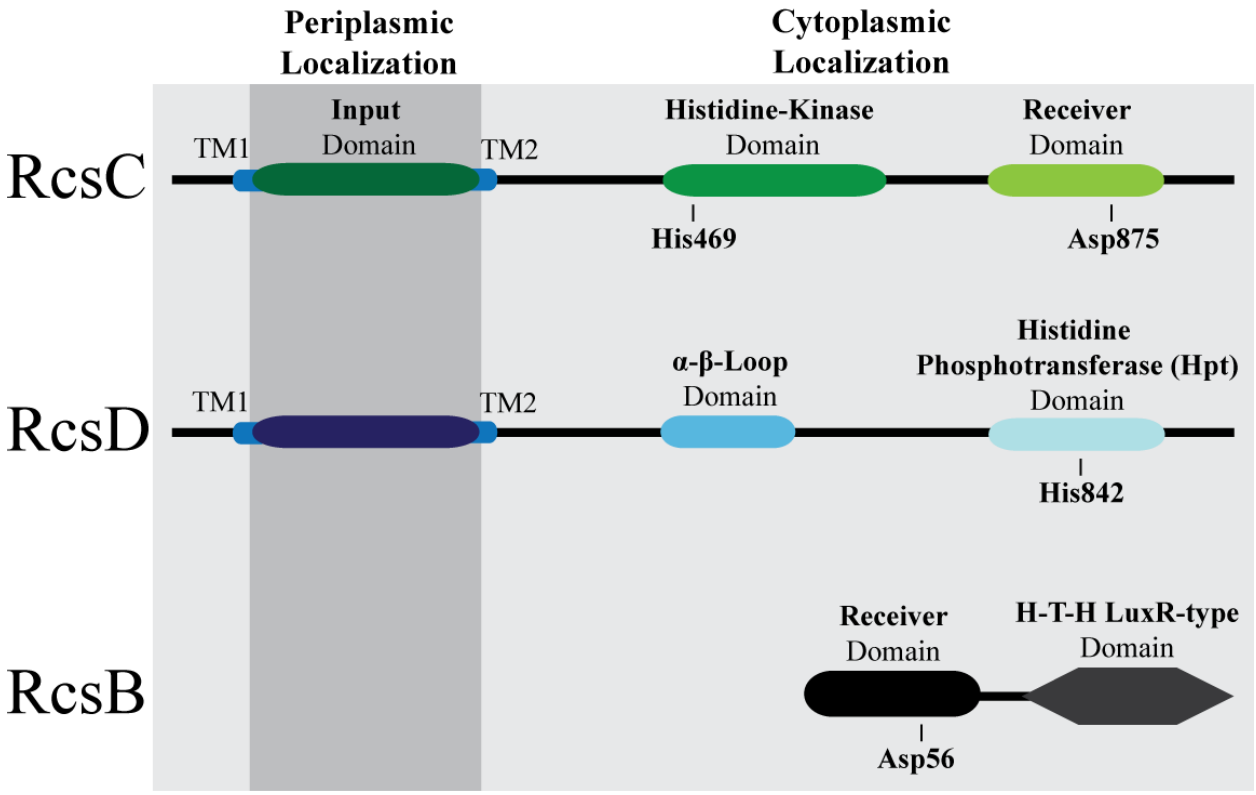

Figure 6 - Functional domains of the Rcs components in *E. coli*
The Rcs phosphorelay is composed of a sensory kinase (RcsC), a histidine phosphotransferase (RcsD), and a response regulator (RcsB). The RcsC sensor kinase is bound to the inner membrane, and has both a periplasmic input domain and a cytosolic histidine kinase and receiver domain for autophosphorylation and phosphotransfer to RcsD. The histidine phosphotransferase RcsD is an adapter protein which functions as an additional control for regulation phosphorylation of the response regulator RcsB. To receive the phosphate from RcsC, the RcsB response regulator must bind at the RcsD-ABL domain.

favor phosphatase activity, CpxA and RcsC, the cognate response regulator can be phosphorylated by, and respond to levels of, acetyl phosphate (Aiso et al., 2011; Batchelor et al., 2005). When excess carbon is present, particularly glucose, cells can accumulate acetyl phosphate. Similar levels of acetyl phosphate accumulation are observed following the mutation of *ackA*, the product of which is key in the Pta-AckA cycle for acetyl-coA and acetogenesis. In this reversible pathway, Pta synthesizes acetyl phosphate and coenzyme A (CoA) from acetyl-CoA, and AckA generates ATP and acetate from acetyl phosphate (Wolfe, 2005). Therefore, mutations or growth conditions which favor the accumulation of acetyl phosphate promote the promiscuous phosphorylation of RcsB, and can directly affect motility and virulence gene regulation in *E. coli* (Aiso et al., 2011; Wolfe, 2010). Beyond phosphorylation, the presence of a lysine acetylation domain was recently reported for RcsB which serves to regulate its activity at the *rprA* promoter, and is dependent on the lysine de-acetylase CobB (Hu et al., 2013; Stelzer et al., 2006).

While the RcsCDB mutli-component signal transduction pathway contains a sensor histidine kinase, activation and autophosphorylation requires the function of two membrane-tethered proteins, specifically DjiA and RcsF (Clarke et al., 1997; Majdalani et al., 2005) (**Fig. 7**). The overproduction of the membrane anchored DnaJ-like protein DjiA has been shown to significantly increase capsular polysaccharide production, dependent on GrpE and DnaK (Kelley and Georgopoulos, 1997). In the cytoplasmic membrane, the transmembrane domain of DjiA facilitates the formation of a DjiA-homodimer. However, while the transmembrane domain is required for DjiA-dependent activation of CPS production, dimerization alone is not sufficient to activate the Rcs phosphorelay (Clarke et al., 1997; Toutain et al., 2003). The specific factors which stimulate the dimerization of DjiA and subsequent activation of CPS production have not

yet been elucidated. Constitutively high production of DjiA is ultimately toxic to the cell. Not surprisingly, the production of DjiA is tightly regulated and transcription is dependent on the extracytoplasmic-function sigma factor, RpoE (Kelley and Georgopoulos, 1997). Similarly, overproduction of RcsF has been shown to induce CPS production in an RcsC dependent manner (Gervais and Drapeau, 1992; Majdalani et al., 2005).

RcsF is a ~14-kDa outer-membrane bound lipoprotein which orients towards the periplasm and its activation has been demonstrated for mutations that affect the proper folding of periplasmic proteins, as well as those which disrupt the proper synthesis and localization of lipopolysaccharides and lipoproteins (Castanie-Cornet et al., 2006; Tao et al., 2012). The activity of RcsF is dependent on the formation of nonconsecutive dislufides and requires an unstructured proline rich region to properly convey signals to the sensor kinase RcsC for Rcs phosphorelay activation (Leverrier et al., 2011; Umekawa et al., 2013). Among enteric gram-negative bacteria that contain RcsF, the C-terminus contains high levels of amino acid sequence similarity, while the membrane anchored N-terminal domain is less conserved (Rogov et al., 2011). While the current model of RcsF-RcsC activation is believed to be through direct interaction of the periplasmic domains of both proteins, experiments performed to validate this hypothesis have been unable to confirm specific interaction (Rogov et al., 2011). Therefore, it remains a possibility that some other factor mediates signal transduction between RcsF and RcsC. Similar to RcsF, overproduction of the putative lipoprotein YpdI is also able to activate the Rcs phosphorelay in an RcsF-independent and RcsA-dependent manner, however little is known about its specific function or role in *E. coli* (Rendon et al., 2007). Both DjiA and RcsF therefore fit within a model previously described for the outer membrane lipoprotein NlpE, which serves as an activator of the CpxAR stress response two-component system (Hirano et al., 2007; Snyder

et al., 1995). Interestingly, the lipoprotein-specific molecular chaperone LolA is required for efficient localization and trafficking of membrane bound lipoproteins, and *lolA* mutant or overexpression derivative *E. coli* strains result in Rcs activation directed through RcsF (Tao et al., 2012), a finding that supports the role for RcsF activation by misfolded/mislocalized periplasmic proteins.

The genes encoding RcsD, RcsB, and RcsC are organized into two distinct operons, with *rcsDB* and *rcsC* oriented and transcribed divergently. The *rcsB* and *rcsC* ORFs were identified prior to that of *rcsD*, and early work suggested that their independent transcription might reflect a need to control the transcription of each gene alone (Stout and Gottesman, 1990). For example, transcription of *rcsB* was suggested to be under the control of LexA and the alternative sigma factor RpoN, however direct experimental evidence for the latter has been contradictory (Gervais et al., 1992). In one case, loss of *rpoN* resulted in decreased *rcsB* transcription, while another group independently reported no significant impact on *rcsB* following mutation of *rpoN* (Gervais et al., 1992; Stout and Gottesman, 1990). A putative sigma-54 (RpoN) binding site was identified upstream of *rcsB*, within the *rcsD* ORF (Stout and Gottesman, 1990), but further work is required to determine if RpoN plays a significant direct role in the regulation of *rcsB*. In *E. coli* strain K-12, the *rcsDB* operon is transcribed from a sigma-70 promoter upstream of *rcsDB*, and the *rcsB* gene is independently transcribed from at least two sigma-70 promoters intracistronic to *rcsD*, $rcsB_{P1}$ and $rcsB_{P2}$ (Krin et al., 2010). Importantly, transcription from the *rcsD* promoter, but not the *rcsB* promoters, is actively repressed through direct binding of H-NS (Krin et al., 2010). This model of regulation suggests a control scheme wherein the histidine phospho-transferase RcsD is a rate limiting step in the phosphorelay, preventing RcsB phosphorylation through the canonical RcsC-RcsD-RcsB route. While the Rcs component genes

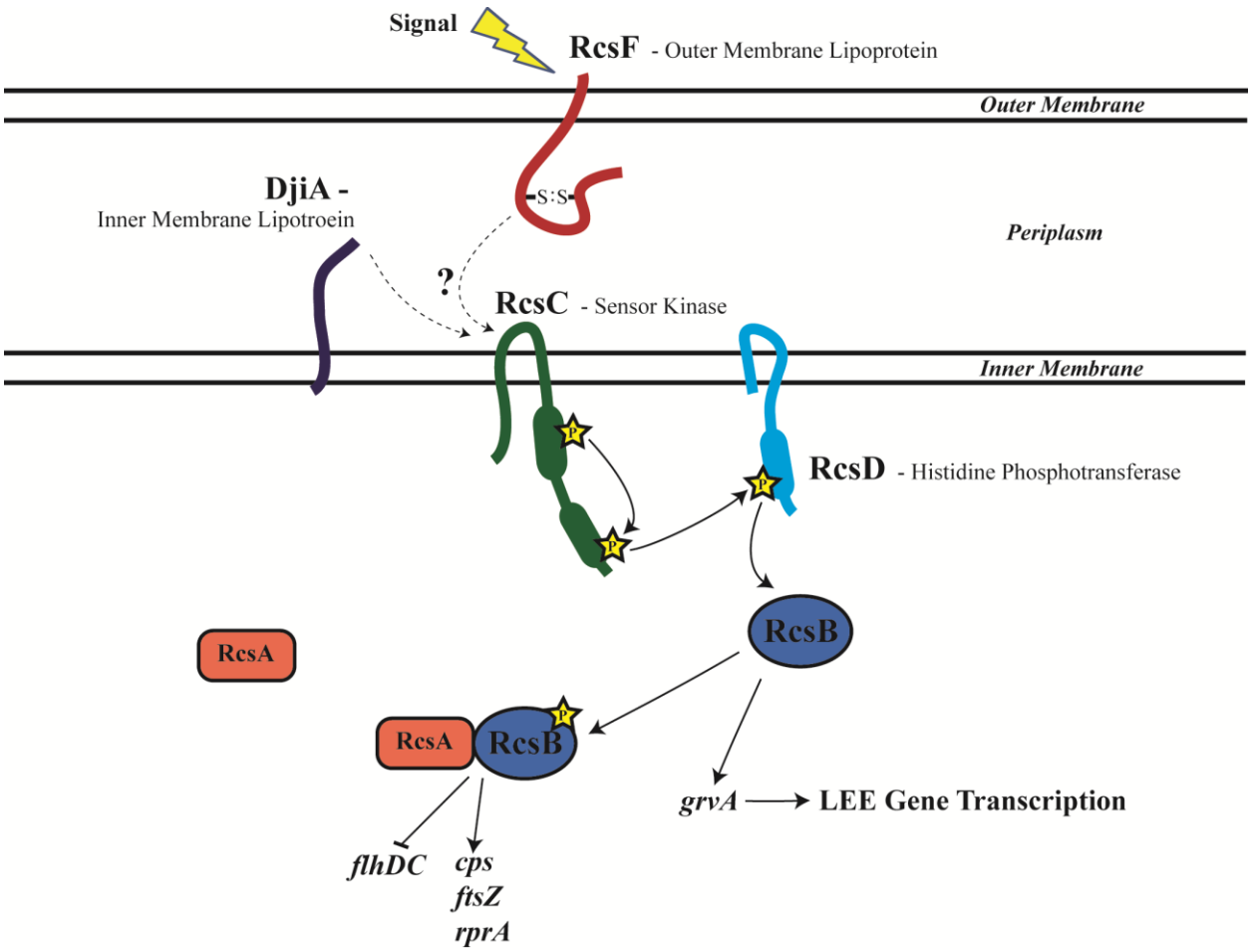

Figure 7 - RcsF and DjiA activation of the Rcs phosphorelay
The current model for Rcs phosphorelay activation includes the components of the relay itself (RcsCDB), but also includes inner- and outer-membrane lipoproteins DjiA and RcsF. Overproduction of DjiA or RcsF has been shown to facilitate signal transduction, through an unknown mechanism, to the sensor kinase RcsC. The functional domains of DjiA are not well described, however the functional domains RcsF lipoprotein have been explored. RcsF contains a disordered proline rich region and a disulfide bond that is required for

are typically conserved in different gram-negative bacteria, their regulatory patterns can be divergent. For example, an analysis of *rcsB* regulation in the enteric pathogen *Salmonella enterica* serovar Typhimurium identified an additional stationary phase inducible *rcsB* promoter, and revealed a model of RcsB negative auto-regulation at the *rcsD* promoter to modulate swarming behavior (Pescaretti Mde et al., 2010; Pescaretti Mde et al., 2009); however, no such model of Rcs auto-regulation has been reported for *E. coli*. More recently, epinephrine sensing histidine sensor kinase QseE was shown to negatively regulate transcription of *rcsB* in EHEC, and therefore negatively affect virulence gene transcription (Deng et al., 2010).

The Rcs phosphorelay plays an important role during conditions which cause damage to the host membrane integrity, such as osmotic shock from high glucose or sodium chloride concentrations, and can protect the cell from desiccation (Sledjeski and Gottesman, 1996). Additionally, the loss of *tolA*, encoding a membrane spanning protein involved in cell envelope integrity, has been shown to activate the Rcs system through stimulation of the sensor kinase RcsC (Clavel et al., 1996). Mutation of *tolA* leads to highly mucoid colonies and decreased adherence in *E. coli* strain MG1655, a phenotype that is completely dependent on the membrane bound lipoprotein RcsF (Vianney et al., 2005). Further examination into activation of Rcs in response to different stimuli reveals that it plays a dynamic role in gene activation relative to growth phase and conditions. Specifically, the co-regulator of colonic acid synthesis RcsA binds with RcsB following phosphorylation at low temperatures, owing to temperature dependent Lon protease activity (Torres-Cabassa and Gottesman, 1987). Independent of RcsA, activation in the presence of $ZnCl_2$, Fe^{3+} and low Mg^{2+} leads to induction of *ugd* under specific conditions and is dependent on the regulator PhoP (Hagiwara et al., 2003; Mouslim et al., 2003). Beyond cell envelope stress, the Rcs response regulator RcsB is required for survival following exposure to

low acidic conditions, such as those present during gastric passage (Castanie-Cornet et al., 2007). This dependence is due to the heterodimerization of RcsB with the acid fitness island (AFI) regulator GadE, which is required for transcription of several key AFI encoded genes (Johnson et al., 2011; Krin et al., 2010). Interestingly, the de novo generation of cell shape following lysozyme treatment was recently shown to require RcsB, revealing a specific role in the recovery from insults to the outer membrane, suggesting that the Rcs phosphorelay might play a role in survival following exposure to host immune responses leading to membrane perturbation (Ranjit and Young, 2013). Likewise, following exposure to human serum, extraintestinal pathogenic *E. coli* (ExPEC) activates the Rcs phosphorelay, along with other envelope stress regulators, as a protective measure in response to cell wall damage (Mellies et al., 2012). Furthermore, the Rcs components were required for survival during exposure to antibiotics that inhibit peptidoglycan synthesis, including the β-lactamases cefsulodin and amdinocillin, independent of RcsA, and more recently the exposure to antimicrobial peptides was observed to activate the Rcs phosphorelay through the membrane bound lipoprotein RcsF (Laubacher and Ades, 2008; Tucker et al., 2010).

While the Rcs phosphorelay has a distinct role in survival during specific stress conditions, it has also been shown to regulate the expression of virulence factors in *E. coli* and other enteric pathogens. Virulence and motility gene regulation has been shown to occur through the RcsC-RcsD-RcsB His-Asp phosphorelay system in *E. coli* (Francez-Charlot et al., 2003; Krin et al., 2010; Tobe et al., 2005). Importantly, overexpression of RcsB has been observed to increase LEE gene activity and attachment to HeLa cells (Tobe et al., 2005). RcsB was shown to positively regulate transcription of the LEE regulator *ler* by positively regulating *grvA*, an activator of *ler* (Tobe et al., 2005). The role for RcsB in TW14359 virulence, and the mechanism

by which RcsB contributes to the LEE overexpression and adhesion phenotype, is unknown. In *Salmonella enterica* serovar Typhimurium, RcsB binds and represses transcription from the *flhDC* promoter in an RcsA dependent manner, and subsequently impairs swarming motility and swimming (Chaand and Dziejman, 2013). However, unlike EHEC, virulence is significantly attenuated in Salmonella following Rcs activation. Specifically, a constitutively active RcsC allelic variant significantly decreases the expression of genes involved in macrophage survival and the invasion of non-phagocytic cells (Krogh et al., 2001). Conversely, virulence of enteropathogenic *Yersinia pseudotuberculosis* requires an intact Rcs phosphorelay (Sayed and Foster, 2009). In contrast to enteropathogenic *Yersinia*, the gene encoding RcsD has undergone mutational attrition in *Yersinia pestis*; this fact is important in light of a study demonstrating that RcsB negatively regulates biofilm formation in *Yersinia pestis*, indicating that *rcsD* was evolutionarily deselected to decrease RcsB phosphorylation (Sun et al., 2012). Beyond virulence in animal hosts, RcsB regulation of virulence in gram-negative pathogenic bacteria has also been reported. For the rosaceous plant pathogen *Erwinia amylovoran*, RcsB is required for the production of the exopolysaccharide amylovoran and directly contributes to bacterial survival and the disease symptom formation (Bereswill and Geider, 1997; Kelm et al., 1997; Santander et al., 2014). Ultimately, RcsB plays a broad role in the regulation of genes involved in survival and virulence gene regulation for a diverse population of gram-negative bacterial pathogens.

1.5 The G. *mellonella* virulence model

Galleria mellonella, the greater wax worm, has been used as a virulence model in several important human pathogenic gram-negative bacteria, such as *Pseudomonas*, *Listeria*, *Yersinia*, *Campylobacter*, *Klebsiella*, and *Legionella* (Champion et al., 2009; Harding et al., 2012; Insua et

al., 2013; Miyata et al., 2003; Mukherjee et al., 2010; Senior et al., 2011). Importantly, the *G. mellonella* model has shown a positive correlation of virulence patterns in mice for major virulence determinants in gram-negative human pathogens, such as *Pseudomonas aeruginosa* and enteropathogenic *Escherichia coli* (EPEC) (Jander et al., 2000; Leuko and Raivio, 2012). Infection of larvae with bacteria results in a robust host immune response characterized by the formation of melanotic nodules, recruitment of hemocytes (Jiang et al., 2010), and the production of both antimicrobial peptides and inhibitors of microbial proteinases (Vogel et al., 2011). The *G. mellonella* model has not yet been used to explore the virulence properties of EHEC or, more specifically, factors which are unique to the O157:H7 serotype. However, at least in EPEC, loss of the T3SS resulted in attenuated virulence, suggesting that the *G. mellonella* model could be used to explore the contribution of GrvA to the overall virulence of EHEC, and specifically strain TW14359.

1.6 Project aim

Variation in virulence has been described between distantly related EHEC strains, specifically with higher levels of LEE gene transcription and subsequent adherence in strains which have been characterized with a high incidence of HUS. More specifically, the 2006 U.S spinach outbreak strain TW14359 possess increased adherence and Stx2 production when compared with the less virulent EHEC strain Sakai. Transcriptomic studies for TW14359 revealed markedly higher levels of LEE gene transcription and decreased transcription of motility associated genes, likely contributing to the increased adherence phenotype. However, the specific genetic mechanism underlying differential virulence had not yet been described. The recently published genome of TW14359 identified numerous factors which were unique to TW14359, and further

revealed polymorphisms which have not been observed in other EHEC strains to-date. It is hypothesized that the hypervirulence of this strain, and closely allied clade 8 strains, is due to the increased expression of virulence factors common to all O157:H7 strains, as well as novel strain-specific factors. Accordingly, the aim of this project is to identify the specific factor(s) which direct increased adherence in TW14359 and to further explore polymorphisms unique to TW14359 which contribute to altered virulence gene regulation. Overall, identifying factors which contribute to differential virulence will provide insight into the evolution of virulence in enterohemorrhagic *E. coli*.

Chapter 2: RcsB determines the locus of enterocyte effacement (LEE) expression and adherence phenotype of *Escherichia coli* O157:H7 spinach outbreak strain TW14359 and coordinates bicarbonate-dependent LEE activation with repression of motility

Note to Reader. Portions of these results have been previously published (Morgan et al., 2013) and are utilized with permission of the publisher (Appendix A)

2.1 Background

Enterohemorrhagic *Escherichia coli* (EHEC) O157:H7 is a virulent human pathogen attributed to sporadic cases and large outbreaks of bloody diarrhea (hemorrhagic colitis) (Rangel et al., 2005). In 2006, an outbreak in the United States of O157:H7 due to the consumption of tainted spinach was associated with unusually high rates of hospitalization and life-threatening sequelae (i.e. hemolytic uremic syndrome) (Manning et al., 2008). Phylogenetic analysis of over five hundred clinical O157:H7 isolates, suggested that the strain which caused this outbreak, TW14359, belongs to a discrete genetic group referred to as clade 8, the members of which are highly virulent (Manning et al., 2008). Consistent with this hypothesis, DNA sequencing of this strain has revealed the presence of virulence factors that are absent in the reference genomes of sequenced O157:H7 strains Sakai (1996 Japan) and EDL933 (1982 USA) (Kulasekara et al., 2009; Manning et al., 2008). In addition, a virulence expression phenotype has been described for strain TW14359 characterized by increased basal transcription of locus of enterocyte effacement (LEE) genes, as well as Shiga toxin 2 genes (*stx2AB*) and Stx2 protein relative to

other O157:H7 strains (Abu-Ali et al., 2010a; Abu-Ali et al., 2010b; Neupane et al., 2011). Elevated basal LEE expression in TW14359 has further been correlated to increased adherence to bovine epithelial cells (Abu-Ali et al., 2010b).

The LEE is a 35.6-kb pathogenicity island that encodes a type III secretion apparatus required for competitive colonization of the intestine and attaching/effacing (A/E) lesion formation in EHEC and enteropathogenic *E. coli* (EPEC) (Elliott et al., 1998; McDaniel and Kaper, 1997; Perna et al., 1998), and in the mouse pathogen *Citrobacter rodentium* (Schauer and Falkow, 1993). Regulation of LEE expression has been intensively studied (Mellies et al., 2007; Tree et al., 2009), but is still not fully understood. Four LEE-encoded proteins are currently known to control its expression: Ler (LEE encoded regulator), Mcp (multiple point controller), GrlR (global regulator of LEE repressor) and GrlA (global regulator of LEE activator). *ler* is the first gene of the *LEE1* operon, and is a master regulator of the LEE, activating transcription from all five LEE operons (Elliott et al., 1998; Sperandio et al., 1999). Mcp, when overexpressed, down-regulates LEE expression through interaction with Ler, and GrlA directly activates *ler* transcription (and thus the LEE), whereas GrlR represses *ler* transcription through interactions with GrlA (Creasey et al., 2003; Deng et al., 2004; Huang and Syu, 2008; Lio and Syu, 2004). In addition, a myriad of non-LEE encoded regulators modulate LEE expression through *ler* in response to environmental cues such as growth phase, bicarbonate, stress, and others (Abe et al., 1997; Abe et al., 2002; Bergholz et al., 2007a; Friedberg et al., 1999; Grant et al., 2003; Kenny et al., 1997a; Shin et al., 2001; Sperandio et al., 1999; Tobe et al., 2005; Umanski et al., 2002).

In this study, the role for RcsB, a response regulator of the Rcs phosphorelay system, in the virulence expression phenotype of strain TW14359 was examined. In particular, the importance of RcsB to enhanced LEE expression and adherence characteristic of this strain was

investigated. In addition, the study sought to define the regulatory contribution of RcsB to bicarbonate-dependent activation of the LEE and LEE-dependent repression of motility.

2.2 Methods

2.2.1 Bacterial strains and culture conditions

The strains and plasmids used in this study are listed in **Table 2**. Strains were stocked at -80°C in glycerol diluted (15% v/v final) in Luria Broth (LB), and were maintained in LB or on LB with 1.5 % agar (LBA). Unless otherwise noted, overnight (18-20 h) cultures grown in LB were used to inoculate fresh LB or LB buffered with sodium bicarbonate (44 mM $NaHCO_3$) or fresh Dulbecco's Modified Eagle's Medium (DMEM) (4 g l^{-1} glucose, 4 mM glutamine, 44 mM $NaHCO_3$, pH 7) to a final optical density 600 nm (OD_{600}) of 0.05. Cultures were grown at 37°C in a rotary shaker (200 RPM) using a 1:10 media-to-flask volume. The growth of strains was monitored by taking OD_{600} readings at 1 h intervals for 11 h. Antibiotics (Sigma-Aldrich, St. Louis, MO) were added to cultures when required. For maximum expression from the P_{BAD} promoter of pBAD22 (Guzman et al., 1995), cultures were grown in DMEM containing L-arabinose (0.5% w/v) and glycerol (0.4% v/v).

2.2.2 Genetic manipulations and chromosomal FLAG-fusion construction

Primers used for the genetic manipulation of TW14359 and Sakai are provided in **Table 3**. Gene deletion and kanamycin (Kan) replacement mutants were constructed using the λ Red recombinase-assisted approach (Murphy and Campellone, 2003) and as described (Riordan et al., 2010). To make a TW14359 *grlA* overexpression strain, an *Eco*RI/*Xba*I digested 413-bp PCR fragment containing the promoterless *grlA* ORF was cloned into similarly digested pBAD22

(Guzman et al., 1995) to yield pRJM-15, which was then transformed by electroporation into TW14359 as described (Riordan et al., 2010). For *rcsB* complementation, a *Bam*HI/*Xho*I digested 3,424-bp PCR fragment, containing the *rcsB* ORF and native promoters, was cloned into similarly digested pACYC177 to yield pRJM20, which was then transformed into TW14359Δ*rcsB*. To construct FLAG fusions to *rcsB* and *tir*, the approach of Uzzau et al. (Uzzau et al., 2001) was used. Primers FLAG-F and P2 used to amplify the FLAG epitope and Kan resistance cassette from pSU312 (Uzzau et al., 2001) were constructed with 40-bp oligonucleotide 5' extensions with homology to a 3' region of the target ORF and a downstream intergenic region, respectively. Homologous recombination of this product using λ Red recombinase replaces the native stop codon with the FLAG sequence in-frame with the target ORF. When expressed, the fusion protein contains a seven amino acid C-terminal epitope (FLAG) that can be detected by western blots using anti-FLAG mAbs (Uzzau et al., 2001). All genetic constructs were validated using a combination of PCR and restriction mapping, qRT-PCR, and DNA sequencing (Eurofins MWG Operon, Huntsville, AL). DNA was purified using the QIAquick PCR Purification kit (Qiagen).

2.2.3 Protein extraction, SDS-PAGE and western blots

Protein extraction, purification and western blots were performed as described previously (Mitra et al., 2012). To extract and purify secreted proteins, mid-exponential phase (OD_{600}=0.5) cultures were centrifuged at 5,000 x *g* for 5 minutes and supernatants were passed through sterile 0.22 μm Millex-GV syringe filters (Millipore, Billerica, MA). Filtrates were precipitated overnight (18-20 h) in 15% (v/v) trichloroacetic acid at 4°C and then centrifuged at 15,000 x *g* for 30 minutes at 4°C. Protein pellets were washed twice with 100% ice cold acetone before re-

suspension in 1M triethyl ammonium bicarbonate (TEAB). The amount of protein loaded on SDS-PAGE gels for western blots was measured by a Bradford protein assay standard curve, and equal loading was validated by western blots for GroEL using anti-GroEL mAbs (Bio-Rad, Hercules, CA). Monoclonal antibodies against FLAG (Sigma-Aldrich) were also used. Each experiment was repeated a minimum of three times in independent trials. Densitometry was used to estimate differences in protein levels for select experiments using a ChemiDoc XRS+ Imaging System and Image Lab 3.0 (BioRad).

2.2.4 Proteomic analysis

Isobaric tag for relative and absolute quantitation (iTRAQ)-based mass spectrometry of strains TW14359 and Sakai followed a previously described protocol (Rivera et al., 2012). DMEM cultures (n=4 for cytosolic; n=3 for secreted) of TW14359 and Sakai were grown to OD_{600}=0.5 (2.5 to 3 h) before sampling for protein extraction (see above Methods). Peptide labeling with isobaric tags 114 and 116 (strain Sakai) and 115 and 117 (strain TW14359) for iTRAQ was performed using the iTRAQ™ Reagents 4-plex reaction kit (Applied Biosystems) following the manufacturer's instructions. Spectra data files (.RAW) were searched using Mascot Daemon ver. 2.3 against a Uniprot TW14359 protein database (http://www.uniprot.org/taxonomy/544404) downloaded on April 18th, 2011, containing 10,510 total sequences (forward and reverse) using the Mascot search algorithm (Matrix Science). Data analysis for proteomics experiments followed a previously described procedure (Rivera et al., 2012). Raw data files (.dat and .RAW) have been deposited in ProteomeXchange through the Proteomics Identification Database (PRIDE) (Vizcaino et al., 2009) (accession #PXD000023).

2.2.5 RNA purification and quantitative real-time PCR (qRT-PCR)

Primers for qRT-PCR are provided in Table S1. RNA purification, cDNA synthesis, qRT-PCR cycling conditions and data analysis followed previously described protocols (Riordan et al., 2010). For *ler* mRNA stability, cultures were growth to mid-exponential phase (OD_{600}=0.4) before addition of a sub-inhibitory concentration of the transcription inhibitor rifampin (300 µg/ml final). Sampling for RNA extraction was performed immediately before addition of rifampin (Rif), and at 4 min intervals thereafter for 12 min. qRT-PCR was performed using a Realplex2 Mastercycler (Eppendorf). Cycle threshold (C_t) data were normalized to *rrsA* (16S rRNA gene) and normalized cycle threshold values (ΔC_t) were transformed to arbitrary transcript expression levels using $2^{-\Delta Ct}/10^{-6}$ as described (Livak and Schmittgen, 2001; Riordan et al., 2010). Expression levels were compared using the appropriate t-test or by Tukey's HSD following a significant F-test ($n \geq 3$, α=0.05) (R. ver. 2.13.0).

2.2.6 Construction of *lacZ* transcriptional promoter fusions and β-galactosidase assays

The construction of *lacZ* reporter transcriptional fusions to the promoters of *ler*, *rcsB*, *rcsD*, and *flhD*, followed a previously described protocol using vector pRS551 (Simons et al., 1987). For ler_{P905}-*lacZ*, a 904-bp *BamH*I/*EcoR*I-digested PCR fragment generated using primers ler-905/EcoRI and ler-1/BamHI was cloned into similarly digested pRS551 using T4 DNA ligase (Fisher Scientific) to produce pRJM-2. Similarly, *rcsB*, *rcsD*, and *flhD* promoter fragments were cloned into pRS551 following *BamH*I/*EcoR*I digestion using primers rcsB-1/BamHI and rcsB-1000/EcoRI ($rcsB_{P1000}$-*lacZ*), rcsD-501/EcoRI and rcsD-1/BamHI ($rcsD_{P501}$-*lacZ*), and flhD-1/BamHI and flhD-1000/EcoRI ($flhD_{P1000}$-*lacZ*). *ler*-, *rcsB*-, *rcsD*-, and *flhD*- *lacZ* transcriptional fusion plasmids were transformed into WT and derivative backgrounds of strains

TW14359 and Sakai. All *lacZ* fusion constructs were confirmed by PCR and sequencing (Eurofins MWG Operon). β-galactosidase activity (Miller Units) was measured as previously described and compared between strains using a Student's t-test or by Tukey's HSD following a significant F-test ($n \geq 3$, $\alpha = 0.05$) (R) (Miller, 1972; Mitra et al., 2012).

2.2.7 Adherence assays

Adherence to epithelial cells was determined following the method of Abe et al. (Abe et al., 2002). Briefly, human HT-29 (ATCC HTB-38, Manassas, VA) colonic epithelial cells were grown to confluence on polylysine-treated glass coverslips placed within the wells of 24 well culture plates at 37°C with 5% CO_2. Overnight DMEM cultures were diluted 1:40 (v/v) in fresh DMEM and 0.05 ml of this dilution was used to inoculate each well which already contained 0.45 ml of sterile DMEM. Culture plates were then gently centrifuged (1000 x *g*) for 5 min and incubated as above. After 3 h, plate wells were washed five times with PBS (137 mM NaCl, 2.7 mM KCl, 10 mM Na_2HPO_4, pH 7) to remove non-adherent bacteria from the coverslips, and fresh DMEM was then added before incubating for an additional 3 h. Plate wells were subsequently washed three times in PBS, and then fixed with ice cold (−20°C) 100% methanol for 10 min before staining with Giemsa diluted in PBS 1:20 (v/v) for 20 min. Giemsa stain was aspirated from the wells, and each stained coverslip was then examined at 1000X magnification by oil immersion bright field microscopy using a binocular microscope (Fisher Scientific). Microcolonies, defined as a pattern of localized adherence (McKee and O'Brien, 1995; Nataro and Kaper, 1998), were scored as discrete clusters of five or more bacterial cells as previously defined (Abe et al., 2002; Iyoda and Watanabe, 2004). For each sample, a minimum of ten viewing frames were observed and the average number of microcolonies was reported per 80

HT-29 cells. Microcolony counts were compared between strains by Tukey's HSD following a significant F-test ($n \geq 3$, $\alpha=0.05$) (R).

2.2.8 Motility assays

Overnight LB cultures were diluted in fresh LB to $OD_{600}=0.5$ and 2 µl samples were inoculated onto LB plates containing 0.25% (w/v) agar following a previous method (Krin et al., 2010). Plates were incubated upright for 5 hours at 37°C before the diameter of lateral growth on the agar surface was examined for each strain. Experiments were repeated in multiple trials using at least three biological replicates per trial.

2.3 Results

2.3.1 The LEE expression phenotype of strain TW14359

Quantitative real-time PCR of LEE transcript levels revealed the upregulation of LEE regulatory (*ler*, 3.8-fold), structural (*espA*, 2.3-fold), effector (*tir*, 2.7-fold) and effector chaperone (*cesT*, 2.3-fold) genes in TW14359 when compared to strains Sakai and EDL933 during exponential growth ($OD_{600}=0.5$) ($p<0.05$) (**Fig. 8A**), consistent with studies of LEE expression in TW14359 grown in DMEM when co-cultured with bovine mammary epithelial (MAC-T) cells (Abu-Ali et al., 2010b). Although expression of the LEE activator gene *grlA* was elevated 1.6-fold in TW14359, levels did not differ significantly when compared to Sakai and EDL933. Transcript levels for all LEE genes did not differ between Sakai and EDL933. The expression of LEE genes decreased markedly in stationary phase ($OD_{600}=3.0$) for all strains and did not differ between them (**Fig. 8A**). This pattern of expression in DMEM is consistent with

previous observations of LEE gene expression during exponential and stationary growth phases in MOPS minimal media (Bergholz et al., 2007b).

Expression from the *ler* promoter, as measured by β-galactosidase activity from ler_{P903}-*lacZ*, increased in both the TW14359 and Sakai backgrounds during exponential growth, and decreased as cultures transitioned into stationary phase (**Fig. 8B**), in agreement with qRT-PCR data (**Fig. 8A**). In TW14359 however, *ler* expression was consistently and significantly higher than in Sakai ($p<0.05$) during mid-exponential growth (between 2 and 3 h growth, corresponding to OD_{600}=0.3 to 0.6), indicating that increased transcription was occurring at the *ler* promoter. Examination of DNA sequence for the *ler* ORF in TW14359 (ECSP_4703) and in Sakai (ECs4588), as well as *ler* core promoters P1 and P2 and 1,200-bp upstream of the translation initiation site revealed 100% nucleotide identity between these strains (NCBI). Adding to this, the stability of *ler* mRNA during exponential growth following treatment of cultures with rifampin did not differ between strains; the *ler* mRNA half-life being estimated at 2.0-min for TW14359 and 2.1-min for Sakai (**Fig. 9**), which is congruent with a previous estimate (Laaberki et al., 2006). It was therefore hypothesized that the LEE expression phenotype in TW14359 is directed through increased transcription from the *ler* promoter by the influence of some *trans*-acting factor(s) during exponential growth.

2.3.2 Role for RcsB in the LEE expression and adherence phenotype of strain TW14359

Quantitative analysis of the relative differences in protein levels using iTRAQ-based proteomics revealed a total of 116 proteins increased or decreased in abundance by at least 1.5-fold in TW14359 relative to strain Sakai during exponential growth (OD_{600}=0.5). In support of

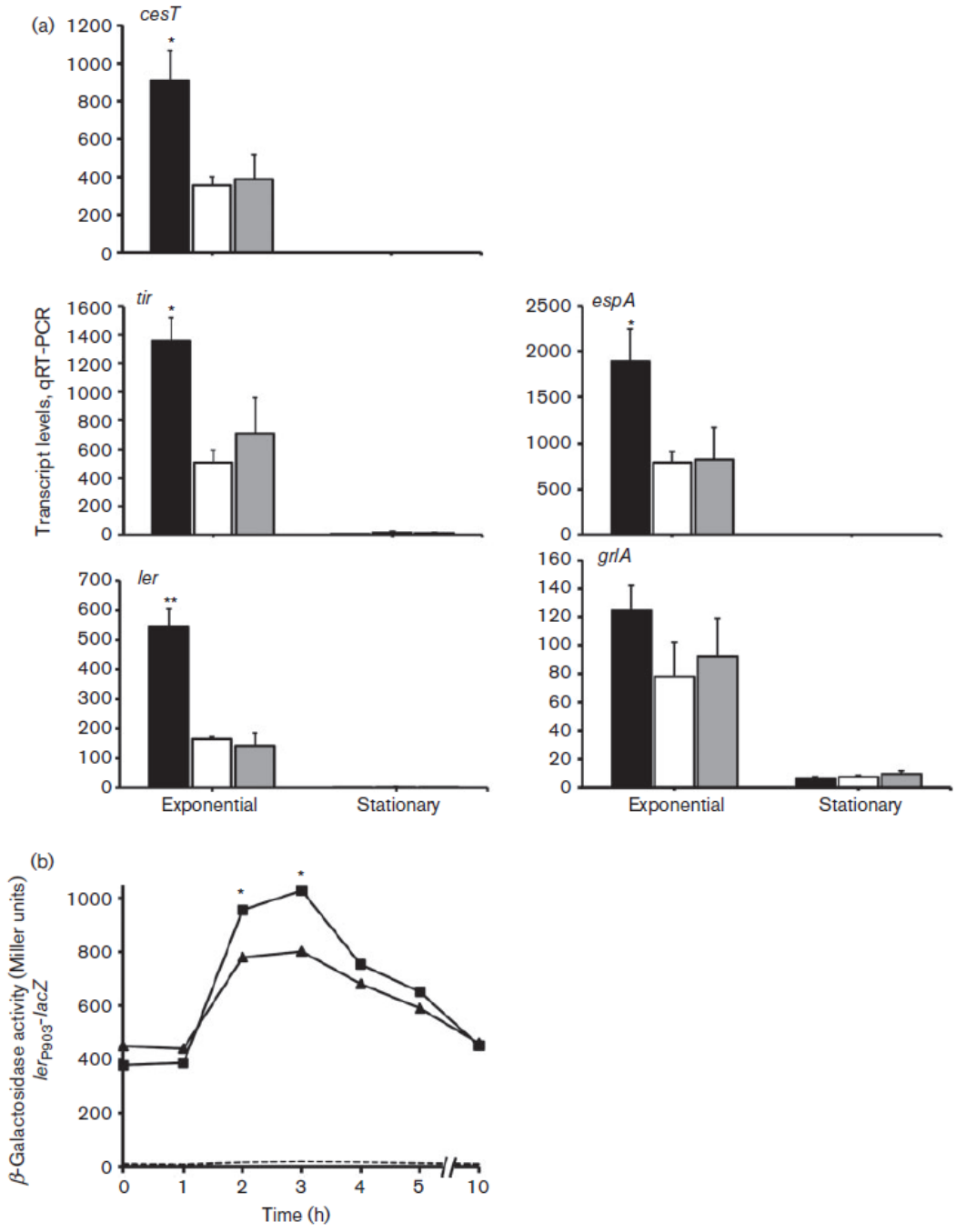

Figure 8 - The LEE expression phenotype of strain TW14359

(1A): Transcript levels for LEE genes are plotted for exponential (OD_{600}=0.5) and stationary (OD_{600}=3.0) phase DMEM cultures of strains TW14359 (filled), Sakai (empty) and EDL933 (grey). (1B): β-galactosidase activity in Miller Units for TW14359 (squares) and Sakai (triangles) containing a ler_{P903}-*lacZ* fusion plotted against time during growth in DMEM. TW14359 containing an empty vector (pRS551) control is denoted by the hatched line. Asterisks denote significant differences in transcript levels of TW14359 compared to other strains by Tukey's HSD following a significant F-test for 1A or Student's t-test for 1B ($p<0.05$ [*], $p<0.01$ [**], $n\geq3$). Error bars denote standard deviation.

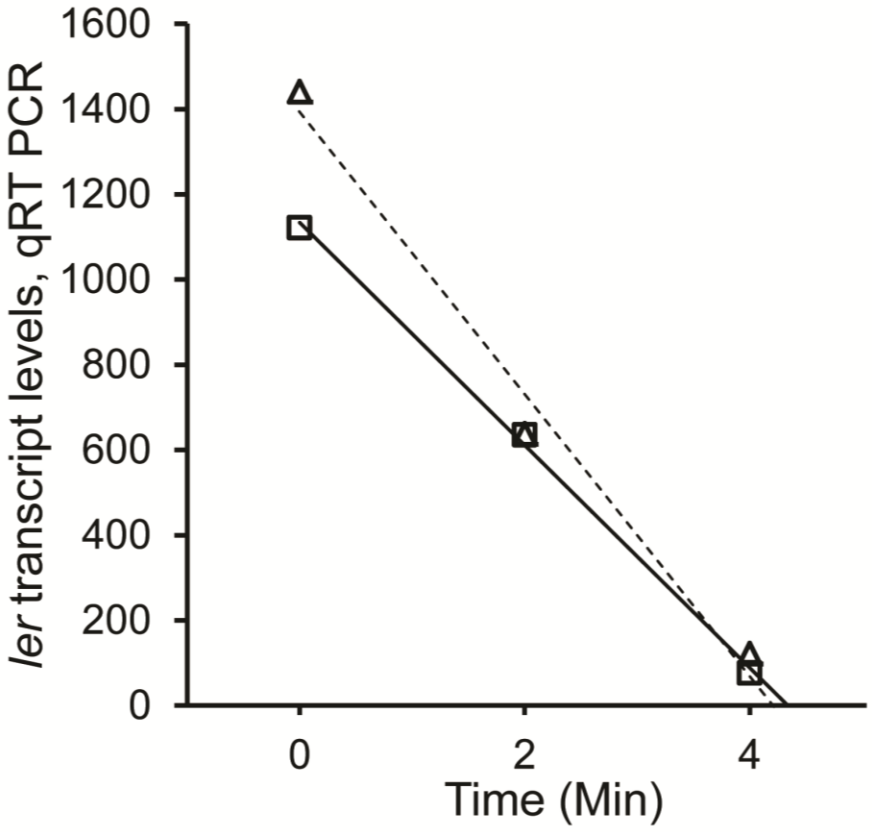

Figure 9 - qRT-PCR for *ler* mRNA stability in TW14359 and Sakai.
Stability of *ler* mRNA in EHEC strains TW14359 (dotted line) and Sakai (solid line) was determined for exponential phase (OD_{600}= 0.5) DMEM cultures at 0, 2, and 4 minutes following the addition of rifampin. Data represents the average of three independent experiments.

previous microarray studies, a number of LEE-encoded proteins were increased in both cytosolic and secreted protein fractions of TW14359 compared to Sakai, including the T3SS needle protein EscF (1.94-fold), the EspA chaperone, CesA (1.72-fold), the type II secretion system protein EtpG (2.06-fold), Ler (1.74-fold), the T3SS translocon apparatus proteins EspA (2.45-fold) and EspB (2.41-fold), the translocated intimin receptor Tir (1.56-fold), and other LEE-encoded proteins (**Table 1**). Also increased in TW14359 was the IIA subunit of Stx2 by 2.11-fold and RcsB (6.86-fold), the response regulator for a multi-component regulator of capsule synthesis (Rcs) phosphorelay system (**Table 1**). Importantly, when overexpressed, RcsB has been shown to activate *ler* transcription and increases adherence to Caco-2 cells (Tobe et al., 2005). It was thus of interest to determine whether the LEE expression and adherence phenotype of TW14359 was attributable to elevated levels of RcsB.

Western blots revealed that the basal level of RcsB in TW14359 was elevated ~2.7-fold when compared to Sakai, congruent with iTRAQ (**Fig. 10A**). In addition, expression of *rcsB* transcript was significantly higher in TW14359 compared to Sakai (p=0.001) (**Fig. 10B**), however, *rcsD*, which is transcribed as a dicistron with *rcsB* (i.e. *rcsDB*) from an upstream $rcsD_P$ promoter (Krin et al., 2010; Pescaretti Mde et al., 2009), was not altered in expression between strains (**Fig. 10B**). This suggests that basal levels of *rcsB* are intrinsically upregulated in TW14359 in a manner which is dependent on a promoter(s) that is intracistronic to *rcsD*. Consistent with a role for RcsB in the LEE expression phenotype of TW14359, *ler* transcript levels were higher in TW14359 than Sakai (p=0.017), but did not differ between TW14359Δ*rcsB* and SakaiΔ*rcsB* (**Fig. 11A**). Complementation of TW14359Δ*rcsB* and SakaiΔ*rcsB* with *rcsB* did not restore differential *ler* expression as observed for WT strains (**Fig. 11A**), supporting the hypothesis that the elevated basal expression of *rcsB* in TW14359 relative

Table 1 - Select list of proteins identified by iTRAQ proteomics

Protein Name[a]	Gene/ORF[a]	Fold change[b]	SD[c]
Intracellular			
DNA-binding response regulator for Rcs phosphorelay	*rcsB*	6.86	0.11
Protein-export protein secB	*secB*	2.93	1.99
Envelope stress induced periplasmic protein	*spy*	2.72	1.73
Conserved metal-binding protein	*yodA*	2.39	1.23
Predicted DNA-binding transcriptional regulator	*yheO*	2.14	1.61
Type II secretion protein	*etpG*	2.06	1.37
Predicted DNA-binding transcriptional regulator	*yhaJ*	2.00	1.43
Mannonate dehydratase	*uxuA*	1.99	0.94
Nucleoside (Except guanosine) transporter	*nupC*	1.98	1.26
Conserved protein	*ycaO*	1.98	1.58
LEE-encoded type III secretion system component	*escF*	1.94	0.98
Predicted chaperone	*yegD*	1.86	0.54
Aminoacyl-histidine dipeptidase (Peptidase D)	*pepD*	1.84	1.04
AMP nucleosidase	*amn*	1.81	0.90
Putative uncharacterized protein; homolog of pO157p81	ECSP_6104	1.78	0.67
Isoprenoid biosynthesis protein	*elbB*	1.76	0.54
Locus of enterocyte effacement (LEE)-encoded regulator	*ler*	1.74	0.70
Bifunctional nitric oxide dioxygenase	*hmp*	1.73	0.10
LEE-encoded chaperone	*cesA*	1.72	0.69
Putative cytoplasmic membrane export protein	ECSP_0558	1.71	0.31
Selenide, water dikinase	*selD*	1.67	0.98
Protein assembly complex, lipoprotein component	*yfgL*	1.65	0.83
Malic enzyme predicted oxidoreductase	*maeB*	1.65	0.61
Colicin resistance and tellurite resistance protein	*terE*	1.64	0.76
Ferrichrome outer membrane transporter	*fhuA*	1.64	0.15
3-methyl-2-oxobutanoate hydroxymethyltransferase	*panB*	1.63	0.42

[a] Protein/gene names and open reading frame (ORF) IDs based on EHEC strain TW14359 (accession NC_013008, NCBI) and K-12 strain MG1655 (EcoCyc, REF).

[b] Mean fold change in protein level as determined by iTRAQ MS for strain TW14359 relative to Sakai.

[c] Standard deviation (SD) of the mean fold change.

Table 1 - Select list of proteins identified by iTRAQ proteomics, continued.

Protein Name[a]	Gene/ORF[a]	Fold change[b]	SD[c]
10 kDa chaperonin	*groS*	4.57	2.92
Stress protein, member of the CspA-family	*cspC*	4.53	3.24
Osmotically inducible, stress-inducible membrane protein	*osmC*	4.42	3.83
Conserved protein	*yifE*	4.35	2.52
Phosphohistidinoprotein-hexose phosphotransferase	*ptsH*	4.34	3.07
30S ribosomal subunit protein S1	*rpsA*	4.08	1.96
Conserved metal-binding protein	*yodA*	4.05	1.31
Component of a tripartite ferrous iron transporter	*efeO*	3.93	1.05
Glycine cleavage system H protein	*gcvH*	3.80	2.02
50S ribosomal protein L24	*rplX*	3.71	1.73
Periplasmic chaperone	*hlpA*	3.70	0.85
Scaffold protein	*iscU*	3.64	1.79
Phosphate transporter subunit	*pstS*	3.61	3.59
30S ribosomal protein S14	*rpsN*	3.55	2.53
Glutaredoxin 3	*grxC*	3.51	2.27
50S ribosomal protein L9	*rplI*	3.38	1.73
tetrahydrodipicolinate succinylase subunit	*dapD*	3.29	0.72
Peptidyl-prolyl cis-trans isomerase (PPIase)	*surA*	3.26	0.74
High-affinity zinc uptake system periplasmic protein	*znuA*	3.18	0.88
Thioredoxin 1	*trxA*	3.12	1.59
Ecotin	*eco*	2.70	0.74
LEE-encoded type III secreted effector	*espF*	2.66	0.65
Ribosome-recycling factor	*frr*	2.62	0.51
Heme oxygenase	*chuS*	2.59	0.43
Periplasmic protein	*osmY*	2.58	0.70
DnaK suppressor protein	*dksA*	2.52	0.75
Secreted protein EspA	*espA*	2.45	1.98
Secreted protein EspB	*espB*	2.41	2.04
Catalase-peroxidase 2	*katP*	2.38	2.39
Conserved protein	*yebT*	2.31	2.74

[a] Protein/gene names and open reading frame (ORF) IDs based on EHEC strain TW14359 (accession NC_013008, NCBI) and K-12 strain MG1655 (EcoCyc, REF).

[b] Mean fold change in protein level as determined by iTRAQ MS for strain TW14359 relative to Sakai.

[c] Standard deviation (SD) of the mean fold change.

Table 1 - Select list of proteins identified by iTRAQ proteomics, continued.

Protein Name[a]	Gene/ORF[a]	Fold change[b]	SD[c]
Glucose-specific enzyme IIA component of PTS	*crr*	2.26	1.16
Protein grpE	*grpE*	2.18	0.90
Serine endoprotease (Protease Do), membrane-associated	*degP*	2.13	0.14
Shiga toxin II subunit A	*stx2A*	2.11	1.51
Protein TolB	*tolB*	2.09	0.13
Porphobilinogen deaminase	*hemC*	2.03	0.38
Alkyl hydroperoxide reductase, C22 subunit	*ahpC*	2.00	1.10
DNA-binding transcriptional repressor	*cspE*	1.91	1.30
Thiol:disulfide interchange protein DsbA	*dsbA*	1.82	0.56
Chaperone Hsp70, co-chaperone with DnaJ	*dnaK*	1.80	0.31
Putative uncharacterized protein	ECSP_3241	1.79	0.48
Carbon storage regulator	*csrA*	1.79	1.39
50S ribosomal protein L23	*rplW*	1.70	1.13
Predicted uncharacterized protein	ECSP_0343	1.66	1.03
Adenylate kinase	*adk*	1.65	0.43
Glutamine synthetase	*glnA*	1.56	0.26
Translocated intimin receptor protein	*tir*	1.56	1.20
60 kDa chaperonin	*groL*	1.55	1.49
Thiosulfate:cyanide sulfurtransferase (Rhodanese)	*pspE*	1.54	0.36
Sorbitol-6-phosphate dehydrogenase	*srlD*	-1.50	0.02
Putative exoprotein-precursor	*espP*	-1.50	0.68
F9 fimbriae chaperone	*fmlB*	-1.53	0.17
Molybdate transporter subunit	*modA*	-1.66	0.69
Hydrogenase 2, large subunit	*hybC*	-1.72	0.25
Cystine transporter subunit	*fliY*	-1.78	0.75
Predicted protein; homolog of VT2-Sap55 in Sakai	ECSP_3238	-2.04	0.14
D-ribose transporter subunit	*rbsB*	-3.21	0.06
L-rhamnose isomerase	*rhaA*	-3.44	0.01
Oligopeptide transporter subunit	*oppA*	-3.49	0.21
Putative uncharacterized prophage protein	ECSP_2949	-4.21	0.21
Predicted protein	ECSP_5384	-6.07	0.22

[a] Protein/gene names and open reading frame (ORF) IDs based on EHEC strain TW14359 (accession NC_013008, NCBI) and K-12 strain MG1655 (EcoCyc, REF).

[b] Mean fold change in protein level as determined by iTRAQ MS for strain TW14359 relative to Sakai.

[c] Standard deviation (SD) of the mean fold change.

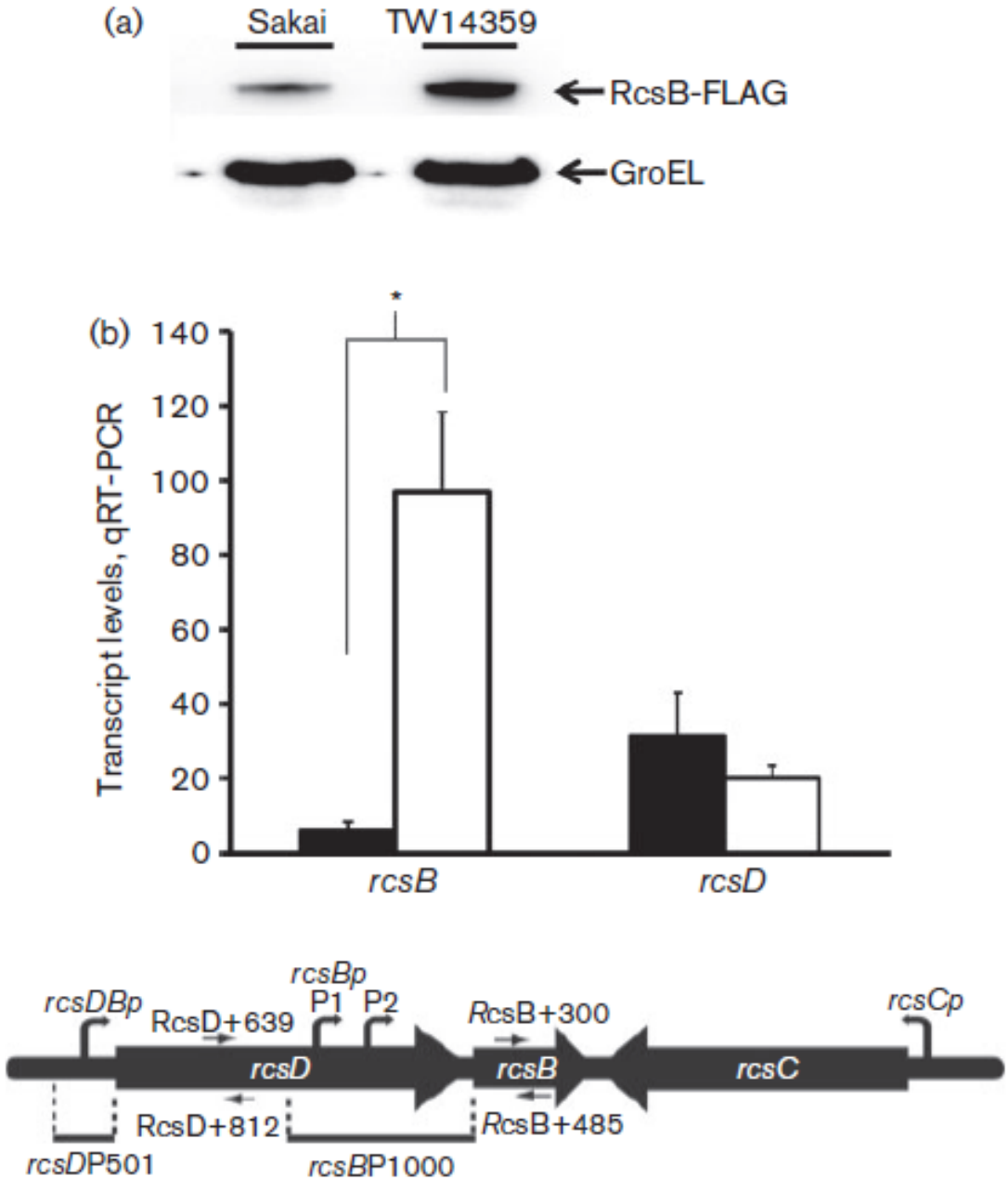

Figure 10 - *rcsB* expression in Sakai and TW14359.
(2A): Representative western blot for FLAG-tagged RcsB in strains Sakai and TW14359 grown in DMEM (OD_{600}=0.5). Equal loading was controlled for by westerns for GroEL. (2B, top): Transcript levels of *rcsB* and *rcsD* plotted for Sakai (filled) and TW14359 (empty) grown in DMEM. The asterisk denotes significant differences between strains by Student's t-test (p=0.001, n≥3). Error bars denote standard deviation. (2B, bottom): Graphic depicts the *rcsDB* and *rcsC* open reading frames with their respective promoters, the location of qRT-PCR priming sites, and the location of amplified promoter *lacZ* fusion fragments for *rcsD* and *rcsD* in pRS551.

to Sakai is responsible for the LEE expression phenotype. The fact that *ler* transcript levels were higher in *rcsB* complement strains relative to WT (**Fig. 11A**), likely reflects expression from pACYC177. Although this plasmid is low-copy, *rcsB* transcript levels were still 20-fold higher in complement strains compared to WT (data not shown). In strain Sakai, the activation of *ler* by *rcsB* overexpression *in-trans* requires an intact global regulator of virulence (*grvA*) gene, the product of which activates transcription from the *LEE1* promoter (Tobe et al., 2005). As such, this study sought to determine if in TW14359, which intrinsically overexpresses *rcsB*, *ler* activation also required *grvA*, or if activation was through a different pathway. Deletion of *grvA* reduced *ler* expression to the same extent as observed for TW14359Δ*rcsB* when compared to TW14359 (**Fig. 11B**) ($p<0.05$). Moreover, deletion of *grvA* in TW14359Δ*rcsB* did not further significantly alter *ler* expression when compared to TW14359Δ*rcsB* or TW14359Δ*grvA*. The expression of *ler* was however slightly, but significantly higher in the TW14359Δ*rcsB*Δ*grvA* backgrounds when compared to Sakai ($p<0.05$). Therefore, increased basal expression of *rcsB* in TW14359 and interaction with *grvA* is required for the LEE expression phenotype of this strain.

This study further ascertained the contribution of intrinsic *rcsB* overexpression to the TW14359 adherence phenotype using the human colonic cell line HT-29. As observed for bovine MAC-T cells (Abu-Ali et al., 2010a), adherence to HT-29 cells, as measured by microcolony formation, was significantly higher for TW14359 than Sakai ($p=0.006$) (**Fig. 11C**). Consistent with *ler* expression data, adherence did not differ between Sakai and Sakai Δ*rcsB*, but was reduced in TW1359Δ*rcsB* to a level comparable to Sakai and Sakai Δ*rcsB*. As anticipated, the adherence of T3SS-deficient TW14359Δ*escN* and Sakai Δ*escN* strains to HT-29 cells was significantly reduced when compared to WT and *rcsB* isogenic backgrounds ($p<0.05$), but not between *escN* isogenic strains (**Fig. 11C**), indicating that the adherence phenotype of TW14359 is dependent

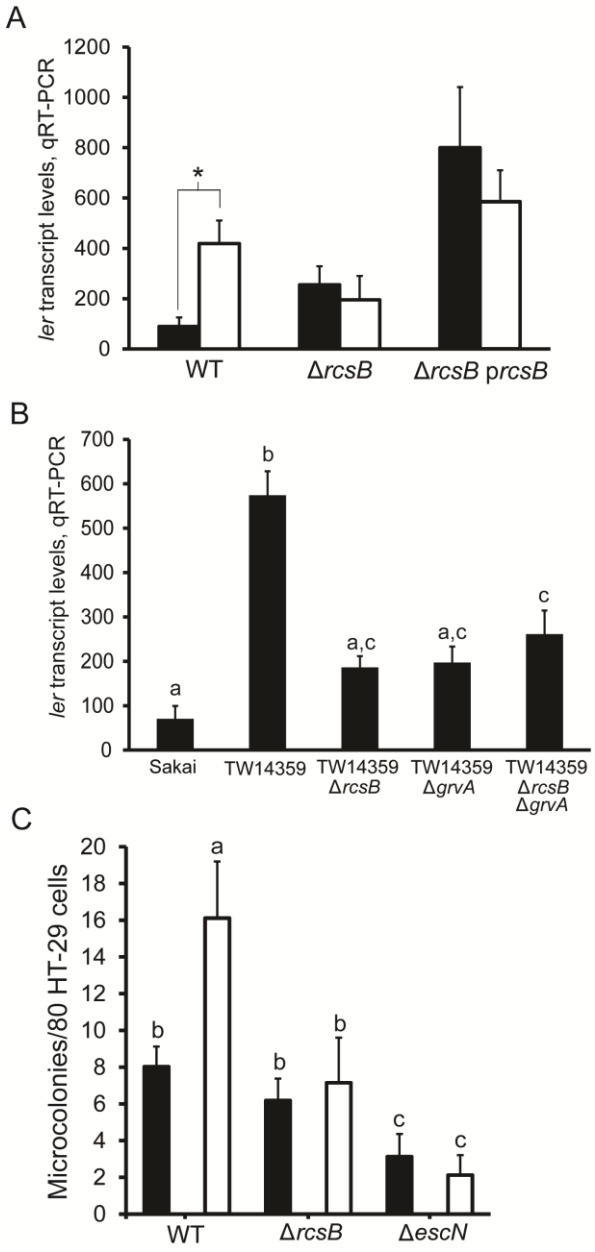

Figure 11 - *rcsB, grvA* and the LEE expression and adherence phenotype of TW14359.
(3A): *ler* transcript levels plotted for WT, Δ*rcsB* , and complement Δ*rcsB* p*rcsB* versions of Sakai (solid) and TW14359 (empty) grown in DMEM (OD_{600}=0.5). (3B): *ler* transcript levels plotted for WT strains and mutant derivative strains of TW14359 during growth in DMEM. (3C): Adherence to HT-29 cells as measured by microcolony formation plotted for WT, Δ*rcsB* and Δ*escN* versions of Sakai (solid) and TW14359 (empty). For 3A, the asterisk denotes a significant difference between Sakai and TW14359 by Student's t-test ($p=0.017$, $n\geq3$). For 3B and 3C, plots which differ by lower case letter, differ significantly by Tukey's HSD following a significant F-test ($p<0.05$, $n\geq3$). Error bars denote standard deviation for all panels.

on intrinsic *rcsB* upregulation, as well as a functional T3SS.

2.3.3 Control of *rcsB* by the LEE-encoded regulator GrlA, and GrlA-RcsB dependent repression of motility

In TW14359, genes associated with motility, including structural and regulatory genes for flagellar biosynthesis (*flg* and *fli* genes), and chemotaxis (*cheB*, *tsr* and *tar*) are reduced in expression compared to Sakai (Abe et al., 2002; Abu-Ali et al., 2010a). In the present study, this has been observed to correspond with a 30-40% reduction in the lateral growth of TW14359 on motility plates relative to Sakai (**Fig. 12A**). Importantly, both RcsB and LEE-encoded activator GrlA are known to negatively regulate motility (Francez-Charlot et al., 2003; Iyoda et al., 2006), and both are increased in expression in TW14359. It was therefore of interest to investigate the potential genetic interaction of *rcsB* and *grlA*, and their contribution to the regulation of motility in TW14359.

As expected, deletion of *rcsB* in TW14359 enhanced the lateral growth of TW14359 on motility plates by 30-40% (**Fig. 13A**), suggesting that the motility deficiency of TW14359 when compared to Sakai is connected to intrinsic *rcsB* overexpression. Also, the inactivation of *grlR* (strain TW14359*grlR*::*kan*) leading to *grlA* overexpression (**Fig. 12**) (Iyoda et al., 2006), substantially impaired lateral growth on motility plates (**Fig. 13A**). Most importantly, deletion of *rcsB* in the TW14359*grlR*::*kan* background restored lateral growth on motility plates to the level observed for TW14359Δ*rcsB*, revealing that the control of motility by *grlA* is epistatic to *rcsB*. Negative regulation of motility by RcsB has been shown to result from direct transcriptional repression of the global regulator of motility genes *flhDC* (Francez-Charlot et al., 2003). Consistent with this, expression from the $flhD_P$ promoter, as measured by β-galactosidase

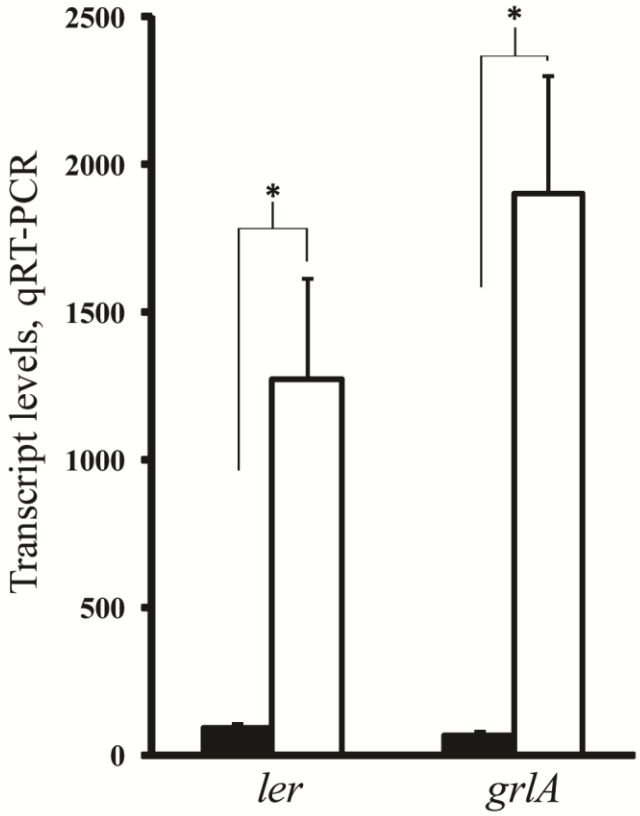

Figure 12 - qRT-PCR for *ler* and *grlA* mRNA in TW14359 and TW14359*grlR*::*kan*.
TW14359 and TW14359*grlR*::*kan* grown to mid-logarithmic phase (OD_{600}=0.5) in LB. The asterisks denotes significance by a Student's t-test ($p<0.05$, $n\geq3$). Error bars indicate standard deviation for both plots.

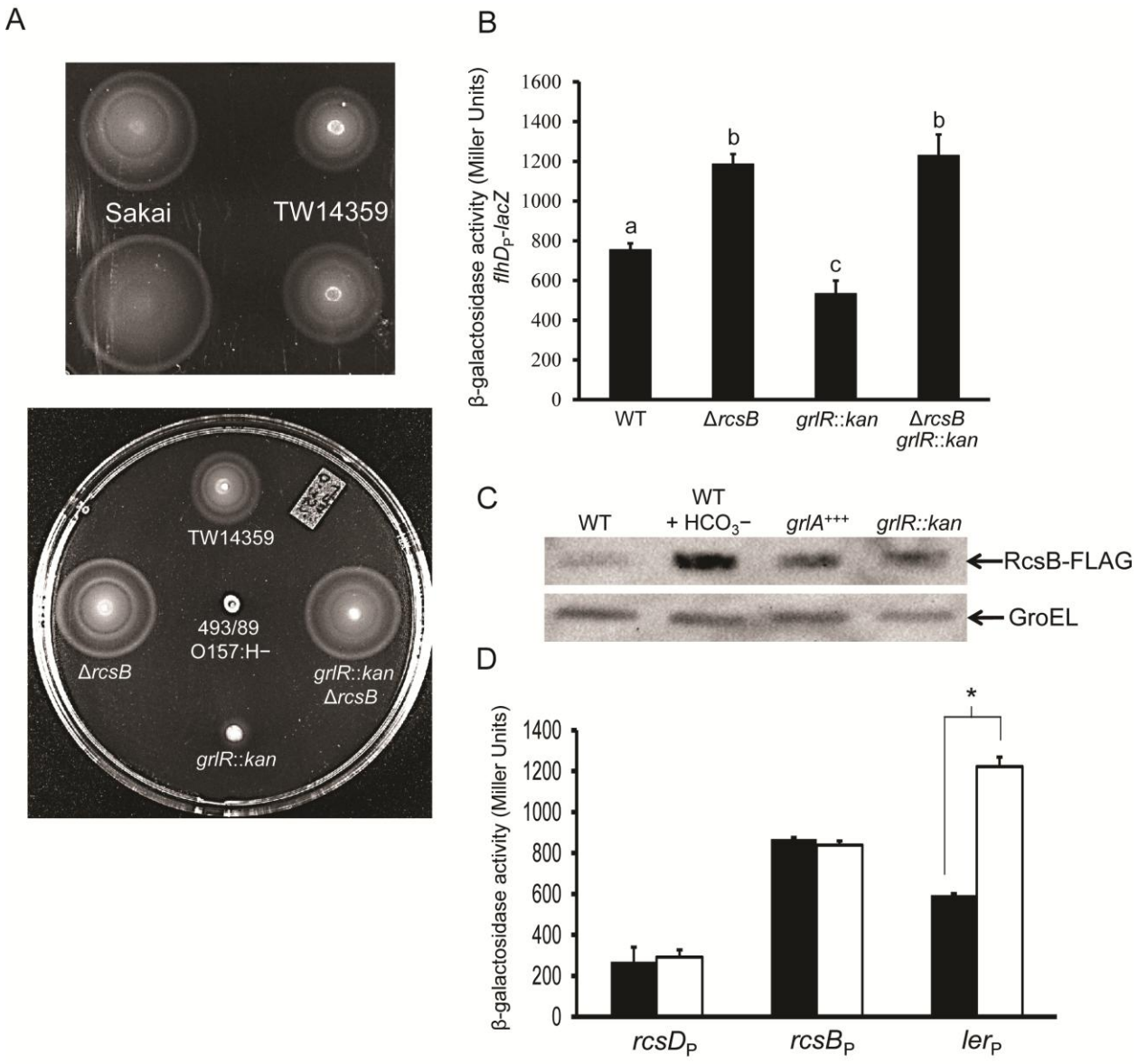

Figure 13 - GrlA-RcsB dependent repression of motility.
(4A): Motility as measured by lateral growth on representative motility plates for Sakai and TW14359 (top), and mutant derivatives of TW14359 (bottom); EHEC O157:H− strain 493/89 is included as a non-motile control. (4B): β-galactosidase activity in Miller Units for TW14359 and mutant derivatives containing an *fhlD*$_{P1000}$-*lacZ* fusion during growth in DMEM. (4C): Representative western blot for FLAG-tagged RcsB in LB plotted for TW14359 (WT) with and without 44 mM HCO_3−, and for *grlA* overexpression strains of TW14359 (*grlA*$^{+++}$ and *grlR*::*kan*). Equal loading was controlled for by westerns for GroEL. (4D): β-galactosidase activity in Miller Units plotted for TW14359 (filled) and TW14359*grlR*::*kan* (empty) grown in LB and containing *rcsD*$_{P501}$-*lacZ*, *rcsB*$_{P1000}$-*lacZ*, or *ler*$_{P903}$-*lacZ* fusions. For 4B, plots which differ by lower case letter, differ significantly by Tukey's HSD following a significant F-test ($p<0.05$, $n\geq3$). For 4D, the asterisk denotes significance by a Student's t-test ($p=0.010$, $n\geq3$). Error bars indicate standard deviation for all panels.

activity from *flhD*$_{P1000}$-*lacZ*, was significantly increased in TW14359Δ*rcsB*, but decreased in TW14359*grlR*::*kan* when compared to WT ($p<0.05$) (**Fig. 13B**). *flhD*$_P$ promoter expression did not differ however between TW14359*grlR*::*kan*Δ*rcsB* and TW14359Δ*rcsB* indicating that RcsB-dependent repression of *flhDC* and motility is positively regulated by GrlA. In further support of this, levels of RcsB were increased (~2.4-fold) in TW14359*grlR*::*kan* and in a *grlA* overexpression strain compared to WT (**Fig. 13C**). Interestingly however, expression from *rcsD*$_P$ or *rcsB*$_P$ promoters was not observed to be altered in TW14359*grlR*::*kan* (**Fig. 13D**), indicating that control of RcsB by GrlA is at the post-transcriptional level; increased expression from the *ler*$_P$ promoter was included as a positive control for *grlA* overexpression. Collectively, these experiments reveal a reciprocating regulatory mechanism in which RcsB and LEE-encoded GrlA coordinate LEE activation with repression of *flhDC* and motility.

2.3.4 Role for Rcs phosphorelay and *grvA* in bicarbonate-dependent activation of the LEE

In the preceding experiments the addition of bicarbonate to TW14359 cultures growing in LB, and added as a positive control for LEE stimulation (Abe et al., 2002), was also observed to increase RcsB levels ~5.4-fold (**Fig. 13C**). The bicarbonate ion (HCO_3^-) has been shown to activate LEE expression and adherence in a dose-dependent manner in EHEC (Abe et al., 2002). This has been reported to be through increased transcription from the *grlRA* promoter in *C. rodentium* (Tauschek et al., 2010), however the mechanism by which bicarbonate stimulates LEE expression in EHEC is unknown. In this study, the increase in RcsB levels with bicarbonate was higher than that observed for *grlA* overexpression strains (**Fig. 13C**), suggesting that this added bicarbonate stimulation of RcsB was, at least in part, independent of *grlA*. It was therefore predicted that the Rcs phosphorelay system was in some way involved in bicarbonate-directed

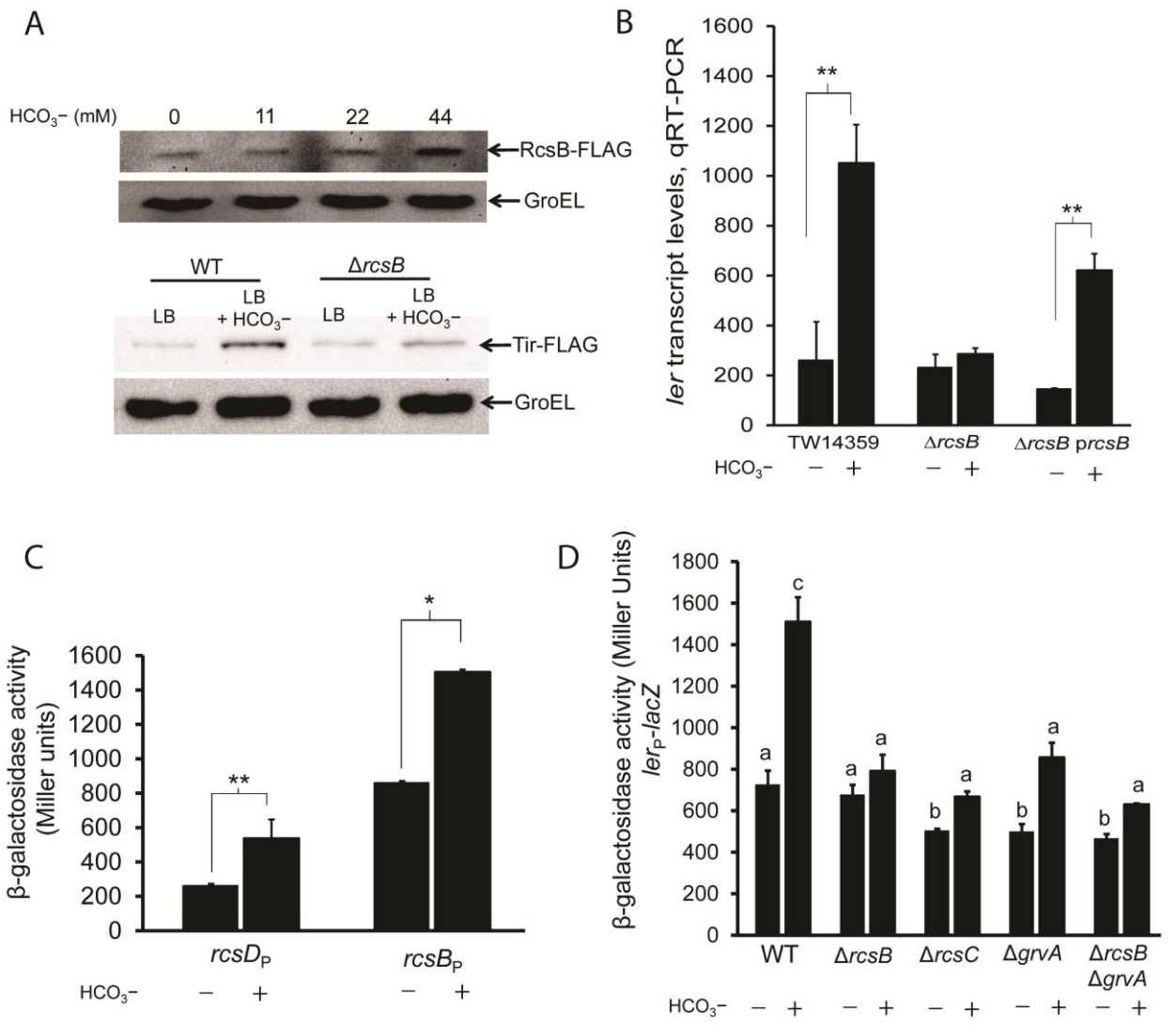

Figure 14 - Effect of bicarbonate on RcsB, and *rcsB*-dependent LEE activation.
(5A): Representative western blot for FLAG-tagged RcsB as a function of increasing bicarbonate (HCO_3^-) molarity (mM) (top), and for FLAG-tagged Tir in TW14359 and TW14359Δ*rcsB* grown in LB or LB with 44 mM HCO_3^- (OD_{600}=0.5) (bottom). Equal loading was controlled for by westerns for GroEL. (4B): *ler* transcript levels plotted for TW14359, TW14359Δ*rcsB*, and complement TW14359Δ*rcsB*p*rcsB* strains grown in LB (−) or LB with 44 mM HCO_3^- (+) (OD_{600}=0.5). (4C): β-galactosidase activity in Miller Units plotted for TW14359 and TW14359 containing $rcsD_{P501}$-*lacZ* or $rcsB_{P1000}$-*lacZ* fusions grown in LB (−) or LB with 44 mM HCO_3^- (+). (4D): β-galactosidase activity in Miller Units plotted for TW14359 (WT) and mutant derivative strains containing ler_{P903}-*lacZ* and grown in LB (−) or LB with 44 mM HCO_3^- (+). For 5B and 5C, the asterisks denote a significant difference between treatments by Student's t-test ($p<0.05$ [*], $p<0.01$ [**], $n\geq3$). For 5D, plots which differ by lower case letter differ significantly by Tukey's HSD following a significant F-test ($p<0.05$, $n\geq3$). Error bars denote standard deviation for all panels.

activation of LEE expression. In agreement with the dose-dependence of bicarbonate for LEE stimulation, the addition of bicarbonate up to 44 mM (a physiologically relevant molarity) (Feldman, 1983) to LB was observed to incrementally increase RcsB levels (**Fig. 14A**). *rcsB* was shown to be required for full activation of LEE expression in response to bicarbonate, as the levels of Tir protein were increased substantially in TW14359 grown with bicarbonate, but only marginally increased in the TW14359Δ*rcsB* background (**Fig. 14A**). In addition, growth with bicarbonate increased *ler* transcript levels 5-fold in the WT ($p=0.001$) compared to only 1.24-fold in TW14359Δ*rcsB* (**Fig. 14B**). Bicarbonate stimulation of *ler* was restored in complement strain TW14359Δ*rcsB* p*rcsB*.

Expression from both $rcsD_P$ and $rcsB_P$ promoters was significantly increased in the presence of bicarbonate ($p<0.05$) (**Fig. 14C**), revealing that bicarbonate is stimulating transcription of *rcsDB* from the $rcsD_P$ promoter, as well as *rcsB* alone from at least one of two mapped promoters intracistronic to *rcsD*. Expression from the ler_P promoter was expectedly increased with bicarbonate addition for TW14359 ($p<0.05$), but not for TW14359Δ*rcsB* (**Fig. 14D**). In addition, deletion of the Rcs phosphorelay sensor kinase *rcsC* significantly reduced bicarbonate stimulation of ler_P promoter activity compared to WT ($p<0.05$). And consistent with an RcsB-GrvA dependent pathway of LEE activation, ler_P promoter expression with bicarbonate addition was reduced in TW14359Δ*grvA* and TW14359Δ*rcsB*Δ*grvA* when compared to WT ($p<0.05$), but not compared to TW14359Δ*rcsB* or TW14359Δ*rcsC* (**Fig. 14D**). Collectively, this reveals that bicarbonate-dependent stimulation of LEE expression in EHEC is at least partly dependent on components of the Rcs phosphorelay system, and on the RcsB-GrvA pathway of LEE activation.

2.4 Discussion

It is predicted that *rcsB*, encoding the response regulator of the Rcs system, is intrinsically upregulated in TW14359, and that this is responsible for the enhanced LEE expression and adherence phenotype of this strain. It is not yet clear why *rcsB* is upregulated in TW14359. *rcsB* is co-transcribed as the second gene of a dicistron with *rcsD* (Krin et al., 2010) and yet *rcsD* transcript levels by qRT-PCR (**Fig. 10**) and protein levels by iTRAQ proteomics did not differ in TW14359 when compared to Sakai. This is consistent with the observation that *rcsB* overexpression can upregulate the LEE independent of *rcsD* (Tobe et al., 2005). Alternatively, *rcsB* can be expressed as a monocistron from at least two promoters which are intracistronic to *rcsD* (i.e. $rcsB_{P1}$ and $rcsB_{P2}$) (Krin et al., 2010), but upstream of the priming sites used for qRT-PCR in this study. Since there are no differences in the sequence of these promoters between TW14359 and Sakai, it is predicted that intrinsic upregulation of *rcsB* is therefore dependent on some *trans*-factor(s) acting on the $rcsB_{P1}$ and/or $rcsB_{P2}$ promoters. Unfortunately, how these promoters are expressed and regulated is unknown, and needs to be further examined. A genetic polymorphism unique to strain TW14359 was initially hypothesized in this study to be important for the *rcsB* expression phenotype of this strain. Kulasekara et al. (Kulasekara et al., 2009) had described a 90-bp insertion in the ORF of *tolA*, the product of which is an inner membrane component of the Tol-Pal envelope complex involved in maintaining cell envelope integrity (Bernadac et al., 1998; Cascales et al., 2000). Importantly, mutations in *tolA* have been reported to substantially upregulate *rcsB* (Clavel et al., 1996). Indeed, *rcsB* expression in strains TW14359*tolA*::*kan* and Sakai*tolA*::*kan* was increased compared to their WT counterparts. However, the level of *rcsB* transcript was still proportionately increased in TW14359*tolA*::*kan* relative to Sakai*tolA*::*kan* ($p=0.016$), suggesting

that the *tolA* polymorphism is not responsible for increased basal expression of *rcsB* in TW14359.

The results also indicated that deletion of *rcsB* had no effect on *ler* expression or HT-29 adherence in strain Sakai. This latter finding is inconsistent with a study demonstrating that both the overexpression and deletion of *rcsB* in Sakai can lead to increased LEE expression and adherence through independent regulatory pathways: RcsB was predicated to upregulate the LEE through activation of *grvA*, and downregulate LEE expression through repression of *pchA*, a positive regulator of the LEE (Tobe et al., 2005). The reason for this disparity in results is not yet known. However, the direction and magnitude at which RcsB regulates LEE expression is likely to be sensitive to differences in growth phase, nutrient availability, as well as signals which activate Rcs phosphorelay. In this study, the influence of RcsB on *ler* expression was only examined in mid-exponential cultures (OD_{600}=0.5), and may differ substantially with even a subtle change in the phase of growth or experimental condition. For example, in Tobe et al (Tobe et al., 2005) Caco-2 cells were used for adherence studies, whereas this study utilized HT-29 cells.

The RcsB-dependent LEE expression phenotype of strain TW14359 was further shown to require an intact global regulator of virulence *grvA* gene. The mechanism by which RcsB controls *grvA*, and how RcsB-GrvA regulate *ler* is unknown. Tobe et al. (Tobe et al., 2005) observed increased expression of *grvA* in response to *rcsB* overexpression and described RcsB boxes in the predicted *grvA* promoter region with some homology to the RcsB consensus (Wehland and Bernhard, 2000), suggesting direct regulation of *grvA* transcription. Alternatively, RcsB may interact with GrvA to directly activate the expression of *ler* and other genes. There is precedent for this, as RcsB has been shown to regulate transcription as a heterodimer with RcsA

(Francez-Charlot et al., 2003; Stout et al., 1991), GadE (Castanie-Cornet et al., 2010), and BglJ (Venkatesh et al., 2010). If RcsB-GrvA activate *ler* transcription as a heterodimer, they likely bind upstream of the core promoter region (i.e. upstream of -35) as is typical for RcsB promoter activation (Boulanger et al., 2005; Castanie-Cornet et al., 2010; Sturny et al., 2003; Venkatesh et al., 2010). However, there is no RcsB binding site upstream of and including the *ler* P1 and P2 promoters.

The results of this study suggest that RcsB is involved in the inverse regulation of genes that control motility (i.e. *flhDC*) and those for intimate colonization (i.e. the LEE) in EHEC. This opposing relationship between colonization and motility may be important for the establishment of *E. coli* in the gut. For example, constitutive expression of FlhDC regulon in EHEC markedly reduced adherence to HeLa cells (Iyoda et al., 2006), whereas the deletion of *flhDC* and lack of motility in K12 increased colonization in a murine model (Gauger et al., 2007; Leatham et al., 2005). It is important to note however that FlhDC also controls the expression of genes which serve no direct role in motility but which could contribute in some way to colonization. In EHEC, the LEE encoded activator GrlA indirectly downregulates transcription of *flhDC* leading to reduced motility (Iyoda et al., 2006). This study has revealed that mutation of *rcsB* masks the negative regulatory effect of GrlA on motility and *flhDC* transcription, and that the overexpression of *grlA* increases RcsB levels. This suggests that RcsB and GrvA are members of a reciprocating regulatory mechanism in EHEC which, at a minimum, coordinates the upregulation of LEE genes with a downregulation of the *flhDC* flagellar regulon. Activation of RcsB by GrlA appears to be at the post-transcriptional level, as increased protein levels did not correspond with increased transcription from promoters driving expression of *rcsDB* or *rcsB*.

In EHEC, bicarbonate has been shown to stimulate LEE transcription through *ler*, and to increase adherence to Caco-2 cells in a pH-independent manner (Abe et al., 2002). It has been hypothesized that bicarbonate produced naturally in the small bowel to neutralize gastric acid may serve as a biological cue for T3SS-dependent colonization (Abe et al., 1997; Abe et al., 2002). In *C. rodentium* bicarbonate interacts with the AraC-type regulator RegA to directly upregulate *grlA* expression (Tauschek et al., 2010). In EHEC and EPEC however, there are no homologs of RegA, and the genetic determinant(s) which regulate bicarbonate-dependent induction of the LEE in these pathogens is unknown. This study has shown that Rcs phosphorelay components RcsB and RcsC and the global regulator of virulence GrvA are required for full stimulation of the LEE in response to bicarbonate in EHEC. Despite the interplay of GrlA and RcsB in the control of *flhDC* and motility, there is no evidence that *grlA* is important for bicarbonate dependent LEE expression through this pathway. For instance, overexpression of *grlA* did not increase *rcsB* transcription, whereas bicarbonate addition did enhance *rcsB* transcription (Figs. **13D** and **14C**). Furthermore, the level of RcsB induction was markedly higher in WT cells grown with bicarbonate than in strains which overexpress *grlA* alone (**Fig. 13C**). Therefore in EHEC it is predicted that bicarbonate stimulates LEE expression through an RcsB-GrvA-Ler activation pathway.

To conclude, the LEE expression phenotype of TW14359 is hypothesized to result from intrinsically increased basal levels of the response regulator RcsB, activating LEE expression through a GrvA-Ler pathway. In addition, increased adherence of strain TW14359 to intestinal cells was shown to be dependent on elevated *rcsB* expression and a functional T3SS. Whether or not this dysregulated pathway is responsible for the severe disease attributed to infections with this strain is not yet clear. Furthermore, the LEE-encoded activator GrlA was determined to

require *rcsB* for repression of the *flhDC* flagellar regulon, suggesting that GrlA and RcsB work together to coordinate the activation of genes for colonization with the repression of genes for motility. Finally, bicarbonate was proposed to be a physiological signal for an Rcs phosphorelay- and GrvA-directed pathway activating LEE expression and colonization in EHEC.

2.5 Acknowledgments

The authors thank Sergio Uzzau (University of Sassari, Italy) for kindly providing vector pSA312 for FLAG fusion construction, Edward G. Dudley (Pennsylvania State University) for providing vector pRS551 for lacZ fusions, and Robert Buzzeo (University of South Florida) for technical assistance with adherence assays. We also thank the University of South Florida Center for Drug Discovery and Innovation (CDDI) for technical assistance with proteomics and mass spectrometry.

Table 2 - Strains and plasmids used in Chapter 2

Strain/plasmid	Relevant characteristics	Reference	Nucleotide[a] Position
Strain name:			
DH5α	Vector propagation, *rec*A1 *end*A1		
Sakai	WT 1996 outbreak, Osaka Japan	Michino, 1999	
TW14359	WT 2006 outbreak, western U.S.A.	Manning, 2008	
EDL933	WT 1982 outbreak, MI and OR, U.S.A.	Riley, 1983	
EcRJM-1	TW14359Δ*escN*	This study	4665071-4666029
EcRJM-2	SakaiΔ*escN*	This study	4605926-4606884
EcRJM-3	TW14359Δ*sepD*	This study	4670066-4670518
EcRJM-5	TW08264Δ*rcsB*	This study	3049164-3049814
EcRJM-6	TW14359Δ*rcsB*	This study	3045397-3046047
EcRJM-7	TW14359Δ*rcsC*	This study	3046247-3049096
EcRJM-8	TW08264*rcsB*-FLAG::*kan*	This study	3049812-3049864
EcRJM-9	TW14359*rcsB*-FLAG::*kan*	This study	3046045-3046097
EcRJM-10	TW14359*rcsB*-FLAG	This study	3046045-3046097
EcRJM-11	TW14359Δ*grvA*	This study	1282113-1282867
EcRJM-12	TW14359Δ*rcsB* Δ*grvA*	This study	
EcRJM-13	TW14359*tir*-FLAG	This study	4659012-4659077
EcRJM-14	TW08264*tir*-FLAG	This study	4599867-4599932
EcRJM-15	TW14359Δ*rcsB tir*-FLAG	This study	
EcRJM-16	TW08264Δ*rcsB tir*-FLAG	This study	
EcRJM-22	Sakai pRJM-2	This study	
EcRJM-23	TW14359 pRJM-2	This study	
EcRJM-29	TW14359 pRJM-7	This study	
EcRJM-34	TW14359 pRJM-8	This study	
EcRJM-35	TW14359Δ*grlR::kan*	This study	4673380-4673731
EcRJM-36	TW14359Δ*grlR::kan* pRJM-2	This study	
EcRJM-37	TW14359Δ*grlR::kan* pRJM-8	This study	
EcRJM-38	TW14359Δ*grlR::kan* pRJM-7	This study	
EcRJM-39	TW14359Δ*rcsB* pRJM-2	This study	
EcRJM-40	TW14359Δ*rcsC* pRJM-2	This study	
EcRJM-55	TW14359 pRJM-15	This study	

[a] Nucleotide positions based on the published Sakai (NC_002695) and TW14359 (NC_013008) genome sequences (NCBI)

Table 2 **Strains and plasmids used in Chapter 2, continued.**

Strain/plasmid	Relevant characteristics	Reference	Nucleotide[a] Position
Strain name:			
EcRJM-59	TW14359Δ*rcsB* Δ*grlR::kan*	This study	
EcRJM-60	TW14359Δ*grlR::kan* pRJM-17	This study	
EcRJM-61	TW14359Δ*rcsB* Δ*grlR::kan* pRJM-17	This study	
EcRJM-62	TW14359Δ*rcsB* pRJM-17	This study	
EcRJM-63	TW14359Δ*rcsC* pRJM-17	This study	
EcRJM-64	TW14359Δ*grvA* pRJM-17	This study	
EcRJM-65	TW14359Δ*rcsB* Δ*grvA* pRJM-17	This study	
EcRJM-66	TW14359Δ*escN* Δ*sepD*	This study	
EcRJM-67	TW14359Δ*escN* Δ*sepD* pRJM-10	This study	
EcRJM-68	SakaiΔ*tolA*::*kan*	This study	860848-862032
EcRJM-69	TW14359Δ*tolA*::*kan*	This study	865712-866986
EcRJM-70	SakaiΔ*tolA::kan* pRJM-19	This study	
EcRJM-71	TW14359Δ*tolA::kan* pRJM-18	This study	
Plasmid name:			
pACYC177	Low copy cloning vector, Amp^R Kan^R	Chang, 1978	
pBAD22	Ara inducible expression vector, Amp^R	Guzman, 1995	
pRS551	*lac* fusion vector, Amp^R Kan^R $lacZ^+$	Simons, 1987	
pCP20	Flp recombinase expression vector	Datsenko, 2000	
pKD4	Template plasmid for Kan cassette	Datsenko, 2000	
pKM208	Red-recombinase expression vector	Datsenko, 2000	
pBAD-TOPO®	Ara inducible expression vector	Invitrogen	
pSU312	FLAG epitope template, Amp^R, Kan^R	Uzzau, 2001	
pRJM-2	pRS551 containing ler_{P905}-*lacZ*	This study	4680206-4679303
pRJM-7	pRS551 containing $rcsB_{P1000}$-*lacZ*	This study	3044397-3045396
pRJM-8	pRS551 containing $rcsD_{P501}$-*lacZ*	This study	3042208-3042707
pRJM-15	pBAD22 containing *grlA*	This study	4672912-4673325
pRJM-17	pRS551 containing $flhD_{P1000}$-*lacZ*	This study	2485401-2486400
pRJM-18	pACYC177-*tolA* (Sakai)	This study	860790-862067
pRJM-19	pACYC177-*tolA* (TW14359)	This study	865654-867021

[a] Nucleotide positions based on the published Sakai (NC_002695) and TW14359 (NC_013008) genome sequences

Table 3 - Primers used in Chapter 2

Primer name	Sequence (5'→ 3')	Function/Ref.
FLAG-F	gactacaaagatgacgacga	Uzzau, 2001
P1	gtgtaggctggagctgcttc	Datsenko, 2000
P2	catatgaatatcctccttag	Datsenko, 2000
RcsB+609/Flag-F	TTATCTCTCTTCAGTAACGTTAAGTCCGGCAGATAAAGACgactacaaagatgacgacga	FLAG fusion
RcsB+741/P2	CGTAGGACGGATAAGGCGTTTACGCCGCATCCGGCAATCGcatatgaatatcctccttag	FLAG fusion
RcsB+585	CGAGAACGATATCGCCCTGC	FLAG fusion validation
RcsB+831	CCGCATCTGGCATTCAGTGC	FLAG fusion validation
Tir-1635/Flag-F	TTCGAATAACCCACCAGCGCCGGGATCCCATCGTTTCGTCgactacaaagatgacgacga	FLAG fusion
Tir-1741/P2	AGCTCAAGAGTTGCCCATCCTGCAGCAATGTTATTCCCTGcatatgaatatcctccttag	FLAG fusion
Tir+1613	GGAGTAATAGCGCTGTGAAT	FLAG fusion validation
Tir+1968	AATTTCCCACAGACACCATA	FLAG fusion validation
EspD+1083/Flag-F	TTCAGCACGGGTAAATAGTCGTATTGTTAGTGGCCGAATTgactacaaagatgacgacga	FLAG fusion
EspD+1136/P2	CGTTACTTGAGTATTATCAATAGTATTCATAATAAAATTCcatatgaatatcctccttag	FLAG fusion
EspD+1042	CAGGCGAGCTATTTACAAAG	FLAG fusion validation
EspD+1198	CTCTCCGAAGCGGAATTAAC	FLAG fusion validation
EscN+0/P1	ATGATTTCAGAGCATGATTCTGTATTGGAAAAATACCCACgtgtaggctggagctgcttc	Deletion primer
EscN+1338/P2	GGCAACCACTTTGAATAGGCTTTCAATCGTTTTTTCGTAAcatatgaatatcctccttag	Deletion primer
EscN-45	GGAGGTTGGGAATAATATCG	Deletion validation
EscN+1405	CCATTGATTCTCTCAATCGG	Deletion validation
RcsB-41/P1	AGTTATGTCAAGAGCTTGCTGTAGCAAGGTAGCCTATTACgtgtaggctgagctgcttc	Deletion primer
RcsB+691/P2	CAGATAAGACACTAACGCGTCTTATCTGGCCTACAGATGAcatatgaatatcctccttag	Deletion primer
RcsB-95	CTGATTCGTGAGAAGGATGT	Deletion validation

[a] Restriction sites indicated by bolded and underlined nucleotides

Table 3 Primers used in Chapter 2, cont.		
Primer name	**Sequence (5'→ 3')**	**Function/Ref.**
RcsB+880	GAGAGGGTCAGGAAATCGCG	Deletion validation
GrlR-41/P1	AAATTGAAAGGAGTGAGGTTAGTATGAAACTGAGTGAGTTgtgtaggctggagctgcttc	Deletion primer
GrlR+412/P2	TTATTTGATAAATAAATCGACATAAAAAACATACATAAAAcatatgaatatcctccttag	Deletion primer
GrlR-78	GGTCTCCATTATTCTTGATATTGCTTATGG	Deletion validation
GrlR+472	CTGAGTCAGGAATTACATAGTCGCCATTTT	Deletion validation
RcsC-41 /P1	ACCACACTCCATCGGTCACCTGAGGCGGAGCTTCGCCCCTgtgtaggctggagctgcttc	Deletion primer
RcsC+2890/P2	ACCACACTCCATCGGTCACCTGAGGCGGAGCTTCGCCCCTcatatgaatatcctccttag	Deletion primer
RcsC-207	GGATATAACCATTAACAAGC	Deletion validation
RcsC+2974	CTTATCCGTCCTACGATTCC	Deletion validation
TolA+1/P1	GTGTCAAAGGCAACCGAACAAAACGACAAGCTCAAGCGGGgtgtaggctggagctgcttc	Deletion primer
TolA+1185/P2	TTACGGTTTGAAGTCCAATGGCGCGTTTTTGAACACTTCAcatatgaatatcctccttag	Deletion primer
TolA-93	GGTTGGTTTAATGACGCAGC	Deletion validation
TolA+1346	CCAAATGCTACTCGTAATGC	Deletion validation
GrvA-41/P1	AATACTGGATTTGTAATACACAACTAAGGTATAAAATGTAgtgtaggctggagctgcttc	Deletion primer
GrvA+795/P2	GAGAGAGTTGCAATTATTTGGTGATTCAGAGTTTAACATCcatatgaatatcctccttag	Deletion primer
GrvA-115/F-Val	CAGATAATTCAGATTTGCAT	Deletion validation
GrvA+959/R-Val	CGGTGAAATTAATAACATGG	Deletion validation
Ler-905/EcoRI	CG**GAATTC**TCTTTATAGAGGGGCGCATT	*lacZ* promoter fusion
Ler-1/BamHI	CG**GGATCC**AATAAATAATCTCCGCATGC	pRS551 *lacZ* fusion

[a] Restriction sites indicated by bolded and underlined nucleotides

Table 3	**Primers used in Chapter 2, cont.**	
Primer name	**Sequence (5'→ 3')**	**Function/Ref.**
RcsB-1,000/EcoRI	CGCG**GAATTC**CGCGGCGATCGCGATGCATTACGACGTATT	pRS551 *lacZ* fusion
RcsB-1/BamHI	CGCG**GGATCC**GTAATAGGCTACCTTGCTACAGCAAGCTCT	pRS551 *lacZ* fusion
RcsD-501/EcoRI	CGCG**GAATTC**ATAATAATTCAAGGTTAAAATCAATAACTT	pRS551 *lacZ* fusion
RcsD-1/BamHI	CGCG**GGATCC**TCGTGTTTATGACCTGTTAAAACTTCGCGA	pRS551 *lacZ* fusion
GrlA+1/EcoRI	CG**GAATTC**ATGGAATCTAAAAATAAAAATGGCGACTAT	pBAD22 cloning
GrlA+414/XbaI	GC**TCTAGA**TTATTTTAAATAAACTTGTG	pBAD22 cloning
ECSP_3286+1	**GAGGAATAATAA**ATGACCACTATAACCGATAA	pBAD-TOPO cloning
ECSP_3286+504	**TCAGTGGTGGTGGTGGTGGTG**CAGTAGAGATGCATGGTGTAAC	pBAD-TOPO cloning
ECSP_0242+1	**GAGGAATAATAA**ATGGAGGAAGCCAATGGGGGGGAG	pBAD-TOPO cloning
ECSP_0242+747	**TCAGTGGTGGTGGTGGTGGTG**TTCAGAAACATGAGAAATATAACC	pBAD-TOPO cloning
ECSP_1773+1	**GAGGAATAATAA**ATGAAAATAATATCCACTGTTATTCAAACAC	pBAD-TOPO cloning
ECSP_1773+588	**TCAGTGGTGGTGGTGGTGGTG**TAAATATTTTCTGTTTAATAATGAATAAAAATC	pBAD-TOPO cloning

[a] Restriction sites indicated by bolded and underlined nucleotides

Chapter 3: Function and regulation of the RcsB-GrvA pathway controlling virulence and fitness factors in enterohemorrhagic *Escherichia coli*

3.1 Background

Enterohemorrhagic *Escherichia coli* (EHEC) O157:H7 is a virulent intestinal pathogen, attributed to food-borne outbreaks of bloody diarrhea (hemorrhagic colitis) and the life-threatening kidney disease hemolytic uremic syndrome (HUS) (Nataro and Kaper, 1998; Rangel et al., 2005). Intimate attachment of this pathogen to the intestine requires a functional type III secretion system (T3SS) and is characterized by the formation of attaching and effacing (A/E) lesions (Kaper et al., 2004). This T3SS is encoded on a 36-kb pathogenicity island referred to as the locus of enterocyte effacement (LEE) containing 41 genes organized into five operons (*LEE1-LEE5*) (McDaniel et al., 1995). The master LEE regulator Ler, encoded as the first gene of the *LEE1* operon, positively stimulates LEE gene transcription by relieving H-NS mediated repression while negatively regulating its own transcription. Ler is also able to stimulate production of other LEE encoded regulators including GrlA and GrlR, which activate and repress *ler* transcription, respectively (Berdichevsky et al., 2005; Deng et al., 2004; Elliott et al., 2000; Haack et al., 2003; Islam et al., 2011; Sperandio et al., 2000). The genes *grlA* and *grlR* are encoded as a discistron from an H-NS/Ler regulated promoter (Barba et al., 2005), and GrlA binds directly to the *LEE1* promoter region (Huang and Syu, 2008); Further regulation of LEE gene transcription is mediated by numerous non-LEE encoded factors that converge on the *ler* and *grlA* promoters to direct the proper spatio-temporal production of the T3SS (Flockhart et al., 2012; Hansen and Kaper, 2009; Iyoda and Watanabe, 2004; Kendall et al., 2010; Leverton and

Kaper, 2005; Luzader et al., 2013; Nakanishi et al., 2006; Russell et al., 2007; Sharp and Sperandio, 2007; Zhang et al., 2004).

One such regulator, RcsB, has been shown to both activate and repress LEE transcription, and more recently to be required for upregulation of the LEE in response to the bicarbonate ion (Morgan et al., 2013; Tobe et al., 2005). RcsB is the response regulator of the Rcs phosphorelay system, a multi-component signaling pathway including RcsC (sensor kinase), RcsD (histidine phosphotransferase) and RcsB, which is activated by cell envelope stresses (Brill et al., 1988; Gottesman and Stout, 1991; Huang et al., 2006; Stout and Gottesman, 1990). Upon phosphorylation, RcsB can bind to target promoters as either a homodimer or as a heterodimer in conjunction with other regulatory proteins, such as BglJ, GadE, or RcsA (Gottesman et al., 1985; Johnson et al., 2011; Venkatesh et al., 2010). Binding occurs at specific RcsB consensus sites (Francez-Charlot et al., 2003; Wehland and Bernhard, 2000), and the location of binding relative to the -35 consensus sequence can dictate whether RcsB positively or negatively affects transcription (Majdalani and Gottesman, 2005). RcsB mediated regulation of the LEE requires LEE transcriptional regulators PchA and GrvA. In one study, overexpression of RcsB was observed to repress LEE transcription through down-regulation of LEE activator, PchA, while positive stimulation of the LEE by RcsB overexpression occurs through transcriptional activation of *grvA* (Tobe et al., 2005). In agreement with this mechanism, a strain that intrinsically overexpressed RcsB is characterized by *grvA*-dependent increased LEE expression (Morgan et al., 2013).

EHEC contains a number of horizontally acquired, multi-genic, elements termed O-islands that contribute roughly 1.3 Mb of genomic content that is not present in K-12 (Hayashi et al., 2001). The genes contained within O-islands (OI) are diverse in function, and play a

significant role in EHEC fitness and virulence. The OI-47 locus, containing *grvAB*, is inserted between the *ycdU* and *ycdT* K-12 backbone genes, and is only present within the O157:H7 and O55:H7 pathogenic *E. coli* serotypes. GrvA is a predicted ToxR family membrane-bound transcriptional regulator. Analysis of the amino acid sequence, using the TMHMM v2.0 analysis program (http://www.cbs.dtu.dk/services/TMHMM/) (Krogh et al., 2001), suggests that GrvA contains a single transmembrane domain, similar to ToxR of *Vibrio cholera* encoded on the *toxRS* operon. The downstream gene, *grvB,* encodes a product with a single transmembrane domain, and may serve to allow GrvA to dimerize and form an active transcriptional complex, as is the case with ToxR and ToxS (DiRita and Mekalanos, 1991). While *grvAB* is found in EPEC O55:H7 and EHEC O157:H7 serotypes, another ToxR homolog, YqeI, is encoded within the defunct ETT2 type III secretion system found in pathogenic and some non-pathogenic *E. coli* strains (Ren et al., 2004). The gene downstream of *yqeI* also encodes a protein with a single transmembrane domain, similar to that of ToxS (*Vibrio*), GrvB (EHEC), and FidL (*Salmonella*). The ToxR family of regulators identified in *E. coli* contain significant amino acid sequence diversity compared between each other and homologues found in *Salmonella*. YqeI from EHEC and MarT from *Salmonella* share 41.5% amino acid homology, whereas GrvA and MarT share only 28.3% homology. Interestingly, GrvA and YqeI share only 29.5% amino acid sequence homology, suggesting divergent functions even within the strain.

While GrvA homologues were not identified through BLASTp search, several homologues for YqeI were identified among *Escherichia*, *Yersinia, Serratia*, and *Pseudoalteromonas* strains. The ToxR homolog identified in *Pseudoalteromonas tunicata,* WmpR, has been shown to regulate genes associated with biofilm, virulence, and survival in low iron media (Stelzer et al., 2006). Additionally, VttRA and VttRB are ToxRS homologues of non-

O1/non-O139 serogroup strains of *V. cholera* that regulate bile-dependent TTSS activation, stress responses, and motility (Alam et al., 2010; Chaand and Dziejman, 2013). The ToxR family of regulators is diverse in function and, to-date, have been largely associated with virulence and fitness gene regulation.

The specific factors that function at the *grvA* promoter are not presently known and, although a putative RcsB consensus sequence upstream of *grvA* was identified, direct transcriptional control at the *grvA* promoter by RcsB has not been shown. Importantly, overproduction of RcsB cannot activate transcription from the *ler* promoter in K-12 without co-expression of *grvA* (Tobe et al., 2005). While the RcsB-GrvA-Ler regulatory pathway has been previously shown, the contribution of GrvA to the virulence of O157 strains and the specific mechanism through which GrvA regulates LEE gene transcription have not yet been described. The goals of this study were to explore the RcsB-GrvA mechanism of LEE gene activation, characterize the GrvA regulon in EHEC O157:H7, and explore its significance in virulence and stress fitness. As such, the transcriptome of GrvA was determined by RNA sequencing, and increased stress fitness was observed for the *grvA* isogenic mutant. This study further expands the role of GrvA in virulence of EHEC, and reveals a novel pathway for LEE gene regulation by GrvA, through the acid resistance regulator *gadE*.

3.2 Methods

3.2.1 Bacterial strains and culture conditions

The strains and plasmids used in this study are listed in **Table 6**. Strains were stocked at -80°C in glycerol diluted (15% v/v final) in Luria Broth (LB), and were maintained in LB or on LB with 1.5% agar (LBA). Unless otherwise noted, overnight (18-20 h) cultures grown in LB

were used to inoculate fresh LB or LB buffered with sodium bicarbonate (44 mM $NaHCO_3$) or fresh Dulbecco's Modified Eagle's Medium (DMEM) (4 g/l glucose, 4 mM glutamine, 44 mM $NaHCO_3$, pH 7.4) to a final optical density 600 nm (OD_{600}) of 0.05. Cultures were grown at 37°C in a rotary shaker (200 RPM) using a 1:10 media-to-flask volume. Antibiotics (Sigma-Aldrich, St. Louis, MO) were added to cultures when required.

3.2.2 Genetic manipulations and complementation

Primers used for genetic manipulation and complementation are listed in **Table 7**. For construction of deletion mutants and chromosomal FLAG-epitope fusions the λ-Red assisted one-step deletion method, adapted for EHEC, was used as described (Datsenko and Wanner, 2000; Lippolis et al., 2009; Morgan et al., 2013). A previously published approach was used to construct FLAG fusions to *rcsB*, *tir*, and *zinT* (Morgan et al., 2013) based on the method of Uzzau et al. (Uzzau et al., 2001). When expressed, the fusion protein contains a seven amino acid C-terminal epitope (FLAG) that can be detected by western immunoblots using anti-FLAG mAbs (Sigma-Aldrich. St. Louis, MO). Confirmation of genetic constructs was done using a combination of B*cc*I (NEB) restriction mapping and DNA sequencing (MWG Operon, Huntsville, AL).

Complementation of *rcsB* was performed using vector pRJM-20, as previously described (Morgan et al., 2013). Additionally, a fragment containing the entire *rcsDB* operon, including the *rcsD* promoter region (nucleotide positions 3041665-3046191, GenBank Ref# NC_013008.1), was cloned into *Bam*HI/*Xba*I-digested low-copy expression vector pMPM-K3 (Kan^R) (Mayer, 1995) using primers RcsB-3732/BamHI and RcsB+794/XbaI, to produce pRJM-21. To complement *grvA*, a PCR product corresponding to the *grvA* ORF and including a 267-bp

upstream region of *grvA* containing the predicted promoter (nucleotide positions 1281984-1283134, GenBank Ref# NC_013008.1), was produced using primers GrvA-268/XhoI and GrvA+884/BamHI, and cloned into *Xho*I/*Bam*HI digested low-copy expression vector pMPM-A2 (Amp^R) (Mayer, 1995), creating pRJM-22. To create a vector expressing a C-terminal 6xHIS tagged variant of GrvA under the control of the native *grvA* promoter, a PCR product including the *grvA* ORF and a region extending 267-bp upstream and 810-bp downstream of the translational start site (including the predicted promoter but not the native stop codon) (nucleotide positions 1282059-1283134, GenBank Ref# NC_013008.1), was produced using primers GrvA-268/XbaI and GrvA+810/EcoRI-6xHIS, with the reverse primer containing the nucleotide sequence for the 6xHIS epitope. This PCR product was cloned into *Xba*I/*Eco*RI digested pUC19 to create pRJM-32.

To complement *gadE*, a PCR product corresponding to the *gadE* ORF and 762-bp upstream of *gadE* (containing the native promoters) (nucleotide positions 4458857-4460195, GenBank Ref# NC_013008.1) was produced using primers GadE-763/XbaI and GadE+577/BamHI, and cloned into the *Xba*I/*Bam*HI digested vector pMPM-A2, to create pRJM-30.

3.2.3 Protein extraction, SDS-PAGE and western immunoblots

Protein extraction, purification and western immunoblots were performed as described previously (Mitra et al., 2012). The amount of protein loaded on SDS-PAGE gels for western blots was measured by a Bradford protein assay standard curve, and equal loading was validated by western blots for GroEL using anti-GroEL mAbs (Bio-Rad, Hercules, CA). Monoclonal antibodies against FLAG (Sigma-Aldrich, St. Louis, MO) were also used. Each experiment was

repeated a minimum of three times in independent trials. Densitometry was used to estimate differences in protein levels for select experiments using a ChemiDoc XRS+ Imaging System and Image Lab 3.0 (BioRad).

3.2.4 RNA purification and quantitative real-time PCR (qRT-PCR)

Primers for qRT-PCR are provided in **Table 7** in supplemental materials. RNA purification, cDNA synthesis, qRT-PCR cycling conditions and data analysis followed previously described protocols (Riordan et al., 2010). qRT-PCR was performed using a Realplex2 Mastercycler (Eppendorf). Cycle threshold (C_t) data were normalized to *rrsH* (16S rRNA gene) and normalized cycle threshold values (ΔC_t) were transformed to arbitrary transcript expression levels using $2^{-\Delta Ct}/10^{-6}$ as described (Livak and Schmittgen, 2001; Mitra et al., 2012). Expression levels were compared statistically using the appropriate t-test or by Tukey's HSD following a significant F-test ($n \geq 3$, $\alpha = 0.05$) (R. ver. 3.1.0).

3.2.5 Construction of single copy *luxE* operon fusions

Strains containing single-copy chromosome-plasmid *luxE* reporter fusions were constructed using a protocol adapted from Shimizu et. al. (Shimizu et al., 2011). To make *rcsDB-luxE* and *grvAB-luxE* fusions, the *kan* cassette and flanking FRT sites were amplified from pKD4 (Datsenko and Wanner, 2000) using primers pKD4forward/SacI and pKD4reverse/BamHI. This product was *Sac*I/*Bam*HI-digested and cloned into the *Bam*HI/*Sac*I site of pMPM-T3 (Mayer, 1995) to produce pMPM-T3-*kan*. An *Xho*I/*Bam*HI-digested PCR product containing the *luxE* gene and native RBS was amplified from placlux8 (Shimizu et al., 2011) using primers LuxE-18/XhoI and LuxE+1,450/BamHI and cloned into the *Xho*I/*Bam*HI

site of similarly digested pMPM-T3-*kan* to create pMPM-T3-*luxE-kan*. For *rcsDB-luxE*, a *luxE-kan* PCR product amplified from pMPM-T3-*luxE-kan* using primers RcsB+625/LuxE and RcsB+838/P2 and Phusion© High-Fidelity DNA Polymerase (NEB) was fused to a region 13-bp downstream of the *rcsB* ORF, and 53-bp downstream of the convergently-transcribed *rcsC* ORF (nucleotide position in TW14359) using λ Red assisted homologous recombination (Datsenko and Wanner, 2000). A similar approach was used to construct *grvAB-luxE* using primers GrvA+1,283/LuxE and GrvA+1,431/P2. Kanamycin resistance cassettes were removed using FLP recombinase as described (Datsenko and Wanner, 2000), and *luxE* fusion constructs were validated using a combination of restriction mapping and DNA sequencing (MWG Operon). *lux* operon genes *luxCDAB* were constitutively expressed *in trans* in TW14359*rcsDB-luxE* and TW14359*grvAB-luxE* backgrounds from pluxCDAB3 (Shimizu et al., 2011; Shimizu et al., 2012).

3.2.6 Luciferase plate assays

Overnight cultures grown in either LB or DMEM were used to inoculate fresh LB containing 44 mM $NaHCO_3$, or DMEM with 44 mM $NaHCO_3$ and ampicillin (100 µg/ml) to an OD_{600}=0.05. Cultures (0.2 ml) were inoculated into 96-well, clear bottom white-walled plates (Greiner Bio-One 655098) and incubated at 37°C in a rotary shaker (200 RPM). Luciferase and OD_{600} measurements were taken every hour for 10 hours using a Biotek Synergy 2 plate reader (1 sec integration) pre-warmed to 37°C. Assays were performed in quadruplicate (n=4), and mean luciferase activity was compared using the appropriate t-test (n=4, α=0.05) (R. ver. 3.1.0).

3.2.7 Electrophoretic mobility shift assay (EMSA)

EMSA experiments were performed as previously described (Mitra et al. 2014). Briefly, the forward primer used to PCR amplify *rcsB* from TW14359 DNA contained a new start codon and a 6xHis epitope tag, and the PCR product was cloned into the *Nco*I/*Xho*I sites of similarly digested vector pET-24d, to create pRJM-27. N-terminal 6xHis-RcsB fusion proteins have wild-type RcsB activity (Carballes et al., 1999). N-terminal 6xHis tagged RcsB was purified from strain BL21(DE3)pLysS using Ni-NTA Spin Columns (Qiagen) according to the manufacturer's protocol. Briefly, overnight cultures grown in LB (supplemented with 1 mM IPTG and Kan (50 µg/ml), at 18°C and 200 rpm) were pelleted and re-suspended in 1.5 ml of Lysis Buffer (50 mM NaH_2PO_4, 300 mM NaCl, 10 mM imidazole, pH 8.0) and lysed by sonication for 3 min (50 % amplitude, 10 sec interval, 30 sec pause) while chilled on ice. The lysate was centrifuged at 21,000 x g to remove insoluble cellular debris, and the supernatant was used for column purification, and subsequently eluted with Elution Buffer (50 mM NaH_2PO_4, 300 mM NaCl, 500 mM imidazole, pH 8.0). Purified 6xHis-RcsB protein was quantified using a Bradford protein assay. 5'-biotin labeled primers (IDT Oligos) were used to amplify the *grvA* promoter region containing the RcsB consensus binding site. An additional fragment, with no predicted RcsB consensus sequence, was amplified and used as a negative binding control. Amplified biotin labeled probes were gel purified (QIAquick Gel Extraction Kit), and diluted to a concentration of 0.5 ng/µl. All EMSA experiments were performed using the LightShift Chemiluminescent EMSA Kit (Thermo Pierce) according to the manufacturer's specifications. Prior to electrophoresis, purified 6xHis-RcsB and biotin labeled fragments were co-incubated for 40 min in Binding Buffer (1x binding buffer, 50 ng/µl sheared salmon sperm DNA, 2.5% glycerol, 0.05% NP-40, 5 mM $MgCl_2$, 50 mM KCl, and 1 mM EDTA) at room temperature. Samples were

loaded into a pre-run and cooled, 8% native polyacrylamide gel, and run at 20 V/cm for 1 hour. Following electrophoresis, biotin labeled DNA was transferred (25V for 20 minutes) to a Biodyne B Pre-Cut Modified Nylon Membrane (Thermo Pierce) and UV crosslinked for 60 sec. Biotin labeled DNA fragments were detected using Streptavidin-HRP conjugated antibodies (1:300) in blocking buffer, and membranes were washed, equilibrated, and subsequently detected using luminol/enhancer solutions in a ChemiDoc XRS+ Imaging System and Image Lab 3.0 (BioRad).

3.2.8 Construction of *lacZ* transcriptional promoter fusions and β-galactosidase assays

Construction of the *grvA*$_P$-*lacZ* reporter transcriptional fusion followed a previously described protocol using vector pRS551 (Morgan et al., 2013). Briefly, a 306-bp PCR product containing the predicted *grvA* promoter was amplified from TW14359 genomic DNA using primers GrvA-268/EcoRI and GrvA+38/BamHI, *Bam*HI/*Eco*RI digested, and cloned into the similarly digested pRS551, resulting in pRJM-31. Four different *gadE*$_P$-*lacZ* promoter fusions were created by cloning *Bam*HI/*Eco*RI-digested PCR products into similarly digested pRS551 using primers GadE-320/EcoRI and GadE-1/BamHI, GadE-276/EcoRI and GadE-516/BamHI, GadE-773/EcoRI and GadE-497/BamHI, and GadE-773/EcoRI and GadE-1/BamHI. β-galactosidase activity (Miller Units) was measured as previously described and compared between strains using the appropriate t-test or by Tukey's HSD following a significant F-test ($n \geq 3$, $\alpha = 0.05$) (R ver. 3.1.0) (Miller, 1972; Mitra et al., 2012).

3.2.9 RNA-seq and data analysis

RNA sequencing experiments were performed as previously described (Weiss et al., 2014). RNA extractions were performed as described for qRT-PCR, except residual genomic DNA was digested using TURBO™ DNase (Ambion, cat. AM2238) following the manufacturers' protocol. Three independent RNA samples for each strain (TW14359, TW14359Δ*grvA*, and TW14359Δ*rcsB*Δ*grvA*) were mixed in a 1:1:1 ratio to account for inter-sample variability, and rRNA was removed using the MICROBExpress™ Bacterial mRNA Enrichment Kit (Ambion, cat. AM1905) according to instructions. The integrity and concentration of purified and enriched mRNA was determined using an Agilent 2100 Bioanalyzer (Agilent Technologies). mRNA was converted to strand specific cDNA using the Ion Total RNA-Seq Kit v2 (Ion Torrent™, cat. 4475936) and samples were sequenced using an Ion Personal Genome Machine® (PGM™) System (Ion Torrent™). Sequence mapping and data analysis was performed using CLC Main Workbench 6 (CLC bio). Subsequent RPKM (reads per kilobase per million mapped reads) values were converted to fold change relative to wild-type TW14359 for both TW14359Δ*grvA* and TW14359Δ*rcsB*Δ*grvA*. Genes of interest with an RPKM below the 1-RPKM cut-off were individually examined for significance between samples. Circular plots were created using Circos v0.65 (http://www.circos.ca) (Krzywinski et al., 2009).

3.2.10 Adherence assays

The maintenance and culture of HT-29 colonic intestinal cells was performed as previously described (Morgan et al., 2013). Adherence competition indexes were determined using the method of Gabbianelli et al. (Gabbianelli et al., 2011). Briefly, overnight DMEM cultures were used to inoculate fresh DMEM to OD_{600}=0.05, and were incubated for 3 hours at

37°C with shaking (200 RPM). Cultures were then diluted to an OD_{600} = 0.5 and mixed in a 1:1 ratio (test strain:control strain), and 200 µl of each was used to inoculate HT-29 cells in 6-well culture plates. For the control strain, the entire *lacZ* ORF was deleted in TW14359 to produce a strain incapable of utilizing lactose, for use in differential selection in competition assays. Each plate was gently mixed before centrifugation at 500 x *g* for 5 min and then incubated as above. Following 3 h of incubation, each well was washed four times using sterile PBS to remove non-adherent cells and adherent cells were removed using 500 µl of 0.1% Triton X-100. Cells were enumerated (CFU/ml) by serial dilution in PBS and plating onto MacConkey agar, which is a differential media used to indicate lactose utilization. After overnight growth on MacConkey agar, pink colonies (Lac+) were scored as test strain CFU/ml, whereas white colonies (Lac-) were scored as TW14359Δ*lacZ* CFU/ml. The competitive index was derived by dividing CFU/ml of the test strain by the CFU/ml of TW14359Δ*lacZ*, and was compared statistically using the appropriate t-test ($n \geq 3$, $\alpha = 0.05$) (R ver. 3.1.0).

3.2.11 Acid resistance assays

Acid resistance by the glutamate-dependent system was measured as described (Riordan et al., 2010) with slight adaptations. Mid-exponential phase (OD_{600}=0.5) DMEM cultures were inoculated to 10^6 CFU/ml final cell density in E minimal glucose (EG) media with or without 5.7 mM L-glutamate at pH 7 (control) or acidified with HCl (pH 2). For cell counts (CFU/ml) and percent survival determinations, samples were serially-diluted in PBS (pH 7), plated to LBA and incubated overnight at 37°C.

3.3 Results

3.3.1 Expression profiles of the *rcsDB* and *grvAB* operons, and molecular basis for *grvA* activation by RcsB

Previous work has shown RcsB to be an activator of *grvA*, and that both factors are required for bicarbonate-dependent upregulation of the LEE-encoded regulator, Ler, and subsequent stimulation of LEE expression in EHEC (Tobe et al; Morgan et al 2013). RcsB is predicted to act upstream of *grvA* in the regulation of *ler*, yet the mechanism underlying the control of *grvA* by RcsB is as yet unknown. In addition, the expression profile for both *rcsDB* and *grvAB* operons under LEE-inducing conditions has not been determined

In both DMEM and LB, expression of *rcsDB* was highest during exponential phase growth as measured by luciferase activity (**Fig. 15A**). For DMEM, *rcsDB* expression declined during transition into stationary phase (after 3 h growth), but for LB, expression declined earlier (after 1 h growth) and during exponential phase. For both DMEM and LB, *rcsDB* expression continued to decline into stationary phase. The expression of *rcsDB* was significantly higher (2- to -4-fold) in DMEM over the course of the first 6 h of growth compared to LB ($p<0.05$) (**Fig. 15A**). Addition of bicarbonate to LB increased *rcsDB* expression during early exponential growth (1 h) ($p=0.001$), however levels were still significantly less than that observed for DMEM at the same time point ($p<0.001$ and **Fig. 15A**). Furthermore, during the later stages of growth (5–10 h), *rcsDB* expression in LB with bicarbonate was significantly lower than LB. This suggests that, while bicarbonate is able to stimulate *rcsDB* transcription, growth in DMEM leads to markedly higher levels of *rcsDB* transcription during early stages of growth. Finally, this data indicates that bicarbonate stimulation of *rcsDB* expression in LB is dependent on growth-phase.

Like *rcsDB*, *grvAB* expression was growth-phase dependent. In both DMEM and LB,

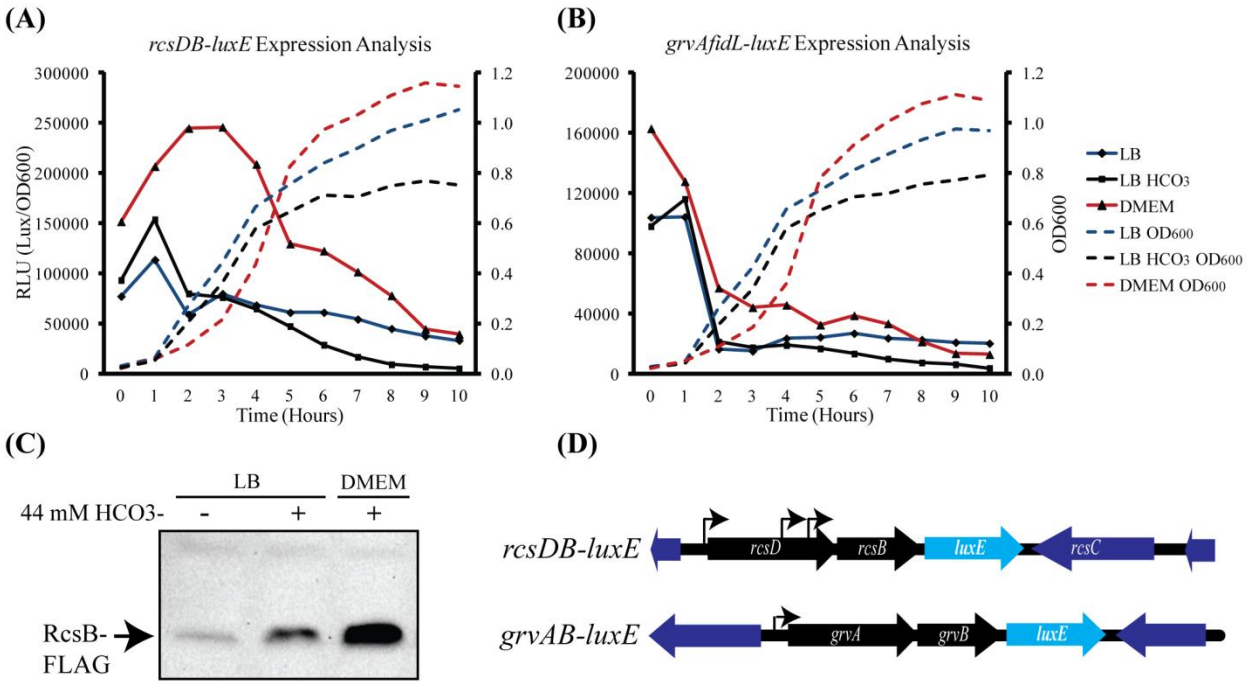

Figure 15 - Temporal expression of *rcsDB* and *grvAB* operons in TW14359
Analysis of *rcsB* promoter activity and temporal expression of the *rcsDB* and *grvAB* operons in TW14359. Luciferase activity of (A) *rcsDB-luxE* and (B) *grvAB-luxE* strains containing plasmid pluxCDAB3, measured over 10 hours, in DMEM with 44 mM bicarbonate (triangle), LB (diamond), and LB with 44 mM bicarbonate (square). RLU values are a function of total luciferase activity divided by OD_{600} measurements at each time point. The OD_{600} valuse of all cultures are indicated by dashed lines. The means at each time point varied by less than 10% for each sample. (C) Representative western blot for RcsB-FLAG grown to mid-exponential phase (OD_{600}=0.5) in LB, LB supplemented with 44 mM bicarbonate, and DMEM. Non-specific binding was used as to control for loading. (D) Schematic diagram for the construction of chromosomal *rcsDB*- and *grvAB-luxE* fusions in TW14359.

expression peaked during early exponential phase, declining rapidly between 1-2 h growth to substantially lower levels of expression for the remaining course of the experiment (2-10 h) (**Fig. 15B**). As for *rcsDB*, *grvAB* expression was significantly higher (1.5- to 3.5-fold) in DMEM compared with LB up until transition to stationary phase (0-4 h) ($p<0.05$). Bicarbonate addition to LB increased *grvAB* expression slightly during early exponential growth, however for stationary-phase cultures, levels were significantly less in LB with bicarbonate ($p<0.05$, 5-10 h) (**Fig. 15B**). The patterns of *rcsDB* and *grvAB* expression were consistent with cytosolic levels of RcsB during exponential (OD600=0.5, or 2 h) growth, with higher levels of proteins observed in LB with HCO_3, and substantially higher levels during growth in DMEM (**Fig. 15D**). This data indicates that GrvA controls several genes, including those involved in colonization and acid resistance, but also includes a number of genes which are not associated with virulence directly.

While RcsB has been shown to upregulate *grvA* (Tobe et al., 2005), the mode of activation is not known. Overexpression of *rcsDB in trans* in a *grvAB-luxE* reporter background (strain EcRJM105) substantially increased RLUs of luciferase (**Fig. 16A**), suggesting that RcsB is working directly on the promoter of *grvAB* for activation. Consistent with this, two putative RcsB boxes were identified in tandem and proximal to a predicted -35 site (nucleotides 1282968-1282982 in TW14359) of the *grvA* promoter ($grvA_P$) (Wehland and Bernhard, 2000) (Tobe et al., 2005) (**Fig. 16B**). To test this hypothesis, purified RcsB was co-incubated with a fragment of the core $grvA_P$ element including the putative RcsB boxes and analyzed using electrophoretic mobility shift assays (EMSA). As anticipated, the 235-bp $grvA_P$ fragment was visibly shifted with the addition of increasing amounts (1-12 μg) of purified RcsB, while no shift was observed for the control fragment (**Fig. 16C**). Based on these findings, it is predicted that RcsB is a direct transcriptional activator of *grvA* and that activation occurs at the *grvA* promoter region

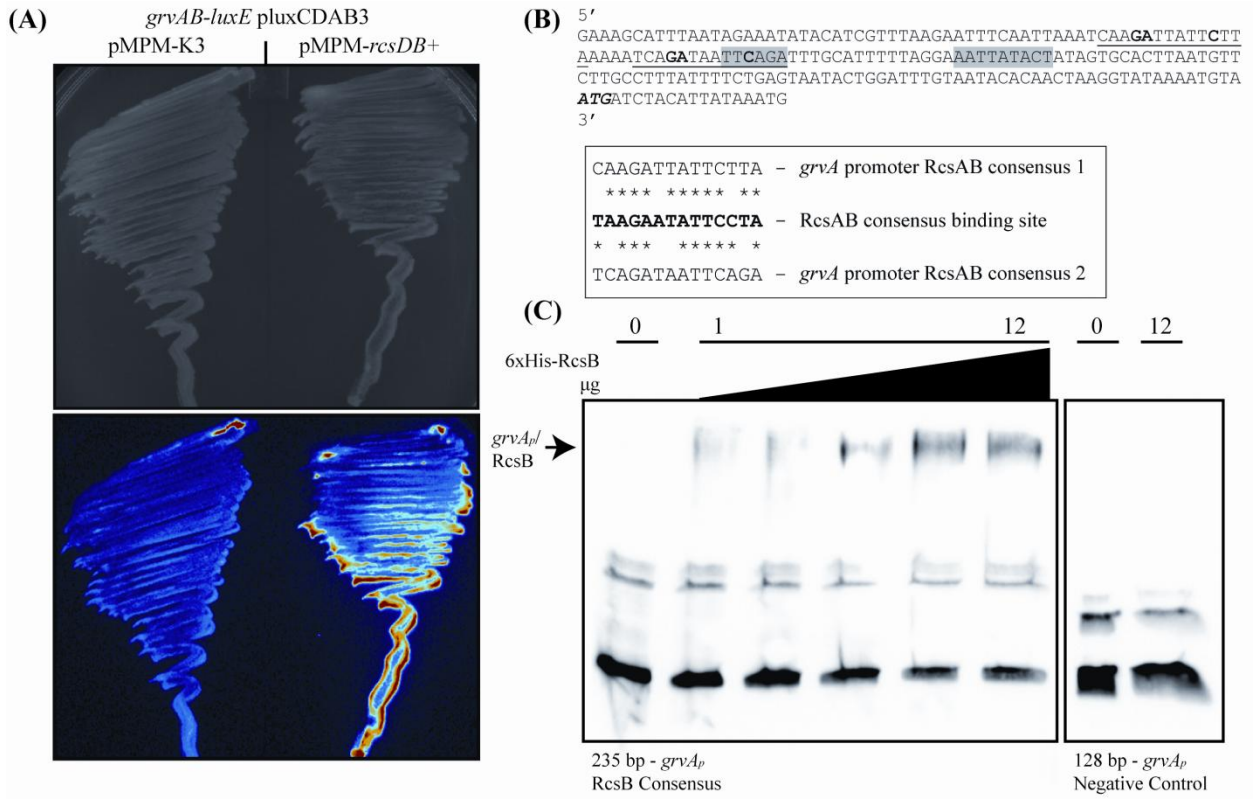

Figure 16 - Direct transcriptional regulation of *grvA* by RcsB
(A) Luminesence was visualized from strain TW14359 *grvAB-luxE* pluxCDAB3 with empty vector pMPM-K3 or vector pMPM-*rcsDB*. Empty vector and *rcsDB* expressing strains were streaked onto an LBA plate and incubated at 37°C for 8 hours before detection. (B) Genomic DNA sequence upstream of *grvA* ORF containing the putative sigma-70 promoter (grey fill), RcsB consensus binding sites (unerlined), and *grvA* translational start site (bold italics) (C) Electrophoretic mobility shift assay for biotinylated *grvA* promoter fragments containing an (bottom left) RcsB consensus sequence and (bottom right) no consensus sequence. RcsB concentration was increased from 1 to 12 µg for the fragment containing the RcsB consensus binding site, and at 12 µg for the fragment with no consensus binding site. The arrow indicates location of the shifted *grvA* sequence.

containing at least one RcsB box.

3.3.2 The GrvA regulon of EHEC

While GrvA clearly contributes to the regulation of Ler (Tobe et al 2005; Morgan et al 2013), the precise mechanism by which it upregulates the LEE and the breadth of genes controlled by GrvA is unknown. To determine this, the transcriptome of EHEC O157:H7 strain TW14359 and its *grvA* isogenic derivative (TW14359Δ*grvA*) was measured by RNA-seq analysis during exponential growth (OD_{600}=0.5) in DMEM. As RcsB is a direct activator of *grvA* (above) and required for GrvA-dependent control of the LEE (Tobe et al; Morgan et al), the transcriptome of TW14359Δ*rcsB*Δ*grvA* was measured in parallel.

In TW14359Δ*grvA*, 765 genes were altered in expression >2-fold above the RPKM cutoff when compared to TW14359 (**Fig. 17A** and **17B**); of these, 264 were upregulated and 501 were downregulated. Gene ontologies were determined based on known and predicted gene product function and included 31% as cellular and metabolic roles (74 up; 162 down), 9% as known or predicted regulators (23 up; 45 down), and 8% involved in transport (18 up; 42 down) (**Table 4**). For those genes in which GrvA is dependent on *rcsB* for regulation, it was expected that the direction and magnitude of expression would not differ between TW14359Δ*grvA* and TW14359Δ*grvA*Δ*rcsB* backgrounds. Of the genes differentially expressed in TW14359Δ*grvA*, 33% (250/765) were similarly altered in expression for TW14359Δ*grvA*Δ*rcsB* (**Table 4**; **Fig. 17A** and **17B**). However, while 63% (485/765) of genes altered in TW14359Δ*grvA* were unchanged in TW14359Δ*grvA*Δ*rcsB*, 4% (30/765) were altered in the opposite direction. Specifically, 13 genes which were upregulated in TW14359Δ*grvA* were down in

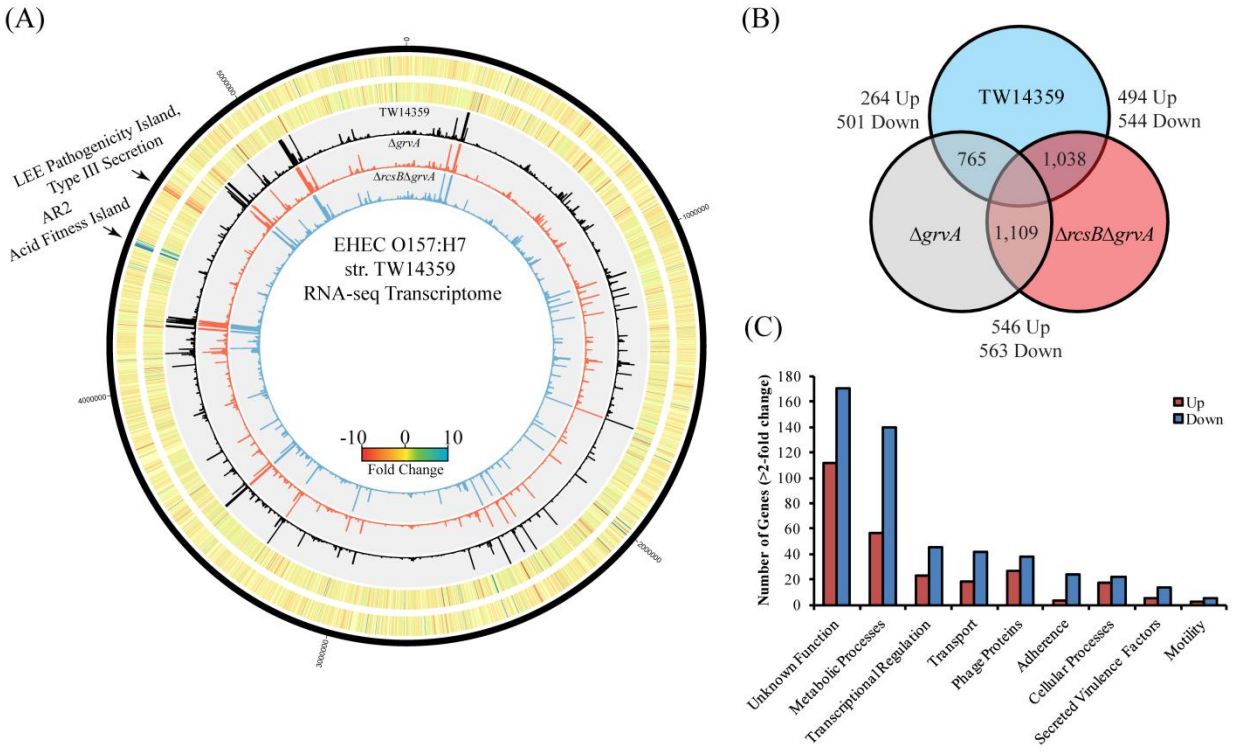

Figure 17 - Circular plot of RNA-Seq in EHEC strain TW14359 and mutant derivatives
(A) Circular plots represent data from RNA sequencing of strains TW14359, TW14359Δ*grvA*, and TW14359Δ*grvA*Δ*rcsB*. Plots represent data and information as follows: (outer, black) Numeric genomic location based on nucleotide position. Heatmaps of fold change in expression for TW14359Δ*grvA* (outer) and TW14359Δ*grvA*Δ*rcsB* (inner), with select key locations indicated with black arrows; fold changes represented as the wild type RPKM divided by the mutant derivative RPKM value for each gene. The inner three histograms represent the RPKM of TW14359 (black), TW14359Δ*grvA* (red), and TW14359Δ*grvA*Δ*rcsB* (blue). Circular plots created using Circos v0.65 (http://www.circos.ca). (B) Venn diagram representing the number of genes up- or down-regulated by at least 2-fold between TW14359 (blue), TW14359Δ*grvA* (grey), and TW14359Δ*grvA*Δ*rcsB* (red). (C) Ontological grouping of genes influenced by GrvA in TW14359. A total of 765 genes showed at least 2-fold alteration up (red) or down (blue) in expression, and genes are grouped by their known or predicted ontologies.

Table 4 - RNA-seq transcriptome data

		Fold Change[b]		
LEE PAI genes, and non-LEE encoded effectors				
ECSP ID[a]	**Gene**	**Δ*grvA***	***grvA*rcsB**	**Description**
ECSP_4665	*espF*	-3.08	-1.18	LEE-encoded type III secreted effector
ECSP_4666	*orf29*	-3.36	-5.13	LEE-encoded predicted type III secretion system factor
ECSP_4667	*escF*	-5.79	-5.06	LEE-encoded type III secretion system component
ECSP_4668	*cesD2*	-8.31	-5.08	predicted chaperone
ECSP_4669	*espB*	-6.55	-5.82	secreted protein EspB
ECSP_4670	*espD*	-4.49	-3.85	secreted protein EspD
ECSP_4671	*espA*	-4.39	-4.31	secreted protein EspA
ECSP_4672	*sepL*	-4.53	-5.69	LEE-encoded type III secretion system component
ECSP_4673	*escD*	-4.03	-3.36	LEE-encoded type III secretion system component
ECSP_4674	*eae*	-4.76	-2.91	intimin adherence protein
ECSP_4675	*cesT*	-5.95	-3.98	molecular chaperone
ECSP_4676	*tir*	-4.01	-3.10	translocated intimin receptor protein
ECSP_4677	*map*	-4.42	-3.48	type III secreted effector protein
ECSP_4678	*cesF*	ND (-)	-1.08	chaperone for type III secretion of EspF
ECSP_4679	*espH*	-4.79	-5.49	LEE-encoded type III secreted effector
ECSP_4680	*escQ*	-1.91	-2.79	LEE-encoded type III secretion system factor
ECSP_4681	*orf16*	-8.06	-6.16	LEE-encoded predicted type III secretion system factor
ECSP_4682	*orf15*	-1.21	-6.16	LEE-encoded predicted type III secretion system factor
ECSP_4683	*escN*	-2.70	-1.69	LEE-encoded type III secretion system factor
ECSP_4684	*escV*	-2.29	-3.59	LEE-encoded type III secretion system factor
ECSP_4685	*orf12*	-1.26	ND (-)	LEE-encoded predicted type III secretion system factor
ECSP_4686	*espZ*	-3.48	-1.85	translocated effector protein
ECSP_4687	*escI*	-1.28	1.09	LEE-encoded predicted type III secretion system component
ECSP_4688	*escJ*	-2.80	-4.53	LEE-encoded type III secretion system factor
ECSP_4689	*sepD*	-1.26	-1.93	LEE-encoded type III secretion system component
ECSP_4690	*escC*	-1.73	-2.38	type III needle complex subunit
ECSP_4691	*cesD*	-1.08	-5.78	LEE-encoded type III secretion system factor
ECSP_4692	*grlA*	-1.11	-4.62	LEE-encoded positive regulator of transcription
ECSP_4693	*grlR*	-1.93	-2.72	LEE-encoded negative regulator of transcription

Table 4 - RNA-seqtTranscriptome data, continued.

ECSP_4694	*etgA*	-1.51	ND (-)	predicted lytic transglycosylase
ECSP_4695	*escU*	ND (+)	1.02	LEE-encoded type III secretion system factor
ECSP_4696	*escT*	ND (-)	-2.70	LEE-encoded type III secretion system factor
ECSP_4697	*escS*	3.97	-1.54	LEE-encoded type III secretion system factor
ECSP_4698	*escR*	-1.64	ND (-)	LEE-encoded type III secretion system factor
ECSP_4699	*escL*	-2.94	-3.85	LEE-encoded predicted type III secretion system factor
ECSP_4700	*orf4*	-1.83	-4.47	LEE-encoded type III secretion system factor
ECSP_4701	*cesA*	-1.01	1.14	LEE-encoded chaperone
ECSP_4702	*escE*	-1.13	-2.60	LEE-encoded type III secretion system factor
ECSP_4703	*ler*	-2.45	-2.33	locus of enterocyte effacement (LEE)-encoded regulator
ECSP_4704	*espG*	-3.69	-1.61	LEE-encoded type III secreted effector
ECSP_4705	*rorf1*	-1.01	ND (-)	LEE-encoded type III secretion system factor
ECSP_0061	*espY1*	1.98	3.25	non-LEE-encoded type III secreted effector
ECSP_0866	*nleC*	-2.27	-3.08	non-LEE-encoded type III secreted effector
ECSP_0868	*nleD*	-1.66	-1.97	non-LEE-encoded type III secreted effector
ECSP_1702	*nleA*	-4.03	-2.46	non-LEE-encoded type III secreted effector
ECSP_1704	*nleH2*	2.25	1.21	non-LEE-encoded type III secreted effector
ECSP_1705	*nleF*	-3.69	-3.99	non-LEE-encoded type III secreted effector
ECSP_3954	*nleE*	-4.03	-4.11	non-LEE-encoded type III secreted effector

Metabolism and Acid Resistance

ECSP ID	Gene	Δ*grvA*	*grvArcsB*	Description
ECSP_0704	*gltL*	-3.89	-4.56	glutamate and aspartate transporter subunit, ATP-binding component of ABC superfamily
ECSP_0705	*gltK*	-3.02	-3.29	glutamate and aspartate transporter subunit, membrane component of ABC superfamily
ECSP_0706	*gltJ*	-2.49	-2.99	glutamate and aspartate transporter subunit, membrane component of ABC superfamily
ECSP_0707	*gltI*	-2.98	-2.39	glutamate and aspartate transporter subunit, periplasmic-binding component of ABC superfamily
ECSP_0906	*glnQ*	-2.35	-2.06	glutamine transporter subunit; ATP-binding component of ABC superfamily

Table 4 - RNA-seq transcriptome data, continued.

ECSP_0907	*glnP*	-2.33	-1.24	glutamine transporter subunit; membrane component of ABC superfamily
ECSP_0908	*glnH*	-1.51	-1.36	glutamine transporter subunit; periplasmic binding component of ABC superfamily
ECSP_1977	*gadC*	15.63	1.79	predicted glutamate:gamma-aminobutyric acid antiporter
ECSP_1978	*gadB*	14.58	1.30	glutamate decarboxylase B, PLP-dependent
ECSP_2312	*astE*	-4.03	-2.93	succinylglutamate desuccinylase
ECSP_2313	*astB*	-5.95	-5.34	succinylarginine dihydrolase
ECSP_2314	*astD*	-9.07	-5.74	succinylglutamic semialdehyde dehydrogenase
ECSP_2315	*astA*	ND (+)	-11.87	arginine succinyltransferase
ECSP_2316	*astC*	-66.00	-11.40	succinylornithine transaminase, PLP-dependent
ECSP_2329	*gdhA*	-1.84	-2.32	glutamate dehydrogenase
ECSP_3185	*argT*	-3.53	-1.78	lysine/arginine/ornithine transporter subunit, periplasmic-binding component of ABC superfamily
ECSP_4065	*uxaA*	1.69	4.10	altronate hydrolase
ECSP_4066	*uxaC*	1.76	4.91	uronate isomerase
ECSP_4486	*slp*	1.98	3.56	outer membrane lipoprotein
ECSP_4498	*hdeB*	ND (+)	1.00	acid-resistance protein
ECSP_4499	*hdeA*	ND (+)	ND (+)	stress response protein acid-resistance protein
ECSP_4500	*hdeD*	ND (+)	ND (+)	acid-resistance membrane protein
ECSP_4501	*gadE*	ND (+)	ND (+)	acid-induced positive regulator of glutamate-dependent acid resistance
ECSP_4502	*mdtE*	ND (+)	ND (+)	multidrug resistance efflux transporter
ECSP_4503	*mdtF*	ND (+)	ND (+)	multidrug transporter, RpoS-dependent
ECSP_4504	*gadW*	ND (+)	ND (+)	DNA-binding transcriptional activator

Table 4 - RNA-seq transcriptome data, continued.

ECSP_4505	-	1.00	1.00	hypothetical protein
ECSP_4506	*gadX*	ND (+)	ND (+)	DNA-binding transcriptional dual regulator
ECSP_4507	*gadA*	ND (+)	ND (+)	glutamate decarboxylase A, PLP-dependent
ECSP_4508	*yhjA*	1.00	ND (+)	predicted cytochrome C peroxidase
ECSP_4509	*treF*	ND (+)	ND (+)	cytoplasmic trehalase
ECSP_4510	*yhjB*	1.00	ND (+)	predicted DNA-binding response regulator in two-component regulatory system
ECSP_4511	*yhjC*	ND (+)	ND (+)	predicted DNA-binding transcriptional regulator
ECSP_4512	*yhjD*	ND (+)	ND (+)	conserved inner membrane protein
ECSP_4513	*yhjE*	87.33	159.09	predicted transporter
ECSP_4921	-	ND	ND (+)	hypothetical protein
ECSP_4922	-	-1.06	1.44	hypothetical protein
ECSP_4923	*glnG*	-3.74	-5.30	fused DNA-binding response regulator in two-component regulatory system
ECSP_4924	*glnL*	-3.71	-7.85	sensory histidine kinase in two-component regulatory system with GlnG
ECSP_4925	*glnA*	-4.32	-6.22	glutamine synthetase
ECSP_0518	*glnK*	ND (+)	ND (+)	nitrogen assimilation regulatory protein for GlnL, GlnE, and AmtB
ECSP_0519	*amtB*	-74.77	-69.89	ammonium transporter
ECSP_4793	*asnC*	-2.02	-4.62	DNA-binding transcriptional dual regulator
ECSP_4794	*asnA*	-4.97	-6.59	asparagine synthetase A
ECSP_0721	*asnB*	-7.58	-6.67	asparagine synthetase B
ECSP_2651	*cbl*	-4.79	-10.97	DNA-binding transcriptional activator of cysteine biosynthesis

Table 4 - RNA-seq transcriptome data, continued.

ECSP_2652	*nac*	-63.48	-21.56	DNA-binding transcriptional dual regulator of nitrogen assimilation
ECSP_3790	*galR*	-2.05	1.20	DNA-binding transcriptional repressor
ECSP_3791	*lysA*	-4.28	-3.59	diaminopimelate decarboxylase, PLP-binding
ECSP_3792	*lysR*	-2.77	1.65	DNA-binding transcriptional dual regulator

Metal Stress Response and Import/Export

ECSP ID	Gene	Δ*grvA*	*grvArcsB*	Description
ECSP_0334	*ykgL*	ND (+)	ND (+)	predicted protein
ECSP_0335	*rpmJ*	170.69	438.30	putative second copy of 50S ribosomal protein L36
ECSP_0336	*rpmE2*	565.67	1205.82	Zn(II)-responsive ribosomal protein
ECSP_0622	*cusS*	-1.30	-1.61	sensory histidine kinase in two-component regulatory system with CusR, senses copper ions
ECSP_0623	*cusR*	1.07	-1.79	DNA-binding response regulator in two-component regulatory system with CusS
ECSP_0624	*cusC*	-1.04	-1.67	copper/silver efflux system, outer membrane component
ECSP_0625	*cusF*	-1.79	-5.08	periplasmic copper-binding protein
ECSP_0626	*cusB*	-1.35	-5.78	copper/silver efflux system, membrane fusion protein
ECSP_0627	*cusA*	-1.41	-6.60	copper/silver efflux system, membrane component
ECSP_0731	*fur*	1.69	6.09	DNA-binding transcriptional dual regulator of siderophore biosynthesis and transport
ECSP_2430	*yebA*	4.47	11.31	predicted peptidase
ECSP_2431	*znuA*	17.68	39.94	High-affinity zinc uptake system periplasmic protein
ECSP_2432	*znuC*	2.48	6.41	High-affinity zinc uptake system ATP-binding protein
ECSP_2433	*znuB*	4.23	9.00	High-affinity zinc uptake system membrane protein

Table 4 - RNA-seq transcriptome data, continued.

ECSP_2579	*zinT*	163.75	484.95	conserved metal-binding protein
ECSP_4263	*zntR*	-1.15	-1.17	DNA-binding transcriptional activator in response to Zn(II)
ECSP_4425	*zntA*	-1.39	-3.45	zinc, cobalt and lead efflux system

Other Functions

ECSP ID	Gene	Δ*grvA*	Δ*grvA*Δ*rcsB*	Description
ECSP_1968	*ddpF*	1.10	1.80	D-ala-D-ala transporter subunit, ATP-binding component of ABC superfamily
ECSP_1969	*ddpD*	1.49	1.62	D-ala-D-ala transporter subunit, ATP-binding component of ABC superfamily
ECSP_1970	*ddpC*	1.59	-1.93	D-ala-D-ala transporter subunit, membrane component of ABC superfamily
ECSP_1971	*ddpB*	-6.55	-20.02	D-ala-D-ala transporter subunit, membrane component of ABC superfamily
ECSP_1972	*ddpA*	-28.72	-6.75	D-ala-D-a la transporter subunit, periplasmic-binding component of ABC superfamily
ECSP_1973	*ddpX*	ND (-)	-15.40	D-ala-D-ala dipeptidase, Zn-dependent
ECSP_2574	*yedV*	-1.82	-1.78	predicted sensory kinase in two-component regulatory system with YedW
ECSP_2575	*yedW*	1.00	-5.56	predicted DNA-binding response regulator in two-component system with YedV
ECSP_5434	*yjiA*	2.78	1.91	predicted GTPase
ECSP_5435	*yjiX*	27.79	25.32	conserved protein
ECSP_5436	*yjiY*	3.81	3.00	predicted inner membrane protein
ECSP_2492	-	-2.36	-16.79	hypothetical protein
ECSP_4094	-	-1.87	-25.76	hypothetical protein

[a] Protein/gene names and open reading frame (ORF) IDs based on EHEC strain TW14359 (accession #XXX, NCBI) and K-12 strain MG1655 (EcoCyc, REF).

[b] fold change calculated as either wild-type RPKM value divided by the mutant strain RPKM value.

[c] RPKM denotes Reads Per Kilobase per Million mapped reads

For inclusion, genes were selected with a fold change greater than 2 in either the single or double mutant strains. Additionally, genes that are part of an operon were included, with their respective fold change and RPKM data, if a component gene was notably altered in expression.

TW14359Δ*grvA*Δ*rcsB*, and 17 were downregulated in TW14359Δ*grvA* were upregulated in TW14359Δ*grvA*Δ*rcsB*.

In agreement with the role of GrvA in *ler* activation, 21 LEE-encoded genes were downregulated in TW14359Δ*grvA*, including *ler*, the translocon genes *espA*, *espB* and *espD*, *eaeA* (intimin) and *tir* (translocated intimin receptor) (**Table 4**; **Fig. 17**). As anticipated, LEE expression was also decreased in TW14359Δ*rcsB*Δ*grvA* compared to TW14359, but was not further decreased when compared to TW14359Δ*grvA*. Decreased transcription of *ler* in TW14359Δ*grvA* and TW14359Δ*rcsB*Δ*grvA* was validated by qRT-PCR, and complementation of *grvA* was shown to restore *ler* expression to wild-type levels (**Table 5**).

Interestingly, genes encoded within the 15 kb genomic acid fitness island (AFI), the products of which are required for survival at low pH (Foster, 2004), were upregulated in TW14359Δ*grvA* when compared to TW14359, in which the expression of AFI genes was barely detectable (**Fig. 17**; **Table 4**). Most notably, genes of the glutamate-dependent acid resistance (GDAR) system were upregulated, including *gadA*, *gadE*, *gadW*, *gadX*, and the non-AFI encoded *gadCB* operon. Increased transcription of *gadE*, encoding the central regulator of GDAR, was validated through qRT-PCR, and complementation with *grvA* was shown to restore *gadE* expression to levels observed for TW14359 (**Table 5**). While there was no difference in *gadE* and *gadW* expression between TW14359Δ*grvA* and TW14359Δ*rcsB*Δ*grvA*, the expression of *gadA*, *gadBC*, and *hde* genes was markedly reduced in TW14359Δ*rcsB*Δ*grvA* compared to TW14359Δ*grvA* (**Table 4**). This observation likely reflects the fact that RcsB directly activates transcription from the promoters of these genes as a heterodimer with GadE (Castanie-Cornet et al., 2010; Johnson et al., 2011), and suggests that the effect of *grvA* deletion on the expression of GDAR genes is independent of *rcsB*.

Table 5 - qRT-PCR validation of RNA-seq data

Strain	**Expression Units**[a]			
Gene[b]**:**	***ler***	***gadE***	***astC***	***znuA***
TW14359	1054.77 (51.81)	0.18 (0.06)	111.56 (1.55)	8.02 (2.34)
Δ*grvA*	78.28 (21.68)	61.11 (8.22)	1.21 (0.67)	551.15 (150.90)
Δ*rcsB*Δ*grvA*	127.97 (33.65)	87.87 (4.10)	2.5 (1.49)	622.03 (46.05)
Δ*grvA* p*grvA*	556.98 (180.36)	12.94 (0.81)	6.87 (2.24)	20.46 (8.28)

[a] Expression units for each gene were calculated relative to *rrsH* expression, and standard deviation is in parentheses.

[b] Gene names IDs based on EHEC strain TW14359 (accession #NC_013008.1, NCBI)

Table 5: qRT-PCR validation of RNA-seq data
Select genes (*ler*, *gadE*, *astC*, and *znuA*) were validated through qRT-PCR from exponential phase (OD_{600}=0.5) DMEM cultures. Numbers represent the expression units for each gene in the noted strain, with the standard deviation listed adjacently in parentheses. Each value represents the average of three independent experiments (n=3).

Genes for zinc binding, transport and resistance to zinc and other metals including *znuA*, *znuCB*, *zinT* (formerly *yodA*), *rpmE2*, *rpmJ*, *ykgL*, and *yebA* (Ferianc et al., 1998; Hensley et al., 2012; Kershaw et al., 2007) were upregulated in TW14359Δ*grvA* and TW14359Δ*rcsB*Δ*grvA* compared to TW14359 (**Fig. 17**, **Table 4**); for *rpmE2*, expression was increased by >500-fold in TW14359Δ*grvA* and TW14359Δ*rcsB*Δ*grvA*. Increased expression of *znuC*, encoding a high affinity zinc uptake protein, was validated by qRT-PCR, and expression was restored with complementation (**Table 5**). This data indicates that GrvA controls several genes, including those involved in colonization and acid resistance, but also includes a number of genes which are not associated with virulence directly.

3.3.3 GrvA/GadE control of *ler* and adherence to HT-29 colonic epithelial cells

RNAseq analysis revealed that deletion of *grvA* leads to the de-repression of *gadE*, a recognized transcriptional repressor of the LEE-encoded regulator, *ler* (Kailasan Vanaja et al., 2009). It was thus of interest to determine if this interaction between *grvA* and *gadE* was the underlying mechanism by which GrvA controls LEE expression and influences adherence. In TW14359Δ*grvA*, *ler* expression was observed to be significantly reduced compared to TW14359 and TW14359Δ*gadE* ($p<0.05$), but was increased to near wild-type levels in TW14359Δ*grvA*Δ*gadE* (**Fig. 18A**). In addition, complementation of TW14359Δ*grvA*Δ*gadE* with *gadE* constitutively expressed restored *ler* transcript levels to that observed for TW14359Δ*grvA*. These findings are in agreement with GadE dependent repression of *ler*, and support a hypothesis in which GrvA activation of *ler* is directed through the repression of *gadE*.

The effect of *grvA* and *gadE* interaction on *in-vitro* adherence was determined by a competition assay. Strains were co-incubated in a 1:1 ratio with HT-29 intestinal cells, followed

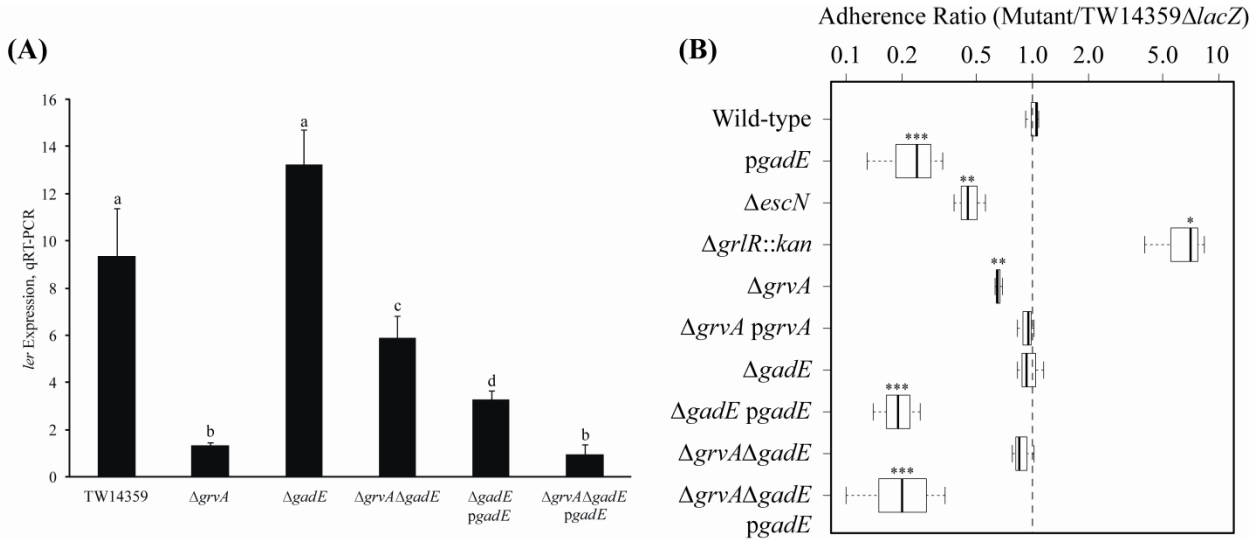

Figure 18 - Analysis of the gadE dependent GrvA regulation of *ler* and competitive adherence to HT-29 colonic epithelial cells

(A) *ler* transcript levels plotted for TW14359, TW14359Δ*grvA*, TW14359Δ*gadE*, TW14359Δ*grvA*Δ*gadE*, complement strain TW14359Δ*gadE* p*gadE*, and complement strain TW14359Δ*grvA*Δ*gadE* p*gadE* grown in DMEM (OD_{600}=0.5). Plots which differ by lower case letter, differ significantly by Tukey's HSD following a significant F-test ($p<0.05$, $n\geq3$). Error bars denote standard deviation. (B) Competitive adherence to confluent monolayers of HT-29 colonic epithelial cells was determined for each strain; adherence was assessed for cultures following 3 hours of co-incubation with HT-29 cells and EHEC strains mixed in a 1:1 ratio with TW14359Δ*lacZ*. Bars represent the ratio of CFU/ml recovered for the strain indicated divided by the CFU/ml of TW14359Δ*lacZ*, as determined by serial dilution and enumeration on MacConkey agar. Asterisks denote significance compared with TW14359, as determined using the Student's t-test (*, $p<0.05$; **, $p<0.01$; ***, $p<0.001$); Error bars denote standard deviation.

by plating and enumeration on MacConkey differential media. The control strain (TW14359Δ*lacZ*) was Lac-, and thus colonies on MacConkey were white, whereas test strains (TW14359 and mutant derivatives) were Lac+, and colonies were thus pink. An adherence index was determined for each test strain from plate counts as the ratio of CFU/ml for the test strain relative to TW14359Δ*lacZ*.

Consistent with the effect of *grvA* and *gadE* interaction on LEE expression, the adherence index of TW14359Δ*grvA* was significantly decreased when compared to TW14359, TW14359Δ*gadE*, and *grvA* complemented strain TW14359Δ*grvA* p*grvA* ($p<0.05$) (**Fig. 18B**). In strains where *gadE* was expressed constitutively *in-trans* (plasmid p*gadE*), the adherence index was uniformly reduced to levels lower than in all other strains, including TTSS-defective strain TW14359Δ*escN* ($p<0.001$) (**Fig. 18B**). These experiments reveal that GrvA-dependent regulation of *ler* and adherence to intestinal cells is dependent on an intact *gadE* gene and are in agreement with a hypothesis in which control of the LEE and LEE-dependent adherence by GrvA is directed through the repression of *gadE*.

3.3.4 Effect of *grvA* mutation on *gadE* promoter activity

GadE is a negative regulator of LEE expression, acting directly on the *LEE1* promoter to repress *ler* transcription (Kailasan Vanaja et al., 2009; Tree et al., 2011). Since GrvA requires *gadE* for LEE activation, it was of interest to define *cis* elements of the *gadE* promoter region, which encompasses over 1-kb of DNA upstream of the ORF, needed for this control. To determine this, transcription from four different *gadE* promoter *lacZ* reporter constructs (**Fig. 19A bottom**) in TW14359 and TW14359Δ*grvA* were compared during exponential and stationary phase growth in DMEM. During exponential growth, transcription from $gadE_{P1\text{-}P3}$-*lacZ* containing

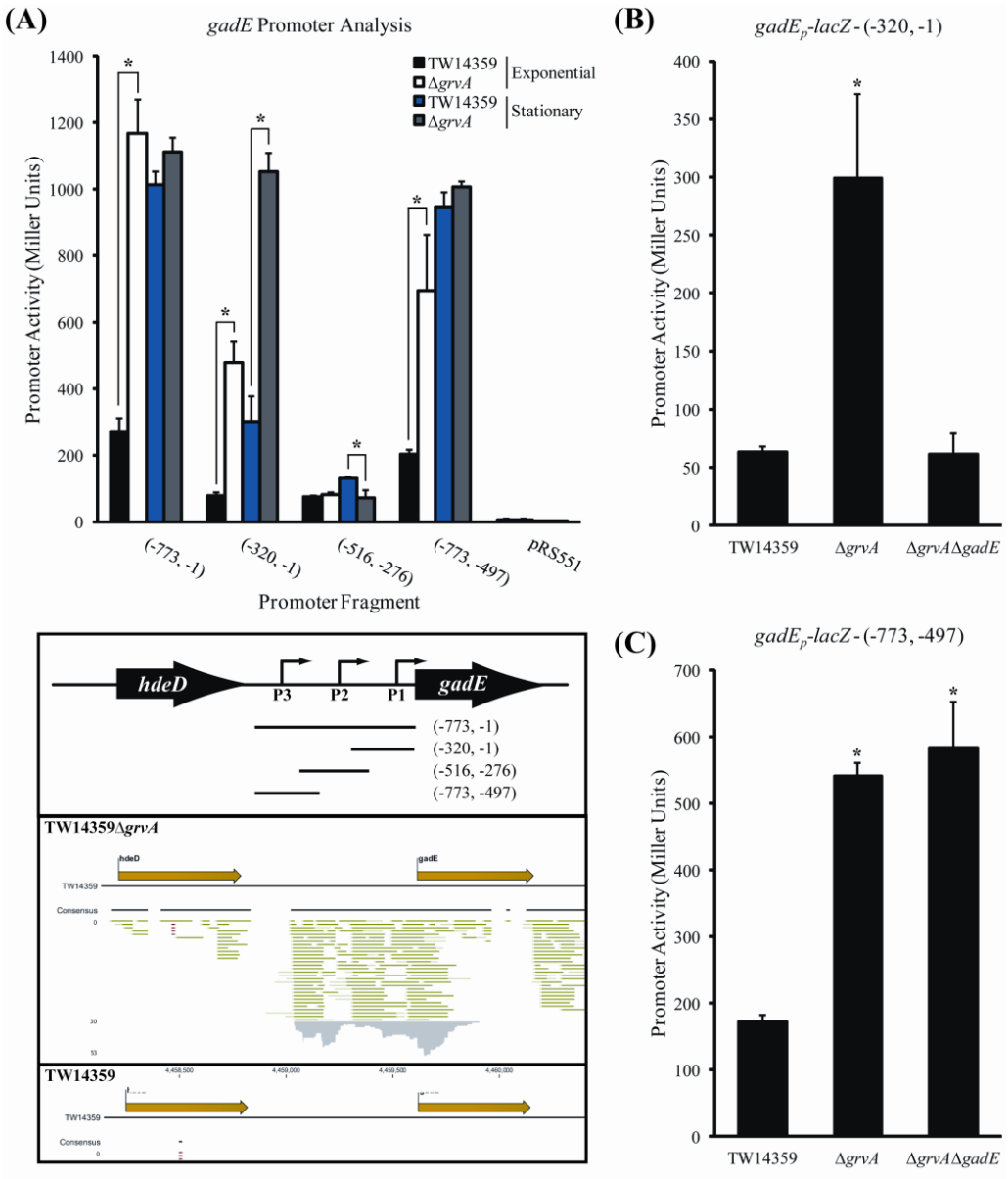

Figure 19 - Investigating the individual contribution of *gadE* promoters using promoter *lacZ* fusions

β-galactosidase activity in Miller Units for TW14359 and mutant derivatives containing a $gadE_P$-*lacZ* fusion during growth in DMEM. (A) (top) Activity measured at an OD_{600}=0.5 (exponential phase) and OD_{600}=2 (stationary phase) for TW14359 and TW14359Δ*grvA*. (bottom) Relative location of amplified P1, P2, P3, and P1P2P3 *gadE* promoter fragments, with location of individual promoters indicated with black arrows; relative location of mapped RNA-seq transcripts are aligned roughly with their relative position in the above *gadE* promoter diagram. (B and C) Activity measured at an OD_{600}=0.5 (exponential phase) for TW14359, TW14359Δ*grvA*, and TW14359Δ*grvA*Δ*gadE* with a *gadE* promoter fusion containing the P1 and P3 fragments, respectively. Asterisks denote significance by a Student's t-test ($p<0.05$, $n\geq3$). Error bars indicate standard deviation for all panels.

all three (P1 though P3) *gadE* promoters was significantly increased in TW14359Δ*grvA* compared to TW14359 (p=0.002) (**Fig. 19A**). Promoter activity from fragments containing the P1 (*gadE*$_{P1}$-*lacZ*) or P3 (*gadE*$_{P3}$-*lacZ*) promoters alone were also significantly higher in TW14359Δ*grvA* (p<0.05), while activity from the fragment containing only the P2 promoter (*gadE*$_{P2}$-*lacZ*) did not differ between TW14359Δ*grvA* and TW14359. As anticipated, promoter activity from all fragments increased significantly during stationary growth for TW14359 (p<0.001), however only slightly for P2 (p<0.001) (**Fig. 19A**). For TW14359Δ*grvA*, promoter activity only further increased from P1 during stationary phase (p=0.015), and was higher than P1 activity in TW14359. This latter observation was predicted to be due to auto-activation of the P1 promoter by GadE, as previously shown (Ma et al., 2004). Indeed, the deletion of *gadE* in TW14359Δ*grvA* completely abrogated P1 activation during exponential growth, but had no effect on P3 activity (**Fig. 19B** and **19C**). Based on these findings it is predicted that GrvA-dependent repression of *gadE* transcription is directed solely through the P3 promoter.

Transcription from the *gadE* P3 promoter is directly controlled by the AFI encoded regulators GadX and GadW (Sayed et al., 2007), and RNAseq analysis of TW14359Δ*grvA* revealed both genes to be elevated in expression when compared to TW14359 (**Table 5**). It was thus suspected that repression of P3 by GrvA was mediated through one or both of these regulators. To test this, the effect of *gadX* and *gadW* deletion in TW14359Δ*grvA* on P3 activity during exponential growth (OD_{600}=0.5) in DMEM was measured. Only the deletion of *gadW* was observed to reduce transcription from P3. Activity from P3 in TW14359Δ*gadW* and TW14359Δ*grvA*Δ*gadW* was reduced significantly compared to TW14359Δ*grvA* (p=0.01 and 0.03, respectively), but not when compared to TW14359 (**Fig. 20**). Conversely, P3 activity was

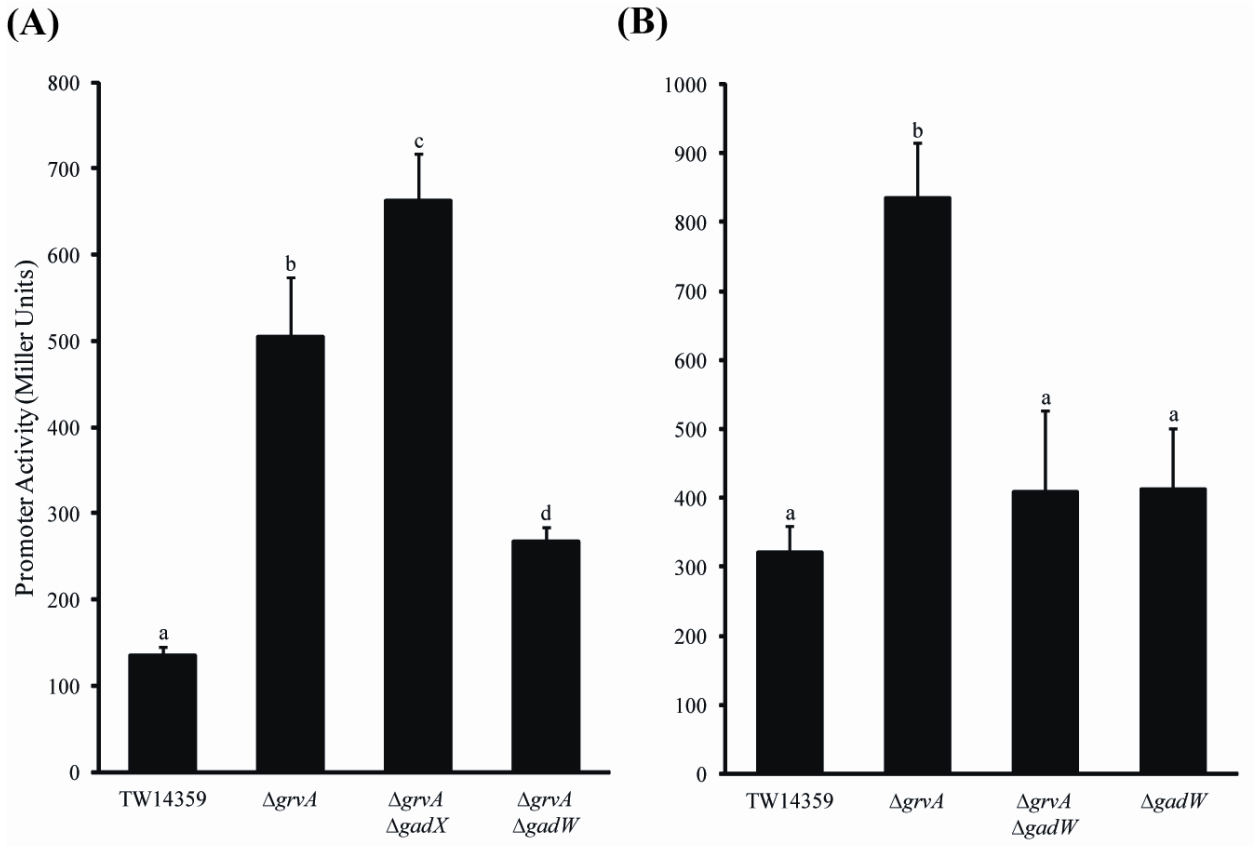

Figure 20 - Investigating the contribution of GadX and GadW to increased *gadE* promoter activity
β-galactosidase activity in Miller Units for TW14359 and mutant derivatives containing a $gadE_{P3}$-*lacZ* fusion during growth in DMEM. Activity measured at an OD_{600}=0.5 (exponential phase) for either (A) TW14359, TW14359Δ*grvA*, TW14359Δ*grvA*Δ*gadX*, and TW14359Δ*grvA*Δ*gadW* or (B) TW14359, TW14359Δ*grvA*, TW14359Δ*grvA*Δ*gadW*, and TW14359Δ*gadW* with a *gadE* promoter fusion containing the P3 fragment. Plots which differ by lower case letter, differ significantly by Tukey's HSD following a significant F-test ($p<0.05$, n=3). Error bars denote standard deviation.

slightly but significantly increased in TW14359Δ*grvA*Δ*gadX* when compared to TW14359Δ*grvA* (p=0.01) (**Fig. 20**). Taken together, this data indicates that GrvA indirectly represses transcription from the *gadE* P3 promoter during exponential growth in a manner that is dependent on *gadW*.

3.3.5 Acid Resistance experiments in TW14359 and *grvA* mutant strains

The expression of glutamate-dependent acid resistance (GDAR) genes is growth phase dependent; it is low during exponential growth and increases markedly as cells transition into stationary phase (Castanie-Cornet et al., 1999). Correspondingly, exponential phase cultures are generally acid susceptible, while stationary phase cultures are acid resistant. Since deletion of *grvA* was shown to de-repress the GadW pathway activating *gadE* during exponential growth (**Table 4**), the contribution of GrvA to the GDAR was determined for exponential cultures and was compared to that of the GDAR phenotype of stationary phase cultures.

As expected, no colonies of wild-type TW14359 could be recovered on LBA after a 1 h exposure of exponential cultures to acidified EG media (pH 2) (**Fig.21A**). However for strain TW14359Δ*grvA*, in which GDAR genes are de-repressed during exponential growth, 400 CFU/ml were recovered, representing 9% of the original inoculum. Complementation of TW14359Δ*grvA* with *grvA* restored wild-type levels of acid sensitivity (**Fig. 21A**). While GDAR genes are upregulated in TW14359Δ*grvA* during exponential growth, the deletion of *rcsB* in TW14359Δ*grvA* counteracts this effect for GDAR structural genes *gadA* and *gadBC* (**Fig. 17**). Decreased expression of these genes in TW14359Δ*grvA*Δ*rcsB* was shown to correspond with a complete loss of the GDAR phenotype during exponential growth in DMEM (**Fig. 21A**).

Complementation with *rcsB* expressed from a low-copy vector and under the control of

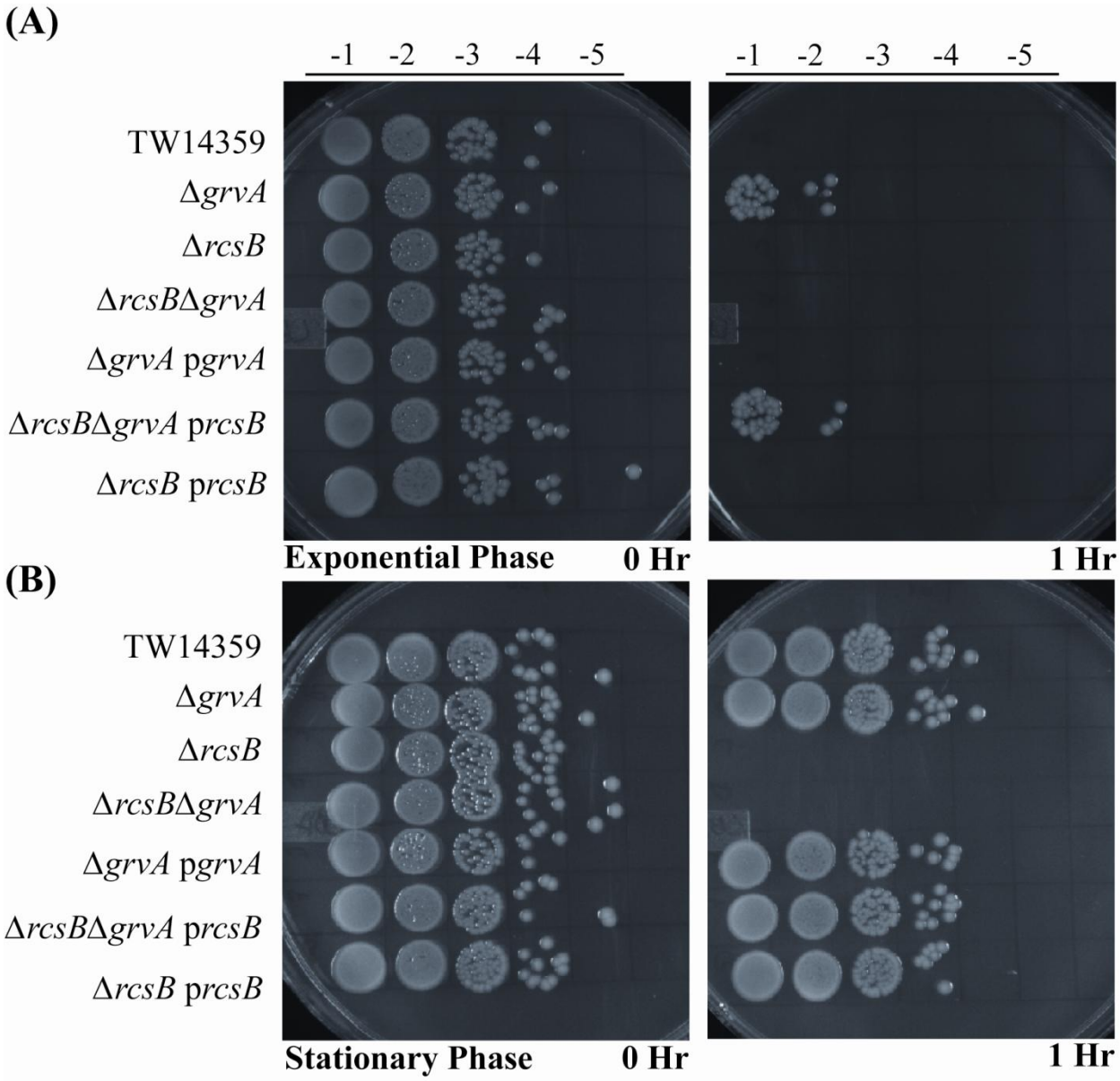

Figure 21 - GrvA dependent exponential phase acid resistance phenotype
Representative experiments for acid resistance in TW14359 and mutant derivative strains during exponential (top) and stationary (bottom) growth. Each plate represents 10-fold microdilutions of control or acid challenged (pH 2.0) samples for each strain before and after acid challenge for 1 hour.

its native promoters restored GDAR in TW14359Δ*grvA*Δ*rcsB*, but not in TW14359Δ*rcsB*, suggesting that expression of the phenotype requires an *rcsB*+ *grvA*$^{-}$ background. During stationary phase, deletion and complementation of *grvA* had no effect on survival in acid with 100% of the initial inoculum being recovered following a 1 h challenge, suggesting that regulation of GDAR genes by GrvA is relegated to exponential phase (**Fig. 21B**). For TW14359Δ*rcsB* and TW14359Δ*grvA*Δ*rcsB* however, no colonies were recovered following acid challenge, while complementation of these mutants with *rcsB* restored wild-type levels of GDAR. This effect of *rcsB* deletion on acid resistance is consistent with its role as an activator of GDAR in both exponential and stationary phase cultures (Johnson et al., 2011). Interestingly however, overexpression of *rcsB* has also been determined to indirectly repress GDAR genes *gadE*, *gadX* and *gadW* (Castanie-Coronet et al 2010). Since *rcsB* overexpression also leads to *grvA* upregulation (Tobe et al., 2005), it is plausible that this negative regulation of GDAR requires the interaction of RcsB and GrvA.

3.4 Discussion

In this study, we examined the TW14359 transcriptome and defined the RcsB-GrvA transcriptome using RNA sequencing, and identified a novel pathway for LEE gene regulation in EHEC. RNA sequencing has been performed with *E. coli* strains in the past, with the commensal MG1655 and the pathogenic EHEC O157:H7 strain Xuzhou21 (Haas et al., 2012; Zhao et al., 2013). Both previous studies were from cultures grown LB media, which is not ideal for examination of LEE gene transcription. In this study, cultures were grown in DMEM supplemented with sodium bicarbonate, conditions known to induce LEE gene expression. And, in agreement with previous accounts of differential gene expression in LB and DMEM (Iyoda et

al., 2006; Tobe et al., 2011), flagellin (*fliC*) was among the most abundant transcripts detected for LB cultures in the aforementioned studies, while motility associated genes were barely detected in our analysis of exponentially growing cultures in DMEM. This observation is congruent with previous work demonstrating increased transcription of genes promoting colonization in DMEM, such as those encoding the *E. coli* common pilus (ECP) and long-polar fimbriae (LPF) (Rendon et al., 2007; Torres et al., 2002). Thus, the results of this study provide insight into the regulatory interplay of the RcsB-GrvA-GadE pathway in conditions which favor colonization, and importantly, transcription of the LEE pathogenicity island.

Transcription of the *rcsDB* and *grvAB* operons was shown to be maximal during growth in DMEM containing 44 mM bicarbonate. *grvAB* is growth phase dependent, indicating tight transcriptional regulation. Previous reports, and our own analyses, have demonstrated that RcsB activates *grvA* transcription from cultures grown at 37°C (Morgan et al., 2013; Tobe et al., 2005). However, a recent report on curli variants in a 1993 hamburger-associated EHEC outbreak strain demonstrated decreased transcription of *grvA* following the repair of a strain specific *rcsB* deletion mutation (Carter et al., 2012). Possible explanations for this disparity may include differences in the experimental conditions employed, specifically growth at 28°C. In support of this, in EHEC strain Sakai, *grvAB* transcription was reported to be decreased following transition to growth at both 25°C and 14°C compared to growth at 35°C (Kocharunchitt et al., 2012). These observations suggest that regulation of *grvAB* at low temperatures may be different from that at physiological temperatures. Importantly, the predicted *grvAB* promoter contains putative RcsAB binding sites upstream of the -35 site, indicating direct transcriptional regulation by at least RcsB. Indeed, purified RcsB was able to shift the *grvA* promoter fragment containing the predicted consensus sequences, validating direct

transcriptional regulation of *grvA* by RcsB alone. It is therefore possible that, during low temperature growth conditions which do not favor Lon-dependent RcsA proteolysis (Torres-Cabassa and Gottesman, 1987), an RcsAB heterodimer may bind at the *grvA* promoter to repress transcription, but at physiological growth temperatures RcsB alone acts as a transcriptional activator. Such a model of transcriptional regulation exists for RcsAB potentiated repression of the *flhDC* promoter (Francez-Charlot et al., 2003). However future work is required to define the specific regulatory factors functioning at the predicted *grvAB* promoter.

Importantly, our data revealed substantially increased transcription of genes involved in acid fitness and metal stress in mutants for strains TW14359Δ*grvA* and TW14359Δ*rcsB*Δ*grvA*. Interestingly, transcription of genes involved in zinc import and acquisition, such as *znuA* and *zinT*, was substantially higher in both mutant strains. Modulation of zinc fitness was of particular interest as zinc has been shown to have a negative effect on type III secretion in EPEC and EHEC (Mellies et al., 2012) and, importantly, to inhibit Stx production (Crane et al., 2011). Previous reports have revealed ZinT as being required for curli production in zinc limiting conditions (Lim et al., 2011), and EHEC *znuA* mutants were deficient in adherence to Caco-2 cells, where a *zinT* mutation alone did not result in decreased adherence (Gabbianelli et al., 2011). Thus, it is clear that alterations in zinc acquisition and export can have pleiotropic effects on EHEC adherence, through direct or indirect means. One possibility is that GrvA effects basal levels of zinc through a metabolic pathway and indirectly contributes to cytosolic zinc transport and export. In such a model, GrvA could indirectly regulate the transcription of Zur-dependent genes, and subsequently alter colonization and pathogenesis through subtle changes in cytosolic zinc concentrations. Interestingly, the Rcs phosphorelay has been shown to be activated by the presence of 1 mM $ZnCl_2$ (Hagiwara et al., 2003), suggesting an even more complex regulatory

relationship between RcsB, GrvA, and the zinc stress response in EHEC. However, this potential regulatory relationship was not examined in this study.

The RNA-seq data also revealed increased transcription of genes encoded within the AR2 acid fitness island, including the transcriptional regulator *gadE* that activates the glutamate-dependent acid resistance (GDAR) system. Importantly, GadE has been shown to repress *LEE1* transcription following overproduction (Kailasan Vanaja et al., 2009), and is able to bind directly to the *LEE1* and *LEE2*/*3* promoters in-vitro (Tree et al., 2011). This is particularly salient in light of recent studies identifying three EHEC specific prophage encoded regulators (PsrA/ PsrB, and PatE) that activate transcription of *gadE* and *hdeA* to direct repression of both the *LEE1* and *LEE2*/*3* operons and modulate acid fitness (Bender et al., 2012; Tree et al., 2011). Conversely, a recent study has suggested that GadE and GadX both negatively regulate the LEE indirectly following exposure to nitric oxide stress (Branchu et al., 2014). Our data suggests that GrvA plays an antagonistic role in regulating the LEE, through *gadE*, to promote transcription of the LEE during early exponential growth. A report in *Salmonella* described a reverse phenotype following expression of *mart-fidL* (a *grvAB* operon homolog) from *S. typhimurium* in *S. typhi*, which lacks the *mart-fidL* genes, where expressing the *marT-fidL* operon in *S. typhi* reduced acid resistance (Retamal et al., 2010). In this study, mutation of *grvA* resulted in increased glutamate-dependent acid resistance (GDAR), but was completely dependent on an intact *rcsB* gene. This finding is markedly consistent with previous accounts of RcsB-dependent activation of several key GadE regulated GDAR genes (Johnson et al., 2011). Thus, while GrvA mediated regulation of exponential phase glutamate-dependent acid resistance through is wholly dependent on RcsB, GrvA regulation of the LEE is independent of RcsB.

Based on the results of this study it is predicted that the $gadE_{P3}$ promoter is likely the target for transcriptional repression by GrvA, either direct or indirect. Indeed, the mapped reads from TW14359Δ*grvA* RNA sequencing correlate well with the mapped location of the $gadE_{P3}$ promoter. This finding was of interest as the previously identified AraC-family prophage encoded regulators PsrA and PsrB bind directly to the $gadE_{P3}$ promoter region to stimulate transcription of *gadE* following attachment (Tree et al., 2011). The 750-bp region upstream of *gadE* contains 3 mapped promoters (P1, P2, and P3) and has been termed a sensory integration region (Sayed and Foster, 2009). Indeed, there exists a complex cascade of regulatory factors that collapse at one or more of the *gadE* promoters to modulate acid resistance in response to growth phase and nutritional availability (Aiso et al., 2011; Ma et al., 2004; Sayed et al., 2007). In this study, during exponential growth, wild-type transcription arising from the $gadE_{P3}$ promoter is repressed activated following deletion of *grvA*. Thus, our results extend the temporal regulation of this region during exponential growth, and further validate GadE auto-regulation at the $gadE_{P1}$ promoter. However, attempts to validate direct binding of GrvA at the *gadE* promoter were unsuccessful (data not shown), suggest that its regulatory effects are indirect.

While both *gadX* and *gadW* were more highly transcribed in TW14359Δ*grvA*, *gadX* transcription in TW14359Δ*grvA*Δ*rcsB* was lower than the isogenic *grvA* mutant alone, but still higher than wild type TW14359. This observation is agreement with RcsB mediated transcriptional activation of the *gadE* independent *gadX* promoter (Johnson et al., 2011). Loss of *gadW* abrogated the increased $gadE_{P3}$ promoter activity observed in TW14359Δ*grvA*, while activity in TW14359Δ*gadX* was not similarly reduced. Therefore, it is proposed that GrvA mediated regulation of acid resistance genes occurs through a GadW-GadE pathway. Transcription of *gadW* can arise from one of two mapped promoters (Tramonti et al., 2008),

though our RNA sequencing data suggests that in TW14359Δ*grvA*, during exponential growth, only the $gadW_{P1}$ promoter is actively transcribed. This is not surprising, as the *gadX* and *gadW* promoters are under complex transcriptional and post-transcriptional regulation (Giangrossi et al., 2005; Sayed et al., 2007; Tramonti et al., 2008). Further analysis is required to determine if GrvA regulation of *gadW* transcription is direct, or if it is functioning through an additional factor to influence transcriptional repression of *gadW*. Because increased *grvAB* transcription was observed during lag and early exponential growth, it is possible that GrvA is required for full repression of *gadE* transcription through *gadW* following transition from stationary to active growth. Such a regulatory pathway would ensure that AFI encoded regulators, such as GadE, are efficiently repressed during periods when adherence is advantageous.

We further went on to show that GrvA mediated activation of *ler* transcription is at least partly dependent on an intact *gadE* gene, establishing a pathway for LEE gene regulation. The possibility remains that one or more additional factors are controlling LEE gene repressing in the absence of GrvA, such as cytosolic zinc levels (discussed above). Competitive adherence assays revealed a dependence on *gadE* for *grvA* mediated regulation of adherence to HT-29 epithelial cells. Interestingly, attempts to complement and express *gadE* ectopically resulted in adherence that was reduced to levels lower even than the TTSS deficient strain TW14359Δ*escN*. One explanation for this observation is that, while loss of *escN* abrogates type III secretion, LEE encoded regulatory genes remain intact. It is possible that some adhesin, under the control of *ler*, is transcriptionally altered by overexpression of *gadE*. Indeed, *lpf* genes, encoding long polar fimbriae, are known to be positively regulated by *ler* (Torres et al., 2007), and could partially account for the disparity.

The 32-kb O-island (OI-47) encoding the *grvAB* operon remains largely uncharacterized. The *vmpA* gene immediately downstream of *grvAB*, encoded in the opposite direction, was recently characterized and encodes a c-di-GMP phosphodiesterase that contributes to biofilm formation and motility in EHEC strain EDL933 (Branchu et al., 2013). Mutation or overexpression of *grvA* was not observed to effect motility in TW14359 (data not shown). The remaining OI-47 genes are functionally diverse, encoding a predicted pilus, adhesin, and usher protein (sharing amino acid homology to the *Klebsiella* Mrk pilus proteins), a predicted hemolysin-like protein, and proteins predicted to be involved in fatty-acid biosynthesis. A CDART search (NCBI) (Geer et al., 2002) of GrvA identified an N-terminal DNA-binding winged HTH-domain and a predicted C-terminal methylenetetrahydrofolate reductase (MTHFR) domain, including a predicted FAD binding domain. The N-terminal domain is predicted to be localized to the periplasmic space, and the C-terminal, DNA-binding domain, is predicted to be located in the cytoplasm. Whether any or all of the OI-47 component genes share regulatory cues or biological functions, or if they are independent of one another, remains to be explored. It is interesting to speculate on the potential for periplasmic FAD activation of GrvA. Additionally, while GrvB shares homology with ToxS, its contribution to GrvA regulation and potential dimerization requires further analysis.

To conclude, we propose a model where, following gastric passage, bicarbonate stimulates activation of the Rcs phosphorelay and transcription of *rcsB*. Subsequent high levels of RcsB directly positively regulate transcription of the *grvAB* operon. As GrvA is activated, transcription of genes associated with acid resistance and gastric passage are down-regulated, and subsequent LEE gene transcription is stimulated to promote colonization. Work remains to be done to establish whether GrvA is indeed a membrane bound regulator and if it binds directly

to the *gadW* promoter. It is also of interest to explore the contribution, if any, of YqeI to virulence and fitness gene regulation in EHEC and other pathogenic *E. coli* strains.

Table 6 - Strains and plasmids used in Chapter 3

Strain/plasmid	Relevant characteristics	Reference
Strain name:		
DH5α	Vector propagation, *recA1 endA1*	
BL21(DE3)pLysS	BL21 with IPTG inducible T7 polymerase	Pan, 2000
MG1655	F-, lambda-, *rph*-1	
E2348/69	*Escherichia coli* O127:H6; (typical EPEC)	Iguchi, 2009
3256-97	*Escherichia coli* O55:H7; (atypical EPEC)	Zhou, 2010
TW14359	WT 2006 outbreak, western U.S.A.	Manning, 2008
EcRJM-1	TW14359Δ*escN*	Morgan, 2013
EcRJM-6	TW14359Δ*rcsB*	Morgan, 2013
EcRJM-10	TW14359*rcsB*-FLAG	Morgan, 2013
EcRJM-11	TW14359Δ*grvA*	Morgan, 2013
EcRJM-12	TW14359Δ*rcsB* Δ*grvA*	Morgan, 2013
EcRJM-13	TW14359*tir*-FLAG	Morgan, 2013
EcRJM-35	TW14359Δ*grlR::kan*	Morgan, 2013
EcRJM-72	TW14359Δ*rcsB* pRJM20	Morgan, 2013
EcRJM-73	TW14359Δ*lacZ*	This study
EcRJM-74	TW14359 pRJM-23	This study
EcRJM-75	TW14359 pRJM-24	This study
EcRJM-76	TW14359 pRJM-25	This study
EcRJM-77	TW14359 pRJM-26	This study
EcRJM-78	TW14359Δ*grvA* pRJM-23	This study
EcRJM-79	TW14359Δ*grvA* pRJM-24	This study
EcRJM-80	TW14359Δ*grvA* pRJM-25	This study
EcRJM-81	TW14359Δ*grvA* pRJM-26	This study
EcRJM-82	TW14359Δ*grvA*Δ*gadE::kan* pRJM-24	This study
EcRJM-110	TW14359Δ*grvA*Δ*gadE::kan* pRJM-26	This study
EcRJM-83	TW14359Δ*grvA* pRJM-22	This study
EcRJM-84	TW14359Δ*rcsB*Δ*grvA* pRJM-22	This study
EcRJM-85	TW14359Δ*rcsB*Δ*grvA* pRJM-20	This study
EcRJM-86	TW14359 *rcsDB-luxE*	This study
EcRJM-87	TW14359 *grvAB-luxE*	This study
EcRJM-88	TW14359 *rcsDB-luxE* pluxCDAB3	This study
EcRJM-89	TW14359 *grvAB-luxE* pluxCDAB3	This study
EcRJM-90	TW14359Δ*gadE::kan*	This study
EcRJM-91	TW14359Δ*grvA*Δ*gadE::kan*	This study
EcRJM-92	TW14359Δ*gadE::kan* pRJM30	This study
EcRJM-93	TW14359Δ*grvA*Δ*gadE::kan* pRJM30	This study
EcRJM-94	TW14359*zinT*-FLAG::*kan*	This study
EcRJM-95	TW14359Δ*grvA zinT*-FLAG::*kan*	This study
EcRJM-96	TW14359 pRJM-31	This study
EcRJM-97	EPEC E2348/69 pRJM-31	This study
EcRJM-98	MG1655 pRJM-31	This study

[a] Nucleotide positions based on the published TW14359 (NC_013008) genome sequences (NCBI)

Table 6 Strains and plasmids used in Chapter 3, continued.

Strain/plasmid	Relevant characteristics	Reference
EcRJM-99	DH5α pRJM-31	This study
EcRJM-100	TW14359 pRJM-32	This study
EcRJM-101	EPEC E2348/69 pRJM-32	This study
EcRJM-102	MG1655 pRJM-32	This study
EcRJM-103	DH5α pRJM-32	This study
EcRJM-104	TW14359 *rcsDB-luxE* pluxCDAB3 pRJM-21	This study
EcRJM-105	TW14359 *grvAB-luxE* pluxCDAB3 pRJM-21	This study
EcRJM-106	TW14359Δ*grvA* pRJM-23	This study
EcRJM-107	TW14359Δ*grvA* pRJM-24	This study
EcRJM-108	TW14359Δ*grvA* pRJM-25	This study
EcRJM-109	TW14359Δ*grvA* pRJM-26	This study
Plasmid name:		
pACYC177	Low copy cloning vector, Amp^R Kan^R P15A	Chang, 1978
pBAD22	Ara inducible expression vector, Amp^R M13	Guzman, 1995
pMPM-A2	Low copy cloning vector, Amp^R pMB1/f1	Mayer, 1995
pMPM-K3	Low copy cloning vector, Kan^R p15A/f1	Mayer, 1995
pMPM-T3	Low copy cloning vector, Tet^R p15A/f1	Mayer, 1995
pUC19	High copy cloning vector, Amp^R pMB1	Yanisch-Perron, 1985
pRS551	*lac* fusion vector, Amp^R Kan^R *lacZ*$^+$ ColE1	Simons, 1987
pCP20	Flp recombinase expression vector	Datsenko, 2000
pKD4	Template plasmid for Kan cassette	Datsenko, 2000
pKM208	Red-recombinase expression vector	Datsenko, 2000
pET-24d	T7 promoter, His tag vector, Kan^R f1, pBR322	Novagen
pSU312	FLAG epitope template, Amp^R, Kan^R, R6K	Uzzau, 2001
pRJM-20	pACYC177-*rcsB*	Morgan, 2013
pRJM-33	pACYC177-*grvAB*	This study
pRJM-21	pMPM-K3-*rcsDB*	This study
pRJM-22	pMPM-A2-*grvA*	This study
pRJM-23	pRS551-$gadE_p$(-773,-1)	This study
pRJM-24	pRS551-$gadE_p$(-320,-1)	This study
pRJM-25	pRS551-$gadE_p$(-516,-276)	This study
pRJM-26	pRS551-$gadE_p$(-773,-497)	This study
pRJM-27	pET-24d-6xHis-*rcsB*	This study
pRJM-28	pMPM-T3-*kan*	This study
pRJM-29	pMPM-T3-*luxE-kan*	This study
pRJM-30	pMPM-A2-*gadE*	This study
pRJM-31	pRS551-$grvA_p$(-268,+38)	This study
pRJM-32	pUC-*grvA*-6xHIS	This study
placlux8	placlux8	Shimizu, 2011
pLuxCDAB3	pLuxCDAB3	Shimizu, 2011

[a] Nucleotide positions based on the published TW14359 (NC_013008) genome sequences (NCBI)

Table 7 - Primers used in Chapter 3

Primers used in this study.

Primer name	Sequence (5'→ 3')[a]	Function/Reference
FLAG-F	gactacaaagatgacgacga	(Uzzau, 2001)
P1	gtgtaggctggagctgcttc	(Datsenko, 2000)
P2	catatgaatatcctccttag	(Datsenko, 2000)
Ler+109	CGAGAGCAGGAAGTTCAA	qRT-PCR Primer/(Mitra, 2012)
Ler+214	GTCCATCATCAGGCACAT	qRT-PCR Primer/(Mitra, 2012)
GadE +309	TGGTAAACACTTGCCCCATA	qRT-PCR Primer/(Mitra, 2012)
GadE +419	AGCGTCGACGTGATATTGCT	qRT-PCR Primer/(Mitra, 2012)
ZnuA+218	AGAACGCGGACTTAGTCGT	qRT-PCR Primer
ZnuA+309	CGTTACCTGCTTCGCTTCT	qRT-PCR Primer
AstC+419	GTCGCACGCTGTTTACTGT	qRT-PCR Primer
AstC+519	GCATGACGGATATCTGGTG	qRT-PCR Primer
GadE-320/EcoRI	CGCG**GAATTC**TCGGATTACTTTTTAACTTT	pRS551 *lacZ* promoter fusion
GadE-1/BamHI	CGCG**GGATCC**AACTTGCTCCTTAGCCGTTA	pRS551 *lacZ* promoter fusion
GadE-276/EcoRI	CGCG**GAATTC**GGTTAAATAAGTAATCCGGG	pRS551 *lacZ* promoter fusion
GadE-516/BamHI	CGCG**GGATCC**GTTTGTGATCTCTGAAGAAT	pRS551 *lacZ* promoter fusion
GadE-773/EcoRI	CGCG**GAATTC**GTCACTTGATGTGACTATGA	pRS551 *lacZ* promoter fusion
GadE-497/BamHI	CGCG**GGATCC**GCAATGTAATCAACGCCAGT	pRS551 *lacZ* promoter fusion
GrvA-268/EcoRI	CGCG**GAATTC**GGAGGATGCGTCCCGTTCTT	pRS551 *lacZ* promoter fusion
GrvA+38/BamHI	CGCG**GGATCC**GAGTTGAATCTTACTTCATC	pRS551 *lacZ* promoter fusion
LuxE-18/XhoI	CCGA**CTCGAG**GGAGGGGTAAAACAGGT	*luxE* cloning primer
LuxE+1450/BamHI	CCGA**GGATCC**TGAGAATTTCCCTCAAATTT	*luxE* cloning primer
pKD4For/SacI	GCG**GAGCTCGT**GTGTAGGCTGGAGCTGCTTC	*kan* from pKD4 primer
pKD4Rev/BamHI	CCGA**GGATCC**CATATGAATATCCTCCTTAG	*kan* from pKD4 primer
GrvA+1283/LuxE	CCACGCTTCATATGTATTTCCCACTAACAGCATTGTTGCTGGAGGGGTAAAACAGGT	*grvAB, luxE* insertion primer

[a] Restriction sites indicated by bolded nucleotides

Table 7 **Primers used in this study, continued.**

Primer name	Sequence (5'→ 3')[a]	Function/Reference
GrvA+1431/P2	CAATGGTATGTAAACAGATAAATAATT AACCAATATTGGAGTGTAGGCTGGAGCT GCTTC	*grvAB, luxE* insertion primer
RcsB+625/LuxE	ACGTTAAGTCCGGCAGATAAAGACTAA TCATCTGTAGGCCGGAGGGGTAAAACAG GT	*rcsDB, luxE* insertion primer
RcsB+838/P2	GTTTACGCCGCATCTGGCATTCAGTGCA AATGCCAGATGCGTGTAGGCTGGAGCTG CTTC	*rcsDB, luxE* insertion primer
LacZ-1/P1	GAAATTGTGAGCGGATAACAATTTCAC ACAGGATACAGCTGTGTAGGCTGGAGCT GCTTC	Deletion primer
LacZ+3115/P2	TTACACGAAATACGGGCAGACATGGCCT GCCCGGTTATTACATATGAATATCCTCC TTAG	Deletion primer
LacZ-178/FVal	CGATTCATTAATGCAGCTGG	Deletion validation
LacZ+3,263/RVal	CCCGTATCACTTTTGCTGAT	Deletion validation
EtpD-43/P1	GCATTTATTGCTGTAGGAGAAAACTGAT TGTTCAGGAAATGTGTAGGCTGGAGCTG CTTC	Deletion primer
EtpD+1,993/P2	CTGTACTACTCTGCTCAAGGGGACGTGA TTCACTGACATTCATATGAATATCCTCC TTAG	Deletion primer
EtpD-122/FVal	GGCGCAGCAGATAATGAAGC	Deletion validation
EtpD+2,077/RVal	GTGTCCTCCATGCAGAACAC	Deletion validation
GadE+35/P2	TACAGGGCTTTTGGCAGTTGAAAGATAA TCACGAAATGATCATATGAATATCCTC CTTAG	Deletion primer
GadE+521/P1	TAAGATGTGATACCCAGGGTGACGATGT CGCTCATACGTCGTGTAGGCTGGAGCTGC TTC	Deletion primer
GadE-74/FVal	CAACGATTCGGACAAGGATG	Deletion validation
GadE+590/RVal	ATGAAATCAGCATCTGCATC	Deletion validation
GadE-763/XbaI	CCGA**TCTAGA**GTGACTATGATCCGATTA ATACTCTCTCCG	pMPM-A2 cloning primer
GadE+577/BamHI	CCGA**GGATCC**CTGCATCCCTCGTCATGCC AGCCATCAATT	pMPM-A2 cloning primer
RcsB-3732/BamHI	CCGA**GGATCC**CTATTTCACAAATAATT AACATCAGCATAA	pMPM-K3 cloning primer
RcsB+794/XbaI	CCGA**TCTAGA**CTGACGCGTCTTATCTGGC CTACTTTAATG	pMPM-K3 cloning primer
GrvAB-679/BamHI	CCGA**GGATCC**CTGCTCCTTATGAGTAAGT AATATTTAAGGG	pACYC177 cloning primer

[a] Restriction sites indicated by bolded nucleotides

Table 7 **Primers used in this study, continued.**

Primer name	Sequence (5'→ 3')[a]	Function/Reference
GadE+577/BamHI	CCGA**GGATCC**CTGCATCCCTCGTCATGCC AGCCATCAATT	pMPM-A2 cloning primer
RcsB-3732/BamHI	CCGA**GGATCC**CTATTTCACAAATAATT AACATCAGCATAA	pMPM-K3 cloning primer
RcsB+794/XbaI	CCGA**TCTAGA**CTGACGCGTCTTATCTGGC CTACTTTAATG	pMPM-K3 cloning primer
GrvAB-679/BamHI	CCGA**GGATCC**TGCTCCTTATGAGTAAGT AATATTTAAGGG	pACYC177 cloning primer
GrvAB+1417 /XhoI	CCGA**CTCGAG**CAGATAAATAATTAACC AATATTGGAATGG	pACYC177 cloning primer
GrvA-268/XhoI	CCGA**CTCGAG**GGAGGATGCGTCCCGTTCT T	pMPM-A2 cloning primer
GrvA+884/BamHI	CCGA**GGATCC**GGCTCAGAATTGCTGCAA TA	pMPM-A2 cloning primer
GrvA-268/XbaI	CCGA**TCTAGA**GGAGGATGCGTCCCGTTCT T	pUC19 cloning primer
GrvA+810-6xHis	CCGA**GAATTC*TCAGTGGTGGTGGTGGT GGTG***CTCCGCTTTATAATAGAGAGAG	pUC19 cloning primer (6xHIS)
GrvA-365/BtFor	CGGATAAAAGACAGTACCGG	EMSA primer
GrvA-238/BtRev	CGTTATAGGGAAAGAACGGG	EMSA primer
GrvA-236/BtFor	GGATACGCAGTTTTTATCAG	EMSA primer
GrvA-1/BtRev	TACATTTTATACCTTAGTTG	EMSA primer

[a] Restriction sites indicated by bolded nucleotides

Chapter 4: A novel promoter drives transcription of the *Escherichia coli* common pilus in the 2006 EHEC O157:H7 spinach outbreak strain TW14359

4.1 Background

Enterohemorrhagic *Escherichia coli* (EHEC) O157:H7 is a virulent pathotype of the gram negative commensal bacteria, *Escherichia coli*. Following host colonization, pathogenesis of EHEC is largely attributed to the production of the Shiga-like toxin (Stx), which damages the kidney vasculature and can lead to the life-threatening hemolytic uremic syndrome (HUS) (Eaton et al., 2008). EHEC adherence to epithelial cells, and subsequent host colonization, is enhanced by a common pilus structure observed almost ubiquitously across *E. coli* strains, the *E. coli* common pilus (ECP) (Rendon et al., 2007). The *E. coli* common pilus is a chaperone-usher fimbrial adhesin, composed of a 21-kDa subunit encoded by the gene *ecpA*, and its production plays a role in early-stage biofilm development for commensal and pathogenic *E. coli* and *Klebsiella pneumonia* strains (Alcantar-Curiel et al., 2013; Garnett et al., 2012; Lehti et al., 2010; Wurpel et al., 2013).

The *ecp* operon contains the gene *ecpR*, encoding a transcriptional regulator of the common pilus operon. In pathogenic and non-pathogenic *E. coli*, the regulator EcpR positively stimulates *ecp* transcription through the *ecpR* promoter, aided by integration host factor (IHF) and RcsB to relieve H-NS mediated repression (Lehti et al., 2012b; Martinez-Santos et al., 2012). Binding of EcpR occurs at a consensus site (TTCCT-$_{N17}$-TTCCT) located upstream of *ecpR*, and is believed to bind as a homodimer (Martinez-Santos et al., 2012). High levels of promoter architecture variation have been described for the *ecpR* (*matA*) promoter sequence in *E.*

coli strains and a phylogenetic organizational model has been previously proposed, with EHEC strains belonging to group E (Lehti et al., 2013a). Within this model, production of ECP varies between groups. For example, *E. coli* strain MG1655, while possessing a functional *ecp* operon, is unable to counteract H-NS mediated repression of the *ecp* promoter and direct production of ECP (Lehti et al., 2013a). Detailed sequence analyses have been performed for the *ecpR* promoter in EHEC (Martinez-Santos et al., 2012), however no reports to-date have identified promotable elements within the *ecpR* ORF, upstream of *ecpA*. Indeed, only the presence of putative temperature sensitive regulatory elements downstream of *ecpR* has been observed from the *ecpA* upstream region (Lehti et al., 2013a).

The remaining products of the *ecpRABCDE* operon include EcpA (the major fimbrial subunit), EcpB (a predicted chaperone), EcpC (a putative usher protein), EcpD (the ECP tip adhesin), and EcpE (a putative chaperone). In meningitic *E. coli* (NMEC) and EHEC strain EDL933, EcpA (MatA in NMEC) is required for efficient biofilm formation (Garnett et al., 2012; Lehti et al., 2010), indicating that successful ECP pilus formation is thus required for attachment and biofilm production in diverse *E. coli* pathotypes. While a number of adhesins produced by Shiga toxin-producing *E. coli* have been identified (reviewed in (Farfan and Torres, 2012)), the specific targets recognized by each adhesin and their contribution to virulence *in-vivo* requires further exploration. ECP production is temperature and oxygen dependent, and increased *ecp* transcription has been observed for cultures grown in DMEM, acetate, and acidic conditions (Lehti et al., 2013a; Rendon et al., 2007). Further, for cultures grown DMEM with 5% CO_2, the addition of ethanolamine was recently shown to significantly increase transcription of *ecp*, and other *E. coli* fimbrial adhesins, in a EutR dependent manner (Gonyar and Kendall, 2013).

Among divergent EHEC O157:H7 lineages, strain TW14359 has been previously reported as having a robust LEE gene expression and adherence phenotype (Abu-Ali et al., 2010a; Abu-Ali et al., 2010b), which is dependent on intrinsically up-regulated *rcsB* transcription, and an intact type III secretion system (Morgan et al., 2013). However, factors that contribute to increased *rcsB* transcription have not yet been characterized. In this study, a novel promotable element within the *ecpR* open reading frame was identified that is able to drive transcription of *ecpA*, and is dependent on a polymorphism specific to the EHEC O157:H7 strain TW14359. Finally, the ECP directed regulation of type III secretion through the response regulator RcsB is explored, and establishes a novel mechanism for co-regulation of adherence factors by distinct and distally encoded adherence factors.

4.2 Methods

4.2.1 Bacterial and mammalian tissue culture

The strains and plasmids used in this study are listed in **Table 7** in the supplemental material. Strains were stocked at -80°C in glycerol diluted (15% v/v final) in Lysogeny Broth (LB), and were maintained in LB or on LB with 1.5% agar (LBA). Unless otherwise noted, overnight (18-20 h) cultures grown in LB were used to inoculate fresh LB or LB buffered with sodium bicarbonate (44 mM $NaHCO_3$) or fresh Dulbecco's Modified Eagle's Medium (DMEM) (4 g/l glucose, 4 mM glutamine, 44 mM $NaHCO_3$, pH 7.4) to a final optical density 600 nm (OD_{600}) of 0.05. Cultures were grown at 37°C in a rotary shaker (200 RPM) using a 1:10 media-to-flask volume. Antibiotics (Sigma-Aldrich, St. Louis, MO) were added to cultures when required.

Maintenance and culture of Caco-2 and HT-29 colonic intestinal cells was performed as previously described (Morgan et al., 2013). Briefly, Caco-2 or HT-29 cells were grown to confluency in multi-well plates at 37°C with 5% CO_2. Prior to infection with bacterial strains, media was aspirated and each well was washed once and replaced with DMEM without FBS. For adherence experiments, bacterial cultures were grown to mid-logarithmic phase (OD_{600} of 0.5) in DMEM, and 200 µl of culture was added to each well of a 6-well plate. Following 3 hours of incubation, each well was washed four times using sterile PBS to remove non-adherent cells, and adherent cells were removed using 500 µl of 0.1% Triton X-100. Finally, cells were enumerated through serial dilution and plating on LBA agar. Each experiment was performed at least 3 times.

4.2.2 Mutagenesis and vector construction

Primers used for the genetic manipulation are provided in **Table 8**. For construction of isogenic deletion mutants and chromosomal FLAG-epitope fusion construction, the λ-Red assisted one-step inactivation method was used, adapted for enterohemorrhagic *Escherichia coli* (Lippolis et al., 2009), and as described (Mitra et al., 2012; Morgan et al., 2013). A previously published approach was used to construct FLAG fusions to *ecpA*, *rcsB*, and *tir* (Morgan et al., 2013) based on the method of Uzzau et al. (Uzzau et al., 2001). When expressed, the fusion protein contains a seven amino acid C-terminal epitope (FLAG) that can be detected by western immunoblots using anti-FLAG mAbs (Sigma-Aldrich. St. Louis, MO). Confirmation of genetic constructs was done using a combination of B*ccI* (NEB) restriction mapping and DNA sequencing (MWG Operon, Huntsville, AL)

Deletion of the *ecpR* promoter region was performed as described above using primers EcpR-388/P2 and EcpR+40/P1. Complementation of *ecpR* was performed by cloning a fragment containing the entire *ecpR* open reading frame, and upstream promoter region, into the *Bam*HI/*Xho*I digested low copy vector pMPM-A2 (Mayer, 1995) using primers EcpR-404/XhoI and EcpR+637/BamHI. To express *ecpR* under the control of the inducible pBAD promoter, the *ecpR* ORF was cloned into the pBAD-TOPO (Invitrogen) expression vector using primers EcpR-1/FpBAD and EcpR+637/RpBAD. A vector expressing the *ecpABCDE* operon, under the control of the TW14359 specific *ecpA* promoter, was created by amplifying the *ecpABDCE* operon using primers EcpA-666/SacI and EcpA+6,220/XbaI, followed by *Sac*I/*Xba*I digestion and ligation into the similarly digested vector pUC19.

4.2.3 RNA purification and quantitative real-time PCR (qRT-PCR)

Primers for qRT-PCR are provided in **Table 8** in supplemental materials. RNA purification, cDNA synthesis, qRT-PCR cycling conditions and data analysis followed previously described protocols (Riordan et al., 2010). qRT-PCR was performed using a Realplex2 Mastercycler (Eppendorf). Cycle threshold (C_t) data were normalized to *rrsH* (16S rRNA gene) and normalized cycle threshold values (ΔC_t) were transformed to arbitrary transcript expression levels using $2^{-\Delta Ct}$ $/10^{-6}$ as described (Livak and Schmittgen, 2001; Riordan et al., 2010). Expression levels were compared using the appropriate t-test or by Tukey's HSD following a significant F-test ($n \geq 3$, $\alpha=0.05$) (R. ver. 2.13.0).

4.2.4 β-galactosidase assays

The construction of the *ecpR*$_P$-*lacZ* reporter transcriptional fusion followed a previously described protocol using vector pRS551 (Morgan et al., 2013). Briefly, a 306-bp fragment, containing the *ecpR* promoter(s), was amplified from TW14359 genomic DNA using primers EcpR-496/BamHI and EcpR-21/BamHI, *Bam*HI/*Eco*RI digested, and cloned into the similarly digested pRS551. To create *ecpA*$_P$-*lacZ* fusions, fragments for regions of the *ecpA* promoter were amplified with forward primers EcpA-666/EcoRI, EcpA-555/EcoRI, EcpA-496/EcoRI, EcpA-387/EcoRI, EcpA-270/EcoRI, EcpA-131/EcoRI, and the reverse primer EcpA-1/BamHI from TW14359 genomic DNA; amplified *ecpA* promoter fragments were digested and cloned into similarly *Eco*RI/*Bam*HI digested pRS551.

Site directed mutagenesis of the *ecpA* promoter nucleotide polymorphism specific to EHEC strain TW14359 was performed by cloning the *ecpA* upstream region (-666 and -1 nucleotides, relative to the *ecpA* translational start site), using primers EcpA-666/EcoRI and EcpA-1/BamHI, into the *Eco*RI/*Bam*HI digested pUC19. Primers containing the desired C to T mutation were designed and used to amplify the entire vector using Phusion© High-Fidelity DNA Polymerase (NEB). The correct sequence identity of both the wild type and mutagenized promoter fragments was confirmed through sequencing (Eurofins MWG Operon, Huntsville, AL). The resulting fragment was digested, gel-purified, and cloned into the *Eco*RI/*Bam*HI site of pRS551. β-galactosidase activity (Miller Units) was measured as previously described and compared between strains using the appropriate t-test or by Tukey's HSD following a significant F-test ($n \geq 3$, $\alpha = 0.05$) (R ver. 3.0.1) (Miller, 1972; Mitra et al., 2012).

4.2.5 Protein extraction and western blotting

Protein extraction, purification and western immunoblots were performed as described previously (Mitra et al., 2012). The amount of protein loaded on SDS-PAGE gels for western blots was measured by a Bradford protein assay standard curve, and equal loading was validated by western blots for GroEL using anti-GroEL mAbs (Bio-Rad, Hercules, CA). Monoclonal antibodies against FLAG (Sigma-Aldrich, St. Louis, MO) were also used. Each experiment was repeated a minimum of three times in independent trials. Densitometry was used to estimate differences in protein levels for select experiments using a ChemiDoc XRS+ Imaging System and Image Lab 3.0 (BioRad).

4.2.6 Flow cytometry

Experiments for flow cytometry to detect relative ECP production were conducted as previously described (Martinez-Santos et al., 2012; Morgan et al., 2013). Briefly, overnight DMEM cultures of TW14359 or mutant derivatives co-incubated with confluent monolayers of Caco-2 cells for 6 hours. After incubation, 10^6 bacteria were formalin fixed for 10 minutes and labeled with anti-ECP antibodies overnight at 4°C. After overnight incubation, samples were washed and labeled with goat-anti rabbit IgG Alexa Fluor 488 conjugated antibodies for 1 hour at 4°C. Bacteria were then labeled with propidium iodide for detection using a 42-nm band pass centered at 585 nm. Emission from Alexa Fluor fluorescence 488 was detected at a 30-nm band pass filter centered at 530 nm. The samples were analyzed in a Becton Dickinson FACScan and 50,000 events were measured.

4.3 Results

4.3.1 Promoter analysis of the *ecpR* and *ecpA* upstream regions in TW14359 identified a novel promotable element within the *ecpR* open reading frame

Our previous transcriptional profiling of EHEC strain TW14359 revealed markedly higher levels of mapped transcripts for the *ecp* operon (**Fig. 22A**) at a region upstream of *ecpA*, but located within the *ecpR* open reading frame (**Fig. 22B**) (Morgan et al., 2013). The promoter region upstream of *ecpR* has been well characterized in EHEC strain EDL933, and our initial experiments in EHEC strain in TW14359, using promoter *lacZ* fusions, revealed significantly higher levels of promoter activity ($p<0.05$) in DMEM compared with LB, in agreement with previous reports (**Fig. 22C**) (Martinez-Santos et al., 2012). However, we sought to further explore potential promotable elements capable of driving *ecpA* transcription, located within the *ecpR* open reading frame. Cloning a fragment 666-bp upstream of the *ecpA* translational start site, lacking any portion of the *ecpR* upstream region, into pRS551 resulted in measurable β-galactosidase activity significantly higher ($p<0.05$) than that of the empty vector. Activity from the $ecpA_P$-*lacZ* reporter was significantly lower than that of the $ecpR_P$-*lacZ* ($p<0.05$), though promoter activity of both constructs was significantly higher for cultures grown in DMEM compared with those in LB (**Fig. 22C**). Maximal promoter activity of the *ecpR* and *ecpA* promoter fragments was observed for late-log phase cultures grown in DMEM ($p<0.05$), and in LB for the *ecpA* promoter fragment, however the *ecpR* promoter fragment was not altered between mid- and late-log phase in LB (**Fig. 22C**). These experiments indicated that *ecp* transcription in EHEC strain TW14359 could be initiated from one of two promotable elements: (1) the promoter(s) upstream of *ecpR*, and (2) a promoter within the *ecpR* open reading frame, and that activity from these promoters is sensitive to changes in growth phase and media.

To identify important regions within the *ecpA* promoter, several *lacZ* fusions were created with truncated fragments of the region upstream of the *ecpA* ORF, and cloned into TW14359Δ*lacZ* for β-galactosidase assays (**Fig. 22D**). The largest fragment, at 666-bp upstream of *ecpA*, had the highest detectable promoter activity. Loss of the first 100-bp resulted in a significant drop in promoter activity ($p<0.05$), which increased slightly following subsequent 100-bp truncation. The final fragment, at 131-bp upstream of *ecpA*, displayed levels which remained significantly higher ($p<0.05$) than that of the empty vector, but were substantially lower than that of the largest fragment (**Fig. 22E**). Collectively, these results support the observations of transcriptional activity from an element upstream of *ecpA*, and reveal a region of importance for maximal activity located upstream of the *ecpA* translational start site, within the *ecpR* open reading frame.

4.3.2 Basal EcpA production independent of the *ecpR* promoter

In the previous experiments, promoter activity was observed for the region upstream of *ecpA* within the *ecpR* open reading frame. It was thus hypothesized that, while primary *ecp* transcription arises from a promoter upstream of *ecpR*, basal activity from a promoter located within the *ecpR* ORF promoter would be sufficient to detect cytosolic EcpA production. To test this, a strain with a chromosomally FLAG tagged *ecpA* gene was created. A *kanamycin* drug cassette was then inserted into the region just upstream of the *ecpR* translational start site, replacing the entire *ecpR* promoter region. Importantly, the *kan* cassette was inserted in a reverse orientation from the *ecp* operon to prevent polar transcription from the *kan* promoter. For cultures grown to mid-logarithmic phase in DMEM, EcpA was observed in the wild type strain with an intact *ecpR* promoter, and EcpA production was substantially increased by

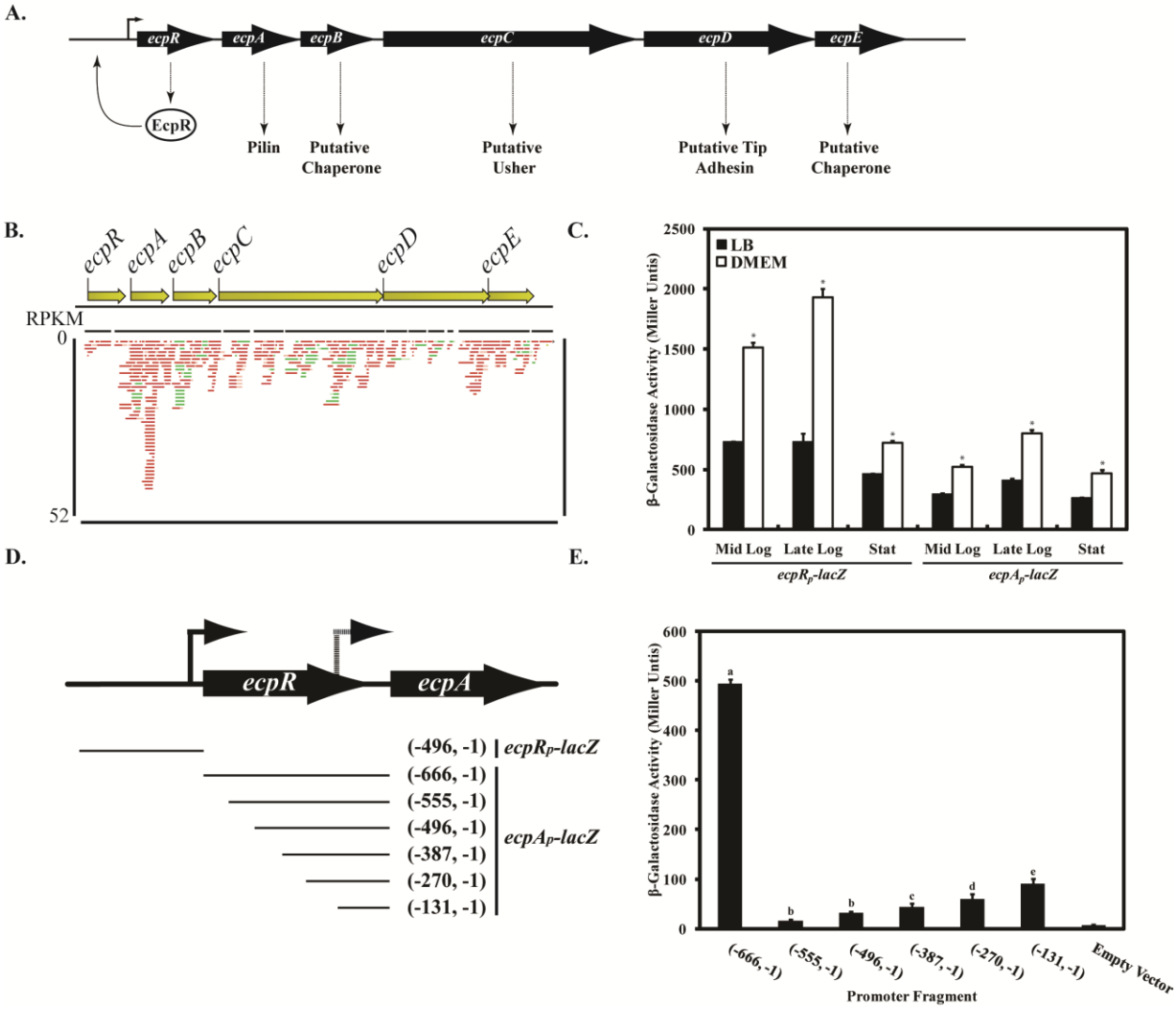

Figure 22 – The transcriptional regulation of *ecpR* and *ecpA*

(A) The *ecp* operon organization with the respective location of the promoter upstream of *ecpR*, and the described or predicted function of each gene. (B) Transcriptome profiling for the *ecp* operon. Mapped transcripts are indicated in green (forward orientation) and red (reverse orientation). (C) β-galactosidase activity in Miller units of $ecpR_{P496}$-*lacZ* and $ecpA_{P666}$-*lacZ* measured during mid log (OD_{600} of 0.5), late log (OD_{600} of 1.0), and stationary (OD_{600} of 2.5) growth phases. Asterisks denote significance by a Student's t-test ($p<0.05$, $n\geq3$). (D) Diagram indicating the relative location of *ecpR* and *ecpA* promoter fragments for *lacZ* transcriptional fusions cloned into pRS551, with the *ecpR* and predicted *ecpA* promoters denoted by a solid or hatched arrow, respectively. (E) β-galactosidase activity in Miller units of each $ecpA_P$-*lacZ* promoter fragment tested, including the empty vector (pRS551) control, in strain TW14359Δ*lacZ*. Plots which differ by lower case letter, differ significantly by Tukey's HSD following a significant F-test ($p<0.05$; $n\geq3$). Error bars indicate standard deviation for all panels.

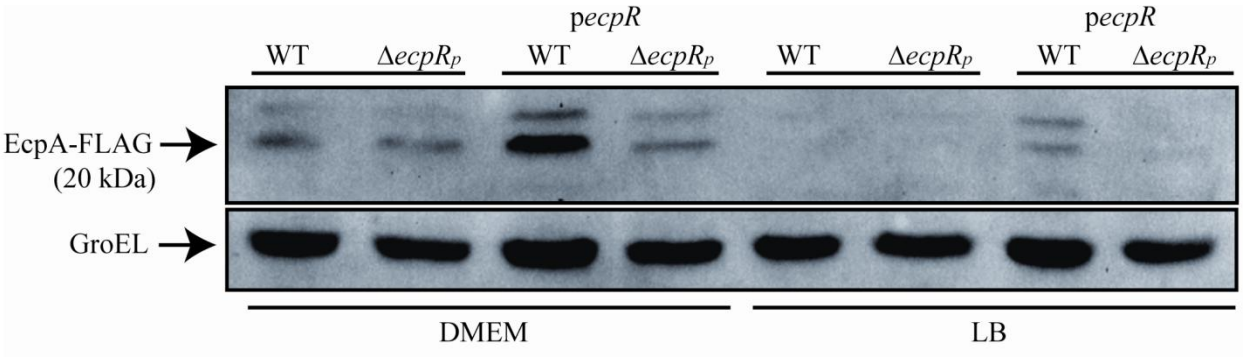

Figure 23 - Western blot analysis of EcpA-FLAG in TW14359
Western blot for EcpA-FLAG, from cultures grown in DMEM or LB during exponential growth (OD_{600} of 0.5), for strains TW14359 and TW14359Δ*ecpR*P::*kan*. GroEL was included as a control for equal loading.

ectopically expressing EcpR from its native promoter on a multi-copy vector (**Fig. 23**). Following deletion of the *ecpR* promoter region, detectable cytosolic EcpA was similar to that of the un-induced wild type strain, though activation of EcpA production by EcpR overproduction was completely abrogated. This observation is in-line with the current model of EcpR mediated transcriptional activation of *ecpR*, at the EcpR binding sites upstream of the *ecpR* promoter, and corroborates basal production of EcpA in EHEC strain TW14359 directed through an additional promoter within the *ecpR* open reading frame.

4.3.3 A single nucleotide polymorphism within the TW14359 *ecpR* open reading frame is required for maximal *ecpA* promoter activity

An alignment of a region 666-bp upstream of the *ecpA* ORF from several pathogenic and non-pathogenic *E. coli* strains revealed substantial sequence diversity (**Fig. 24**). Fragments from several strains, representing a spectrum of sequence variation, were examined using promoter *lacZ* fusions in TW14359Δ*lacZ*. Surprisingly, only the *ecpA* upstream fragment from EHEC strain TW14359 displayed β-galactosidase activity above that of the empty vector control (**Fig. 25A**). Further analysis of the *ecpA* upstream region, compared with other *E. coli* strains, identified a polymorphism unique to TW14359. The most closely related sequence was that of EHEC strain Sakai, which contained a single nucleotide difference within a region predicted, through *in-silico* analysis, to contain a sigma-70 promoter. To explore the significance of this polymorphism, the 666-bp fragment upstream of *ecpA*, from strain TW14395, was cloned into vector pUC19 and the nucleotide thymine was changed to a cytosine using site-directed mutagenesis. The resulting fragment was subsequently cloned into pRS551 assayed for promoter activity. As expected, the T to C mutation resulted in significantly decreased promoter activity

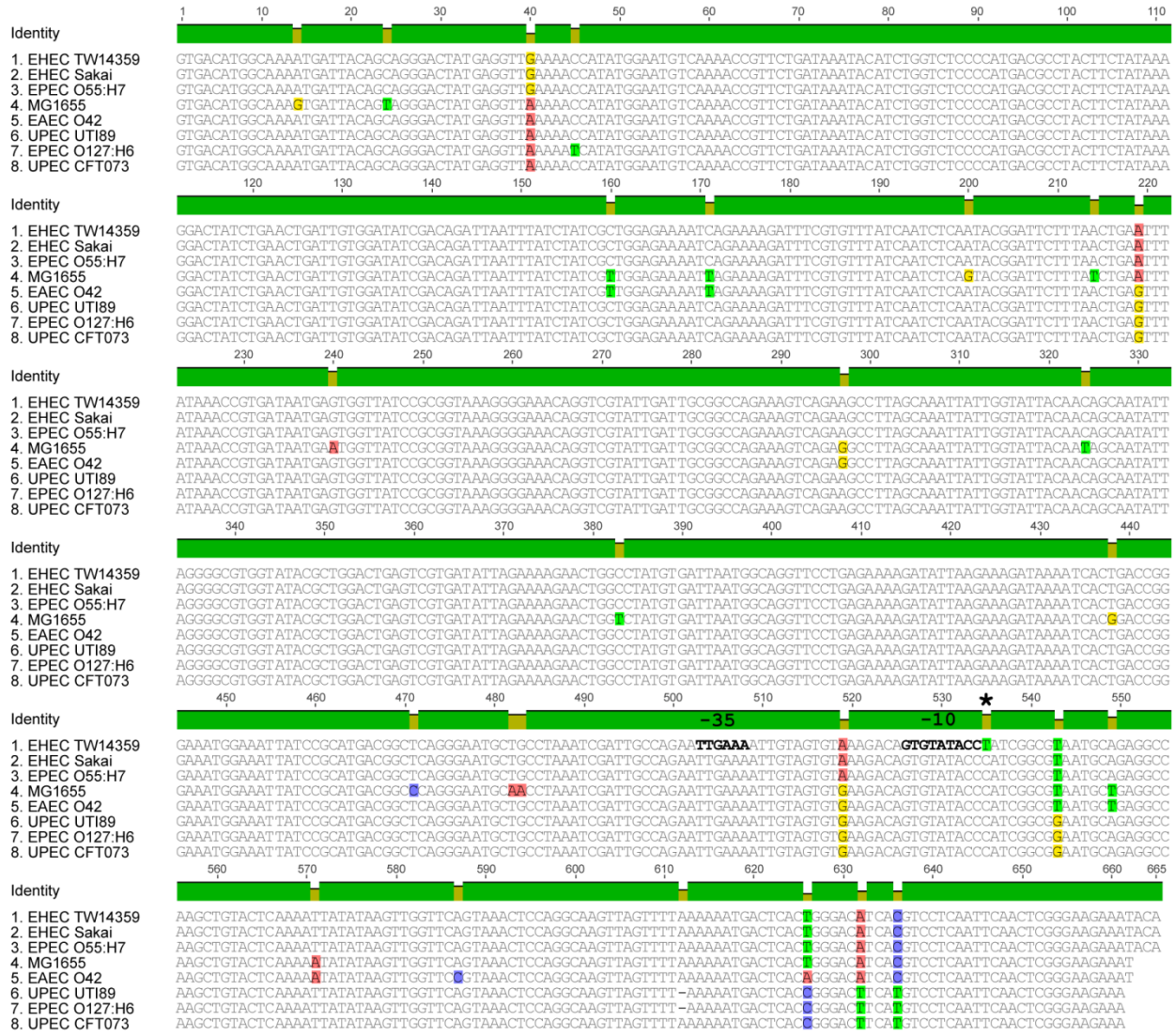

Figure 24 - Alignment of the *ecpA* upstream region from select *E. coli* strains
Alignment for multiple *E. coli* strains for the region upstream of *ecpA*, but not including the *ecpR* upstream region. The predicted *ecpA* promoter is indicated with bold letters, and an asterisk indicates the nucleotide polymorphism unique to EHEC strain TW14359.

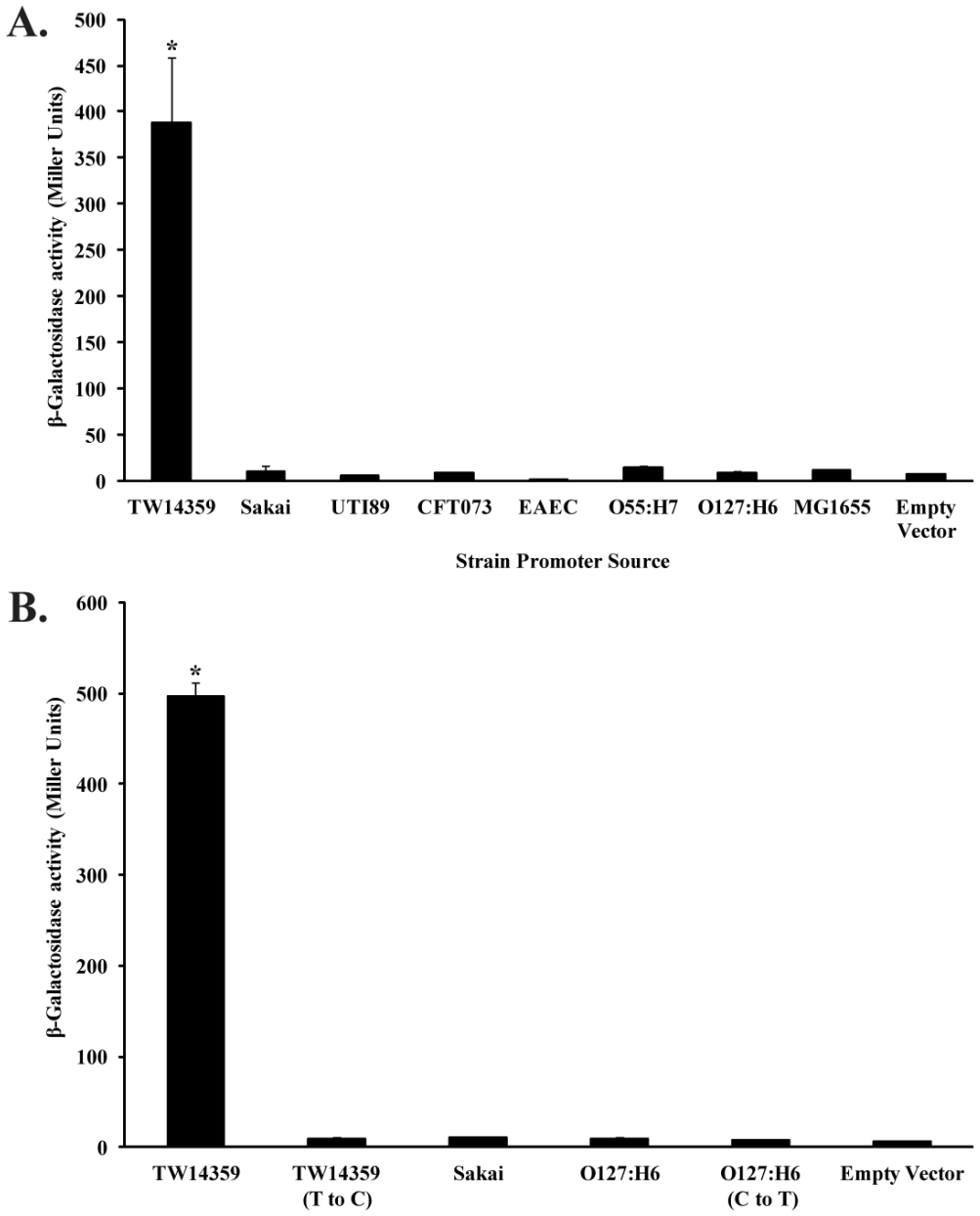

Figure 25 - Characterizing the TW14359 *ecpA* specific promoter polymorphism
(A) β-galactosidase activity in Miller units of $ecpA_{P666}$-*lacZ* for different *E. coli* strains. (B) β-galactosidase activity in Miller units for the *ecpA* promoter of TW14359, Sakai, E2348/69 (EPEC O127:H6), the TW14359 *ecpA* promoter with a site-directed mutation, and the E2348/69 *ecpA* promoter with a site-directed mutation. All experiments were performed using strain TW14359Δ*lacZ*, and the empty vector (pRS551) was included as a negative control. Asterisks denote significance by a Student's t-test ($p<0.05$; $n\geq3$). Error bars denote standard deviation for all panels.

($p<0.05$), comparable to that of strain Sakai (**Fig. 25B**). Collectively these experiments reveal a promotable region located upstream of the *ecpA* ORF, in EHEC strain TW14359, that is dependent on a single nucleotide polymorphism within a predicted sigma-70 promoter region. However, alteration of the same nucleotide from the EPEC O127:H6 *ecpA* upstream region did not yield detectable promoter activity, suggesting that one or more additional nucleotide differences contribute to *ecpA* promoter function.

Activity from the TW14359 *ecpA* promoter was observed to be weaker than that of the *ecpR* promoter (**Fig. 22C**). Since direct binding of H-NS to the *ecpR* open reading frame has been previously described, and has been shown to play an important role in regulation of *ecp* transcription (Lehti et al., 2013a; Martinez-Santos et al., 2012), it was of interest to examine whether the *ecpA* promoter activity observed for TW14359 was under the control of H-NS. Indeed, mutation of *hns* significantly increased activity ($p<0.05$) from the TW14359 *ecpA* promoter fragment, while only slightly increasing promoter activity from the Sakai *ecpA* promoter fragment (**Fig. 26**). Though activation of the Sakai derived *ecpA* promoter was marginal in the absence of H-NS, activity was significantly higher ($p<0.05$) than that of the empty vector alone, suggesting that the fragment contains a very weak promoter which is effectively silenced by H-NS. Taken together, this data suggests that H-NS binding actively represses transcription of the *ecpR* and *ecpA* promoters in TW14359.

4.3.4 Adherence to epithelial cells mediated by ECP in the absence of the *ecpR* promoter

The positive role of the *E. coli* common pilus in adherence to cultured epithelial cells has been previously described (Rendon et al., 2007; Saldana et al., 2009a). Therefore, we sought to explore the contribution of the TW14359 specific *ecpA* promoter in ECP production

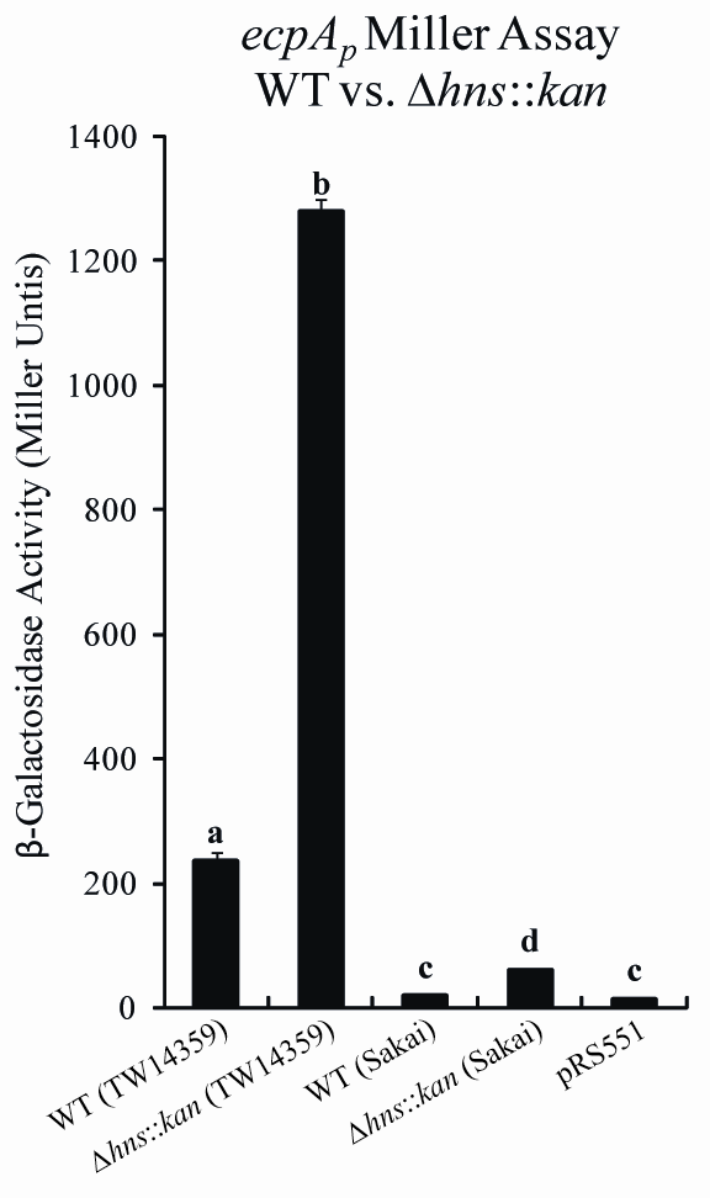

Figure 26 - Regulation of the TW14359 *ecpA* promoter by H-NS
β-galactosidase activity in Miller units of $ecpA_{P666}$-*lacZ* (source of cloned promoter fragment in parentheses, strain TW14359 or Sakai) in wild type TW14359Δ*lacZ* or TW14359Δ*lacZ*Δ*hns*::*kan* from cultures grown to mid-exponential phase (OD_{600} of 0.5) in LB; The empty vector (pRS551) was included as a negative control. Plots which differ by lower case letter, differ significantly by Tukey's HSD following a significant F-test ($p<0.05$; $n\geq3$). Error bars indicate standard deviation for all panels.

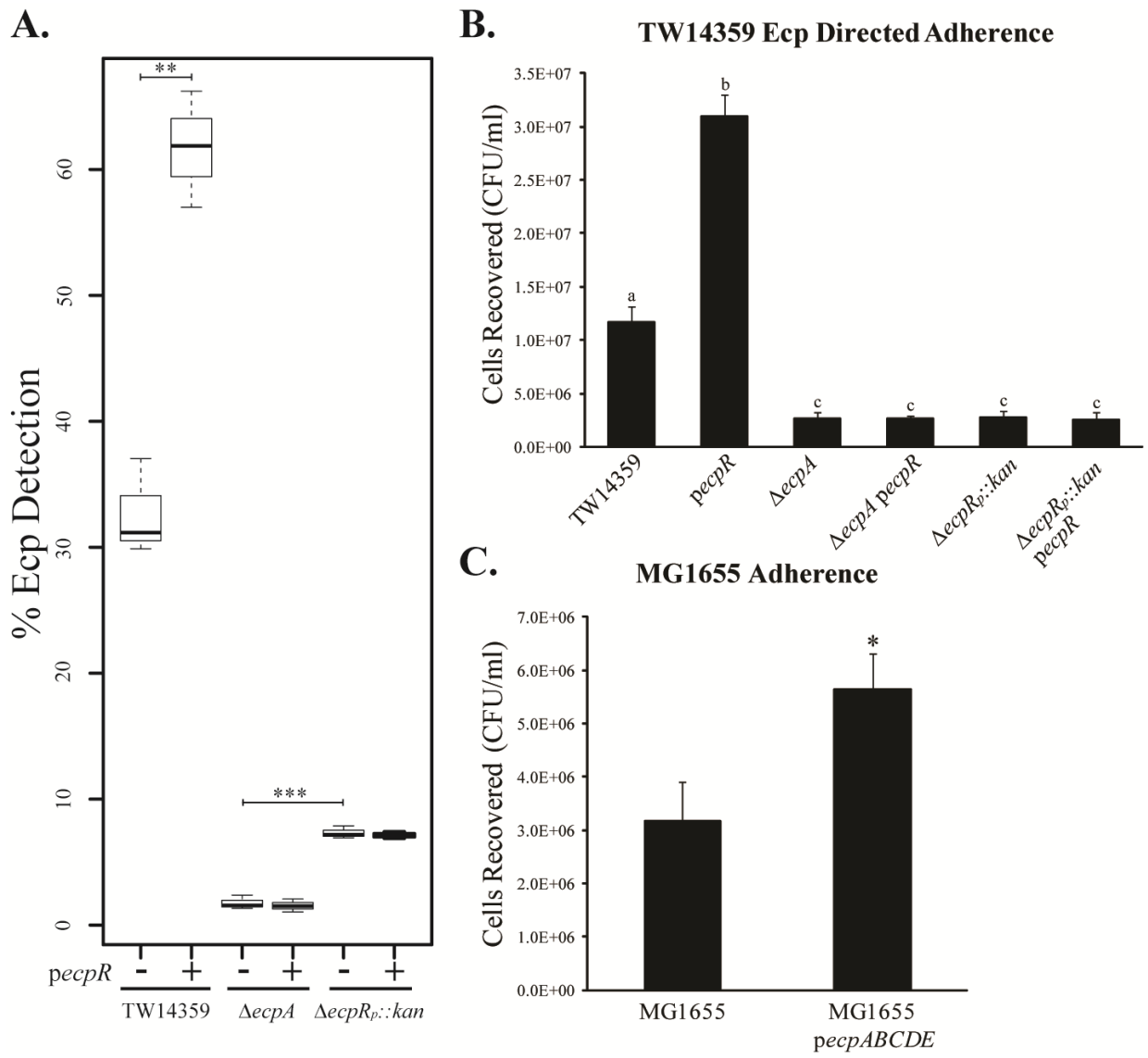

Figure 27 - ECP directed adherence and production of ECP by the *ecpR* and *ecpA* promoters
(left) Box plots for the level of ECP production determined by flow cytometry, in bacteria adhering to Caco-2 cultured epithelial cells, for strains TW14359, TW14359Δ*ecpA*::*kan*, and TW14359Δ*ecpR*$_P$::*kan* with or without p*ecpR*. (top right) CFU/ml of EHEC strain TW14359 recovered following incubation with Caco-2 cells in different *ecp* mutant strains. Asterisks denote significance by a Student's t-test (**, $p<0.01$; ***, $p<0.001$; $n\geq3$). Plots which differ by lower case letter, differ significantly by Tukey's HSD following a significant F-test ($p<0.05$, $n\geq3$). (bottom right) CFU/ml of MG1655 containing p*ecpABCDE* or the empty vector pUC19. Asterisks denote significance by a Student's t-test (*, $p<0.05$; $n\geq3$). Error bars indicate standard deviation for all panels.

and adherence. As expected, overproduction of EcpR led to significantly elevated ECP production ($p<0.01$), compared with wild type, and mutation of *ecpA* resulted in minimal detection of ECP production (**Fig. 27A**). Importantly, while mutation of the *ecpR* promoter region led to a substantial reduction in ECP production, detectable ECP levels were roughly 4.7-fold higher than the *ecpA* mutant, revealing that basal activity from the remaining *ecpA* promoter was able to produce low levels of ECP. In agreement with western blots for EcpA, overproduction of EcpR did not affect basal production of ECP in strain TW14359Δ*ecpR*$_P$::*kan*.

Adherence to Caco-2 cells was observed to significantly increase following overexpression of *ecpR* in wild type TW14359 ($p<0.05$), as expected from previous reports (Rendon et al., 2007) and our own observations (**Fig. 27B**). However, adherence experiments comparing strains TW14359Δ*ecpA* and TW14359Δ*ecpR*$_P$::*kan*, or their respective *ecpR* overexpression strains, were not significantly different from one another, suggesting that transcription from the TW14359 specific *ecpA* promoter alone is not sufficient to alter adherence, at least in the conditions tested in this study. While the preceding experiments were unable to detect noticeable contributions to adherence from the TW14359 specific *ecpA* promoter, it was hypothesized that this might be due to its low level of promoter activity, and subsequent *ecp* transcription, compared with that of the fully activated *ecpR* promoter. To address this, the *ecpABCDE* operon, excluding the entire *ecpR* upstream promoter region, was cloned into a high copy vector under the control of the TW14359 *ecpA* promoter. Because the *ecp* operon is not actively transcribed in *E. coli* strain MG1655, due to mutations inactivating the *ecpR* promoter (Lehti et al., 2010), it was used in adherence experiments with HT-29 human colonic epithelial cells. Indeed, expression of the *ecpABCDE* operon resulted in significantly increased adherence ($p<0.05$), compared to MG1655 containing the empty vector alone (**Fig.**

27C). Collectively, these experiments suggest that, while low levels of ECP production from the native *ecpA* promoter was not able to detectably alter adherence in EHEC strain TW14359, *ecp* transcription arising solely from the TW14359 *ecpA* promoter is able to increase adherence when expressed from a high copy vector.

4.3.5 Overproduction of EcpR increases cytosolic RcsB and Tir protein levels

Transcription of *ecpR* (*matA*) in meningitic *E. coli* has been shown to require the response regulator RcsB (Lehti et al., 2012b). However, in EHEC, the *rcsB* consensus binding site was shown to be dispensable for transcription of *ecpR* in a study using a multi-copy reporter system (Martinez-Santos et al., 2012). In this study, overexpression of *ecpR* led to significantly higher *ecpA* transcription compared with wild-type ($P<0.001$), but did not alter transcription of *ecpA* in TW14359Δ*rcsB* or TW14359Δ*ecpR*$_P$::*kan*, in agreement with previous accounts of RcsB and EcpR dependent *ecp* transcriptional (**Fig. 28A**) (Lehti et al., 2012b; Martinez-Santos et al., 2012).

In EHEC strain TW14359, *rcsB* transcription is intrinsically up-regulated when compared with EHEC strain Sakai (Morgan et al., 2013). However, the specific factors that contribute to this phenotype have not yet been identified. It was therefore of interest to determine whether increased ECP production had a role in transcriptional regulation of *rcsB*. To further explore the potential co-regulation of EcpR and RcsB in EHEC strain TW14359, *ecpR* was cloned into a multi-copy vector and expressed from either an arabinose inducible promoter or from the native

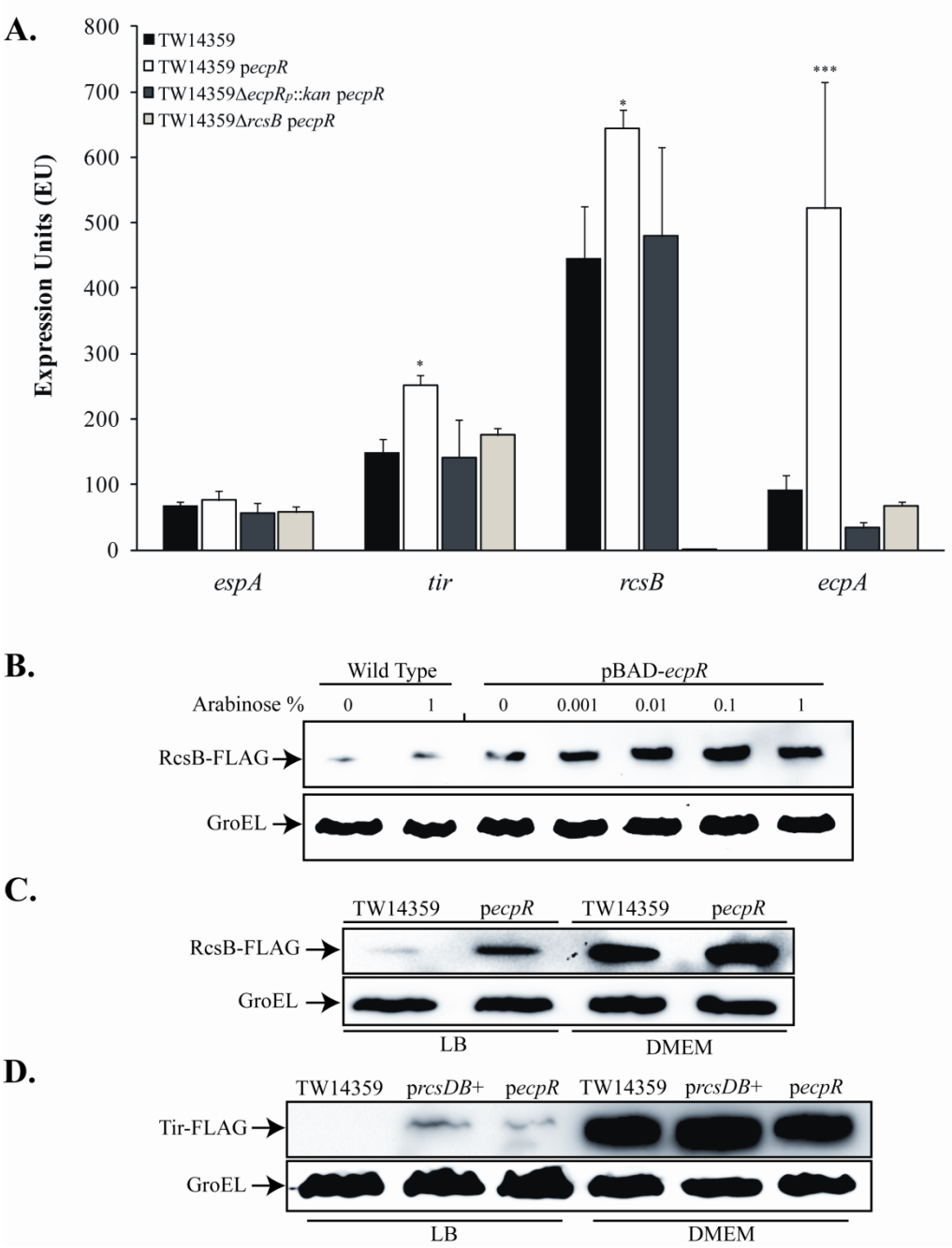

Figure 28 - qRT-PCR and Western blot analysis of *rcsB, ecp,* and LEE gene targets
(A) Transcript levels for *espA*, *tir*, *rcsB,* and *ecpA* in wild type and derivative TW14359 strains expressing *ecpR* on a multi-copy plasmid (p*ecpR*) from its native promoter. Asterisks denote significance by a Student's t-test (*, $p<0.05$; **, $p<0.01$; ***, $p<0.001$; $n\geq3$). Error bars indicate standard deviation for all panels. (B and C) Representative western blots for RcsB-FLAG or (D) Tir-FLAG for cultures grown to mid-exponential phase (OD_{600} of 0.5) in LB or DMEM, with or without vector pBAD-*ecpR*, p*ecpR*, or p*rcsDB.*

ecpR promoter. Overproduction of *ecpR* was observed to slightly but significantly ($p<0.05$) increase transcription of *rcsB* compared with wild-type TW14359, which was dependent upon an intact *ecpR* promoter (**Fig. 28A**). Indeed, overproduction of EcpR, under the control of an arabinose inducible promoter (pBAD-*ecpR*), or its native promoter (p*ecpR*), resulted in visibly increased cytosolic RcsB for cultures grown in LB, with a slight increase for cultures grown in DMEM (**Fig. 28B** and **28C**).

In EHEC O157:H7 strains, RcsB overproduction is able to stimulate LEE gene transcription and subsequent type III secretion (Tobe et al., 2005). Since increased *rcsB* transcription was observed following *ecpR* overexpression, it was hypothesized that this may have an impact on LEE gene transcription. Therefore, transcription and cytosolic levels of the LEE encoded protein Tir was assessed in strains overexpressing *ecpR*. Analysis of *tir* transcription using qRT-PCR revealed significantly increased levels in TW14359 p*ecpR* ($p<0.05$), but not in TW14359Δ*ecpR*$_P$::*kan* p*ecpR* or TW14359Δ*rcsB* p*ecpR* (**Fig. 28A**). Indeed, overproduction of *ecpR* resulted in visibly increased production of cytosolic Tir during growth in LB, but not for cultures grown in DMEM (**Fig. 28D**). As a positive control for LEE activation, expression of the *rcsDB* operon from a multi-copy vector resulted in a similarly increased level of cytosolic Tir during growth in LB, with a slight increase observed during growth in DMEM (**Fig. 28D**). These results demonstrate that overproduction of EcpR is able to increase production of RcsB and LEE encoded Tir. However, it was not clear whether the regulator EcpR was directly influencing their transcription, or whether the effect was indirect.

It was thus hypothesized that production of ECP pilus was indirectly influencing production of RcsB and Tir, rather than direct activation by EcpR. To address this, *rcsB* and *tir*

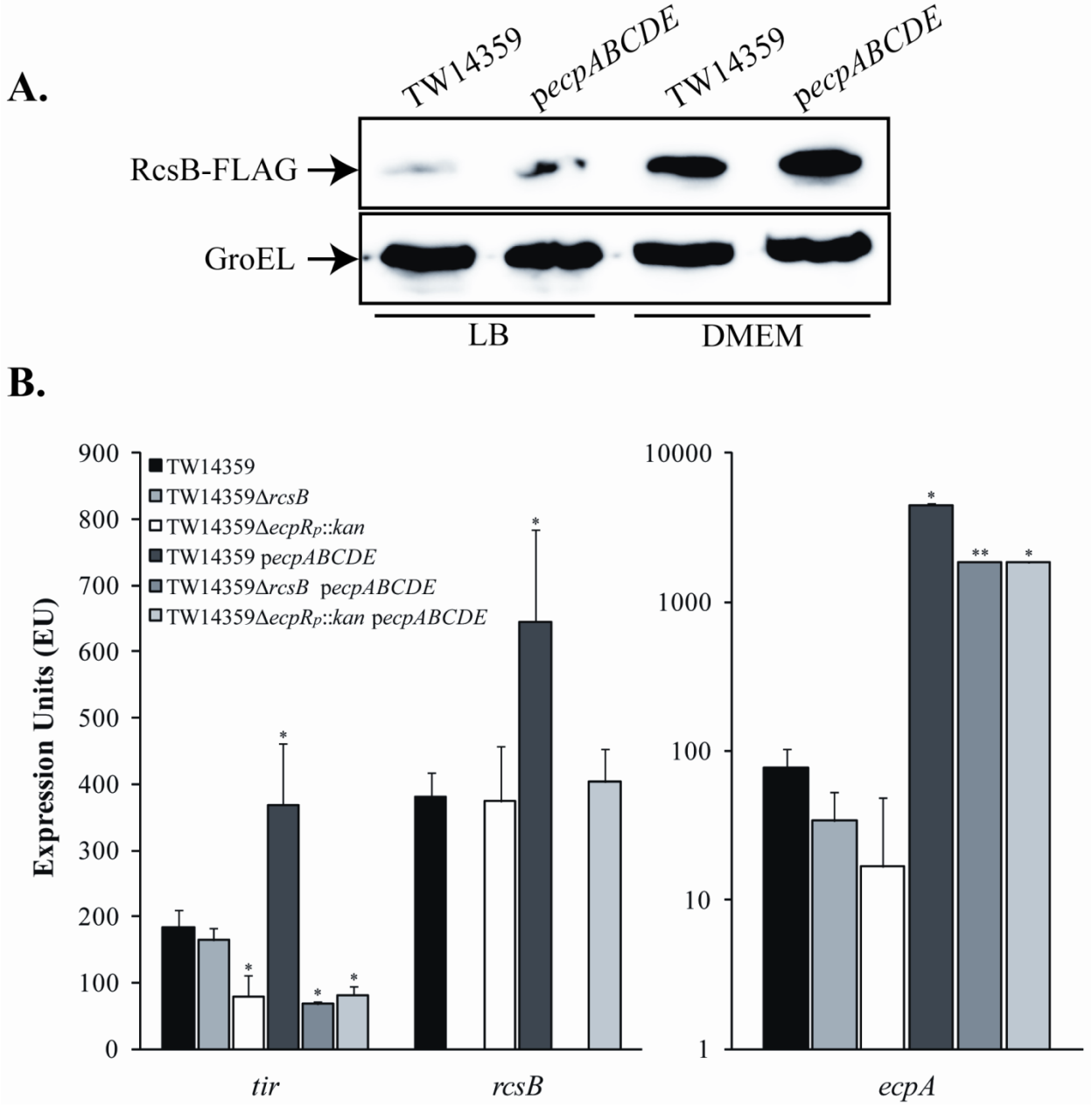

Figure 29 - qRT-PCR and western blot analysis of *rcsB*, *ecp*, and LEE gene targets with *pecpABCDE*

(A) Representative western blots for RcsB-FLAG for cultures grown to mid-exponential phase (OD_{600} of 0.5) in LB or DMEM, with or without vector p*ecpABCDE*. (B) Transcript levels for *tir*, *rcsB*, and *ecpA* in wild type and derivative TW14359 strains expressing p*ecpABCDE* on a multi-copy plasmid from the TW14359 *ecpA* promoter (666 bp upstream of the *ecpA* start codon) for exponential (OD_{600} of 0.5) phase LB cultures. Asterisks denote significance by a Student's t-test (*, $p<0.05$; **, $p<0.01$; ***, $p<0.001$; $n\geq3$). Error bars indicate standard deviation for all panels.

transcript levels were determined in TW14359 containing a vector expressing *ecpABCDE* under the control of the TW14359 specific *ecpA* promoter. In support of this hypothesis, significantly higher levels of transcription ($p<0.05$) were observed for *rcsB* and *tir* compared to wild type TW14359, with concomitantly elevated RcsB protein in strain TW14359 p*ecpABCDE* (**Fig. 29A** and **29B**). And, consistent with the activity of the TW14359 *ecpA* promoter, loss of the *ecpR* upstream region did not completely abrogate *ecpA* transcription (**Fig. 29B**). However, as previously observed, TW14359Δ*ecpR*$_P$::*kan* and TW14359Δ*ecpR*$_P$::*kan* p*ecpABCDE* did not have significantly different levels of *rcsB* or *tir* transcription. Collectively, the results of these experiments suggest that transcriptional activation of *rcsB* and *tir* transcription by *ecpR* requires an intact *ecpR* promoter, and confirm that EcpR mediated transcriptional activation of the *ecp* operon, in EHEC strain TW14359, requires an intact *rcsB* gene.

4.4 Discussion

A number of chaperone-usher fimbriae are encoded within the *E. coli* genome (Wurpel et al., 2013), however their specific contribution to the colonization in the human host, or the specific host targets recognized, remains largely unknown. The contribution of the *E. coli* common pilus for adherence to cultured epithelial cells has been previously described (Rendon et al., 2007), and a report using the commensal *E. coli* strain Nissile 1917 identified *ecpA* as being required for colonization in an infant mouse model (Lasaro et al., 2009); more recently, virulence attenuation was observed for avian pathogenic *E. coli* (APEC) following mutation of the ECP tip adhesin gene, *ecpD* (Stacy et al., 2014). Though, the contribution of ECP to host colonization and virulence for EHEC strains has yet to be definitively shown. Among pathogenic and non-pathogenic *E. coli* strains the *ecp* operon structure is highly conserved; however, a phylogenetic

grouping has been defined based on promoter architecture of *ecpR* (*matA*), and the diverse regulatory patterns of the *ecp* operon among strains are at least in part a direct result of this promoter sequence variation (Lehti et al., 2013a). For example, transcription and production of ECP during growth at physiological temperatures is observed for EHEC strains, but not for NMEC (Lehti et al., 2013a). The results presented in this study identify a regulatory feature of the *ecp* operon that is unique to EHEC strain TW14359, and reveal novel a pathway for ECP mediated *rcsB* transcriptional activation and LEE gene regulation.

Using the mapped transcripts from previous RNA sequencing experiments (Morgan et. al., 2014), the transcriptional profile of the *ecp* operon was examined. In agreement with previous reports (Lehti et al., 2013a), transcription of the *ecp* operon appears to be under the control of a transcriptional terminator (d'Aubenton Carafa et al., 1990), with levels of mapped transcript reduced substantially near the location of the mapped terminator sequence within the *ecpA*-*ecpB* intergenic region. Indeed, modulation of mRNA production through transcriptional termination has been previously described in other pilus and fimbrial operons, and was proposed to regulate stoichiometric levels of adhesin assembly machinery (He et al., 2004; Jordi et al., 1993; Kram et al., 2008). More importantly, while the entire operon was mapped, the highest level of mapped transcript was located within and immediately upstream of *ecpA*. This finding suggested that, though the promoter(s) upstream of *ecpR* can drive production of ECP, another previously cryptic element within the *ecpA* ORF was capable of promoting transcription. In this study, a TW14359 specific polymorphism was characterized within the *ecpR* ORF that is required for $ecpR_P$-independent *ecpA* transcription. While the region upstream of *ecpA* in is largely transcriptionally silent in *E. coli* strains, in EHEC strain TW14359 the promoter activity was detectable. This promoter activity required a single polymorphism located near a predicted

sigma-70 promoter region, and was negatively repressed by H-NS. One possibility is that the polymorphism present in TW14359 alters the binding affinity of some unknown factor required for efficient transcription from the *ecpA* promoter. Alternatively, it may more directly influence the architecture of the promoter itself. A sequence analysis revealed a predicted sigma-70 promoter immediately upstream of polymorphism, and this difference might disrupt or inhibit RNA polymerase binding. Repression by H-NS was present in EHEC strain Sakai, but promoter activity was significantly lower than strain TW14359. It is then possible that the promoter for *ecpA* transcription exists in the other strains assayed, but is cryptic in function. Future work is aimed at determining the specific *ecpA* promoter sequence, and at identifying potential regulatory elements present in TW14359 which may contribute to its distinct regulation when compared with other *E. coli* strains. The results of this study thus show that, even without repression by H-NS, *ecpA* promoter activity from other *E. coli* strains is significantly weaker than that of TW14359.

While EcpR directly regulates transcription from the EcpR promoter, and has been shown to weakly bind to the *ecpA* upstream region (Lehti et al., 2013a), loss of *ecpR* or its overproduction had no effect on transcription from the *ecpA* promoter. This is consistent with the fact that sequence analysis of the *ecpA* upstream region did not reveal any EcpR binding consensus sites (TTCCT-$_{N17}$-TTCCT) (Martinez-Santos et al., 2012) within the region 666-bp upstream of *ecpA*. Overall, this data is consistent with the observation of high levels of mapped transcripts within the *ecpA* ORF, and the presence of a predicted sigma-70 promoter (Huerta and Collado-Vides, 2003). Future experiments are aimed at identifying potential factors or conditions which act through the *ecpA* promoter to direct ECP production independent of primary transcription from the promoter(s) upstream of *ecpR*.

Further, this study has corroborated the contribution of ECP pilus production to cultured epithelial cells (Garnett et al., 2012; Rendon et al., 2007), specifically to Caco-2 and HT-29 epithelial cells. *E. coli* strains have been shown to produce an expansive repertoire of adhesins contributing to adherence, including intimin, curli, hemorrhagic coli pili (HCP), long polar fimbriae (Lpf), the acid inducible YadK, and others (Avelino et al., 2010; Chingcuanco et al., 2012; DeVinney et al., 1999; Elliott et al., 2000; Erdem et al., 2007; Fordtran and Locklear, 1966; Garnett et al., 2012; Giron et al., 2002; Gonyar and Kendall, 2013; Hernandes et al., 2013; Hernandes et al., 2011; Kenny et al., 1997b; Saldana et al., 2009b; Torres et al., 2002; Xicohtencatl-Cortes et al., 2007). It is therefore not difficult to rationalize the variation observed in promoter architecture for different *E. coli* pathotypes, and even further promoter sequence refinement within hemorrhagic *E. coli* strains, where each pathotype alters the expression of surface expressed adhesins to suit its unique biological niche or preferred site of colonization. This is important particularly in light of the co-regulatory nature of different EHEC adhesins, such as Ler (*LEE1* encoded, transcriptional activator of the LEE) mediated activation of Lpf transcription (Elliott et al., 2000; Sperandio et al., 2000; Torres et al., 2007). This dynamic extends beyond just regulation, as the localized adherence pattern of enteropathogenic *Escherichia coli* was shown to be dependent on bundle-forming pili (BFP), the T3SS and ECP working synergistically with other adhesins to coordinate adherence to host epithelial cells (Saldana et al., 2009a). Conversely, a recent study identified factors involved in the formation and microanatomy of *E. coli* strain W3110 macrocolonies, and showed that type I fimbriae and ECP were dispensable, while flagella production played a significant role in macrocolony morphology (Serra et al., 2013). However, for different non-pathogenic *E. coli* strains, such as MG1655 and W3110, the promoter upstream of *ecpR* has undergone mutational attrition and is

no longer able to facilitate active *ecpR* transcription (Lehti et al., 2013a). It is therefore interesting to speculate on the potential contribution of ECP to the formation of the distinct macrocolony structure in ECP strains producing biofilms.

Expression of *ecpR* from a multi-copy vector resulted in substantially increased *ecpA* transcription, but was completely dependent on an intact *rcsB* gene. However, a previous report using EHEC strain EDL933 found that the RcsB consensus site was dispensable for *ecpR* promoter activity (Martinez-Santos et al., 2012). The reason for this disparity might be due to the nature of the expression analysis performed, wherein the authors utilized a multi-copy vector for their expression experiments, which might have masked subtle regulatory interactions between RcsB and EcpR at the *ecpR* promoter. However, this study has corroborated the RcsB dependent regulatory pathway for *ecp* transcriptional activation, through the *ecpR* promoter(s), at least in EHEC strain TW14359.

Strain TW14359 has been previously shown to possess intrinsically upregulated *rcsB* transcription, which was shown to be required for its increased adherence phenotype compared with EHEC strain Sakai (Abu-Ali et al., 2010b; Morgan et al., 2013). However, the specific factors which contribute to increased *rcsB* transcription remained elusive. Since transcription of *matA* (*ecpR*) was shown to be dependent on RcsB (Lehti et al., 2012b), and our own analysis validated this finding in EHEC strain TW14359, the potential contribution of increased ECP biogenesis on RcsB production was explored. Where previous reports aimed at examining the contribution of EcpR (MatA) to the transcriptional regulation of *rcsB* did not identify a significant increase in *rcsB* transcript (Lehti et al., 2012b), this study revealed a slight but significant increase in strain TW14359. Differences in the two strains examined, as well as the specific growth conditions, might account for the disparity in the studies. Furthermore, and in

agreement with RcsB regulation of type III secretion (Tobe et al., 2005), increased *tir* mRNA and cytosolic Tir was detected following overproduction of ECP, specifically following overexpression of *ecpR*. It is important to note that, while overproduction of EcpR did increase cytosolic levels of RcsB, a similar increase was also observed following overexpression of the *ecp* operon alone without *ecpR*. Therefore, one intriguing possibility is that activation of *rcsB* transcription is a result of increased ECP pilus production, rather than a result of direct or indirect activation by EcpR, such as is the case with EcpR mediated repression of motility through the *flhDC* promoter (Lehti et al., 2012a). Bacterial sensing of pilus production has been previously reported during overproduction of the type IV bundle-forming pilus, resulting in activation of the Cpx envelope stress response system (Nevesinjac and Raivio, 2005). And, more recently, loss of *ecpD* (encoding the ECP tip adhesin) was shown to decrease motility in APEC (Stacy et al., 2014). Collectively, these findings indicate that increased production of the ECP pilus is able to modulate transcription of *rcsB*, and thus indirectly effect the production of additional, distally encoded, adherence factors in EHEC strain TW14359. As ECP production has been found to play a critical role in *E. coli* biofilm formation (Lehti et al., 2010; Rendon et al., 2007; Stacy et al., 2014), it is possible that biogenesis of the *E. coli* common pilus may directly or indirectly activate the Rcs phosphorelay and transcription of genes involved in biofilm formation.

To conclude, in EHEC strain TW14359 it was shown that transcription of *ecpA* is under the control of a promoter that is repressed by H-NS. The promoter activity in TW14359 was further shown to be dependent on a strain specific polymorphism, and that mutation of the SNP to that of the closely related Sakai sequence reverted promoter activity to the low level observed for other *E. coli* strains. Furthermore, overproduction of ECP stimulated production of RcsB and

the LEE encoded Tir. And finally, *ecp* transcription, driven by the promoter upstream of *ecpA*, was able to positively affect adherence to cultured epithelial cells.

Table 8 - Strains and plasmids used in Chapter 4

Strain/plasmid	Relevant characteristics	Reference
Strain name:		
DH5α	Vector propagation, *recA1 endA1*	
MG1655	F-, lambda-, *rph*-1	
E2348/69	*Escherichia coli* O127:H6; (typical EPEC)	Iguchi, 2009
3256-97	*Escherichia coli* O55:H7; (atypical EPEC)	Zhou, 2010
TW14359	WT 2006 outbreak, western U.S.A. (EHEC)	Manning, 2008
Sakai	WT 1996 outbreak, Osaka, Japan (EHEC)	Michino, 1998
CFT073	*Escherichia coli* O6:K2:H1 CFT073 (UPEC)	Welch, 2002
EAEC O42	Wild-type Peruvian *Escherichia coli* O44:H18 (EAEC)	Nataro, 1985
UTI89	*Escherichia coli* O18 K1 H7 UTI89 (UPEC)	Chen, 2006
EcRJM-6	TW14359Δ*rcsB*	Morgan, 2013
EcRJM-10	TW14359*rcsB*-FLAG	Morgan, 2013
EcRJM-13	TW14359*tir*-FLAG	Morgan, 2013
EcRJM-73	TW14359Δ*lacZ*	Morgan, 2014
EcRJM-86	TW14359 *rcsDB-luxE*	Morgan, 2014
EcRJM-113	TW14359Δ*ecpR*$_p$::*kan*	This study
EcRJM-114	TW14359Δ*ecpA*::*kan*	This study
EcRJM-115	TW14359 *ecpA*-FLAG	This study
EcRJM-116	TW14359Δ*ecpR*$_p$::*kan ecpA-FLAG*	This study
EcRJM-117	TW14359Δ*lacZ*Δ*hns*::*kan*	This study
Plasmid name:		
pACYC177	Low copy cloning vector, Amp^R Kan^R P15A	Chang, 1978
pBAD-TOPO	Ara inducible expression vector, pBR322	Invitrogen
pMPM-K3	Low copy cloning vector, Kan^R p15A/f1	Mayer, 1995
pUC19	High copy cloning vector, Amp^R pMB1	Yanisch-Perron, 1985
pRS551	*lac* fusion vector, Amp^R Kan^R *lacZ*$^+$ ColE1	Simons, 1987
pCP20	Flp recombinase expression vector	Datsenko, 2000
pKD4	Template plasmid for Kan cassette	Datsenko, 2000
pKM208	Red-recombinase expression vector	Datsenko, 2000
pSU312	FLAG epitope template, Amp^R, Kan^R, R6K	Uzzau, 2001
placlux8	placlux8	Shimizu, 2011
pLuxCDAB3	pLuxCDAB3	Shimizu, 2011
pRJM-34	p*ecpR*, *ecpR* ORF and promoter in vector pMPM-K3	This study
pRJM-35	pBAD-*ecpR*, *ecpR* ORF in pBAD-TOPO vector	This study
pRJM-36	pMPM$_{BAD}$-*ecpR*, *ecpR* ORF and pBAD promoter cloned from pRJM-35 in pMPM-K3	This study
pRJM-37	p*ecpABCDE*, *ecpABCDE* operon cloned into pUC19	This study
pRJM-38	pRS551-*ecpR* (-496,-1), from TW14359	This study
pRJM-39	pRS551-*ecpA* (-666,-1), from TW14359	This study

[a] Nucleotide positions based on the published TW14359 (NC_013008) genome sequences (NCBI)

Table 7 **Strains and plasmids used in Chapter 3, continued.**

Strain/plasmid	Relevant characteristics	Reference
Plasmid name:		
pRJM-40	pRS551-*ecpA* (-555,-1), from TW14359	This study
pRJM-41	pRS551-*ecpA* (-496,-1), from TW14359	This study
pRJM-42	pRS551-*ecpA* (-387,-1), from TW14359	This study
pRJM-43	pRS551-*ecpA* (-270,-1), from TW14359	This study
pRJM-44	pRS551-*ecpA* (-131,-1), from TW14359	This study
pRJM-45	pRS551-*ecpA* (-666,-1), from Sakai	This study
pRJM-46	pRS551-*ecpA* (-666,-1), from UTI89	This study
pRJM-47	pRS551-*ecpA* (-666,-1), from CFT073	This study
pRJM-48	pRS551-*ecpA* (-666,-1), from O55:H7	This study
pRJM-49	pRS551-*ecpA* (-666,-1), from O127:H6	This study
pRJM-50	pRS551-*ecpA* (-666,-1), from MG1655	This study
pRJM-51	pRS551-*ecpA* (-666,-1), from TW14359 (T to C directed mutation)	This study
pRJM-52	pRS551-*ecpA* (-666,-1), from O127:H6 (C to T directed mutation)	This study
pRJM-53	pUC19-$ecpA_P$ (-666,-1), from TW14359	This study
pRJM-54	pUC19-$ecpA_P$ (-666,-1), from TW14359 (T to C directed mutation)	This study
pRJM-55	pUC19-$ecpA_P$ (-666,-1), from O127:H6	This study
pRJM-56	pUC19-$ecpA_P$ (-666,-1), from O127:H6 (C to T directed mutation)	This study
pRJM-21	pMPM-K3-*rcsDB*	Morgan 2014

[a] Nucleotide positions based on the published TW14359 (NC_013008) genome sequences (NCBI)

Table 9 - Primers used in Chapter 4

Primer name	Sequence (5'→ 3')[a,b]	Function/Reference
FLAG-F	gactacaaagatgacgacga	Uzzau, 2001
P1	gtgtaggctggagctgcttc	Datsenko, 2000
P2	catatgaatatcctccttag	Datsenko, 2000
Tir+664	ACTTCCAGCCTTCGTTCAGA	qRT-PCR Primer/Mitra, 2012
Tir+869	TTCTGGAACGCTTCTTTCGT	qRT-PCR Primer/Mitra, 2012
EspA+128	AGGCTGCGATTCTCATGTTT	qRT-PCR Primer/Mitra, 2012
EspA+310	GAAGTTTGGCTTTCGCATTC	qRT-PCR Primer/Mitra, 2012
RcsB+300	TCTGGATATCGAAGGGATCG	qRT-PCR Primer/Morgan, 2013
RcsB+485	AACAGGCGCAGAACTTCACT	qRT-PCR Primer/Morgan, 2013
EcpA+208	CTATTTGACGTGGCTATCG	qRT-PCR Primer
EcpA+291	CTGGGTTAATGTGTTGGTG	qRT-PCR Primer
Hns-41/P1	CCTCAACAAACCACCCCAATATAAGTTT GAGATTACTACAGTGTAGGCTGGAGCTGC TTC	Deletion Primer
Hns+455/P2	CGCCGATGGCGGGATTTTAAGCAAGTGCA ATCTACAAAAGCATATGAATATCCTCCT TAG	Deletion Primer
Hns-83/FVal	CTGAATTTAAGGCTCTATTA	Deletion Validation
Hns+482/RVal	TGTCTTAAACCGGACAATAA	Deletion Validation
EcpR-388/P2	CTTATCATTTAGACTTGTTTTTTTACTAG TCCATTACACACATATGAATATCCTCCT TAG	Deletion Primer
EcpR+40/P1	CAACCTCATAGTCCCTGCTGTAATCATTT TGCCATGTCACGTGTAGGCTGGAGCTGCT TC	Deletion Primer
EcpR-496	GGGATGAACACCCATAACCA	Deletion Validation
EcpR+70	CAGAACGGTTTTGACATTCC	Deletion Validation
EcpA-41/P1	TGGGACATCACGTCCTCAATTCAACTCGG GAAGAAATACAGTGTAGGCTGGAGCTGC TTC	Deletion Primer
EcpR-496	GGGATGAACACCCATAACCA	Deletion Validation
EcpR+70	CAGAACGGTTTTGACATTCC	Deletion Validation
EcpA-41/P1	TGGGACATCACGTCCTCAATTCAACTCGG GAAGAAATACAGTGTAGGCTGGAGCTGC TTC	Deletion Primer
EcpA+610/P2	CCCTGCTGGTACATCAGAGAGATTAACT GGTCCAGGTCGCCATATGAATATCCTCCT TAG	Deletion Primer

[a] Restriction sites indicated by bolded and underlined nucleotides

[b] Nucleotides changed through site-directed mutagenesis are indicated by bold nucleotides.

Table 8 **Primers used in Chapter 4, continued.**

Primer name	Sequence (5'→ 3')[a,b]	Function/Reference
EcpA+546/Flag-F	CGGCGACGTTAGCGTACAGTTCGACGCGACCTGGACCAGTGACTACAAAGATGACGACGA	FLAG Tagging Primer
EcpA+658/P2	GGTGCTTTTTCATAACAATTCCGTCCAGGAATAAAGCTGGCATATGAATATCCTCCTTAG	FLAG Tagging Primer
EcpA+524	CTCTACCGGAAGGCATCTGG	FLAG Validation Primer
EcpA+676	GCAGAGCGAGAAGCAGAAGG	FLAG Validation Primer
EcpR-496/BamHI	CG**GGATCC**GGGATGAACACCCATAACCA	Fragment for pRS551
EcpR-21/BamHI	CG**GGATCC**TACTTTCCAAACCTGTAATT	Fragment for pRS551
EcpA-666/EcoRI (1)	CGCG**GAATTC**GTGACATGGCAAAATGATTAC	Fragment for pRS551
EcpA-555/EcoRI	CGCG**GAATTC**GGACTATCTGAACTGATTGT	Fragment for pRS551
EcpA-496/EcoRI	CGCG**GAATTC**CAGAAAAGATTTCGTGTTTA	Fragment for pRS551
EcpA-387/EcoRI	CGCG**GAATTC**GCGGCCAGAAAGTCAGAAGC	Fragment for pRS551
EcpA-270/EcoRI	CGCG**GAATTC**GGCAGGTTCCTGAGAAAAGA	Fragment for pRS551
EcpA-131/EcoRI	CGCG**GAATTC**ATCGGCGTAATGCAGAGGCC	Fragment for pRS551
EcpA-1/BamHI (1)	CGCG**GGATCC**TGTATTTCTTCCCGAGTTGAA	Fragment for pRS551
EcpA-666/EcoRI (2)	CGCG**GAATTC**GTGACATGGCAAAGTGATTAC	Fragment for pRS551
EcpA-1/BamHI (2)	CGCG**GGATCC**TGCTTTTCTTCCCGAGTTGAA	Fragment for pRS551
EcpA-1/BamHI (3)	CGCG**GGATCC**TGCATTTCTTCCCGAGTTGAA	Fragment for pRS551
ecpAp/SDMForward	AGTGTATACC**C** ATCGGCGTAA	Site-Directed Mutagenesis
ecpAp/SDMReverse	TTACGCCGAT**G** GGTATACACT	Site-Directed Mutagenesis
ecpAp/SDMForward (O127)	AGTGTATACC**T** ATCGGCGGAA	Site-Directed Mutagenesis
ecpAp/SDMReverse (O127)	TTCCGCCGAT**A** GGTATACACT	Site-Directed Mutagenesis

[a] Restriction sites indicated by bolded and underlined nucleotides

[b] Nucleotides changed through site-directed mutagenesis are indicated by bold nucleotides.

Chapter 5: Conclusions and Future Directions

The 2006 EHEC O157:H7 outbreak strain TW14359 is characterized by increased virulence and an increased adherence phenotype when compared with distantly related EHEC strains (Abu-Ali et al., 2010a). Increased virulence is associated with increased LEE and *stx2* gene transcription, with concomitantly increased adherence and Stx2 production compared with the less virulent Sakai outbreak strain (Abu-Ali et al., 2010b). However, no specific factors had been identified which could account for increased virulence gene expression in TW14359 hitherto. Here, the proteome and transcriptome of EHEC strain TW14359 was explored to determine specific factors which contribute to increased virulence gene expression and adherence. Our proteomic analysis identified the Rcs response regulator RcsB as being more abundant in TW14359 when compared with EHEC strain Sakai. Indeed, loss of *rcsB* collapsed the differences in LEE gene expression and adherence between Sakai and TW14359, suggesting that it plays a role in the enhanced virulence phenotype.

The previous finding suggested that one or more factors, acting at one of the *rcsB* promoters, direct hypervirulence in TW14359. It is possible that some factor is directly binding to the *rcsB* promoter to influence transcriptional activation of the response regulator. Our analysis has only shown increased *rcsB* and LEE gene transcription during exponential phase in DMEM, a condition which is known to stimulate LEE gene transcription. Thus, it is possible that the effect is specific to those conditions which mimic the host environment and promote colonization. The production of other colonization factors, such as the *E. coli* common pilus (ECP), are stimulated during growth in DMEM for EHEC (Rendon et al., 2007; Torres et al.,

2002; Torres et al., 2007). While no additional *rcsB* regulators have been identified in this study, a few specific regulators have been previously shown to influence *rcsB* transcription, including QseE and LexA (Gervais et al., 1992; Reading et al., 2010). However, neither regulator was identified as being increased in either previous transcriptional profiles or comparative proteomic analyses herein. It is therefore possible that another unknown factor contributes directly or indirectly to increased *rcsB* transcription in EHEC strain TW14359. One additional possibility is that RcsB is directly regulating its own transcriptional activation through the phosphorelay itself. For example, in *Salmonella* the *rcsDB* operon is negatively regulated by RcsB through direct binding at the *rcsDB* promoter upstream of *rcsD* (Pescaretti Mde et al., 2009). This is particularly salient as it suggests RcsB may directly regulate its own transcription to some degree. However, no such regulatory pathway to-date has been identified in *E. coli*. Moreover, the predicted RcsB binding site upstream of *rcsD* present in *Salmonella* bears little homology to the same site in *E. coli*, opening the possibility for differences in auto-regulation.

Because RcsB is more abundant in TW14359, a strain which has high levels of LEE gene transcription, it was of interest to determine if overproduction of the LEE had a role in transcriptional activation of *rcsB*. While no specific activation of *rcsB* was observed following overproduction of GrlA, elevated RcsB was seen. This finding was particularly interesting since GrlA is known to repress motility in *E. coli*, and this study has shown RcsB is required for GrlA mediated repression of motility. Although increased RcsB was observed in GrlA overexpression strains, *rcsB* transcriptional activation was not. This data suggests some post-translational regulation of RcsB, either direct or indirect, by GrlA. As GrlA has been shown to interact directly with GrlR (Padavannil et al., 2013), it is possible that GrlA interacts with RcsB in some way to promote its stability. Alternatively, GrlA may affect some other factor that is able to post-

translationally modulate cytosolic RcsB levels. To determine potential interactions between GrlA and RcsB, it would be of interest to perform protein-protein interaction analyses using purified tagged variants of both GrlA and RcsB in pull-down studies. Alternatively, a co-immunoprecipitation experiment could be performed with purified GrlA and RcsB to determine specific protein-protein interactions. These experiments would begin to clearly determine if the regulatory effect of GrlA on RcsB abundance is direct, or whether it is through some other factor. In light of the latter findings, it is important to note that a previous study on transcriptional differences between EHEC strains Sakai and TW14359 revealed differences in LEE gene transcription, but also identified decreased transcription in genes associated with motility (Abu-Ali et al., 2010b). This finding was of particular interest as GrlA overexpression was also shown to negatively affect motility through the *flhDC* promoter, though direct interaction has not yet been shown (Iyoda et al., 2006). The results of this study have shown that GrlA mediated repression of motility requires an intact *rcsB* gene. As heterodimerization of RcsB with a number of transcriptional regulators has been previously described (Krin et al., 2010; Torres-Cabassa and Gottesman, 1987; Venkatesh et al., 2010), one possibility is that GrlA and RcsB interact directly to regulate *flhDC* promoter activity. While a specific RcsAB binding consensus site was identified in *E. coli* (Francez-Charlot et al., 2003), no current GrlA consensus sequence has been described. Alternatively, the regulatory effects on motility by GrlA and RcsB could be simply due to the downstream affects of increased RcsB protein levels alone.

As a positive LEE gene expression control, sodium bicarbonate was added to the growth media to stimulate LEE gene transcription. Surprisingly, addition of bicarbonate led to substantially increased cytosolic RcsB protein level (**Fig. 31**), which were elevated above that observed following GrlA overproduction. It was further shown that bicarbonate mediated

transcriptional activation of the *ler* promoter required an intact Rcs phosphorelay, and that full stimulation was also dependent on the EHEC specific regulator GrvA (Morgan et al., 2013; Tobe et al., 2005). To date, numerous studies have shown that LEE gene expression is maximal during active growth, but also in conditions which are similar to the predicted host physiology. These include, but are not limited to, pH, osmolarity, and the availability of different nutrients and host derived signals (Alam et al., 2010; Kendall et al., 2012; Kenny et al., 1997a; Kenny and Finlay, 1995; Pacheco et al., 2012; Sperandio et al., 2002). While this work has demonstrated RcsB dependent bicarbonate induction of the LEE, the method of RcsB activation by bicarbonate remains to be determined. Experiments aimed at elucidating this mechanism could explore factors which are dependent on the bicarbonate ion for function in *E. coli* that might activate the Rcs phosphorelay. For example, the cyclopropane fatty acid synthase (Cfa) is an enzyme which catalyzes the formation of cyclopropane groups in the non-polar region of phospholipids, a process that has a significant role in moderate acid resistance during stationary growth (Brown et al., 1997; Chang and Cronan, 1999). Recent studies have identified a bicarbonate molecule within the Cfa active site, and have further shown that enzyme activity can be inhibited following the addition of the Cfa active site competitor, borate, with a similar planar trigonal structure (Courtois and Ploux, 2005; Iwig et al., 2005). Thus, it is possible that bicarbonate increases enzymatic activity of the Cfa enzyme during exponential growth, when *cfa* transcription is typically lower (Rosenthal et al., 2008), and promotes the addition of cyclopropane groups to the cell membrane. Such a membrane alteration could conceivably activate the Rcs phosphorelay and promote downstream LEE gene transcription. Initial experiments aimed at exploring this hypothesis would be aimed at mutational analysis of *cfa* and the contribution to LEE gene transcription during growth with and without bicarbonate.

Preliminary data (not shown) has shown that addition of borate is able to quench bicarbonate mediated *rcsDB* promoter activation. However, the chemical nature of this is not yet clear as potential chemical reactions with bicarbonate and borate were not fully determined. As an alternative to Cfa, the aminopeptidase A (PepA) catalytic domain utilizes a bicarbonate ion, though it does not require bicarbonate for function (Strater et al., 1999). The PepA aminipeptidase was implicated in bicarbonate mediated virulence gene regulation in Vibrio cholera (Abuaita and Withey, 2009), though no study to-date has fully addressed the hypothesis.

Increased transcription of *rcsB* was observed in EHEC, and the effect was hypothesized to be due to some factor specific to TW14359. A comparative analysis of the TW14359 genome with other EHEC strains was performed (Kulasekara et al., 2009), and identified an insertion in the *tolA* gene which was initially hypothesized to contribute to *rcsB* dysregulation, which would make sense in light of the role for TolA in membrane integrity and subsequent Rcs phosphorelay activation (Clavel et al., 1996; Levengood et al., 1991) (**Fig. 30**). However, while loss of *tolA* in both TW14359 and Sakai EHEC strains did indeed elevate *rcsB* transcription, it was still proportionally higher in TW14359. Although data towards understanding the role for the TW14359 specific insertion in *tolA* did not support the initial hypothesis, further analysis into its role in potential physiological stress response differences in TW14359 is warranted. Specifically, variation in the *E. coli tolA* membrane spanning repeat domain length has recently been shown to affect stress tolerance to 4% sodium dodecyl sulfate (SDS) (Zhou et al., 2012). Furthermore, differences in the TolA transmembrane domain length contribute to distinct stress resistance differences observed for *Salmonella enterica* subsp. enterica serovars *Typhi* and *Typhimurium* (Lahiri et al., 2011). Thus, further examination into the direct role of TolA in EHEC virulence

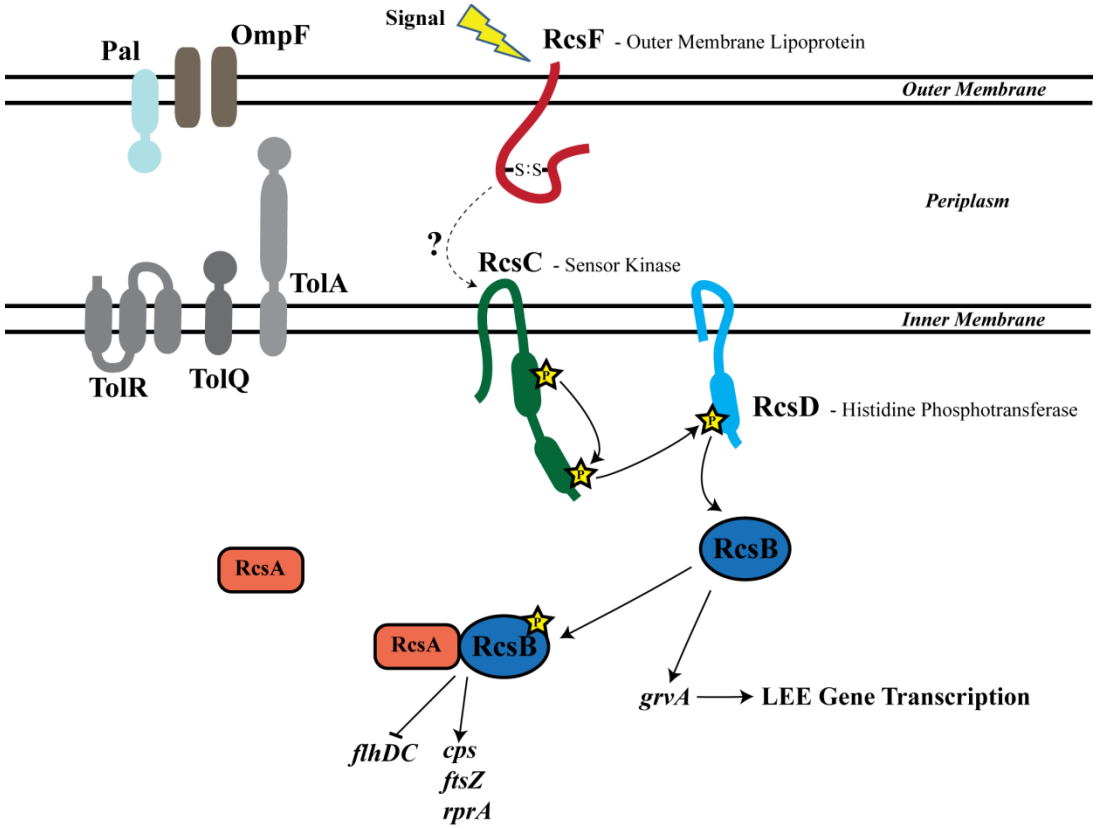

Figure 30 - Schematic model for TolQRA and the Rcs phosphorelay
The TolQRA complex is in E. coli facilitates maintenance of outer membrane integrity and has a role in division (Lloubes et al., 2001). The TolR and TolQ proteins energize TolA by coupling the proton motive force of the periplasmic space (Cascales et al., 2000). TolA is anchored to the inner membrane and has an extended alpha helical which connects the terminal domain that interacts with OmpF and Pal. Loss of TolA leads to outer membrane perturbation and strongly promotes signal transduction between RcsF and RcsC through some unknown mechanism (Clavel et al., 1996). Activation of the Rcs phosphorelay thus leads to transcriptional activation of capsular polysaccharide genes (*cps*) and is predicted to increase LEE gene transcription through the RcsB-GrvA pathway.

could include exploring its specific role in virulence, as observed in *Salmonella* (Paterson et al., 2009), and the mechanism by which *tolA* mutation communicates membrane perturbation to the inner-membrane lipoprotein RcsF (Clavel et al., 1996). As increased *rcsB* transcription was observed in both Sakai and TW14359 following mutation of *tolA*, it is possible that potential auto-activation of RcsB through the Rcs phosphorelay is a contributing factor. Finally, virulence assays for *tolA* mutant EHEC strains could be performed to explore the significance of the membrane spanning protein in pathogenesis and growth fitness in both bovine and mouse models of colonization. The contribution to adherence could be ascertained through adherence assays for EHEC on cultured epithelial cells, with either visual microcolony counts or fluorescent microscopy with antibodies for actin to determine pedestal formation under adherent EHEC cells. The experiment latter would permit detection of type III secretion mediated actin accumulation, and could help to discriminate between adherent cells utilizing other important EHEC adhesins, such as Lpf or HCP.

To identify additional factors unique to EHEC strain TW14359, a further sequence analysis of the TW14359 genome for other factors which might directly affect *rcsB* transcription was performed. Subsequent analysis of nucleotide polymorphisms specific to TW14359 revealed a SNP located upstream of the *ecp* operon encoded gene *ecpA*. This gene, encoding the major fimbrial subunit of the *E. coli* common pilus (ECP), was of particular interest as a regulatory dynamic between RcsB and the major *ecp* promoter had been previously established (Lehti et al., 2012b). A detailed mapping of the promoter, and further site-directed mutagenesis of specific nucleotide polymorphisms, revealed that promoter activity upstream of *ecpA* was significantly higher than all other *E. coli ecpA* promoters tested. And, perhaps more importantly, promoter activity was significantly higher than that of EHEC strain Sakai. This finding was particularly

salient as the only difference between the two promoters was the polymorphism identified. The regulatory region 270-bp upstream of *ecpA* identified had been previously tested for promoter activity (Martinez-Santos et al., 2012), but was performed on a strain lacking the polymorphism unique to TW14359. Likewise, another study has explored transcriptional regulation of the *ecpR* promoter and the region upstream of *ecpA*, specifically mediated by H-NS, and suggested that the sequence located within the *ecpR* open-reading frame may contain an 'upstream regulatory element' (Lehti et al., 2013b). This finding was congruent with our observation of H-NS control over the TW14359 specific *ecpA* promoter, where mutation of *hns* resulted in substantially higher *ecpA* promoter activity. A slight but significant increase was also seen for the promoter fragment derived from EHEC strain Sakai, supporting a model of H-NS regulation through the *ecpA* promoter in *E. coli* strains regardless of the promoter activity strength. Future investigations into the regulation of the *ecpA* promoter could include a more detailed analysis of the sequence differences between TW14359 and more distantly related strains, such as enteropathogenic *E. coli* O127:H6 strain E2348/69. Our initial findings revealed that the TW14359 specific SNP alone was not enough to activate transcription in E2348/69, and that one or more of the other nucleotide sequence differences might be responsible for promoter activity below that of strain TW14359. Identification of factors which directly regulate transcription from the *ecpA* promoter, in TW14359 and other *E. coli* strains, would provide insight into how ECP production is controlled in different nutritional conditions and growth phases, and provide insight into the contribution of unique nucleotide polymorphisms found among divergent *E. coli* strains.

Promoter variation for the primary *ecp* operon promoter, upstream of the *ecp* encoded ECP regulator EcpR, has been previously explored (Lehti et al., 2013b). The latter study

identified phylogenetic group specific variation in transcription that is associated with differences in promoter architecture, and suggests that it may contribute to adaptation among *E. coli* strains in response to different environments and growth conditions. Such a model for promoter adaptation would make sense, in an evolutionary sense, as production of ECP in EHEC has been associated with adherence to both mammalian and plant tissue, specifically to cultured epithelial cells and spinach leaves, respectively (Rendon et al., 2007; Saldana et al., 2011). It is thus possible that enhanced promoter activity of the *ecpA* pilin gene in EHEC strain TW14359 could provide a competitive advantage during colonization of a human or bovine host, or in adherence to spinach leaves. The latter food matrix is particularly interesting as the 2006 EHEC outbreak to which TW14359 was involved occurred largely through contaminated pre-packaged spinach (Wendel et al., 2009). Whether increased *ecpA* promoter activity in TW14359 has a role in adherence to mammalian or plant tissue has yet to be determined, however our analysis of ECP production has shown that ECP is produced in TW14359 in the absence of a functional *ecpR* promoter. Future analyses of TW14359 ECP production could involve experiments for competitive mammalian and plant tissue colonization with strains lacking other major adhesins, such as the type III secretion system, and in strains with distinct ECP expression patterns.

The primary *ecp* promoter upstream of *ecpR* is directly regulated by RcsB, as previously observed for neuromeningitic *E. coli* (NMEC) (Lehti et al., 2012b) and herein observed for EHEC. However, overproduction of EcpR in NMEC only slightly increased *rcsB* promoter activity, while in EHEC strain TW14359 our experiments have shown that a significant increase in mRNA and cytosolic RcsB is observed following expression of *ecpR*. This finding was quite intriguing as it suggests the former observation of increased *ecpA* promoter activity in EHEC strain TW14359 may have a role in dysregulation of *rcsB* when compared with other EHEC

strains (Morgan et al., 2013). As the regulator of the *ecp* operon, EcpR overproduction increases total ECP production. Thus, it is possible that increased *rcsB* transcription could be as a result of significantly increased ECP protuberance. Increased fimbriae production has been observed to activate the Cpx response in *E. coli* (Hung et al., 2001), in accordance with the proposed model. The *ecp* operon contains all of the factors required for ECP production. Specifically, following the chaperone-usher model of pilus biogenesis in *E. coli* (Thanassi et al., 1998; Waksman and Hultgren, 2009), ECP pili require the insertion of an usher protein (EcpC) into the outer-membrane through which the pilus is assembled (Volkan et al., 2013a). For ECP pili, two predicted *ecp* encoded chaperones (EcpB/EcpE) direct the assembly of both the ECP tip adhesin (EcpD) and the major ECP subunit (EcpA) (Garnett et al., 2012; Sauer et al., 1999). Since expression of the *ecp* operon, excluding *ecpR*, resulted in a similarly increased level of *rcsB* transcription, biogenesis of ECP is at least partly able to stimulate *rcsB* transcription (**Fig. 31**). However, as EcpR has been shown to directly regulate additional genes outside of the *ecp* operon, specifically *flhDC* (Lehti et al., 2012a), it remains a possibility that EcpR is able to regulate *rcsB* production in a manner independent of the pilus. How exactly assembly of ECP is capable of activation *rcsB* transcription is still unknown, however a recent study demonstrated that loss of the ECP tip adhesin EcpD, but not the major fimbrial subunit EcpA, significantly reduced motility in avian pathogenic *E. coli* (APEC) (Stacy et al., 2014). One possible explanation for this could be that loss of the ECP tip adhesin results in either mis-assembly or excess accumulation of EcpA in the periplasmic space, where chaperone binding capacity is exceeded. Indeed, previous reports on the basis of pilus biogenesis indicate that pilin subunits in the periplasm can be either chaperone-bound and awaiting assembly through the outer-

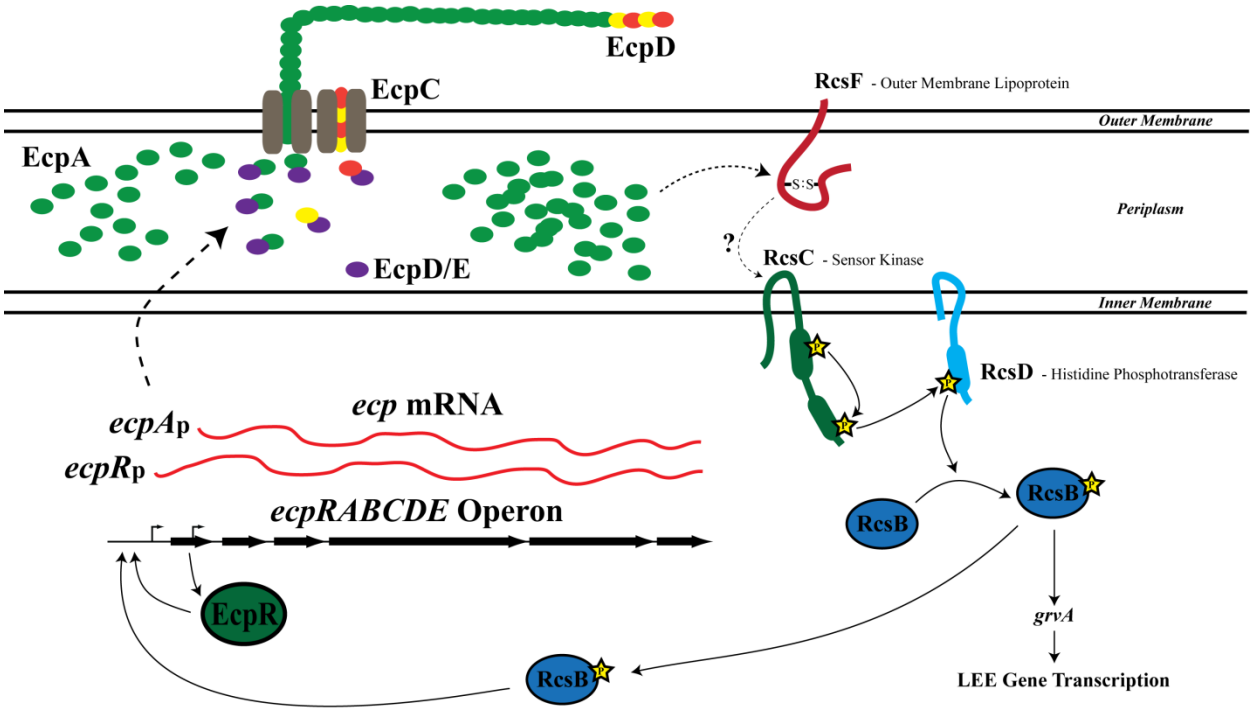

Figure 31 - Model for ECP biogenesis and predicted stimulation of the Rcs phosphorelay
The *E. coli* common pilus is assembled through the chaperon-usher model of pilus biogenesis (Volkan et al., 2013b; Wurpel et al., 2013). The *ecp* operon is regulated by both the *ecp* encoded EcpR and the response regulator RcsB. Though two ecp promoters have been identified in TW14359, only the *ecpR* promoter is directly regulated by EcpR and RcsB. ECP pilus components localize to the periplasmic space where the EcpD and EcpE chaperones guide the major pilin subunit (EcpA) and the tip adhesin (EcpD) to the usher protein (EcpC) for assembly. In this model, accumulation of EcpA could stimulate the Rcs phosphorelay through RcsF, or another unknown mechanism, to promote transcription and production of both RcsB and the LEE.

membrane usher, or alternatively involved OFF-pathway interactions leading to stress pathway activation (Hung et al., 1999; Hung et al., 2001). The outer-membrane lipoprotein RcsF has been shown to sense membrane perturbations and transmit signals to the Rcs sensor kinase (Majdalani et al., 2005; Shiba et al., 2012), and could thus effect transcription of the *rcsB* gene itself. Indeed, as previous studies have shown that mutation of *tolA* results in unambiguous activation of the Rcs phosphorelay (Clavel et al., 1996), loss of *tolA* in TW14359 led to significantly higher *rcsB* transcription (Morgan et al., 2013), in support of the proposed model of RcsB auto-regulation. However, as noted previously, work remains to be done in elucidating specific auto-regulation of the *rcsDB* operon by RcsB.

The LEE gene regulatory pathway through RcsB and GrvA had previously only been functionally described; indeed, the *grvA* dependence for LEE gene transcription had only been shown during overexpression of RcsB or through intrinsic activation of the Rcs phosphorelay through expression of a hyper-phosphorylating variant of RcsC (Tobe et al., 2005). However, the specific regulatory dynamic between RcsB and the *grvA* gene and downstream LEE gene regulation by GrvA remained unknown. Since our work has shown that RcsB binds directly to the *grvA* promoter, direct regulation through phosphorylated RcsB likely occurs at one or both of the tandem RcsB consensus sequences located proximal to the predicted *grvA* sigma-70 promoter. Interestingly, the *grvA* promoter appears to be under tight regulation during all post-lag growth phases, suggesting that some other factor may be involved in transcriptionally regulating its activity. Even during growth in DMEM, a condition which significantly increase *rcsB* transcription, *grvA* promoter activity eventually collapsed following transition to exponential growth. One such possible regulator includes the capsule synthesis regulator RcsA, which is typically under tight proteolytic degradation during growth at physiological

temperatures (Torres-Cabassa and Gottesman, 1987). If RcsA is able to accumulate during stationary phase, transition to growth could ultimately leave a population of the regulator able to act of RcsA/RcsB promoters prior to its eventual degradation. In support of this, the RcsB binding sites upstream of the *grvA* promoter bear high sequence similarity to that of the RcsAB box identified upstream of *flhDC* (Francez-Charlot et al., 2003), a promoter which is actively repressed during RcsA accumulation. To determine whether RcsA is indeed a bona-fide *grvA* regulator, direct interaction could be determined through electrophoretic mobility shift assays or through co-immuno precipitation with epitope tagged RcsA.

While the direct regulation of *grvA* by RcsB was identified, the specific role for GrvA in the regulation of LEE gene transcription had not been shown. RNA sequencing was employed to explore the transcriptional differences in wild type compared with *grvA* and *rcsB* mutant strains. This aim of this approach was to determine the pathway, direct or indirect, through which GrvA transcriptionally regulates the *LEE1* promoter, and downstream type III secretion. However, between the *grvA* isogenic mutant strain and the *rcsB* and *grvA* double mutant, only increased transcription of the GAD acid fitness island (AFI) could account for decreased LEE gene transcription. The AFI encoded transcriptional regulator GadE is a known direct repressor of LEE gene transcription, and is under complex regulation at 3 independent promoters located within a 750-bp sensory region upstream of the *gadE* ORF (Kailasan Vanaja et al., 2009; Sayed and Foster, 2009; Tree et al., 2011). Only the $gadE_{P3}$ promoter was consistently up-regulated in the *grvA* mutant strain and up-regulation required an additional AFI encoded regulator, GadW (**Fig. 32**). This regulatory dynamic is of particular interest as attempts to identify GrvA interaction at the $gadE_{P3}$ promoter, while unsuccessful, revealed an additional unexpected shift with purified membrane fractions independent of GrvA. Thus, the GAD acid fitness island may

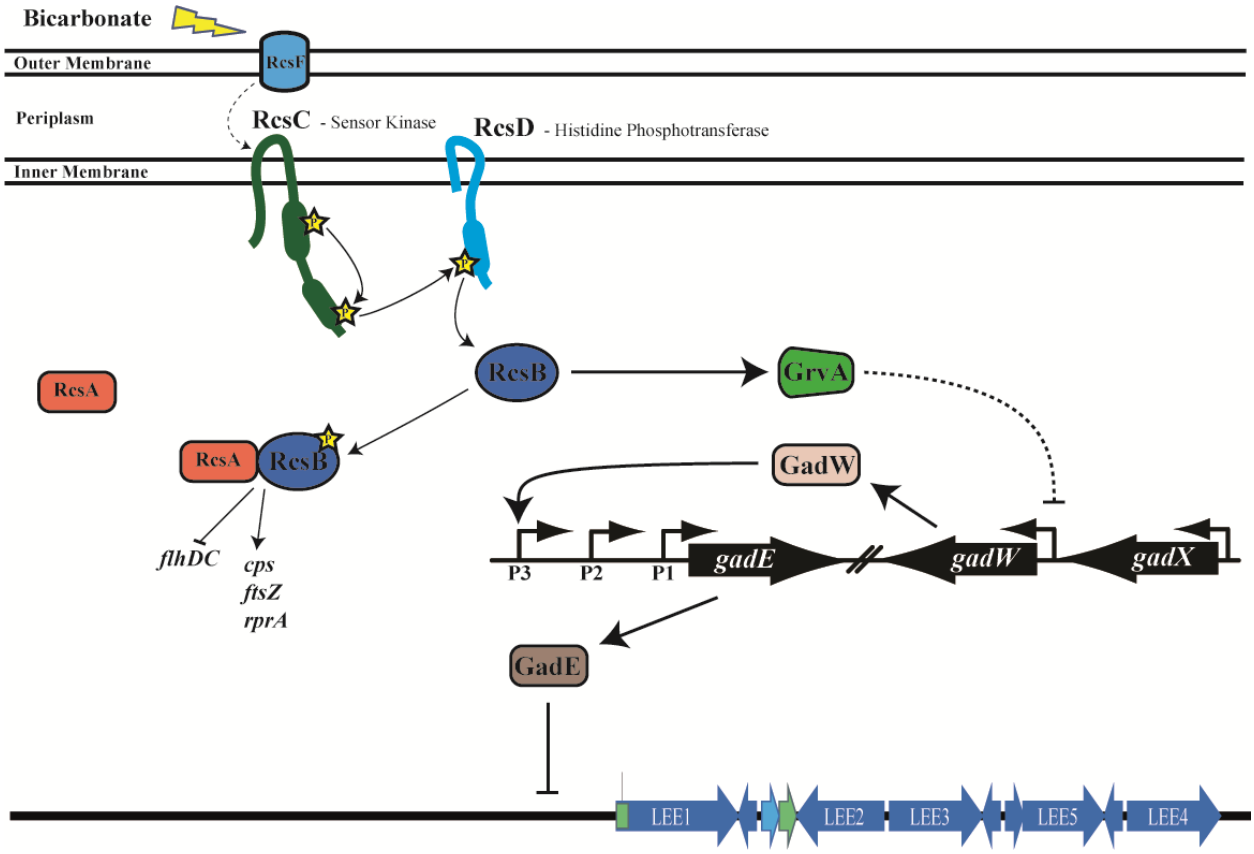

Figure 32 - Schematic model for RcsB-GrvA regulation of the LEE
Bicarbonate is predicted to be a signal of at least RcsC, and its activation results in phosphotransfer to RcsD and thus RcsB. The grvA promoter is activated through direct transcriptional activation by RcsB and, through an as of yet unknown mechanism, is predicted to represses production of the *gadE* positive regulator GadW. Ultimately, de-repression of *gadW* leads to increased GadE production through the $gadE_{P3}$ promoter, and results in both exponential acid resistance and *LEE1* promoter repression.

interact with the inner membrane through direct binding of some factor at the *gadE* P3 promoter. In this model, GrvA bound to the inner membrane could more easily interact with the AFI encoded *gadW* promoter region. This mechanism of transcriptional regulation has been extensively described for the *Vibrio cholerae* toxin regulator ToxR (Kolmar et al., 1995). However, it has not been investigated whether GrvA directly binds to either of the mapped *gadW* promoters, or whether its regulatory role is indirect. Although preliminary evidence does suggest GrvA is localized to the inner membrane (unpublished data), in accordance with the location of its predicted transmembrane domain and high amino acid homology with ToxR.

To conclude, the results presented herein have demonstrated that differences in transcriptional regulation between two genetically distant EHEC strains is as a result of dysregulation of the capsule synthesis regulator RcsB. In the course of experimentation, a reciprocating regulatory loop between the LEE encoded regulator GrlA and RcsB was identified, and bicarbonate mediated virulence gene activation in EHEC was shown to be dependent on an intact Rcs phosphorelay. Further investigations into the genetic differences between EHEC strains Sakai and TW14359 revealed a polymorphism upstream of the ECP major fimbrial subunit gene encoding EcpA, and was subsequently shown to be unique to the 2006 O157:H7 EHEC spinach outbreak strain TW14359. Although increased ECP production results in *rcsB* transcriptional activation, it remains a possibility that other factors contribute to intrinsic dysregulation of the *rcsB* in TW14359. Finally, the RcsB-GrvA pathway was explored using comparative RNA sequencing to elucidate the specific mechanism through which GrvA effects LEE gene transcription, and a pathway wherein GadE, stimulated by GadW, was identified. Taken together, the results presented significantly expand the role for RcsB in virulence gene

regulation for EHEC, identify a novel pathway for ECP stimulated LEE gene activation, and characterize the specific pathway for GrvA regulation of type III secretion.

References

Abe, A., Kenny, B., Stein, M., Finlay, B.B., 1997. Characterization of two virulence proteins secreted by rabbit enteropathogenic Escherichia coli, EspA and EspB, whose maximal expression is sensitive to host body temperature. Infect Immun 65, 3547-3555.

Abe, H., Tatsuno, I., Tobe, T., Okutani, A., Sasakawa, C., 2002. Bicarbonate ion stimulates the expression of locus of enterocyte effacement-encoded genes in enterohemorrhagic Escherichia coli O157:H7. Infect Immun 70, 3500-3509.

Abu-Ali, G.S., Ouellette, L.M., Henderson, S.T., Lacher, D.W., Riordan, J.T., Whittam, T.S., Manning, S.D., 2010a. Increased adherence and expression of virulence genes in a lineage of Escherichia coli O157:H7 commonly associated with human infections. PLoS One 5, e10167.

Abu-Ali, G.S., Ouellette, L.M., Henderson, S.T., Whittam, T.S., Manning, S.D., 2010b. Differences in adherence and virulence gene expression between two outbreak strains of enterohaemorrhagic Escherichia coli O157 : H7. Microbiology 156, 408-419.

Abuaita, B.H., Withey, J.H., 2009. Bicarbonate Induces Vibrio cholerae virulence gene expression by enhancing ToxT activity. Infect Immun 77, 4111-4120.

Aiso, T., Murata, M., Gamou, S., 2011. Transcription of an antisense RNA of a gadE mRNA is regulated by GadE, the central activator of the acid resistance system in Escherichia coli. Genes to cells : devoted to molecular & cellular mechanisms 16, 670-680.

Alam, A., Tam, V., Hamilton, E., Dziejman, M., 2010. vttRA and vttRB Encode ToxR family proteins that mediate bile-induced expression of type three secretion system genes in a non-O1/non-O139 Vibrio cholerae strain. Infect Immun 78, 2554-2570.

Alcantar-Curiel, M.D., Blackburn, D., Saldana, Z., Gayosso-Vazquez, C., Iovine, N.M., De la Cruz, M.A., Giron, J.A., 2013. Multi-functional analysis of Klebsiella pneumoniae fimbrial types in adherence and biofilm formation. Virulence 4, 129-138.

Avelino, F., Saldana, Z., Islam, S., Monteiro-Neto, V., Dall'Agnol, M., Eslava, C.A., Giron, J.A., 2010. The majority of enteroaggregative Escherichia coli strains produce the E. coli common pilus when adhering to cultured epithelial cells. Int J Med Microbiol 300, 440-448.

Barba, J., Bustamante, V.H., Flores-Valdez, M.A., Deng, W., Finlay, B.B., Puente, J.L., 2005. A positive regulatory loop controls expression of the locus of enterocyte effacement-encoded regulators Ler and GrlA. J Bacteriol 187, 7918-7930.

Batchelor, E., Walthers, D., Kenney, L.J., Goulian, M., 2005. The Escherichia coli CpxA-CpxR envelope stress response system regulates expression of the porins ompF and ompC. J Bacteriol 187, 5723-5731.

Bender, J.K., Praszkier, J., Wakefield, M.J., Holt, K., Tauschek, M., Robins-Browne, R.M., Yang, J., 2012. Involvement of PatE, a Prophage-Encoded AraC-Like Regulator, in the Transcriptional Activation of Acid Resistance Pathways of Enterohemorrhagic Escherichia coli Strain EDL933. Appl Environ Microbiol 78, 5083-5092.

Berdichevsky, T., Friedberg, D., Nadler, C., Rokney, A., Oppenheim, A., Rosenshine, I., 2005. Ler is a negative autoregulator of the LEE1 operon in enteropathogenic Escherichia coli. J Bacteriol 187, 349-357.

Bereswill, S., Geider, K., 1997. Characterization of the rcsB gene from Erwinia amylovora and its influence on exoploysaccharide synthesis and virulence of the fire blight pathogen. J Bacteriol 179, 1354-1361.

Bergholz, T.M., Wick, L.M., Qi, W., Riordan, J.T., Ouellette, L.M., Whittam, T.S., 2007a. Global transcriptional response of Escherichia coli O157:H7 to growth transitions in glucose minimal medium. BMC Microbiol 7, 97.

Bergholz, T.M., Wick, L.M., Qi, W., Riordan, J.T., Ouellette, L.M., Whittam, T.S., 2007b. Global transcriptional response of Escherichia coli O157:H7 to growth transitions in glucose minimal medium. BMC Microbiol 7, 97.

Bernadac, A., Gavioli, M., Lazzaroni, J.C., Raina, S., Lloubes, R., 1998. Escherichia coli tol-pal mutants form outer membrane vesicles. J Bacteriol 180, 4872-4878.

Bingle, L.E., Constantinidou, C., Shaw, R.K., Islam, M.S., Patel, M., Snyder, L.A., Lee, D.J., Penn, C.W., Busby, S.J., Pallen, M.J., 2014. Microarray Analysis of the Ler Regulon in Enteropathogenic and Enterohaemorrhagic Escherichia coli Strains. PLoS One 9, e80160.

Boerlin, P., McEwen, S.A., Boerlin-Petzold, F., Wilson, J.B., Johnson, R.P., Gyles, C.L., 1999. Associations between virulence factors of Shiga toxin-producing Escherichia coli and disease in humans. J Clin Microbiol 37, 497-503.

Boulanger, A., Francez-Charlot, A., Conter, A., Castanie-Cornet, M.P., Cam, K., Gutierrez, C., 2005. Multistress regulation in Escherichia coli: expression of osmB involves two independent promoters responding either to sigmaS or to the RcsCDB His-Asp phosphorelay. J Bacteriol 187, 3282-3286.

Branchu, P., Hindre, T., Fang, X., Thomas, R., Gomelsky, M., Claret, L., Harel, J., Gobert, A.P., Martin, C., 2013. The c-di-GMP phosphodiesterase VmpA absent in Escherichia coli K12 strains affects motility and biofilm formation in the enterohemorrhagic O157:H7 serotype. Vet Immunol Immunopathol 152, 132-140.

Branchu, P., Matrat, S., Vareille, M., Garrivier, A., Durand, A., Crépin, S., Harel, J., Jubelin, G., Gobert, A.P., 2014. NsrR, GadE, and GadX Interplay in Repressing Expression of the Escherichia coli O157:H7 LEE Pathogenicity Island in Response to Nitric Oxide. PLoS Pathog 10, e1003874.

Brill, J.A., Quinlan-Walshe, C., Gottesman, S., 1988. Fine-structure mapping and identification of two regulators of capsule synthesis in Escherichia coli K-12. J Bacteriol 170, 2599-2611.

Brown, J.L., Ross, T., McMeekin, T.A., Nichols, P.D., 1997. Acid habituation of Escherichia coli and the potential role of cyclopropane fatty acids in low pH tolerance. Int J Food Microbiol 37, 163-173.

Campellone, K.G., 2010. Cytoskeleton-modulating effectors of enteropathogenic and enterohaemorrhagic Escherichia coli: Tir, EspF and actin pedestal assembly. FEBS J.

Carballes, F., Bertrand, C., Bouche, J.P., Cam, K., 1999. Regulation of Escherichia coli cell division genes ftsA and ftsZ by the two-component system rcsC-rcsB. Mol Microbiol 34, 442-450.

Carter, M.Q., Parker, C.T., Louie, J.W., Huynh, S., Fagerquist, C.K., Mandrell, R.E., 2012. RcsB contributes to the distinct stress fitness among Escherichia coli O157:H7 curli variants of the 1993 hamburger-associated outbreak strains. Appl Environ Microbiol 78, 7706-7719.

Cascales, E., Gavioli, M., Sturgis, J.N., Lloubes, R., 2000. Proton motive force drives the interaction of the inner membrane TolA and outer membrane pal proteins in Escherichia coli. Mol Microbiol 38, 904-915.

Castanie-Cornet, M.P., Cam, K., Bastiat, B., Cros, A., Bordes, P., Gutierrez, C., 2010. Acid stress response in Escherichia coli: mechanism of regulation of gadA transcription by RcsB and GadE. Nucleic Acids Res 38, 3546-3554.

Castanie-Cornet, M.P., Cam, K., Jacq, A., 2006. RcsF is an outer membrane lipoprotein involved in the RcsCDB phosphorelay signaling pathway in Escherichia coli. J Bacteriol 188, 4264-4270.

Castanie-Cornet, M.P., Penfound, T.A., Smith, D., Elliott, J.F., Foster, J.W., 1999. Control of acid resistance in Escherichia coli. J Bacteriol 181, 3525-3535.

Castanie-Cornet, M.P., Treffandier, H., Francez-Charlot, A., Gutierrez, C., Cam, K., 2007. The glutamate-dependent acid resistance system in Escherichia coli: essential and dual role of the His-Asp phosphorelay RcsCDB/AF. Microbiology 153, 238-246.

Chaand, M., Dziejman, M., 2013. Vibrio cholerae VttR(A) and VttR(B) regulatory influences extend beyond the type 3 secretion system genomic island. J Bacteriol 195, 2424-2436.

Champion, O.L., Cooper, I.A., James, S.L., Ford, D., Karlyshev, A., Wren, B.W., Duffield, M., Oyston, P.C., Titball, R.W., 2009. Galleria mellonella as an alternative infection model for Yersinia pseudotuberculosis. Microbiology 155, 1516-1522.

Chang, Y.Y., Cronan, J.E., Jr., 1999. Membrane cyclopropane fatty acid content is a major factor in acid resistance of Escherichia coli. Mol Microbiol 33, 249-259.

Cheng, H.C., Skehan, B.M., Campellone, K.G., Leong, J.M., Rosen, M.K., 2008. Structural mechanism of WASP activation by the enterohaemorrhagic E. coli effector EspF(U). Nature 454, 1009-1013.

Chingcuanco, F., Yu, Y., Kus, J.V., Que, L., Lackraj, T., Levesque, C.M., Barnett Foster, D., 2012. Identification of a novel adhesin involved in acid-induced adhesion of enterohaemorrhagic Escherichia coli O157 : H7. Microbiology 158, 2399-2407.

Chung, C.H., Goldberg, A.L., 1981. The product of the lon (capR) gene in Escherichia coli is the ATP-dependent protease, protease La. Proc Natl Acad Sci U S A 78, 4931-4935.

Clarke, D.J., 2010. The Rcs phosphorelay: more than just a two-component pathway. Future Microbiol 5, 1173-1184.

Clarke, D.J., Holland, I.B., Jacq, A., 1997. Point mutations in the transmembrane domain of DjlA, a membrane-linked DnaJ-like protein, abolish its function in promoting colanic acid production via the Rcs signal transduction pathway. Mol Microbiol 25, 933-944.

Clavel, T., Lazzaroni, J.C., Vianney, A., Portalier, R., 1996. Expression of the tolQRA genes of Escherichia coli K-12 is controlled by the RcsC sensor protein involved in capsule synthesis. Mol Microbiol 19, 19-25.

Courtois, F., Ploux, O., 2005. Escherichia coli cyclopropane fatty acid synthase: is a bound bicarbonate ion the active-site base? Biochemistry 44, 13583-13590.

Crane, J.K., Byrd, I.W., Boedeker, E.C., 2011. Virulence inhibition by zinc in shiga-toxigenic Escherichia coli. Infect Immun 79, 1696-1705.

Crane, J.K., McNamara, B.P., Donnenberg, M.S., 2001. Role of EspF in host cell death induced by enteropathogenic Escherichia coli. Cell Microbiol 3, 197-211.

Cray, W.C., Jr., Moon, H.W., 1995. Experimental infection of calves and adult cattle with Escherichia coli O157:H7. Appl Environ Microbiol 61, 1586-1590.

Creasey, E.A., Delahay, R.M., Daniell, S.J., Frankel, G., 2003. Yeast two-hybrid system survey of interactions between LEE-encoded proteins of enteropathogenic Escherichia coli. Microbiology 149, 2093-2106.

d'Aubenton Carafa, Y., Brody, E., Thermes, C., 1990. Prediction of rho-independent Escherichia coli transcription terminators. A statistical analysis of their RNA stem-loop structures. J Mol Biol 216, 835-858.

Danese, P.N., Silhavy, T.J., 1997. The sigma(E) and the Cpx signal transduction systems control the synthesis of periplasmic protein-folding enzymes in Escherichia coli. Genes Dev 11, 1183-1193.

Datsenko, K.A., Wanner, B.L., 2000. One-step inactivation of chromosomal genes in Escherichia coli K-12 using PCR products. Proc Natl Acad Sci U S A 97, 6640-6645.

Dean, P., Kenny, B., 2009. The effector repertoire of enteropathogenic E. coli: ganging up on the host cell. Curr Opin Microbiol 12, 101-109.

Deng, W., de Hoog, C.L., Yu, H.B., Li, Y., Croxen, M.A., Thomas, N.A., Puente, J.L., Foster, L.J., Finlay, B.B., 2010. A comprehensive proteomic analysis of the type III secretome of Citrobacter rodentium. J Biol Chem 285, 6790-6800.

Deng, W., Li, Y., Hardwidge, P.R., Frey, E.A., Pfuetzner, R.A., Lee, S., Gruenheid, S., Strynakda, N.C., Puente, J.L., Finlay, B.B., 2005. Regulation of type III secretion hierarchy of translocators and effectors in attaching and effacing bacterial pathogens. Infect Immun 73, 2135-2146.

Deng, W., Puente, J.L., Gruenheid, S., Li, Y., Vallance, B.A., Vazquez, A., Barba, J., Ibarra, J.A., O'Donnell, P., Metalnikov, P., Ashman, K., Lee, S., Goode, D., Pawson, T., Finlay, B.B., 2004. Dissecting virulence: systematic and functional analyses of a pathogenicity island. Proc Natl Acad Sci U S A 101, 3597-3602.

DeVinney, R., Stein, M., Reinscheid, D., Abe, A., Ruschkowski, S., Finlay, B.B., 1999. Enterohemorrhagic Escherichia coli O157:H7 produces Tir, which is translocated to the host cell membrane but is not tyrosine phosphorylated. Infect Immun 67, 2389-2398.

DiRita, V.J., Mekalanos, J.J., 1991. Periplasmic interaction between two membrane regulatory proteins, ToxR and ToxS, results in signal transduction and transcriptional activation. Cell 64, 29-37.

Dong, T., Coombes, B.K., Schellhorn, H.E., 2009. Role of RpoS in the virulence of Citrobacter rodentium. Infect Immun 77, 501-507.

Dong, T., Schellhorn, H.E., 2009. Global effect of RpoS on gene expression in pathogenic Escherichia coli O157:H7 strain EDL933. BMC Genomics 10, 349.

Dorel, C., Lejeune, P., Rodrigue, A., 2006. The Cpx system of Escherichia coli, a strategic signaling pathway for confronting adverse conditions and for settling biofilm communities? Res Microbiol 157, 306-314.

Eaton, K.A., Friedman, D.I., Francis, G.J., Tyler, J.S., Young, V.B., Haeger, J., Abu-Ali, G., Whittam, T.S., 2008. Pathogenesis of renal disease due to enterohemorrhagic Escherichia coli in germ-free mice. Infect Immun 76, 3054-3063.

Efromovich, S., Grainger, D., Bodenmiller, D., Spiro, S., 2008. Genome-wide identification of binding sites for the nitric oxide-sensitive transcriptional regulator NsrR. Methods Enzymol 437, 211-233.

Egger, L.A., Park, H., Inouye, M., 1997. Signal transduction via the histidyl-aspartyl phosphorelay. Genes Cells 2, 167-184.

Elliott, S.J., Sperandio, V., Giron, J.A., Shin, S., Mellies, J.L., Wainwright, L., Hutcheson, S.W., McDaniel, T.K., Kaper, J.B., 2000. The locus of enterocyte effacement (LEE)-encoded regulator controls expression of both LEE- and non-LEE-encoded virulence factors in enteropathogenic and enterohemorrhagic Escherichia coli. Infect Immun 68, 6115-6126.

Elliott, S.J., Wainwright, L.A., McDaniel, T.K., Jarvis, K.G., Deng, Y.K., Lai, L.C., McNamara, B.P., Donnenberg, M.S., Kaper, J.B., 1998. The complete sequence of the locus of enterocyte effacement (LEE) from enteropathogenic Escherichia coli E2348/69. Mol Microbiol 28, 1-4.

Elliott, S.J., Yu, J., Kaper, J.B., 1999. The cloned locus of enterocyte effacement from enterohemorrhagic Escherichia coli O157:H7 is unable to confer the attaching and effacing phenotype upon E. coli K-12. Infect Immun 67, 4260-4263.

Endo, Y., Tsurugi, K., Yutsudo, T., Takeda, Y., Ogasawara, T., Igarashi, K., 1988. Site of action of a Vero toxin (VT2) from Escherichia coli O157:H7 and of Shiga toxin on eukaryotic ribosomes. RNA N-glycosidase activity of the toxins. Eur J Biochem 171, 45-50.

Erdem, A.L., Avelino, F., Xicohtencatl-Cortes, J., Giron, J.A., 2007. Host protein binding and adhesive properties of H6 and H7 flagella of attaching and effacing Escherichia coli. J Bacteriol 189, 7426-7435.

Farfan, M.J., Torres, A.G., 2012. Molecular mechanisms that mediate colonization of Shiga toxin-producing Escherichia coli strains. Infect Immun 80, 903-913.

Feldman, M., 1983. Gastric bicarbonate secretion in humans. Effect of pentagastrin, bethanechol, and 11,16,16-trimethyl prostaglandin E2. J Clin Invest 72, 295-303.

Ferianc, P., Farewell, A., Nystrom, T., 1998. The cadmium-stress stimulon of Escherichia coli K-12. Microbiology 144 (Pt 4), 1045-1050.

Ferrieres, L., Clarke, D.J., 2003. The RcsC sensor kinase is required for normal biofilm formation in Escherichia coli K-12 and controls the expression of a regulon in response to growth on a solid surface. Mol Microbiol 50, 1665-1682.

Flockhart, A.F., Tree, J.J., Xu, X., Karpiyevich, M., McAteer, S.P., Rosenblum, R., Shaw, D.J., Low, C.J., Best, A., Gannon, V., Laing, C., Murphy, K.C., Leong, J.M., Schneiders, T., La Ragione, R., Gally, D.L., 2012. Identification of a novel prophage regulator in Escherichia coli controlling the expression of type III secretion. Mol Microbiol 83, 208-223.

Fordtran, J.S., Locklear, T.W., 1966. Ionic constituents and osmolality of gastric and small-intestinal fluids after eating. Am J Dig Dis 11, 503-521.

Foster, J.W., 2004. Escherichia coli acid resistance: tales of an amateur acidophile. Nat Rev Microbiol 2, 898-907.

Francez-Charlot, A., Laugel, B., Van Gemert, A., Dubarry, N., Wiorowski, F., Castanie-Cornet, M.P., Gutierrez, C., Cam, K., 2003. RcsCDB His-Asp phosphorelay system negatively regulates the flhDC operon in Escherichia coli. Mol Microbiol 49, 823-832.

Frenzen, P.D., Drake, A., Angulo, F.J., 2005. Economic cost of illness due to Escherichia coli O157 infections in the United States. J Food Prot 68, 2623-2630.

Friedberg, D., Umanski, T., Fang, Y., Rosenshine, I., 1999. Hierarchy in the expression of the locus of enterocyte effacement genes of enteropathogenic Escherichia coli. Mol Microbiol 34, 941-952.

Gabbianelli, R., Scotti, R., Ammendola, S., Petrarca, P., Nicolini, L., Battistoni, A., 2011. Role of ZnuABC and ZinT in Escherichia coli O157:H7 zinc acquisition and interaction with epithelial cells. BMC Microbiol 11, 36.

Garmendia, J., Phillips, A.D., Carlier, M.F., Chong, Y., Schuller, S., Marches, O., Dahan, S., Oswald, E., Shaw, R.K., Knutton, S., Frankel, G., 2004. TccP is an enterohaemorrhagic Escherichia coli O157:H7 type III effector protein that couples Tir to the actin-cytoskeleton. Cell Microbiol 6, 1167-1183.

Garnett, J.A., Martinez-Santos, V.I., Saldana, Z., Pape, T., Hawthorne, W., Chan, J., Simpson, P.J., Cota, E., Puente, J.L., Giron, J.A., Matthews, S., 2012. Structural insights into the biogenesis and biofilm formation by the Escherichia coli common pilus. Proc Natl Acad Sci U S A 109, 3950-3955.

Gauger, E.J., Leatham, M.P., Mercado-Lubo, R., Laux, D.C., Conway, T., Cohen, P.S., 2007. Role of motility and the flhDC Operon in Escherichia coli MG1655 colonization of the mouse intestine. Infect Immun 75, 3315-3324.

Gauthier, A., Puente, J.L., Finlay, B.B., 2003. Secretin of the enteropathogenic Escherichia coli type III secretion system requires components of the type III apparatus for assembly and localization. Infect Immun 71, 3310-3319.

Geer, L.Y., Domrachev, M., Lipman, D.J., Bryant, S.H., 2002. CDART: protein homology by domain architecture. Genome Res 12, 1619-1623.

Gervais, F.G., Drapeau, G.R., 1992. Identification, cloning, and characterization of rcsF, a new regulator gene for exopolysaccharide synthesis that suppresses the division mutation ftsZ84 in Escherichia coli K-12. J Bacteriol 174, 8016-8022.

Gervais, F.G., Phoenix, P., Drapeau, G.R., 1992. The rcsB gene, a positive regulator of colanic acid biosynthesis in Escherichia coli, is also an activator of ftsZ expression. J Bacteriol 174, 3964-3971.

Giangrossi, M., Zattoni, S., Tramonti, A., De Biase, D., Falconi, M., 2005. Antagonistic role of H-NS and GadX in the regulation of the glutamate decarboxylase-dependent acid resistance system in Escherichia coli. J Biol Chem 280, 21498-21505.

Giron, J.A., Torres, A.G., Freer, E., Kaper, J.B., 2002. The flagella of enteropathogenic Escherichia coli mediate adherence to epithelial cells. Mol Microbiol 44, 361-379.

Gonyar, L.A., Kendall, M.M., 2013. Ethanolamine and choline promote expression of putative and characterized fimbriae in enterohemorrhagic Escherichia coli O157:H7. Infect Immun.

Gottesman, S., Stout, V., 1991. Regulation of capsular polysaccharide synthesis in Escherichia coli K12. Mol Microbiol 5, 1599-1606.

Gottesman, S., Trisler, P., Torres-Cabassa, A., 1985. Regulation of capsular polysaccharide synthesis in Escherichia coli K-12: characterization of three regulatory genes. J Bacteriol 162, 1111-1119.

Grant, A.J., Farris, M., Alefounder, P., Williams, P.H., Woodward, M.J., O'Connor, C.D., 2003. Co-ordination of pathogenicity island expression by the BipA GTPase in enteropathogenic Escherichia coli (EPEC). Mol Microbiol 48, 507-521.

Gupte, G., Woodward, C., Stout, V., 1997. Isolation and characterization of rcsB mutations that affect colanic acid capsule synthesis in Escherichia coli K-12. J Bacteriol 179, 4328-4335.

Guzman, L.M., Belin, D., Carson, M.J., Beckwith, J., 1995. Tight regulation, modulation, and high-level expression by vectors containing the arabinose PBAD promoter. J Bacteriol 177, 4121-4130.

Haack, K.R., Robinson, C.L., Miller, K.J., Fowlkes, J.W., Mellies, J.L., 2003. Interaction of Ler at the LEE5 (tir) operon of enteropathogenic Escherichia coli. Infect Immun 71, 384-392.

Haas, B.J., Chin, M., Nusbaum, C., Birren, B.W., Livny, J., 2012. How deep is deep enough for RNA-Seq profiling of bacterial transcriptomes? BMC Genomics 13, 734.

Hagiwara, D., Sugiura, M., Oshima, T., Mori, H., Aiba, H., Yamashino, T., Mizuno, T., 2003. Genome-wide analyses revealing a signaling network of the RcsC-YojN-RcsB phosphorelay system in Escherichia coli. J Bacteriol 185, 5735-5746.

Hansen, A.M., Kaper, J.B., 2009. Hfq affects the expression of the LEE pathogenicity island in enterohaemorrhagic Escherichia coli. Mol Microbiol 73, 446-465.

Harding, C.R., Schroeder, G.N., Reynolds, S., Kosta, A., Collins, J.W., Mousnier, A., Frankel, G., 2012. Legionella pneumophila pathogenesis in the Galleria mellonella infection model. Infect Immun 80, 2780-2790.

Hayashi, T., Makino, K., Ohnishi, M., Kurokawa, K., Ishii, K., Yokoyama, K., Han, C.G., Ohtsubo, E., Nakayama, K., Murata, T., Tanaka, M., Tobe, T., Iida, T., Takami, H., Honda, T., Sasakawa, C., Ogasawara, N., Yasunaga, T., Kuhara, S., Shiba, T., Hattori, M., Shinagawa, H., 2001. Complete genome sequence of enterohemorrhagic Escherichia coli O157:H7 and genomic comparison with a laboratory strain K-12. DNA Res 8, 11-22.

He, H., Snyder, H.A., Forst, S., 2004. Unique organization and regulation of the mrx fimbrial operon in Xenorhabdus nematophila. Microbiology 150, 1439-1446.

Hemrajani, C., Marches, O., Wiles, S., Girard, F., Dennis, A., Dziva, F., Best, A., Phillips, A.D., Berger, C.N., Mousnier, A., Crepin, V.F., Kruidenier, L., Woodward, M.J., Stevens, M.P., La Ragione, R.M., MacDonald, T.T., Frankel, G., 2008. Role of NleH, a type III secreted effector from attaching and effacing pathogens, in colonization of the bovine, ovine, and murine gut. Infect Immun 76, 4804-4813.

Hengge, R., 2009. Proteolysis of sigmaS (RpoS) and the general stress response in Escherichia coli. Res Microbiol 160, 667-676.

Hensley, M.P., Gunasekera, T.S., Easton, J.A., Sigdel, T.K., Sugarbaker, S.A., Klingbeil, L., Breece, R.M., Tierney, D.L., Crowder, M.W., 2012. Characterization of Zn(II)-responsive ribosomal proteins YkgM and L31 in E. coli. J Inorg Biochem 111, 164-172.

Hernandes, R.T., De la Cruz, M.A., Yamamoto, D., Giron, J.A., Gomes, T.A., 2013. Dissection of the Role of Pili and Type 2 and 3 Secretion Systems in Adherence and Biofilm Formation of an Atypical Enteropathogenic Escherichia coli Strain. Infect Immun 81, 3793-3802.

Hernandes, R.T., Velsko, I., Sampaio, S.C., Elias, W.P., Robins-Browne, R.M., Gomes, T.A., Giron, J.A., 2011. Fimbrial adhesins produced by atypical enteropathogenic Escherichia coli strains. Appl Environ Microbiol 77, 8391-8399.

Hirano, Y., Hossain, M.M., Takeda, K., Tokuda, H., Miki, K., 2007. Structural studies of the Cpx pathway activator NlpE on the outer membrane of Escherichia coli. Structure 15, 963-976.

Horwitz, M.A., Silverstein, S.C., 1980. Influence of the Escherichia coli capsule on complement fixation and on phagocytosis and killing by human phagocytes. J Clin Invest 65, 82-94.

Hu, L.I., Chi, B.K., Kuhn, M.L., Filippova, E.V., Walker-Peddakotla, A.J., Basell, K., Becher, D., Anderson, W.F., Antelmann, H., Wolfe, A.J., 2013. Acetylation of the response regulator RcsB controls transcription from a small RNA promoter. J Bacteriol 195, 4174-4186.

Huang, L.H., Syu, W.J., 2008. GrlA of enterohemorrhagic Escherichia coli O157:H7 activates LEE1 by binding to the promoter region. J Microbiol Immunol Infect 41, 9-16.

Huang, Y.H., Ferrieres, L., Clarke, D.J., 2006. The role of the Rcs phosphorelay in Enterobacteriaceae. Res Microbiol 157, 206-212.

Huerta, A.M., Collado-Vides, J., 2003. Sigma70 promoters in Escherichia coli: specific transcription in dense regions of overlapping promoter-like signals. J Mol Biol 333, 261-278.

Hung, D.L., Pinkner, J.S., Knight, S.D., Hultgren, S.J., 1999. Structural basis of chaperone self-capping in P pilus biogenesis. Proc Natl Acad Sci U S A 96, 8178-8183.

Hung, D.L., Raivio, T.L., Jones, C.H., Silhavy, T.J., Hultgren, S.J., 2001. Cpx signaling pathway monitors biogenesis and affects assembly and expression of P pili. EMBO J 20, 1508-1518.

Insua, J.L., Llobet, E., Moranta, D., Perez-Gutierrez, C., Tomas, A., Garmendia, J., Bengoechea, J.A., 2013. Modelling Klebsiella pneumoniae pathogenesis by infecting the wax moth Galleria mellonella. Infect Immun.

Islam, M.S., Bingle, L.E., Pallen, M.J., Busby, S.J., 2011. Organization of the LEE1 operon regulatory region of enterohaemorrhagic Escherichia coli O157:H7 and activation by GrlA. Mol Microbiol 79, 468-483.

Iwig, D.F., Uchida, A., Stromberg, J.A., Booker, S.J., 2005. The activity of Escherichia coli cyclopropane fatty acid synthase depends on the presence of bicarbonate. J Am Chem Soc 127, 11612-11613.

Iyoda, S., Koizumi, N., Satou, H., Lu, Y., Saitoh, T., Ohnishi, M., Watanabe, H., 2006. The GrlR-GrlA regulatory system coordinately controls the expression of flagellar and LEE-encoded type III protein secretion systems in enterohemorrhagic Escherichia coli. J Bacteriol 188, 5682-5692.

Iyoda, S., Watanabe, H., 2004. Positive effects of multiple pch genes on expression of the locus of enterocyte effacement genes and adherence of enterohaemorrhagic Escherichia coli O157 : H7 to HEp-2 cells. Microbiology 150, 2357-2571.

Iyoda, S., Watanabe, H., 2005. ClpXP protease controls expression of the type III protein secretion system through regulation of RpoS and GrlR levels in enterohemorrhagic Escherichia coli. J Bacteriol 187, 4086-4094.

Jaeger, J.L., Acheson, D.W., 2000. Shiga Toxin-Producing Escherichia coli. Curr Infect Dis Rep 2, 61-67.

Jander, G., Rahme, L.G., Ausubel, F.M., 2000. Positive correlation between virulence of Pseudomonas aeruginosa mutants in mice and insects. J Bacteriol 182, 3843-3845.

Jiang, H., Vilcinskas, A., Kanost, M.R., 2010. Immunity in lepidopteran insects. Adv Exp Med Biol 708, 181-204.

Jimenez, R., Cruz-Migoni, S.B., Huerta-Saquero, A., Bustamante, V.H., Puente, J.L., 2010. Molecular characterization of GrlA, a specific positive regulator of ler expression in enteropathogenic Escherichia coli. J Bacteriol 192, 4627-4642.

Johannes, L., Romer, W., 2010. Shiga toxins--from cell biology to biomedical applications. Nat Rev Microbiol 8, 105-116.

Johnson, M.D., Burton, N.A., Gutierrez, B., Painter, K., Lund, P.A., 2011. RcsB is required for inducible acid resistance in Escherichia coli and acts at gadE-dependent and -independent promoters. J Bacteriol 193, 3653-3656.

Jordi, B.J., op den Camp, I.E., de Haan, L.A., van der Zeijst, B.A., Gaastra, W., 1993. Differential decay of RNA of the CFA/I fimbrial operon and control of relative gene expression. J Bacteriol 175, 7976-7981.

Kailasan Vanaja, S., Bergholz, T.M., Whittam, T.S., 2009. Characterization of the Escherichia coli O157:H7 Sakai GadE regulon. J Bacteriol 191, 1868-1877.

Kaper, J.B., Nataro, J.P., Mobley, H.L., 2004. Pathogenic Escherichia coli. Nat Rev Microbiol 2, 123-140.

Keller, A., Nesvizhskii, A.I., Kolker, E., Aebersold, R., 2002. Empirical statistical model to estimate the accuracy of peptide identifications made by MS/MS and database search. Anal Chem 74, 5383-5392.

Kelley, W.L., Georgopoulos, C., 1997. Positive control of the two-component RcsC/B signal transduction network by DjlA: a member of the DnaJ family of molecular chaperones in Escherichia coli. Mol Microbiol 25, 913-931.

Kelm, O., Kiecker, C., Geider, K., Bernhard, F., 1997. Interaction of the regulator proteins RcsA and RcsB with the promoter of the operon for amylovoran biosynthesis in Erwinia amylovora. Mol Gen Genet 256, 72-83.

Kendall, M.M., Gruber, C.C., Parker, C.T., Sperandio, V., 2012. Ethanolamine controls expression of genes encoding components involved in interkingdom signaling and virulence in enterohemorrhagic Escherichia coli O157:H7. MBio 3.

Kendall, M.M., Rasko, D.A., Sperandio, V., 2010. The LysR-Type Regulator QseA Regulates Both Characterized and Putative Virulence Genes in Enterohemorrhagic Escherichia coli O157:H7. Mol Microbiol.

Kenny, B., Abe, A., Stein, M., Finlay, B.B., 1997a. Enteropathogenic Escherichia coli protein secretion is induced in response to conditions similar to those in the gastrointestinal tract. Infect Immun 65, 2606-2612.

Kenny, B., DeVinney, R., Stein, M., Reinscheid, D.J., Frey, E.A., Finlay, B.B., 1997b. Enteropathogenic E. coli (EPEC) transfers its receptor for intimate adherence into mammalian cells. Cell 91, 511-520.

Kenny, B., Finlay, B.B., 1995. Protein secretion by enteropathogenic Escherichia coli is essential for transducing signals to epithelial cells. Proc Natl Acad Sci U S A 92, 7991-7995.

Kershaw, C.J., Brown, N.L., Hobman, J.L., 2007. Zinc dependence of zinT (yodA) mutants and binding of zinc, cadmium and mercury by ZinT. Biochem Biophys Res Commun 364, 66-71.

Knutton, S., Baldwin, T., Williams, P.H., McNeish, A.S., 1989. Actin accumulation at sites of bacterial adhesion to tissue culture cells: basis of a new diagnostic test for enteropathogenic and enterohemorrhagic Escherichia coli. Infect Immun 57, 1290-1298.

Knutton, S., Lloyd, D.R., McNeish, A.S., 1987. Adhesion of enteropathogenic Escherichia coli to human intestinal enterocytes and cultured human intestinal mucosa. Infect Immun 55, 69-77.

Kocharunchitt, C., King, T., Gobius, K., Bowman, J.P., Ross, T., 2012. Integrated transcriptomic and proteomic analysis of the physiological response of Escherichia coli O157:H7 Sakai to steady-state conditions of cold and water activity stress. Mol Cell Proteomics 11, M111 009019.

Kolmar, H., Hennecke, F., Gotze, K., Janzer, B., Vogt, B., Mayer, F., Fritz, H.J., 1995. Membrane insertion of the bacterial signal transduction protein ToxR and requirements of transcription activation studied by modular replacement of different protein substructures. EMBO J 14, 3895-3904.

Kram, K.E., Hovel-Miner, G.A., Tomich, M., Figurski, D.H., 2008. Transcriptional regulation of the tad locus in Aggregatibacter actinomycetemcomitans: a termination cascade. J Bacteriol 190, 3859-3868.

Kresse, A.U., Rohde, M., Guzman, C.A., 1999. The EspD protein of enterohemorrhagic Escherichia coli is required for the formation of bacterial surface appendages and is incorporated in the cytoplasmic membranes of target cells. Infect Immun 67, 4834-4842.

Krin, E., Danchin, A., Soutourina, O., 2010. RcsB plays a central role in H-NS-dependent regulation of motility and acid stress resistance in Escherichia coli. Res Microbiol 161, 363-371.

Krogh, A., Larsson, B., von Heijne, G., Sonnhammer, E.L., 2001. Predicting transmembrane protein topology with a hidden Markov model: application to complete genomes. J Mol Biol 305, 567-580.

Krzywinski, M., Schein, J., Birol, I., Connors, J., Gascoyne, R., Horsman, D., Jones, S.J., Marra, M.A., 2009. Circos: an information aesthetic for comparative genomics. Genome Res 19, 1639-1645.

Kulasekara, B.R., Jacobs, M., Zhou, Y., Wu, Z., Sims, E., Saenphimmachak, C., Rohmer, L., Ritchie, J.M., Radey, M., McKevitt, M., Freeman, T.L., Hayden, H., Haugen, E., Gillett, W., Fong, C., Chang, J., Beskhlebnaya, V., Waldor, M.K., Samadpour, M., Whittam, T.S., Kaul, R., Brittnacher, M., Miller, S.I., 2009. Analysis of the genome of the Escherichia coli O157:H7 2006 spinach-associated outbreak isolate indicates candidate genes that may enhance virulence. Infect Immun 77, 3713-3721.

Laaberki, M.H., Janabi, N., Oswald, E., Repoila, F., 2006. Concert of regulators to switch on LEE expression in enterohemorrhagic Escherichia coli O157:H7: interplay between Ler, GrlA, HNS and RpoS. Int J Med Microbiol 296, 197-210.

Lahiri, A., Ananthalakshmi, T.K., Nagarajan, A.G., Ray, S., Chakravortty, D., 2011. TolA mediates the differential detergent resistance pattern between the Salmonella enterica subsp. enterica serovars Typhi and Typhimurium. Microbiology 157, 1402-1415.

Lasaro, M.A., Salinger, N., Zhang, J., Wang, Y., Zhong, Z., Goulian, M., Zhu, J., 2009. F1C fimbriae play an important role in biofilm formation and intestinal colonization by the Escherichia coli commensal strain Nissle 1917. Appl Environ Microbiol 75, 246-251.

Laubacher, M.E., Ades, S.E., 2008. The Rcs phosphorelay is a cell envelope stress response activated by peptidoglycan stress and contributes to intrinsic antibiotic resistance. J Bacteriol 190, 2065-2074.

Leatham, M.P., Stevenson, S.J., Gauger, E.J., Krogfelt, K.A., Lins, J.J., Haddock, T.L., Autieri, S.M., Conway, T., Cohen, P.S., 2005. Mouse intestine selects nonmotile flhDC mutants of Escherichia coli MG1655 with increased colonizing ability and better utilization of carbon sources. Infect Immun 73, 8039-8049.

Lehti, T.A., Bauchart, P., Dobrindt, U., Korhonen, T.K., Westerlund-Wikstrom, B., 2012a. The fimbriae activator MatA switches off motility in Escherichia coli by repression of the flagellar master operon flhDC. Microbiology 158, 1444-1455.

Lehti, T.A., Bauchart, P., Heikkinen, J., Hacker, J., Korhonen, T.K., Dobrindt, U., Westerlund-Wikstrom, B., 2010. Mat fimbriae promote biofilm formation by meningitis-associated Escherichia coli. Microbiology 156, 2408-2417.

Lehti, T.A., Bauchart, P., Kukkonen, M., Dobrindt, U., Korhonen, T.K., Westerlund-Wikstrom, B., 2013a. Phylogenetic group-associated differences in regulation of the common colonization factor Mat fimbria in Escherichia coli. Mol Microbiol.

Lehti, T.A., Bauchart, P., Kukkonen, M., Dobrindt, U., Korhonen, T.K., Westerlund-Wikstrom, B., 2013b. Phylogenetic group-associated differences in regulation of the common colonization factor Mat fimbria in Escherichia coli. Mol Microbiol 87, 1200-1222.

Lehti, T.A., Heikkinen, J., Korhonen, T.K., Westerlund-Wikstrom, B., 2012b. The response regulator RcsB activates expression of Mat fimbriae in meningitic Escherichia coli. J Bacteriol 194, 3475-3485.

Leuko, S., Raivio, T.L., 2012. Mutations that impact the enteropathogenic Escherichia coli Cpx envelope stress response attenuate virulence in Galleria mellonella. Infect Immun 80, 3077-3085.

Levengood, S.K., Beyer, W.F., Jr., Webster, R.E., 1991. TolA: a membrane protein involved in colicin uptake contains an extended helical region. Proc Natl Acad Sci U S A 88, 5939-5943.

Leverrier, P., Declercq, J.P., Denoncin, K., Vertommen, D., Hiniker, A., Cho, S.H., Collet, J.F., 2011. Crystal structure of the outer membrane protein RcsF, a new substrate for the periplasmic protein-disulfide isomerase DsbC. J Biol Chem 286, 16734-16742.

Leverton, L.Q., Kaper, J.B., 2005. Temporal expression of enteropathogenic Escherichia coli virulence genes in an in vitro model of infection. Infect Immun 73, 1034-1043.

Lim, J., Lee, K.M., Kim, S.H., Kim, Y., Park, W., Park, S., 2011. YkgM and ZinT proteins are required for maintaining intracellular zinc concentration and producing curli in enterohemorrhagic Escherichia coli (EHEC) O157:H7 under zinc deficient conditions. Int J Food Microbiol 149, 159-170.

Lio, J.C., Syu, W.J., 2004. Identification of a negative regulator for the pathogenicity island of enterohemorrhagic Escherichia coli O157:H7. J Biomed Sci 11, 855-863.

Lippolis, J.D., Bayles, D.O., Reinhardt, T.A., 2009. Proteomic changes in Escherichia coli when grown in fresh milk versus laboratory media. J Proteome Res 8, 149-158.

Livak, K.J., Schmittgen, T.D., 2001. Analysis of relative gene expression data using real-time quantitative PCR and the 2(-Delta Delta C(T)) Method. Methods 25, 402-408.

Lloubes, R., Cascales, E., Walburger, A., Bouveret, E., Lazdunski, C., Bernadac, A., Journet, L., 2001. The Tol-Pal proteins of the Escherichia coli cell envelope: an energized system required for outer membrane integrity? Res Microbiol 152, 523-529.

Luzader, D.H., Clark, D.E., Gonyar, L.A., Kendall, M.M., 2013. EutR is a direct regulator of genes that contribute to metabolism and virulence in enterohemorrhagic Escherichia coli O157:H7. J Bacteriol 195, 4947-4953.

Ma, Z., Masuda, N., Foster, J.W., 2004. Characterization of EvgAS-YdeO-GadE branched regulatory circuit governing glutamate-dependent acid resistance in Escherichia coli. J Bacteriol 186, 7378-7389.

Majdalani, N., Gottesman, S., 2005. The Rcs phosphorelay: a complex signal transduction system. Annu Rev Microbiol 59, 379-405.

Majdalani, N., Heck, M., Stout, V., Gottesman, S., 2005. Role of RcsF in signaling to the Rcs phosphorelay pathway in Escherichia coli. J Bacteriol 187, 6770-6778.

Manning, S.D., Motiwala, A.S., Springman, A.C., Qi, W., Lacher, D.W., Ouellette, L.M., Mladonicky, J.M., Somsel, P., Rudrik, J.T., Dietrich, S.E., Zhang, W., Swaminathan, B., Alland, D., Whittam, T.S., 2008. Variation in virulence among clades of Escherichia coli O157:H7 associated with disease outbreaks. Proc Natl Acad Sci U S A 105, 4868-4873.

Martinez-Santos, V.I., Medrano-Lopez, A., Saldana, Z., Giron, J.A., Puente, J.L., 2012. Transcriptional regulation of the ecp operon by EcpR, IHF, and H-NS in attaching and effacing Escherichia coli. J Bacteriol 194, 5020-5033.

Mayer, M.P., 1995. A new set of useful cloning and expression vectors derived from pBlueScript. Gene 163, 41-46.

McDaniel, T.K., Jarvis, K.G., Donnenberg, M.S., Kaper, J.B., 1995. A genetic locus of enterocyte effacement conserved among diverse enterobacterial pathogens. Proc Natl Acad Sci U S A 92, 1664-1668.

McDaniel, T.K., Kaper, J.B., 1997. A cloned pathogenicity island from enteropathogenic Escherichia coli confers the attaching and effacing phenotype on E. coli K-12. Mol Microbiol 23, 399-407.

McKee, M.L., O'Brien, A.D., 1995. Investigation of enterohemorrhagic Escherichia coli O157:H7 adherence characteristics and invasion potential reveals a new attachment pattern shared by intestinal E. coli. Infect Immun 63, 2070-2074.

Mellies, J.L., Barron, A.M., Carmona, A.M., 2007. Enteropathogenic and enterohemorrhagic Escherichia coli virulence gene regulation. Infect Immun 75, 4199-4210.

Mellies, J.L., Benison, G., McNitt, W., Mavor, D., Boniface, C., Larabee, F.J., 2011. Ler of pathogenic Escherichia coli forms toroidal protein-DNA complexes. Microbiology 157, 1123-1133.

Mellies, J.L., Elliott, S.J., Sperandio, V., Donnenberg, M.S., Kaper, J.B., 1999. The Per regulon of enteropathogenic Escherichia coli : identification of a regulatory cascade and a novel transcriptional activator, the locus of enterocyte effacement (LEE)-encoded regulator (Ler). Mol Microbiol 33, 296-306.

Mellies, J.L., Thomas, K., Turvey, M., Evans, N.R., Crane, J., Boedeker, E., Benison, G.C., 2012. Zinc-induced envelope stress diminishes type III secretion in enteropathogenic Escherichia coli. BMC Microbiol 12, 123.

Miller, J., 1972. Assay of B-galactosidase. In: Experiments in molecular genetics. Cold Spring Harbor, NY. Cold Spring Harbor Laboratory, 352-255.

Mills, E., Baruch, K., Charpentier, X., Kobi, S., Rosenshine, I., 2008. Real-time analysis of effector translocation by the type III secretion system of enteropathogenic Escherichia coli. Cell Host Microbe 3, 104-113.

Mitra, A., Fay, P.A., Morgan, J.K., Vendura, K.W., Versaggi, S.L., Riordan, J.T., 2012. Sigma Factor N, Liaison to an ntrC and rpoS Dependent Regulatory Pathway Controlling Acid Resistance and the LEE in Enterohemorrhagic Escherichia coli. PLoS One 7, e46288.

Miyata, S., Casey, M., Frank, D.W., Ausubel, F.M., Drenkard, E., 2003. Use of the Galleria mellonella caterpillar as a model host to study the role of the type III secretion system in Pseudomonas aeruginosa pathogenesis. Infect Immun 71, 2404-2413.

Moon, H.W., Whipp, S.C., Argenzio, R.A., Levine, M.M., Giannella, R.A., 1983. Attaching and effacing activities of rabbit and human enteropathogenic Escherichia coli in pig and rabbit intestines. Infect Immun 41, 1340-1351.

Morgan, J.K., Vendura, K.W., Stevens, S.M., Jr., Riordan, J.T., 2013. RcsB determines the locus of enterocyte effacement (LEE) expression and adherence phenotype of Escherichia coli O157 : H7 spinach outbreak strain TW14359 and coordinates bicarbonate-dependent LEE activation with repression of motility. Microbiology 159, 2342-2353.

Mouslim, C., Latifi, T., Groisman, E.A., 2003. Signal-dependent requirement for the co-activator protein RcsA in transcription of the RcsB-regulated ugd gene. J Biol Chem 278, 50588-50595.

Mukherjee, K., Altincicek, B., Hain, T., Domann, E., Vilcinskas, A., Chakraborty, T., 2010. Galleria mellonella as a model system for studying Listeria pathogenesis. Appl Environ Microbiol 76, 310-317.

Murphy, K.C., Campellone, K.G., 2003. Lambda Red-mediated recombinogenic engineering of enterohemorrhagic and enteropathogenic E. coli. BMC Mol Biol 4, 11.

Nakanishi, N., Abe, H., Ogura, Y., Hayashi, T., Tashiro, K., Kuhara, S., Sugimoto, N., Tobe, T., 2006. ppGpp with DksA controls gene expression in the locus of enterocyte effacement (LEE) pathogenicity island of enterohaemorrhagic Escherichia coli through activation of two virulence regulatory genes. Mol Microbiol 61, 194-205.

Nakanishi, N., Tashiro, K., Kuhara, S., Hayashi, T., Sugimoto, N., Tobe, T., 2009. Regulation of virulence by butyrate sensing in enterohaemorrhagic Escherichia coli. Microbiology 155, 521-530.

Nataro, J.P., Kaper, J.B., 1998. Diarrheagenic Escherichia coli. Clin Microbiol Rev 11, 142-201.

Navarro Llorens, J.M., Tormo, A., Martinez-Garcia, E., 2010. Stationary phase in gram-negative bacteria. FEMS Microbiol Rev 34, 476-495.

Neidhardt, F.C., Bloch, P.L., Smith, D.F., 1974. Culture medium for enterobacteria. J Bacteriol 119, 736-747.

Neupane, M., Abu-Ali, G.S., Mitra, A., Lacher, D.W., Manning, S.D., Riordan, J.T., 2011. Shiga toxin 2 overexpression in Escherichia coli O157:H7 strains associated with severe human disease. Microb Pathog 51, 466-470.

Nevesinjac, A.Z., Raivio, T.L., 2005. The Cpx envelope stress response affects expression of the type IV bundle-forming pili of enteropathogenic Escherichia coli. J Bacteriol 187, 672-686.

Njoroge, J., Sperandio, V., 2012. Enterohemorrhagic Escherichia coli virulence regulation by two bacterial adrenergic kinases, QseC and QseE. Infect Immun 80, 688-703.

O'Brien, A.O., Lively, T.A., Chen, M.E., Rothman, S.W., Formal, S.B., 1983. Escherichia coli O157:H7 strains associated with haemorrhagic colitis in the United States produce a Shigella dysenteriae 1 (SHIGA) like cytotoxin. Lancet 1, 702.

Ogino, T., Ohno, R., Sekiya, K., Kuwae, A., Matsuzawa, T., Nonaka, T., Fukuda, H., Imajoh-Ohmi, S., Abe, A., 2006. Assembly of the type III secretion apparatus of enteropathogenic Escherichia coli. J Bacteriol 188, 2801-2811.

Ophir, T., Gutnick, D.L., 1994. A role for exopolysaccharides in the protection of microorganisms from desiccation. Appl Environ Microbiol 60, 740-745.

Pacheco, A.R., Curtis, M.M., Ritchie, J.M., Munera, D., Waldor, M.K., Moreira, C.G., Sperandio, V., 2012. Fucose sensing regulates bacterial intestinal colonization. Nature 492, 113-117.

Padavannil, A., Jobichen, C., Mills, E., Velazquez-Campoy, A., Li, M., Leung, K.Y., Mok, Y.K., Rosenshine, I., Sivaraman, J., 2013. Structure of GrlR-GrlA complex that prevents GrlA activation of virulence genes. Nat Commun 4, 2546.

Partridge, J.D., Bodenmiller, D.M., Humphrys, M.S., Spiro, S., 2009. NsrR targets in the Escherichia coli genome: new insights into DNA sequence requirements for binding and a role for NsrR in the regulation of motility. Mol Microbiol 73, 680-694.

Paterson, G.K., Northen, H., Cone, D.B., Willers, C., Peters, S.E., Maskell, D.J., 2009. Deletion of tolA in Salmonella Typhimurium generates an attenuated strain with vaccine potential. Microbiology 155, 220-228.

Patzer, S.I., Hantke, K., 1998. The ZnuABC high-affinity zinc uptake system and its regulator Zur in Escherichia coli. Mol Microbiol 28, 1199-1210.

Perna, N.T., Mayhew, G.F., Posfai, G., Elliott, S., Donnenberg, M.S., Kaper, J.B., Blattner, F.R., 1998. Molecular evolution of a pathogenicity island from enterohemorrhagic Escherichia coli O157:H7. Infect Immun 66, 3810-3817.

Pescaretti Mde, L., Farizano, J.V., Morero, R., Delgado, M.A., 2013. A novel insight on signal transduction mechanism of RcsCDB system in Salmonella enterica serovar typhimurium. PLoS One 8, e72527.

Pescaretti Mde, L., Lopez, F.E., Morero, R.D., Delgado, M.A., 2010. Transcriptional autoregulation of the RcsCDB phosphorelay system in Salmonella enterica serovar Typhimurium. Microbiology 156, 3513-3521.

Pescaretti Mde, L., Morero, R., Delgado, M.A., 2009. Identification of a new promoter for the response regulator rcsB expression in Salmonella enterica serovar Typhimurium. FEMS Microbiol Lett 300, 165-173.

Phillips, T.A., VanBogelen, R.A., Neidhardt, F.C., 1984. lon gene product of Escherichia coli is a heat-shock protein. J Bacteriol 159, 283-287.

Porter, M.E., Mitchell, P., Free, A., Smith, D.G., Gally, D.L., 2005. The LEE1 promoters from both enteropathogenic and enterohemorrhagic Escherichia coli can be activated by PerC-like proteins from either organism. J Bacteriol 187, 458-472.

Pruimboom-Brees, I.M., Morgan, T.W., Ackermann, M.R., Nystrom, E.D., Samuel, J.E., Cornick, N.A., Moon, H.W., 2000. Cattle lack vascular receptors for Escherichia coli O157:H7 Shiga toxins. Proc Natl Acad Sci U S A 97, 10325-10329.

Rangel, J.M., Sparling, P.H., Crowe, C., Griffin, P.M., Swerdlow, D.L., 2005. Epidemiology of Escherichia coli O157:H7 outbreaks, United States, 1982-2002. Emerg Infect Dis 11, 603-609.

Ranjit, D.K., Young, K.D., 2013. The Rcs stress response and accessory envelope proteins are required for de novo generation of cell shape in Escherichia coli. J Bacteriol 195, 2452-2462.

Reading, N.C., Rasko, D., Torres, A.G., Sperandio, V., 2010. A transcriptome study of the QseEF two-component system and the QseG membrane protein in enterohaemorrhagic Escherichia coli O157 : H7. Microbiology 156, 1167-1175.

Ren, C.P., Chaudhuri, R.R., Fivian, A., Bailey, C.M., Antonio, M., Barnes, W.M., Pallen, M.J., 2004. The ETT2 gene cluster, encoding a second type III secretion system from Escherichia coli, is present in the majority of strains but has undergone widespread mutational attrition. J Bacteriol 186, 3547-3560.

Rendon, M.A., Saldana, Z., Erdem, A.L., Monteiro-Neto, V., Vazquez, A., Kaper, J.B., Puente, J.L., Giron, J.A., 2007. Commensal and pathogenic Escherichia coli use a common pilus adherence factor for epithelial cell colonization. Proc Natl Acad Sci U S A 104, 10637-10642.

Rensing, C., Mitra, B., Rosen, B.P., 1997. The zntA gene of Escherichia coli encodes a Zn(II)-translocating P-type ATPase. Proc Natl Acad Sci U S A 94, 14326-14331.

Retamal, P., Castillo-Ruiz, M., Villagra, N.A., Morgado, J., Mora, G.C., 2010. Modified intracellular-associated phenotypes in a recombinant Salmonella Typhi expressing S. Typhimurium SPI-3 sequences. PLoS One 5, e9394.

Riordan, J.T., Tietjen, J.A., Walsh, C.W., Gustafson, J.E., Whittam, T.S., 2010. Inactivation of alternative sigma factor 54 (RpoN) leads to increased acid resistance, and alters locus of enterocyte effacement (LEE) expression in Escherichia coli O157 : H7. Microbiology 156, 719-730.

Rivera, F.E., Miller, H.K., Kolar, S.L., Stevens, S.M., Jr., Shaw, L.N., 2012. The impact of CodY on virulence determinant production in community-associated methicillin-resistant Staphylococcus aureus. Proteomics 12, 263-268.

Roberts, I.S., 1996. The biochemistry and genetics of capsular polysaccharide production in bacteria. Annu Rev Microbiol 50, 285-315.

Rogov, V.V., Rogova, N.Y., Bernhard, F., Lohr, F., Dotsch, V., 2011. A disulfide bridge network within the soluble periplasmic domain determines structure and function of the outer membrane protein RCSF. J Biol Chem 286, 18775-18783.

Rosenshine, I., Ruschkowski, S., Finlay, B.B., 1996. Expression of attaching/effacing activity by enteropathogenic Escherichia coli depends on growth phase, temperature, and protein synthesis upon contact with epithelial cells. Infect Immun 64, 966-973.

Rosenthal, A.Z., Kim, Y., Gralla, J.D., 2008. Regulation of transcription by acetate in Escherichia coli: in vivo and in vitro comparisons. Mol Microbiol 68, 907-917.

Russell, R.M., Sharp, F.C., Rasko, D.A., Sperandio, V., 2007. QseA and GrlR/GrlA regulation of the locus of enterocyte effacement genes in enterohemorrhagic Escherichia coli. J Bacteriol 189, 5387-5392.

Saldana, Z., Erdem, A.L., Schuller, S., Okeke, I.N., Lucas, M., Sivananthan, A., Phillips, A.D., Kaper, J.B., Puente, J.L., Giron, J.A., 2009a. The Escherichia coli common pilus and the bundle-forming pilus act in concert during the formation of localized adherence by enteropathogenic E. coli. J Bacteriol 191, 3451-3461.

Saldana, Z., Sanchez, E., Xicohtencatl-Cortes, J., Puente, J.L., Giron, J.A., 2011. Surface structures involved in plant stomata and leaf colonization by shiga-toxigenic Escherichia coli o157:h7. Front Microbiol 2, 119.

Saldana, Z., Xicohtencatl-Cortes, J., Avelino, F., Phillips, A.D., Kaper, J.B., Puente, J.L., Giron, J.A., 2009b. Synergistic role of curli and cellulose in cell adherence and biofilm formation of attaching and effacing Escherichia coli and identification of Fis as a negative regulator of curli. Environ Microbiol 11, 992-1006.

Santander, R.D., Oliver, J.D., Biosca, E.G., 2014. Cellular, physiological and molecular adaptive responses of Erwinia amylovora to starvation. FEMS Microbiol Ecol.

Sauer, F.G., Futterer, K., Pinkner, J.S., Dodson, K.W., Hultgren, S.J., Waksman, G., 1999. Structural basis of chaperone function and pilus biogenesis. Science 285, 1058-1061.

Sayed, A.K., Foster, J.W., 2009. A 750 bp sensory integration region directs global control of the Escherichia coli GadE acid resistance regulator. Mol Microbiol 71, 1435-1450.

Sayed, A.K., Odom, C., Foster, J.W., 2007. The Escherichia coli AraC-family regulators GadX and GadW activate gadE, the central activator of glutamate-dependent acid resistance. Microbiology 153, 2584-2592.

Schauer, D.B., Falkow, S., 1993. Attaching and effacing locus of a Citrobacter freundii biotype that causes transmissible murine colonic hyperplasia. Infect Immun 61, 2486-2492.

Schmoe, K., Rogov, V.V., Rogova, N.Y., Lohr, F., Guntert, P., Bernhard, F., Dotsch, V., 2011. Structural insights into Rcs phosphotransfer: the newly identified RcsD-ABL domain enhances interaction with the response regulator RcsB. Structure 19, 577-587.

Senior, N.J., Bagnall, M.C., Champion, O.L., Reynolds, S.E., La Ragione, R.M., Woodward, M.J., Salguero, F.J., Titball, R.W., 2011. Galleria mellonella as an infection model for Campylobacter jejuni virulence. J Med Microbiol 60, 661-669.

Serra, D.O., Richter, A.M., Klauck, G., Mika, F., Hengge, R., 2013. Microanatomy at cellular resolution and spatial order of physiological differentiation in a bacterial biofilm. mBio 4, e00103-00113.

Sharp, F.C., Sperandio, V., 2007. QseA directly activates transcription of LEE1 in enterohemorrhagic Escherichia coli. Infect Immun 75, 2432-2440.

Shiba, Y., Miyagawa, H., Nagahama, H., Matsumoto, K., Kondo, D., Matsuoka, S., Hara, H., 2012. Exploring the relationship between lipoprotein mislocalization and activation of the Rcs signal transduction system in Escherichia coli. Microbiology 158, 1238-1248.

Shimizu, T., Ohta, Y., Tsutsuki, H., Noda, M., 2011. Construction of a novel bioluminescent reporter system for investigating Shiga toxin expression of enterohemorrhagic Escherichia coli. Gene 478, 1-10.

Shimizu, T., Tsutsuki, H., Matsumoto, A., Nakaya, H., Noda, M., 2012. The nitric oxide reductase of enterohaemorrhagic Escherichia coli plays an important role for the survival within macrophages. Mol Microbiol 85, 492-512.

Shin, S., Castanie-Cornet, M.P., Foster, J.W., Crawford, J.A., Brinkley, C., Kaper, J.B., 2001. An activator of glutamate decarboxylase genes regulates the expression of enteropathogenic Escherichia coli virulence genes through control of the plasmid-encoded regulator, Per. Mol Microbiol 41, 1133-1150.

Simons, R.W., Houman, F., Kleckner, N., 1987. Improved single and multicopy lac-based cloning vectors for protein and operon fusions. Gene 53, 85-96.

Sledjeski, D.D., Gottesman, S., 1996. Osmotic shock induction of capsule synthesis in Escherichia coli K-12. J Bacteriol 178, 1204-1206.

Snyder, W.B., Davis, L.J., Danese, P.N., Cosma, C.L., Silhavy, T.J., 1995. Overproduction of NlpE, a new outer membrane lipoprotein, suppresses the toxicity of periplasmic LacZ by activation of the Cpx signal transduction pathway. J Bacteriol 177, 4216-4223.

Sorg, J.A., Miller, N.C., Schneewind, O., 2005. Substrate recognition of type III secretion machines--testing the RNA signal hypothesis. Cell Microbiol 7, 1217-1225.

Sperandio, V., Li, C.C., Kaper, J.B., 2002. Quorum-sensing Escherichia coli regulator A: a regulator of the LysR family involved in the regulation of the locus of enterocyte effacement pathogenicity island in enterohemorrhagic E. coli. Infect Immun 70, 3085-3093.

Sperandio, V., Mellies, J.L., Delahay, R.M., Frankel, G., Crawford, J.A., Nguyen, W., Kaper, J.B., 2000. Activation of enteropathogenic Escherichia coli (EPEC) LEE2 and LEE3 operons by Ler. Mol Microbiol 38, 781-793.

Sperandio, V., Mellies, J.L., Nguyen, W., Shin, S., Kaper, J.B., 1999. Quorum sensing controls expression of the type III secretion gene transcription and protein secretion in enterohemorrhagic and enteropathogenic Escherichia coli. Proc Natl Acad Sci U S A 96, 15196-15201.

Stacy, A.K., Mitchell, N.M., Maddux, J.T., De la Cruz, M.A., Duran, L., Giron, J.A., rd, R.C., Mellata, M., 2014. Evaluation of the Prevalence and Production of Common Pilus among Avian Pathogenic and Its Role in Virulence. PLoS One 9, e86565.

Stelzer, S., Egan, S., Larsen, M.R., Bartlett, D.H., Kjelleberg, S., 2006. Unravelling the role of the ToxR-like transcriptional regulator WmpR in the marine antifouling bacterium Pseudoalteromonas tunicata. Microbiology 152, 1385-1394.

Stock, J.B., Ninfa, A.J., Stock, A.M., 1989. Protein phosphorylation and regulation of adaptive responses in bacteria. Microbiol Rev 53, 450-490.

Stout, V., Gottesman, S., 1990. RcsB and RcsC: a two-component regulator of capsule synthesis in Escherichia coli. J Bacteriol 172, 659-669.

Stout, V., Torres-Cabassa, A., Maurizi, M.R., Gutnick, D., Gottesman, S., 1991. RcsA, an unstable positive regulator of capsular polysaccharide synthesis. J Bacteriol 173, 1738-1747.

Strater, N., Sun, L., Kantrowitz, E.R., Lipscomb, W.N., 1999. A bicarbonate ion as a general base in the mechanism of peptide hydrolysis by dizinc leucine aminopeptidase. Proc Natl Acad Sci U S A 96, 11151-11155.

Sturny, R., Cam, K., Gutierrez, C., Conter, A., 2003. NhaR and RcsB independently regulate the osmCp1 promoter of Escherichia coli at overlapping regulatory sites. J Bacteriol 185, 4298-4304.

Sun, Y.C., Guo, X.P., Hinnebusch, B.J., Darby, C., 2012. The Yersinia pestis Rcs phosphorelay inhibits biofilm formation by repressing transcription of the diguanylate cyclase gene hmsT. J Bacteriol 194, 2020-2026.

Takeda, S., Fujisawa, Y., Matsubara, M., Aiba, H., Mizuno, T., 2001. A novel feature of the multistep phosphorelay in Escherichia coli: a revised model of the RcsC --> YojN --> RcsB signalling pathway implicated in capsular synthesis and swarming behaviour. Mol Microbiol 40, 440-450.

Tao, K., Narita, S., Tokuda, H., 2012. Defective lipoprotein sorting induces lolA expression through the Rcs stress response phosphorelay system. J Bacteriol 194, 3643-3650.

Tauschek, M., Yang, J., Hocking, D., Azzopardi, K., Tan, A., Hart, E., Praszkier, J., Robins-Browne, R.M., 2010. Transcriptional analysis of the grlRA virulence operon from Citrobacter rodentium. J Bacteriol 192, 3722-3734.

Thanassi, D.G., Saulino, E.T., Hultgren, S.J., 1998. The chaperone/usher pathway: a major terminal branch of the general secretory pathway. Curr Opin Microbiol 1, 223-231.

Thomas, N.A., Deng, W., Puente, J.L., Frey, E.A., Yip, C.K., Strynadka, N.C., Finlay, B.B., 2005. CesT is a multi-effector chaperone and recruitment factor required for the efficient type III secretion of both LEE- and non-LEE-encoded effectors of enteropathogenic Escherichia coli. Mol Microbiol 57, 1762-1779.

Tobe, T., Ando, H., Ishikawa, H., Abe, H., Tashiro, K., Hayashi, T., Kuhara, S., Sugimoto, N., 2005. Dual regulatory pathways integrating the RcsC-RcsD-RcsB signalling system control enterohaemorrhagic Escherichia coli pathogenicity. Mol Microbiol 58, 320-333.

Tobe, T., Nakanishi, N., Sugimoto, N., 2011. Activation of motility by sensing short-chain fatty acids via two steps in a flagellar gene regulatory cascade in enterohemorrhagic Escherichia coli. Infect Immun 79, 1016-1024.

Torres-Cabassa, A.S., Gottesman, S., 1987. Capsule synthesis in Escherichia coli K-12 is regulated by proteolysis. J Bacteriol 169, 981-989.

Torres, A.G., Giron, J.A., Perna, N.T., Burland, V., Blattner, F.R., Avelino-Flores, F., Kaper, J.B., 2002. Identification and characterization of lpfABCC'DE, a fimbrial operon of enterohemorrhagic Escherichia coli O157:H7. Infect Immun 70, 5416-5427.

Torres, A.G., Lopez-Sanchez, G.N., Milflores-Flores, L., Patel, S.D., Rojas-Lopez, M., Martinez de la Pena, C.F., Arenas-Hernandez, M.M., Martinez-Laguna, Y., 2007. Ler and H-NS, regulators controlling expression of the long polar fimbriae of Escherichia coli O157:H7. J Bacteriol 189, 5916-5928.

Torruellas, J., Jackson, M.W., Pennock, J.W., Plano, G.V., 2005. The Yersinia pestis type III secretion needle plays a role in the regulation of Yop secretion. Mol Microbiol 57, 1719-1733.

Touchon, M., Hoede, C., Tenaillon, O., Barbe, V., Baeriswyl, S., Bidet, P., Bingen, E., Bonacorsi, S., Bouchier, C., Bouvet, O., Calteau, A., Chiapello, H., Clermont, O., Cruveiller, S., Danchin, A., Diard, M., Dossat, C., Karoui, M.E., Frapy, E., Garry, L., Ghigo, J.M., Gilles, A.M., Johnson, J., Le Bouguenec, C., Lescat, M., Mangenot, S., Martinez-Jehanne, V., Matic, I., Nassif, X., Oztas, S., Petit, M.A., Pichon, C., Rouy, Z., Ruf, C.S., Schneider, D., Tourret, J., Vacherie, B., Vallenet, D., Medigue, C., Rocha, E.P., Denamur, E., 2009. Organised genome dynamics in the Escherichia coli species results in highly diverse adaptive paths. PLoS Genet 5, e1000344.

Toutain, C.M., Clarke, D.J., Leeds, J.A., Kuhn, J., Beckwith, J., Holland, I.B., Jacq, A., 2003. The transmembrane domain of the DnaJ-like protein DjlA is a dimerisation domain. Mol Genet Genomics 268, 761-770.

Tramonti, A., De Canio, M., De Biase, D., 2008. GadX/GadW-dependent regulation of the Escherichia coli acid fitness island: transcriptional control at the gadY-gadW divergent promoters and identification of four novel 42 bp GadX/GadW-specific binding sites. Mol Microbiol 70, 965-982.

Tree, J.J., Roe, A.J., Flockhart, A., McAteer, S.P., Xu, X., Shaw, D., Mahajan, A., Beatson, S.A., Best, A., Lotz, S., Woodward, M.J., La Ragione, R., Murphy, K.C., Leong, J.M., Gally, D.L., 2011. Transcriptional regulators of the GAD acid stress island are carried by effector protein-encoding prophages and indirectly control type III secretion in enterohemorrhagic Escherichia coli O157:H7. Mol Microbiol 80, 1349-1365.

Tree, J.J., Wolfson, E.B., Wang, D., Roe, A.J., Gally, D.L., 2009. Controlling injection: regulation of type III secretion in enterohaemorrhagic Escherichia coli. Trends Microbiol 17, 361-370.

Trisler, P., Gottesman, S., 1984. lon transcriptional regulation of genes necessary for capsular polysaccharide synthesis in Escherichia coli K-12. J Bacteriol 160, 184-191.

Tucker, N.P., Le Brun, N.E., Dixon, R., Hutchings, M.I., 2010. There's NO stopping NsrR, a global regulator of the bacterial NO stress response. Trends Microbiol 18, 149-156.

Tyler, J.S., Beeri, K., Reynolds, J.L., Alteri, C.J., Skinner, K.G., Friedman, J.H., Eaton, K.A., Friedman, D.I., 2013. Prophage induction is enhanced and required for renal disease and lethality in an EHEC mouse model. PLoS Pathog 9, e1003236.

Umanski, T., Rosenshine, I., Friedberg, D., 2002. Thermoregulated expression of virulence genes in enteropathogenic Escherichia coli. Microbiology 148, 2735-2744.

Umekawa, M., Miyagawa, H., Kondo, D., Matsuoka, S., Matsumoto, K., Hara, H., 2013. Importance of the proline-rich region for the regulatory function of RcsF, an outer membrane lipoprotein component of the Escherichia coli Rcs signal transduction system. Microbiology 159, 1818-1827.

Unkmeir, A., Schmidt, H., 2000. Structural analysis of phage-borne stx genes and their flanking sequences in shiga toxin-producing Escherichia coli and Shigella dysenteriae type 1 strains. Infect Immun 68, 4856-4864.

Uzzau, S., Figueroa-Bossi, N., Rubino, S., Bossi, L., 2001. Epitope tagging of chromosomal genes in Salmonella. Proc Natl Acad Sci U S A 98, 15264-15269.

van Elsas, J.D., Semenov, A.V., Costa, R., Trevors, J.T., 2011. Survival of Escherichia coli in the environment: fundamental and public health aspects. ISME J 5, 173-183.

Venkatesh, G.R., Kembou Koungni, F.C., Paukner, A., Stratmann, T., Blissenbach, B., Schnetz, K., 2010. BglJ-RcsB heterodimers relieve repression of the Escherichia coli bgl operon by H-NS. J Bacteriol 192, 6456-6464.

Vianney, A., Jubelin, G., Renault, S., Dorel, C., Lejeune, P., Lazzaroni, J.C., 2005. Escherichia coli tol and rcs genes participate in the complex network affecting curli synthesis. Microbiology 151, 2487-2497.

Vizcaino, J.A., Cote, R., Reisinger, F., Foster, J.M., Mueller, M., Rameseder, J., Hermjakob, H., Martens, L., 2009. A guide to the Proteomics Identifications Database proteomics data repository. Proteomics 9, 4276-4283.

Vogel, H., Altincicek, B., Glockner, G., Vilcinskas, A., 2011. A comprehensive transcriptome and immune-gene repertoire of the lepidopteran model host Galleria mellonella. BMC Genomics 12, 308.

Volkan, E., Kalas, V., Pinkner, J.S., Dodson, K.W., Henderson, N.S., Pham, T., Waksman, G., Delcour, A.H., Thanassi, D.G., Hultgren, S.J., 2013a. Molecular basis of usher pore gating in Escherichia coli pilus biogenesis. Proc Natl Acad Sci U S A 110, 20741-20746.

Volkan, E., Kalas, V., Pinkner, J.S., Dodson, K.W., Henderson, N.S., Pham, T., Waksman, G., Delcour, A.H., Thanassi, D.G., Hultgren, S.J., 2013b. Molecular basis of usher pore gating in Escherichia coli pilus biogenesis. Proc Natl Acad Sci U S A.

Waksman, G., Hultgren, S.J., 2009. Structural biology of the chaperone-usher pathway of pilus biogenesis. Nat Rev Microbiol 7, 765-774.

Wehland, M., Bernhard, F., 2000. The RcsAB box. Characterization of a new operator essential for the regulation of exopolysaccharide biosynthesis in enteric bacteria. J Biol Chem 275, 7013-7020.

Weiss, A., Ibarra, J.A., Paoletti, J., Carroll, R.K., Shaw, L.N., 2014. The delta Subunit of RNA Polymerase Guides Promoter Selectivity and Virulence in Staphylococcus aureus. Infect Immun 82, 1424-1435.

Wendel, A.M., Johnson, D.H., Sharapov, U., Grant, J., Archer, J.R., Monson, T., Koschmann, C., Davis, J.P., 2009. Multistate outbreak of Escherichia coli O157:H7 infection associated with consumption of packaged spinach, August-September 2006: the Wisconsin investigation. Clin Infect Dis 48, 1079-1086.

Whitfield, C., 2006. Biosynthesis and assembly of capsular polysaccharides in Escherichia coli. Annu Rev Biochem 75, 39-68.

Whitfield, C., Paiment, A., 2003. Biosynthesis and assembly of Group 1 capsular polysaccharides in Escherichia coli and related extracellular polysaccharides in other bacteria. Carbohydr Res 338, 2491-2502.

Winnen, B., Schlumberger, M.C., Sturm, A., Schupbach, K., Siebenmann, S., Jenny, P., Hardt, W.D., 2008. Hierarchical effector protein transport by the Salmonella Typhimurium SPI-1 type III secretion system. PLoS One 3, e2178.

Wolfe, A.J., 2005. The acetate switch. Microbiol Mol Biol Rev 69, 12-50.

Wolfe, A.J., 2010. Physiologically relevant small phosphodonors link metabolism to signal transduction. Curr Opin Microbiol 13, 204-209.

Wurpel, D.J., Beatson, S.A., Totsika, M., Petty, N.K., Schembri, M.A., 2013. Chaperone-usher fimbriae of Escherichia coli. PLoS One 8, e52835.

Xicohtencatl-Cortes, J., Monteiro-Neto, V., Ledesma, M.A., Jordan, D.M., Francetic, O., Kaper, J.B., Puente, J.L., Giron, J.A., 2007. Intestinal adherence associated with type IV pili of enterohemorrhagic Escherichia coli O157:H7. J Clin Invest 117, 3519-3529.

Xu, J., Bjursell, M.K., Himrod, J., Deng, S., Carmichael, L.K., Chiang, H.C., Hooper, L.V., Gordon, J.I., 2003. A genomic view of the human-Bacteroides thetaiotaomicron symbiosis. Science 299, 2074-2076.

Yang, J., Hart, E., Tauschek, M., Price, G.D., Hartland, E.L., Strugnell, R.A., Robins-Browne, R.M., 2008. Bicarbonate-mediated transcriptional activation of divergent operons by the virulence regulatory protein, RegA, from Citrobacter rodentium. Mol Microbiol 68, 314-327.

Yen, H., Ooka, T., Iguchi, A., Hayashi, T., Sugimoto, N., Tobe, T., 2010. NleC, a type III secretion protease, compromises NF-kappaB activation by targeting p65/RelA. PLoS Pathog 6, e1001231.

Yip, C.K., Kimbrough, T.G., Felise, H.B., Vuckovic, M., Thomas, N.A., Pfuetzner, R.A., Frey, E.A., Finlay, B.B., Miller, S.I., Strynadka, N.C., 2005. Structural characterization of the molecular platform for type III secretion system assembly. Nature 435, 702-707.

Zarivach, R., Vuckovic, M., Deng, W., Finlay, B.B., Strynadka, N.C., 2007. Structural analysis of a prototypical ATPase from the type III secretion system. Nat Struct Mol Biol 14, 131-137.

Zhang, L., Chaudhuri, R.R., Constantinidou, C., Hobman, J.L., Patel, M.D., Jones, A.C., Sarti, D., Roe, A.J., Vlisidou, I., Shaw, R.K., Falciani, F., Stevens, M.P., Gally, D.L., Knutton, S., Frankel, G., Penn, C.W., Pallen, M.J., 2004. Regulators encoded in the Escherichia coli type III secretion system 2 gene cluster influence expression of genes within the locus for enterocyte effacement in enterohemorrhagic E. coli O157:H7. Infect Immun 72, 7282-7293.

Zhao, H., Chen, C., Xiong, Y., Xu, X., Lan, R., Wang, H., Yao, X., Bai, X., Liu, X., Meng, Q., Zhang, X., Sun, H., Zhao, A., Cheng, Y., Chen, Q., Ye, C., Xu, J., 2013. Global transcriptional and phenotypic analyses of Escherichia coli O157:H7 strain Xuzhou21 and its pO157_Sal cured mutant. PLoS One 8, e65466.

Zhou, K., Michiels, C.W., Aertsen, A., 2012. Variation of intragenic tandem repeat tract of tolA modulates Escherichia coli stress tolerance. PLoS One 7, e47766.

Appendices

Appendix A: Copyright Permissions

USF

Jason Morgan <jkmorgan@mail.usf.edu>

Permission to Re-Use content in paper

3 messages

Jason Morgan <jkmorgan@mail.usf.edu> Tue, Mar 4, 2014 at 11:38 AM
To: micro.permission@sgm.ac.uk

Greetings,

I am a Ph.D. student currently writing my dissertation, and I am the primary author on the 2013 Microbiology publication:

"RcsB determines the locus of enterocyte effacement (LEE) expression and adherence phenotype of Escherichia coli O157:H7 spinach outbreak strain TW14359 and coordinates bicarbonate-dependent LEE activation with repression of motility"

I am writing to determine if I need any special permissions to re-use any portions of the paper in the preparation of my dissertation.

Regards,

Jason Morgan

Journals <sgmjournals@sgm.ac.uk> Wed, Mar 5, 2014 at 1:41 AM
To: Jason Morgan <jkmorgan@mail.usf.edu>

Dear Jason,

Thank you for your permission request. SGM no longer responds to individual permission requests; these are now handled by the Copyright Clearance Center.

If you are an author (or an author's representative) of the content for which you are requesting permission:

The copyright transfer agreement/licence to publish that was signed by the authors gives express permission for authors to reuse their own content, provided that the journal is acknowledged as the original source. No further permission is required.

If another publisher requires confirmation that permission has been granted, please forward this email to them.

If you are NOT an author of the content for which you are requesting permission:

Please click on the '© Get Permissions' link that appears with the online article. Alternatively, you can visit www.copyright.com.

Please note that the Copyright Clearance Center will charge a processing fee for each request. Additional charges may apply for reuse for "for-profit" purposes.

Best wishes,

Cath Hicklin
Microbiology Editorial Office

Jason Morgan <jkmorgan@mail.usf.edu>

Permission to Re-Use content in paper for dissertation

3 messages

Jason Morgan <jkmorgan@mail.usf.edu> Tue, Mar 4, 2014 at 11:43 AM
To: license@plos.org

Greetings,

I am a Ph.D. student currently writing my dissertation, and I am a co-author on the 2012 PLoS One publication:

"Sigma Factor N, Liaison to an ntrC and rpoS Dependent Regulatory Pathway Controlling Acid Resistance and the LEE in Enterohemorrhagic Escherichia coli"

I am writing to determine if I need any special permissions to re-use portions of the paper in the preparation of my dissertation, assuming proper citation.

Regards,

Jason Morgan

PLOS <PLOS@plos.org> Tue, Mar 4, 2014 at 12:44 PM
To: Jason Morgan <jkmorgan@mail.usf.edu>

Dear Jason,

Thank you for your enquiry.

We are an open access publisher and as such everything we publish is freely available online throughout the world, for you to read, download, copy, distribute, and use (with attribution) any way you wish.

No permission required.

For information on the Creative Commons Attribution License please follow this link http://www.plos.org/about/open-access/license/

Hope this is helpful.

Thank you,

Appendix B: Manuscripts

Microbiology (2013), **159**, 2342–2353 DOI 10.1099/mic.0.070201-0

RcsB determines the locus of enterocyte effacement (LEE) expression and adherence phenotype of *Escherichia coli* O157 : H7 spinach outbreak strain TW14359 and coordinates bicarbonate-dependent LEE activation with repression of motility

Jason K. Morgan, Khoury W. Vendura, Stanley M. Stevens Jr and James T. Riordan

Correspondence
James T. Riordan
jtriordan@usf.edu

Department of Cell Biology, Microbiology, and Molecular Biology, University of South Florida, Tampa, FL 33620, USA

The 2006 US spinach outbreak of *Escherichia coli* O157 : H7, characterized by unusually severe disease, has been attributed to a strain (TW14359) with enhanced pathogenic potential, including elevated virulence gene expression, robust adherence and the presence of novel virulence factors. This study proposes a mechanism for the unique virulence expression and adherence phenotype of this strain, and further expands the role for regulator RcsB in control of the *E. coli* locus of enterocyte effacement (LEE) pathogenicity island. Proteomic analysis of TW14359 revealed a virulence proteome consistent with previous transcriptome studies that included elevated levels of the LEE regulatory protein Ler and type III secretion system (T3SS) proteins, secreted T3SS effectors and Shiga toxin 2. Basal levels of the LEE activator and Rcs phosphorelay response regulator, RcsB, were increased in strain TW14359 relative to O157 : H7 strain Sakai. Deletion of *rcsB* eliminated inherent differences between these strains in *ler* expression, and in T3SS-dependent adherence. A reciprocating regulatory pathway involving RcsB and LEE-encoded activator GrlA was identified and predicted to co-ordinate LEE activation with repression of the *flhDC* flagellar regulator and motility. Overexpression of *grlA* was shown to increase RcsB levels, but did not alter expression from promoters driving *rcsB* transcription. Expression of *rcsDB* and RcsB was determined to increase in response to physiological levels of bicarbonate, and bicarbonate-dependent stimulation of the LEE was shown to be dependent on an intact Rcs system and *ler* activator *grvA*. The results of this study significantly broaden the role for RcsB in enterohaemorrhagic *E. coli* virulence regulation.

Received 6 June 2013
Accepted 28 August 2013

INTRODUCTION

Enterohaemorrhagic *Escherichia coli* (EHEC) O157 : H7 is a virulent human pathogen attributed to sporadic cases and large outbreaks of bloody diarrhoea (haemorrhagic colitis) (Rangel *et al.*, 2005). In 2006, an outbreak in the United States of O157 : H7 due to the consumption of tainted spinach was associated with unusually high rates of hospitalization and life-threatening sequelae (i.e. haemolytic uraemic syndrome) (Manning *et al.*, 2008). Phylogenetic analysis of over 500 clinical O157 : H7 isolates suggested that the strain which caused this outbreak, TW14359, belongs to a discrete genetic group referred to as clade 8, members of which are highly virulent (Manning *et al.*, 2008). Consistent with this hypothesis, DNA sequencing of this strain has revealed the presence of virulence factors that are absent in the reference genomes of sequenced O157 : H7 strains Sakai (1996 Japan) and EDL933 (1982 USA) (Kulasekara *et al.*, 2009; Manning *et al.*, 2008). In addition, a virulence expression phenotype has been described for strain TW14359 characterized by increased basal transcription of locus of enterocyte effacement (LEE) genes, as well as Shiga toxin 2 genes (*stx2AB*) and Stx2 protein relative to other O157 : H7 strains (Abu-Ali *et al.*, 2010a, b; Neupane *et al.*, 2011). Elevated basal LEE expression in TW14359 has

Abbreviations: EHEC, enterohaemorrhagic *Escherichia coli*; EPEC, enteropathogenic *E. coli*; HSD, honestly significant difference; iTRAQ, isobaric tag for relative and absolute quantification; Kan, kanamycin; LEE, locus of enterocyte effacement; qRT-PCR, quantitative real-time PCR; Rif, rifampicin; T3SS, type III secretion system; WT, wild-type.

Four supplementary figures and three supplementary tables are available with the online version of this paper.

further been correlated with increased adherence to bovine epithelial cells (Abu-Ali *et al.*, 2010a).

The LEE is a 35.6 kb pathogenicity island that encodes a type III secretion apparatus required for competitive colonization of the intestine and attaching/effacing lesion formation in EHEC and enteropathogenic *E. coli* (EPEC) (Elliott *et al.*, 1998; McDaniel & Kaper, 1997; Perna *et al.*, 1998), and in the mouse pathogen *Citrobacter rodentium* (Schauer & Falkow, 1993). Regulation of LEE expression has been intensively studied (Mellies *et al.*, 2007; Tree *et al.*, 2009), but is still not fully understood. Four LEE-encoded proteins are currently known to control its expression: Ler (LEE-encoded regulator), Mcp (multiple point controller), GrlR (global regulator of LEE repressor) and GrlA (global regulator of LEE activator). *ler* is the first gene of the *LEE1* operon, and is a master regulator of the LEE, activating transcription from all five LEE operons (Elliott *et al.*, 1998; Sperandio *et al.*, 1999). Mcp, when overexpressed, downregulates LEE expression through interaction with Ler, and GrlA directly activates *ler* transcription (and thus the LEE), whereas GrlR represses *ler* transcription through interactions with GrlA (Creasey *et al.*, 2003; Deng *et al.*, 2004; Huang & Syu, 2008; Lio & Syu, 2004). In addition, a myriad of non-LEE-encoded regulators modulate LEE expression through *ler* in response to environmental cues such as growth phase, bicarbonate and stress (Abe *et al.*, 1997, 2002; Bergholz *et al.*, 2007b; Friedberg *et al.*, 1999; Grant *et al.*, 2003; Kenny *et al.*, 1997; Shin *et al.*, 2001; Sperandio *et al.*, 1999; Tobe *et al.*, 2005; Umanski *et al.*, 2002).

In this study, a role for RcsB, a response regulator of the Rcs phosphorelay system, in the virulence expression phenotype of strain TW14359 was examined. In particular, the importance of RcsB to enhanced LEE expression and adherence characteristic of this strain was investigated. In addition, the study sought to define the regulatory contribution of RcsB to bicarbonate-dependent activation of the LEE and LEE-dependent repression of motility.

METHODS

Bacterial strains and culture conditions. The strains and plasmids used in this study are listed in Table 1. Strains were stocked at −80 °C in glycerol diluted (15 %, v/v, final concentration) in Luria broth (LB), and were maintained in LB or on LB with 1.5 % agar (LBA). Unless otherwise noted, overnight (18–20 h) cultures grown in LB were used to inoculate fresh LB or LB buffered with sodium bicarbonate (44 mM $NaHCO_3$) or fresh Dulbecco's modified Eagle's medium (DMEM) (4 g glucose l^{-1}, 4 mM glutamine, 44 mM $NaHCO_3$, pH 7) to a final OD_{600} of 0.05. Cultures were grown at 37 °C in a rotary shaker (200 r.p.m.) using a 1 : 10 media-to-flask volume. Growth of strains was monitored by taking OD_{600} readings at 1 h intervals for 11 h (Fig. S1, available in *Microbiology* Online). Antibiotics (Sigma-Aldrich) were added to cultures when required. For maximum expression from the P_{BAD} promoter of pBAD22 (Guzman *et al.*, 1995), cultures were grown in DMEM containing L-arabinose (0.5 %, w/v) and glycerol (0.4 %, v/v).

Genetic manipulations and chromosomal FLAG-fusion construction. Primers used for the genetic manipulation of strains TW14359 and Sakai are provided in Table S1. Gene deletion and kanamycin (Kan) replacement mutants were constructed using the λ Red recombinase-assisted approach (Datsenko & Wanner, 2000; Murphy & Campellone, 2003) and as described (Riordan *et al.*, 2010). To make a TW14359 *grlA* overexpression strain, an *Eco*RI/*Xba*I-digested 413 bp PCR fragment containing the promoterless *grlA* ORF was cloned into similarly digested pBAD22 (Guzman *et al.*, 1995) to yield pRJM-15, which was then transformed by electroporation into TW14359 as described (Riordan *et al.*, 2010). For *rcsB* complementation, a *Bam*HI/*Xho*I-digested 3424 bp PCR fragment, containing the *rcsB* ORF and native promoters, was cloned into similarly digested pACYC177 to yield pRJM20, which was then transformed into TW14359Δ*rcsB*. To construct FLAG fusions to *rcsB* and *tir*, the approach of Uzzau *et al.* (2001) was used. Primers FLAG-F and P2 used to amplify the FLAG epitope and Kan resistance cassette from pSU312 (Uzzau *et al.*, 2001) were constructed with 40 bp oligonucleotide 5′ extensions with homology to a 3′ region of the target ORF and a downstream intergenic region, respectively. Homologous recombination of this product using λ Red recombinase replaces the native stop codon with the FLAG sequence in-frame with the target ORF. When expressed, the fusion protein contains a 7 aa C-terminal epitope (FLAG) that can be detected by Western blots using anti-FLAG mAbs (Uzzau *et al.*, 2001). All genetic constructs were validated using a combination of PCR and restriction mapping, quantitative real-time PCR (qRT-PCR) and DNA sequencing (Eurofins MWG Operon). DNA was purified using the QIAquick PCR Purification kit (Qiagen).

Protein extraction, SDS-PAGE and Western blots. Protein extraction, purification and Western blots were performed as described previously (Mitra *et al.*, 2012). To extract and purify secreted proteins, mid-exponential phase (OD_{600} of 0.5) cultures were centrifuged at 5000 ***g*** for 5 min and supernatants were passed through sterile 0.22 μm Millex-GV syringe filters (Millipore). Filtrates were precipitated overnight (18–20 h) in 15 % (v/v) trichloroacetic acid at 4 °C and then centrifuged at 15 000 ***g*** for 30 min at 4 °C. Protein pellets were washed twice with 100 % ice-cold acetone before resuspension in 1 M triethyl ammonium bicarbonate. The amount of protein loaded on SDS-PAGE gels for Western blots was measured using a Bradford protein assay standard curve, and equal loading was validated by Western blots for GroEL using anti-GroEL mAbs (Bio-Rad). mAbs against FLAG (Sigma-Aldrich) were also used. Each experiment was repeated a minimum of three times in independent trials. Densitometry was used to estimate differences in protein levels for select experiments using a ChemiDoc XRS + Imaging System and Image Lab 3.0 (Bio-Rad).

Proteomic analysis. Isobaric tag for relative and absolute quantification (iTRAQ)-based MS of strains TW14359 and Sakai followed a previously described protocol (Rivera *et al.*, 2012). DMEM cultures (n=4 for cytosolic; n=3 for secreted) of strains TW14359 and Sakai were grown to an OD_{600} of 0.5 (2.5–3 h) before sampling for protein extraction (see above Methods). Peptide labelling with isobaric tags 114 and 116 (strain Sakai) and 115 and 117 (strain TW14359) for iTRAQ was performed using the iTRAQ™ Reagents 4-plex reaction kit (Applied Biosystems) following the manufacturer's instructions. Spectra data files (.RAW) were searched using Mascot Daemon ver. 2.3 against a Uniprot TW14359 protein database (http://www.uniprot.org/taxonomy/544404) downloaded on 18 April 2011, containing 10 510 total sequences (forward and reverse) using the Mascot search algorithm (Matrix Science). Data analysis for proteomics experiments followed a previously described procedure (Rivera *et al.*, 2012). Raw data files (.dat and .RAW) have been deposited in ProteomeXchange through the Proteomics Identification Database (PRIDE) (Vizcaíno *et al.*, 2009) (accession no. PXD000023).

RNA purification and qRT-PCR. Primers for qRT-PCR are provided in Table S1. RNA purification, cDNA synthesis, qRT-PCR cycling

Table 1. Strains and plasmids used in this study

Strain/plasmid	Relevant characteristics	Reference/source
Strain		
DH5α	Vector propagation, *recA1 endA1*	
Sakai	WT 1996 outbreak, Osaka, Japan	Michino *et al.* (1999)
TW14359	WT 2006 outbreak, western USA	Manning *et al.* (2008)
EDL933	WT 1982 outbreak, MI and OR, USA	Riley *et al.* (1983)
EcRJM-1	TW14359Δ*escN*	This study
EcRJM-2	SakaiΔ*escN*	This study
EcRJM-5	TW08264Δ*rcsB*	This study
EcRJM-6	TW14359Δ*rcsB*	This study
EcRJM-7	TW14359Δ*rcsC*	This study
EcRJM-8	TW08264*rcsB*-FLAG	This study
EcRJM-10	TW14359*rcsB*-FLAG	This study
EcRJM-11	TW14359Δ*grvA*	This study
EcRJM-12	TW14359Δ*rcsB* Δ*grvA*	This study
EcRJM-13	TW14359*tir*-FLAG	This study
EcRJM-14	TW08264*tir*-FLAG	This study
EcRJM-15	TW14359Δ*rcsB tir*-FLAG	This study
EcRJM-16	TW08264Δ*rcsB tir*-FLAG	This study
EcRJM-35	TW14359*grlR*::*kan*	This study
EcRJM-59	TW14359Δ*rcsB grlR*::*kan*	This study
Plasmid		
pACYC177	Low-copy cloning vector, Amp^R Kan^R P15A	Chang & Cohen (1978)
pBAD22	Ara inducible expression vector, Amp^R M13	Guzman *et al.* (1995)
pRS551	*lac* fusion vector, Amp^R Kan^R $lacZ^+$ ColE1	Simons *et al.* (1987)
pBAD-TOPO®	Ara inducible expression vector, lacZ V5-His pBR322	Invitrogen
pSU312	FLAG epitope template, Amp^R, Kan^R, R6K	Uzzau *et al.* (2001)
pRJM-1	pACYC177 containing *rcsB*	This study
pRJM-2	pRS551 containing ler_{P905}–*lacZ*	This study
pRJM-7	pRS551 containing $rcsB_{P1000}$–*lacZ*	This study
pRJM-8	pRS551 containing $rcsD_{P501}$–*lacZ*	This study
pRJM-15	pBAD22 containing *grlA*	This study
pRJM-17	pRS551 containing $flhD_{P1000}$–*lacZ*	This study

conditions and data analysis followed previously described protocols (Riordan *et al.*, 2010). For *ler* mRNA stability, cultures were growth to mid-exponential phase (OD_{600} of 0.4) before addition of a subinhibitory concentration of the transcription inhibitor rifampicin (Rif; 300 μg ml^{-1} final concentration). Sampling for RNA extraction was performed immediately before addition of Rif, and at 4 min intervals thereafter for 12 min. qRT-PCR was performed using a Realplex2 Mastercycler (Eppendorf). Cycle threshold (C_t) data were normalized to *rrsA* (16S rRNA gene) and normalized cycle threshold values (ΔC_t) were transformed to arbitrary transcript expression levels using $2^{-\Delta Ct}/10^{6}$ as described (Livak & Schmittgen, 2001; Riordan *et al.*, 2010). Expression levels were compared using the appropriate *t*-test or by Tukey's honestly significant difference (HSD) test following a significant F-test ($n \geqslant 3$, $\alpha=0.05$) (R. ver. 2.13.0).

Construction of *lacZ* transcriptional promoter fusions and β-galactosidase assays. Construction of *lacZ* reporter transcriptional fusions to the promoters of *ler*, *rcsB*, *rcsD* and *flhD* followed a previously described protocol using vector pRS551 (Simons *et al.*, 1987). For ler_{P905}-*lacZ*, a 904 bp *Bam*HI/*Eco*RI-digested PCR fragment generated using primers ler-905/*Eco*RI and ler-1/*Bam*HI was cloned into similarly digested pRS551 using T4 DNA ligase (Fisher Scientific) to produce pRJM-2. Similarly, *rcsB*, *rcsD* and *flhD* promoter fragments were cloned into pRS551 following *Bam*HI/*Eco*RI digestion using primers rcsB-1/*Bam*HI and rcsB-1000/*Eco*RI ($rcsB_{P1000}$-*lacZ*), rcsD-501/*Eco*RI and rcsD-1/*Bam*HI ($rcsD_{P501}$-*lacZ*), and flhD-1/*Bam*HI and flhD-1000/*Eco*RI ($flhD_{P1000}$-*lacZ*). *ler*-, *rcsB*-, *rcsD*-, and *flhD*-*lacZ* transcriptional fusion plasmids were transformed into wild-type (WT) and derivative backgrounds of strains TW14359 and Sakai. All *lacZ* fusion constructs were confirmed by PCR and sequencing (Eurofins MWG Operon). β-Galactosidase activity (Miller units) was measured as previously described and compared between strains using a Student's *t*-test or by Tukey's HSD test following a significant F-test ($n \geqslant 3$, $\alpha=0.05$) (R) (Miller, 1972; Mitra *et al.*, 2012).

Adherence assays. Adherence to epithelial cells was determined following the method of Abe *et al.* (2002). Briefly, human HT-29 (ATCC HTB-38) colonic epithelial cells were grown to confluence on polylysine-treated glass coverslips placed within the wells of 24-well culture plates at 37 °C with 5 % CO_2. Overnight DMEM cultures were diluted 1 : 40 (v/v) in fresh DMEM and 0.05 ml of this dilution was used to inoculate each well, which already contained 0.45 ml sterile DMEM. Culture plates were then gently centrifuged (1000 ***g***) for 5 min and incubated as above. After 3 h, plate wells were washed five times with PBS (137 mM NaCl, 2.7 mM KCl, 10 mM Na_2HPO_4, pH 7) to remove non-adherent bacteria from the coverslips, and fresh DMEM was then added before incubating for an additional 3 h. Plate wells were subsequently washed three times in PBS, and then fixed with ice-cold (−20 °C) 100 % methanol for 10 min before staining with Giemsa diluted in PBS (1 : 20, v/v) for 20 min. Giemsa stain was

aspirated from the wells, and each stained coverslip was then examined at 1000× magnification by oil immersion bright-field microscopy using a binocular microscope (Fisher Scientific). Microcolonies, defined as a pattern of localized adherence (McKee & O'Brien, 1995; Nataro & Kaper, 1998), were scored as discrete clusters of five or more bacterial cells as previously defined (Abe *et al.*, 2002; Iyoda & Watanabe, 2004). For each sample, a minimum of ten viewing frames were observed and the mean number of microcolonies was reported per 80 HT-29 cells. Microcolony counts were compared between strains by Tukey's HSD test following a significant F-test ($n \geqslant 3$, $\alpha=0.05$) (R).

Motility assays. Overnight LB cultures were diluted in fresh LB to an OD_{600} of 0.5 and 2 µl samples were inoculated onto LB plates containing 0.25 % (w/v) agar following a previous method (Krin *et al.*, 2010). Plates were incubated upright for 5 h at 37 °C before the diameter of lateral growth on the agar surface was examined for each strain. Experiments were repeated in multiple trials using at least three biological replicates per trial.

RESULTS

LEE expression phenotype of strain TW14359

qRT-PCR of LEE transcript levels revealed the upregulation of LEE regulatory (*ler*, 3.8-fold), structural (*espA*, 2.3-fold), effector (*tir*, 2.7-fold) and effector chaperone (*cesT*, 2.3-fold) genes in TW14359 when compared with strains Sakai and EDL933 during exponential growth (OD_{600} of 0.5) ($P<0.05$) (Fig. 1a), consistent with studies of LEE expression in TW14359 grown in DMEM when co-cultured with bovine mammary epithelial (MAC-T) cells (Abu-Ali *et al.*, 2010a). Although expression of the LEE activator gene *grlA* was elevated 1.6-fold in TW14359, levels did not differ significantly when compared with Sakai and EDL933. Transcript levels for all LEE genes did not differ between Sakai and EDL933. The expression of LEE genes decreased markedly in stationary phase (OD_{600} of 3.0) for all strains and did not differ between them (Fig. 1a). This pattern of expression in DMEM is consistent with previous observations of LEE gene expression during exponential and stationary growth phases in MOPS minimal media (Bergholz *et al.*, 2007a).

Expression from the *ler* promoter, as measured by β-galactosidase activity from ler_{P903}–*lacZ*, increased in both the TW14359 and the Sakai backgrounds during exponential growth, and decreased as cultures transitioned into stationary phase (Fig. 1b), in agreement with qRT-PCR data (Fig. 1a). In TW14359, however, *ler* expression was consistently and significantly higher than in Sakai ($P<0.05$) during mid-exponential growth (between 2 and 3 h growth, corresponding to OD_{600} of 0.3–0.6), indicating that increased transcription was occurring at the *ler* promoter. Examination of DNA sequence for the *ler* ORF in TW14359 (ECSP_4703) and in Sakai (ECs4588), as well as *ler* core promoters P1 and P2 and 1200 bp upstream of the translation initiation site, revealed 100 % nucleotide identity between these strains (NCBI). In addition, the stability of *ler* mRNA during exponential growth following treatment of cultures with Rif did not differ between strains; the *ler* mRNA half-life was estimated at 2.0 min for TW14359 and 2.1 min for Sakai (Fig. S2), in agreement with a previous estimate (Laaberki *et al.*, 2006). It was therefore hypothesized that the LEE expression phenotype in TW14359 is directed through increased transcription from the *ler* promoter by the influence of some *trans*-acting factor(s) during exponential growth.

Role for RcsB in the LEE expression and adherence phenotype of strain TW14359

Quantitative analysis of the relative differences in protein levels using iTRAQ-based proteomics revealed a total of 116 proteins increased or decreased in abundance by at least 1.5-fold in TW14359 relative to strain Sakai during exponential growth (OD_{600} of 0.5) (Table S2). In support of previous microarray studies, a number of LEE-encoded proteins were increased in both cytosolic and secreted protein fractions of TW14359 compared with Sakai, including the type III secretion system (T3SS) needle protein EscF (1.94-fold), the EspA chaperone, CesA (1.72-fold), the type II secretion system protein EtpG (2.06-fold), Ler (1.74-fold), the T3SS translocon apparatus proteins EspA (2.45-fold) and EspB (2.41-fold), the translocated intimin receptor Tir (1.56-fold), and other LEE-encoded proteins (Table S2). Also increased in TW14359 was the IIA subunit of Stx2 (2.11-fold) and RcsB (6.86-fold), the response regulator for a multi-component regulator of capsule synthesis (Rcs) phosphorelay system (Table S2). Importantly, when overexpressed, RcsB has been shown to activate *ler* transcription and increases adherence to Caco-2 cells (Tobe *et al.*, 2005). It was thus of interest to determine whether the LEE expression and adherence phenotype of TW14359 was attributable to elevated levels of RcsB.

Western blots revealed that the basal level of RcsB in TW14359 was elevated ~2.7-fold when compared with Sakai, congruent with iTRAQ (Fig. 2a). In addition, expression of *rcsB* transcript was significantly higher in TW14359 than in Sakai ($P=0.001$) (Fig. 2b); however, *rcsD*, which is transcribed as a dicistron with *rcsB* (i.e. *rcsDB*) from an upstream $rcsD_P$ promoter (Krin *et al.*, 2010; Pescaretti *et al.*, 2009), was not altered in expression between strains (Fig. 1b). This suggests that basal levels of *rcsB* are intrinsically upregulated in TW14359 in a manner that is dependent on a promoter(s) that is intracistronic to *rcsD*. Consistent with a role for RcsB in the LEE expression phenotype of TW14359, *ler* transcript levels were higher in TW14359 than in Sakai ($P=0.017$), but did not differ between TW14359Δ*rcsB* and SakaiΔ*rcsB* (Fig. 3a). Complementation of TW14359Δ*rcsB* and SakaiΔ*rcsB* with *rcsB* did not restore differential *ler* expression as observed for WT strains (Fig. 3a), supporting the hypothesis that the elevated basal expression of *rcsB* in TW14359 relative to Sakai is responsible for the LEE expression phenotype. The fact that *ler* transcript levels were higher in *rcsB* complement strains relative to WT (Fig. 3a) probably reflects expression

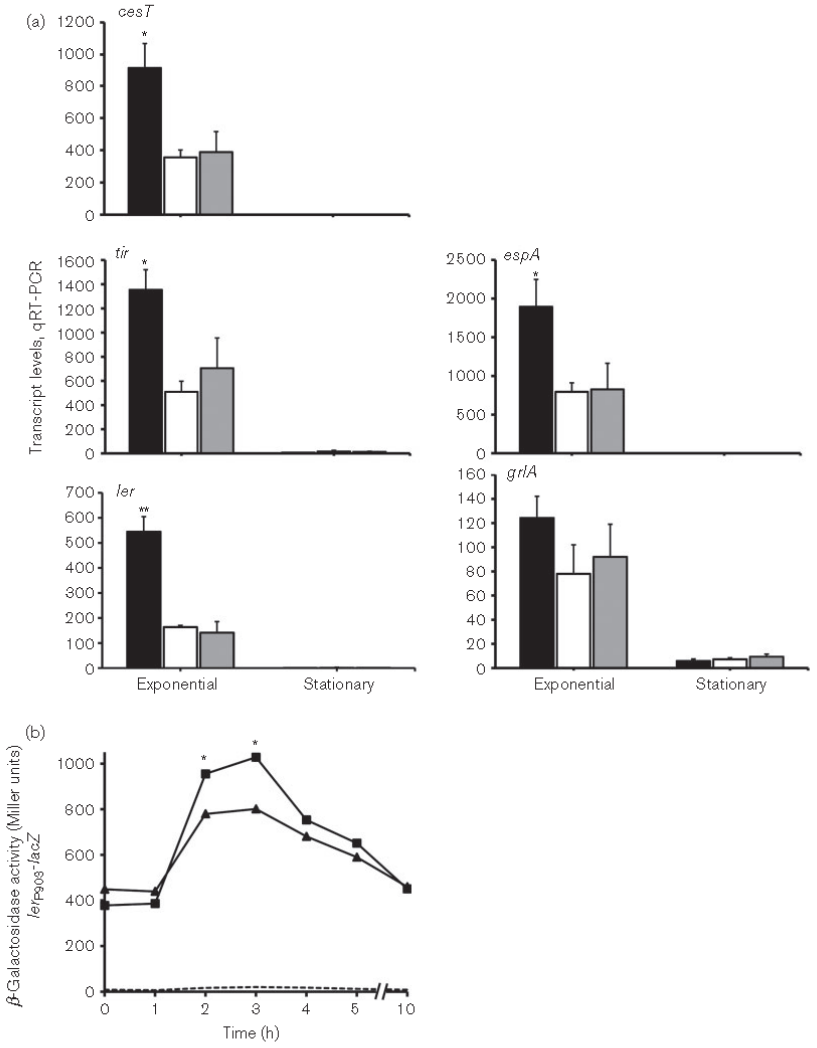

Fig. 1. The LEE expression phenotype of strain TW14359. (a) Transcript levels for LEE genes are plotted for exponential (OD_{600} of 0.5) and stationary (OD_{600} of 3.0) phase DMEM cultures of strains TW14359 (filled), Sakai (empty) and EDL933 (grey). (b) β-Galactosidase activity in Miller units for TW14359 (squares) and Sakai (triangles) containing a ler_{P903}–*lacZ* fusion plotted against time during growth in DMEM. TW14359 containing an empty vector (pRS551) control is denoted by the hatched line. Asterisks denote significant differences in transcript levels of TW14359 compared with other strains by Tukey's HSD test following a significant F-test (a) or Student's *t*-test (b) (*$P<0.05$, **$P<0.01$, $n\geqslant3$). Error bars denote SD.

from pACYC177. Although this plasmid is low-copy, *rcsB* transcript levels were still 20-fold higher in complement strains compared with WT (data not shown). In strain Sakai, the activation of *ler* by *rcsB* overexpression *in trans* requires an intact global regulator of virulence (*grvA*) gene, the product of which activates transcription from the *LEE1* promoter (Tobe *et al.*, 2005). As such, this study sought to determine if in TW14359, which intrinsically overexpresses *rcsB*, *ler* activation also required *grvA*, or if activation was through a different pathway. Deletion of *grvA* reduced *ler*

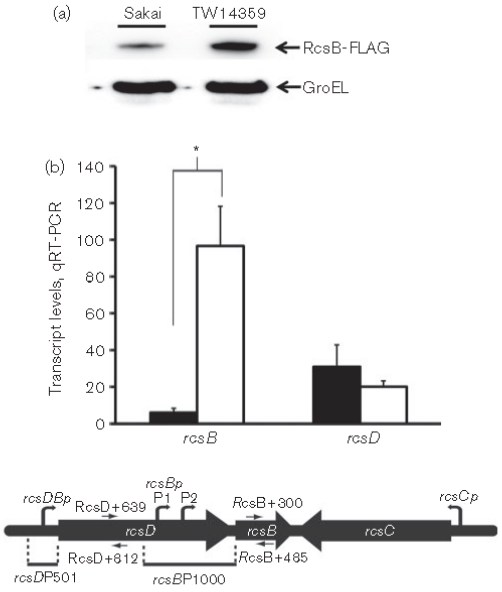

Fig. 2. Expression of *rcsB* in Sakai and TW14359. (a) Representative Western blot for FLAG-tagged RcsB in strains Sakai and TW14359 grown in DMEM (OD_{600} of 0.5). Equal loading was controlled for by Western blots for GroEL. (b) (Top) Transcript levels of *rcsB* and *rcsD* plotted for Sakai (filled) and TW14359 (empty) grown in DMEM. The asterisk denotes significant differences between strains by Student's *t*-test ($P=0.001$, $n\geqslant3$). Error bars denote SD. (Bottom) Graphic depicting the *rcsDB* and *rcsC* ORFs with their respective promoters, the location of qRT-PCR priming sites, and the location of amplified promoter *lacZ* fusion fragments for *rcsD* and *rcsB* in pRS551.

expression to the same extent as observed for TW14359Δ*rcsB* when compared with TW14359 (Fig. 3b) ($P<0.05$). Moreover, deletion of *grvA* in TW14359Δ*rcsB* did not further significantly alter *ler* expression when compared with TW14359Δ*rcsB* or TW14359Δ*grvA*. The expression of *ler* was, however, slightly but significantly higher in the TW14359Δ*rcsB*Δ*grvA* backgrounds when compared with Sakai ($P<0.05$). Therefore, increased basal expression of *rcsB* in TW14359 and interaction with *grvA* is required for the LEE expression phenotype of this strain.

This study further ascertained the contribution of intrinsic *rcsB* overexpression to the TW14359 adherence phenotype using the human colonic cell line HT-29. As observed for bovine MAC-T cells (Abu-Ali *et al.*, 2010b), adherence to HT-29 cells, as measured by microcolony formation, was significantly higher for TW14359 than for Sakai ($P=0.006$) (Fig. 3c). Consistent with *ler* expression data, adherence did not differ between Sakai and SakaiΔ*rcsB*, but was reduced in TW1359Δ*rcsB* to a level comparable to Sakai and

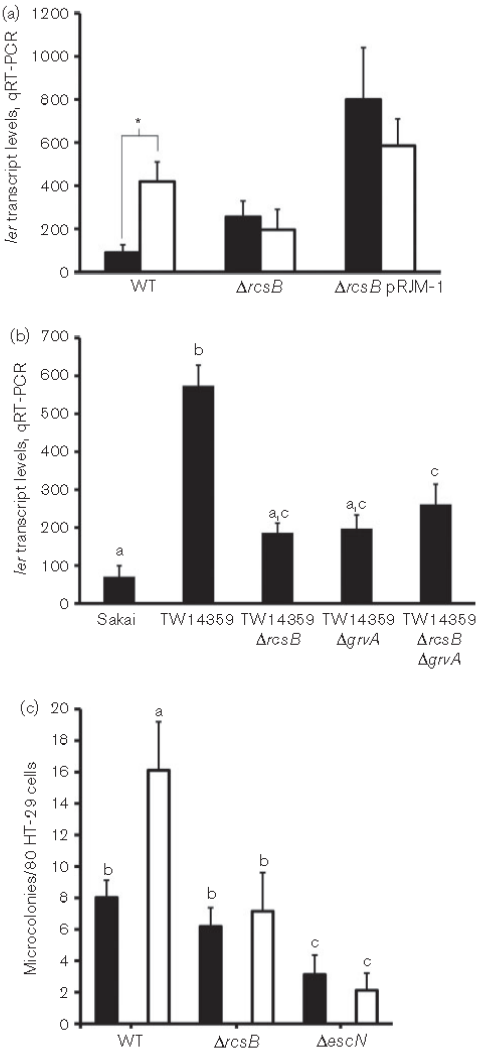

Fig. 3. Expression of *rcsB*, *grvA* and the LEE and adherence phenotype of TW14359. (a) Transcript levels of *ler* plotted for WT, Δ*rcsB* and complement Δ*rcsB* p*rcsB* versions of Sakai (solid) and TW14359 (empty) grown in DMEM (OD_{600} of 0.5). (b) Transcript levels of *ler* plotted for WT strains and mutant derivative strains of TW14359 during growth in DMEM. (c) Adherence to HT-29 cells as measured by microcolony formation plotted for WT, Δ*rcsB* and Δ*escN* versions of Sakai (solid) and TW14359 (empty). For (a), the asterisk denotes a significant difference between Sakai and TW14359 by Student's *t*-test ($P=0.017$, $n\geqslant3$). For (b) and (c), plots with different lower-case letters differ significantly by Tukey's HSD test following a significant F-test ($P<0.05$, $n\geqslant3$). Error bars denote SD.

SakaiΔ*rcsB*. As anticipated, the adherence of T3SS-deficient TW14359Δ*escN* and SakaiΔ*escN* strains to HT-29 cells was significantly reduced when compared with WT and *rcsB* isogenic backgrounds ($P<0.05$), but not between *escN* isogenic strains (Fig. 3c), indicating that the adherence phenotype of TW14359 is dependent on intrinsic *rcsB* upregulation, as well as a functional T3SS.

Control of *rcsB* by the LEE-encoded regulator GrlA, and GrlA-RcsB-dependent repression of motility

In TW14359, genes associated with motility, including structural and regulatory genes for flagellar biosynthesis (*flg* and *fli* genes), and chemotaxis (*cheB*, *tsr* and *tar*) are reduced in expression compared with Sakai (Abe *et al.*, 2002; Abu-Ali *et al.*, 2010b). In the present study, this has been observed to correspond with a 30–40 % reduction in the lateral growth of TW14359 on motility plates relative to Sakai (Fig. 4a). Importantly, both RcsB and LEE-encoded activator GrlA are known to negatively regulate motility (Francez-Charlot *et al.*, 2003; Iyoda *et al.*, 2006), and both are increased in expression in TW14359. It was therefore of interest to investigate the potential genetic interaction of *rcsB* and *grlA*, and their contribution to the regulation of motility in TW14359.

As expected, deletion of *rcsB* in TW14359 enhanced the lateral growth of TW14359 on motility plates by 30–40 %

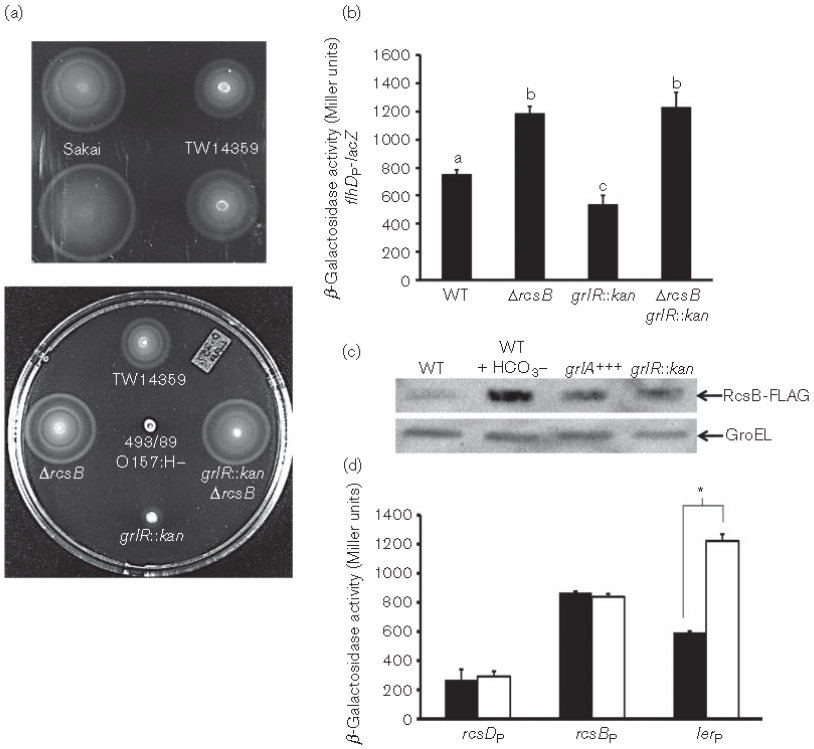

Fig. 4. GrlA–RcsB-dependent repression of motility. (a) Motility as measured by lateral growth on representative motility plates for Sakai and TW14359 (top), and mutant derivatives of TW14359 (bottom); EHEC O157 :H– strain 493/89 is included as a non-motile control. (b) β-Galactosidase activity in Miller units for TW14359 and mutant derivatives containing an $fhlD_{P1000}$–*lacZ* fusion during growth in DMEM. (c) Representative Western blot for FLAG-tagged RcsB in LB plotted for TW14359 (WT) with and without 44 mM HCO_3^-, and for *grlA* overexpression strains of TW14359 ($grlA^{+++}$ and *grlR*::*kan*). Equal loading was controlled for by Western blots for GroEL. (d) β-Galactosidase activity in Miller units plotted for TW14359 (filled) and TW14359*grlR*::*kan* (empty) grown in LB and containing $rcsD_{P501}$–*lacZ*, $rcsB_{P1000}$–*lacZ* or ler_{P903}–*lacZ* fusions. For (b), plots with different lower-case letters differ significantly by Tukey's HSD test following a significant F-test ($P<0.05$, $n\geqslant3$). For (d), the asterisk denotes significance by Student's *t*-test ($P=0.010$, $n\geqslant3$). Error bars indicate SD.

(Fig. 4a, Table S3), suggesting that the motility deficiency of TW14359 when compared with Sakai is connected to intrinsic *rcsB* overexpression. Also, the inactivation of *grlR* (strain TW14359*grlR*::*kan*) leading to *grlA* overexpression (Fig. S4) (Iyoda *et al.*, 2006) substantially impaired lateral growth on motility plates (Fig. 4a). Most importantly, deletion of *rcsB* in the TW14359*grlR*::*kan* background restored lateral growth on motility plates to the level observed for TW14359Δ*rcsB*, revealing that the control of motility by *grlA* is epistatic to *rcsB*. Negative regulation of motility by RcsB has been shown to result from direct transcriptional repression of the global regulator of motility genes *flhDC* (Francez-Charlot *et al.*, 2003). Consistent with this, expression from the $flhD_P$ promoter, as measured by β-galactosidase activity from $flhD_{P1000}$-*lacZ*, was significantly increased in TW14359Δ*rcsB*, but decreased in TW14359*grlR*::*kan* when compared with WT ($P<0.05$) (Fig. 4b). $flhD_P$ promoter expression did not differ, however, between TW14359*grlR*::*kan*Δ*rcsB* and TW14359Δ*rcsB*, indicating that RcsB-dependent repression of *flhDC* and motility is positively regulated by GrlA. In further support of this, levels of RcsB were increased (~2.4-fold) in TW14359*grlR*::*kan* and in a *grlA* overexpression strain compared with WT (Fig. 4c). Interestingly, however, expression from $rcsD_P$ or $rcsB_P$ promoters was not altered in TW14359*grlR*::*kan* (Fig. 4d), indicating that control of RcsB by GrlA is at the post-transcriptional level; increased expression from the ler_P promoter was included as a positive control for *grlA* overexpression. Collectively, these experiments reveal a reciprocating regulatory mechanism in which RcsB and LEE-encoded GrlA co-ordinate LEE activation with repression of *flhDC* and motility.

Role for Rcs phosphorelay and *grvA* in bicarbonate-dependent activation of the LEE

In the preceding experiments the addition of bicarbonate to TW14359 cultures growing in LB, and added as a positive control for LEE stimulation (Abe *et al.*, 2002), was also observed to increase RcsB levels ~5.4-fold (Fig. 4c). The bicarbonate ion (HCO_3^-) has been shown to activate LEE expression and adherence in a dose-dependent manner in EHEC (Abe *et al.*, 2002). This has been reported to be through increased transcription from the *grlRA* promoter in *C. rodentium* (Tauschek *et al.*, 2010), although the mechanism by which bicarbonate stimulates LEE expression in EHEC is unknown. In this study, the increase in RcsB levels with bicarbonate was higher than that observed for *grlA* overexpression strains (Fig. 4c), suggesting that this added bicarbonate stimulation of RcsB was, at least in part, independent of *grlA*. It was therefore predicted that the Rcs phosphorelay system was in some way involved in bicarbonate-directed activation of LEE expression. In agreement with the dose dependence of bicarbonate for LEE stimulation, the addition of bicarbonate up to 44 mM (a physiologically relevant molarity) (Feldman, 1983) to LB was observed to increase RcsB levels incrementally (Fig. 5a). Also, *rcsB* was shown to be required for full activation of LEE expression in response to bicarbonate, as the levels of Tir protein were increased substantially in TW14359 grown with bicarbonate, but only marginally increased in the TW14359Δ*rcsB* background (Fig. 5a). In addition, growth with bicarbonate increased *ler* transcript levels 5-fold in the WT ($P=0.001$) compared with only 1.24-fold in TW14359Δ*rcsB* (Fig. 5b). Bicarbonate stimulation of *ler* was restored in complement strain TW14359Δ*rcsB* p*rcsB*.

Expression from both $rcsD_P$ and $rcsB_P$ promoters was significantly increased in the presence of bicarbonate ($P<0.05$) (Fig. 5c), revealing that bicarbonate is stimulating transcription of *rcsDB* from the $rcsD_P$ promoter, as well as *rcsB* alone from at least one of two mapped promoters intracistronic to *rcsD*. Expression from the ler_P promoter was, as expected, increased with bicarbonate addition for TW14359 ($P<0.05$), but not for TW14359Δ*rcsB* (Fig. 5d). In addition, deletion of the Rcs phosphorelay sensor kinase *rcsC* significantly reduced bicarbonate stimulation of ler_P promoter activity compared with WT ($P<0.05$). And consistent with an RcsB-GrvA-dependent pathway of LEE activation, ler_P promoter expression with bicarbonate addition was reduced in TW14359Δ*grvA* and TW14359Δ*rcsB*Δ*grvA* when compared with WT ($P<0.05$), but not compared with TW14359Δ*rcsB* or TW14359Δ*rcsC* (Fig. 5d). Collectively, this reveals that bicarbonate-dependent stimulation of LEE expression in EHEC is at least partly dependent on components of the Rcs phosphorelay system, and on the RcsB-GrvA pathway of LEE activation.

DISCUSSION

It is predicted that *rcsB*, encoding the response regulator of the Rcs system, is intrinsically upregulated in TW14359, and that this is responsible for the enhanced LEE expression and adherence phenotype of this strain. It is not yet clear why *rcsB* is upregulated in TW14359. The *rcsB* gene is co-transcribed as the second gene of a dicistron with *rcsD* (Krin *et al.*, 2010) and yet *rcsD* transcript levels by qRT-PCR (Fig. 3) and protein levels by iTRAQ proteomics did not differ in TW14359 when compared with Sakai. This is consistent with the observation that *rcsB* overexpression can upregulate the LEE independent of *rcsD* (Tobe *et al.*, 2005). Alternatively, *rcsB* can be expressed as a monocistron from at least two promoters which are intracistronic to *rcsD* (i.e. $rcsB_{P1}$ and $rcsB_{P2}$) (Krin *et al.*, 2010), but upstream of the priming sites used for qRT-PCR in this study. As there are no differences in the sequence of these promoters between TW14359 and Sakai, it is predicted that intrinsic upregulation of *rcsB* is therefore dependent on some *trans*-factor(s) acting on the $rcsB_{P1}$ and/or $rcsB_{P2}$ promoters. Unfortunately, how these promoters are expressed and regulated is unknown, and needs to be examined further. A genetic polymorphism unique to strain TW14359 was initially hypothesized in this study to be important for the *rcsB* expression phenotype of this strain. Kulasekara *et al.* (2009) had described a 90 bp

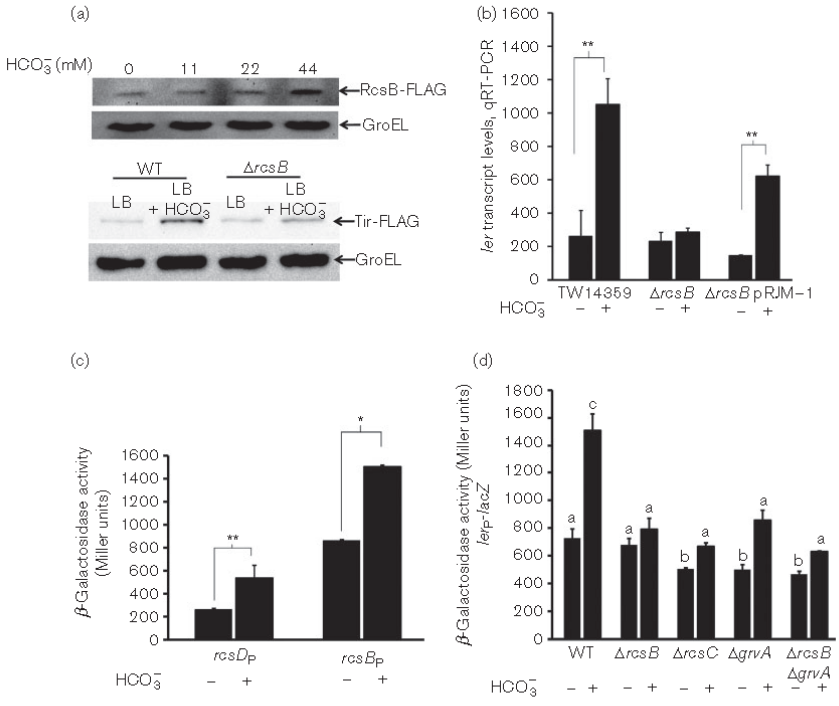

Fig. 5. Effect of bicarbonate on RcsB, and *rcsB*-dependent LEE activation. (a) Representative Western blot for FLAG-tagged RcsB as a function of increasing bicarbonate (HCO_3^-) molarity (mM) (top), and for FLAG-tagged Tir in TW14359 and TW14359Δ*rcsB* grown in LB or LB with 44 mM HCO_3^- (OD_{600} of 0.5) (bottom). Equal loading was controlled for by Western blots for GroEL. (b) Transcript levels of *ler* plotted for TW14359, TW14359Δ*rcsB* and complement TW14359Δ*rcsB*p*rcsB* strains grown in LB (–) or LB with 44 mM HCO_3^- (+) (OD_{600} of 0.5). (c) β-Galactosidase activity in Miller units plotted for TW14359 and TW14359 containing $rcsD_{P501}$–*lacZ* or $rcsB_{P1000}$–*lacZ* fusions grown in LB (–) or LB with 44 mM HCO_3^- (+). (d) β-Galactosidase activity in Miller units plotted for TW14359 (WT) and mutant derivative strains containing ler_{P903}–*lacZ* and grown in LB (–) or LB with 44 mM HCO_3^- (+). For (b) and (c), the asterisks denote a significant difference between treatments by Student's *t*-test (*$P<0.05$, **$P<0.01$, $n\geq3$). For (d), plots with different lower-case letters differ significantly by Tukey's HSD test following a significant F-test ($P<0.05$, $n\geq3$). Error bars denote SD.

insertion in the ORF of *tolA*, the product of which is an inner membrane component of the Tol–Pal envelope complex involved in maintaining cell envelope integrity (Bernadac *et al.*, 1998; Cascales *et al.*, 2000). Importantly, mutations in *tolA* have been reported to substantially upregulate *rcsB* (Clavel *et al.*, 1996). Indeed, *rcsB* expression in strains TW14359*tolA*::*kan* and Sakai*tolA*::*kan* was increased compared with their WT counterparts (Fig. S3). However, the level of *rcsB* transcript was still proportionately increased in TW14359*tolA*::*kan* relative to Sakai*tolA*::*kan* ($P=0.016$), suggesting that the *tolA* polymorphism is not responsible for increased basal expression of *rcsB* in TW14359.

The results also indicated that deletion of *rcsB* had no effect on *ler* expression or HT-29 adherence in strain Sakai. This latter finding is inconsistent with a study demonstrating that both the overexpression and deletion of *rcsB* in Sakai can lead to increased LEE expression and adherence through independent regulatory pathways: RcsB was predicted to upregulate the LEE through activation of *grvA*, and down-regulate LEE expression through repression of *pchA*, a positive regulator of the LEE (Tobe *et al.*, 2005). The reason for this disparity in results is not yet known. However, the direction and magnitude at which RcsB regulates LEE expression are likely to be sensitive to differences in growth phase, nutrient availability as well as signals which activate Rcs phosphorelay. In this study, the influence of RcsB on *ler* expression was only examined in mid-exponential cultures (OD_{600} of 0.5) and may differ substantially with even a subtle change in the phase of growth or experimental condition. For example, in Tobe *et al.* (2005) Caco-2 cells were used for adherence studies, whereas this study utilized HT-29 cells.

The RcsB-dependent LEE expression phenotype of strain TW14359 was further shown to require an intact global regulator of virulence *grvA* gene. The mechanism by which RcsB controls *grvA*, and how RcsB–GrvA regulate *ler*, is unknown. Tobe *et al.* (2005) observed increased expression of *grvA* in response to *rcsB* overexpression and described RcsB boxes in the predicted *grvA* promoter region with some homology to the RcsB consensus (Wehland & Bernhard, 2000), suggesting direct regulation of *grvA* transcription. Alternatively, RcsB may interact with GrvA to directly activate the expression of *ler* and other genes. There is precedent for this, as RcsB has been shown to regulate transcription as a heterodimer with RcsA (Francez-Charlot *et al.*, 2003; Stout *et al.*, 1991), GadE (Castanié-Cornet *et al.*, 2010) and BglJ (Venkatesh *et al.*, 2010). If RcsB–GrvA activate *ler* transcription as a heterodimer, they probably bind upstream of the core promoter region (i.e. upstream of −35) as is typical for RcsB promoter activation (Boulanger *et al.*, 2005; Castanié-Cornet *et al.*, 2010; Sturny *et al.*, 2003; Venkatesh *et al.*, 2010). However, there is no RcsB binding site upstream of and including the *ler* P1 and P2 promoters.

The results of this study suggest that RcsB is involved in the inverse regulation of genes that control motility (i.e. *flhDC*) and those for intimate colonization (i.e. the LEE) in EHEC. This opposing relationship between colonization and motility may be important for the establishment of *E. coli* in the gut. For example, constitutive expression of the FlhDC regulon in EHEC markedly reduced adherence to HeLa cells (Iyoda *et al.*, 2006), whereas deletion of *flhDC* and lack of motility in K12 increased colonization in a murine model (Gauger *et al.*, 2007; Leatham *et al.*, 2005). Note, however, that FlhDC also controls the expression of genes which serve no direct role in motility but which could contribute in some way to colonization. In EHEC, the LEE-encoded activator GrlA indirectly downregulates transcription of *flhDC* leading to reduced motility (Iyoda *et al.*, 2006). This study has revealed that mutation of *rcsB* masks the negative regulatory effect of GrlA on motility and *flhDC* transcription, and that the overexpression of *grlA* increases RcsB levels. This suggests that RcsB and GrvA are members of a reciprocating regulatory mechanism in EHEC which, at a minimum, co-ordinates the upregulation of LEE genes with a downregulation of the *flhDC* flagellar regulon. Activation of RcsB by GrlA appears to be at the post-transcriptional level, as increased protein levels did not correspond with increased transcription from promoters driving expression of *rcsDB* or *rcsB*.

In EHEC, bicarbonate has been shown to stimulate LEE transcription through *ler*, and to increase adherence to Caco-2 cells in a pH-independent manner (Abe *et al.*, 2002). It has been hypothesized that bicarbonate produced naturally in the small bowel to neutralize gastric acid may serve as a biological cue for T3SS-dependent colonization (Abe *et al.*, 1997, 2002). In *C. rodentium* bicarbonate interacts with the AraC-type regulator RegA to directly upregulate *grlA* expression (Tauschek *et al.*, 2010). In EHEC and EPEC, however, there are no homologues of RegA, and the genetic determinant(s) which regulates bicarbonate-dependent induction of the LEE in these pathogens is unknown. This study has shown that Rcs phosphorelay components RcsB and RcsC and the global regulator of virulence GrvA are required for full stimulation of the LEE in response to bicarbonate in EHEC. Despite the interplay of GrlA and RcsB in the control of *flhDC* and motility, there is no evidence that *grlA* is important for bicarbonate-dependent LEE expression through this pathway. For instance, overexpression of *grlA* did not increase *rcsB* transcription, whereas bicarbonate addition did enhance *rcsB* transcription (Figs 4d and 5c). Furthermore, the level of RcsB induction was markedly higher in WT cells grown with bicarbonate than in strains which overexpress *grlA* alone (Fig. 4c). Therefore, in EHEC it is predicted that bicarbonate stimulates LEE expression through an RcsB–GrvA–Ler activation pathway.

To conclude, the LEE expression phenotype of TW14359 is hypothesized to result from intrinsically increased basal levels of the response regulator RcsB, activating LEE expression through a GrvA–Ler pathway. In addition, increased adherence of strain TW14359 to intestinal cells was shown to be dependent on elevated *rcsB* expression and a functional T3SS. Whether this dysregulated pathway is responsible for the severe disease attributed to infections with this strain is not yet clear. Furthermore, the LEE-encoded activator GrlA was determined to require *rcsB* for repression of the *flhDC* flagellar regulon, suggesting that GrlA and RcsB work together to co-ordinate the activation of genes for colonization with the repression of genes for motility. Finally, bicarbonate was proposed to be a physiological signal for an Rcs phosphorelay- and GrvA-directed pathway activating LEE expression and colonization in EHEC.

ACKNOWLEDGEMENTS

We thank Sergio Uzzau (University of Sassari, Italy) for kindly providing vector pSA312 for FLAG-fusion construction, Edward G. Dudley (Pennsylvania State University) for providing vector pRS551 for *lacZ* fusions and Robert Buzzeo (University of South Florida) for technical assistance with adherence assays. We also thank the University of South Florida Center for Drug Discovery and Innovation (CDDI) for technical assistance with proteomics and MS.

REFERENCES

Abe, A., Kenny, B., Stein, M. & Finlay, B. B. (1997). Characterization of two virulence proteins secreted by rabbit enteropathogenic *Escherichia coli*, EspA and EspB, whose maximal expression is sensitive to host body temperature. *Infect Immun* **65**, 3547–3555.

Abe, H., Tatsuno, I., Tobe, T., Okutani, A. & Sasakawa, C. (2002). Bicarbonate ion stimulates the expression of locus of enterocyte effacement-encoded genes in enterohemorrhagic *Escherichia coli* O157:H7. *Infect Immun* **70**, 3500–3509.

Abu-Ali, G. S., Ouellette, L. M., Henderson, S. T., Whittam, T. S. & Manning, S. D. (2010a). Differences in adherence and virulence gene

expression between two outbreak strains of enterohaemorrhagic *Escherichia coli* O157:H7. *Microbiology* **156**, 408–419.

Abu-Ali, G. S., Ouellette, L. M., Henderson, S. T., Lacher, D. W., Riordan, J. T., Whittam, T. S. & Manning, S. D. (2010b). Increased adherence and expression of virulence genes in a lineage of *Escherichia coli* O157:H7 commonly associated with human infections. *PLoS ONE* **5**, e10167.

Bergholz, T. M., Wick, L. M., Qi, W., Riordan, J. T., Ouellette, L. M. & Whittam, T. S. (2007a). Global transcriptional response of *Escherichia coli* O157:H7 to growth transitions in glucose minimal medium. *BMC Microbiol* **7**, 97.

Bergholz, T. M., Wick, L. M., Qi, W., Riordan, J. T., Ouellette, L. M. & Whittam, T. S. (2007b). Global transcriptional response of *Escherichia coli* O157:H7 to growth transitions in glucose minimal medium. *BMC Microbiol* **7**, 97.

Bernadac, A., Gavioli, M., Lazzaroni, J. C., Raina, S. & Lloubès, R. (1998). *Escherichia coli tol-pal* mutants form outer membrane vesicles. *J Bacteriol* **180**, 4872–4878.

Boulanger, A., Francez-Charlot, A., Conter, A., Castanié-Cornet, M. P., Cam, K. & Gutierrez, C. (2005). Multistress regulation in *Escherichia coli*: expression of *osmB* involves two independent promoters responding either to σ^S or to the RcsCDB His-Asp phosphorelay. *J Bacteriol* **187**, 3282–3286.

Cascales, E., Gavioli, M., Sturgis, J. N. & Lloubès, R. (2000). Proton motive force drives the interaction of the inner membrane TolA and outer membrane *pal* proteins in *Escherichia coli*. *Mol Microbiol* **38**, 904–915.

Castanié-Cornet, M. P., Cam, K., Bastiat, B., Cros, A., Bordes, P. & Gutierrez, C. (2010). Acid stress response in *Escherichia coli*: mechanism of regulation of *gadA* transcription by RcsB and GadE. *Nucleic Acids Res* **38**, 3546–3554.

Chang, A. C. & Cohen, S. N. (1978). Construction and characterization of amplifiable multicopy DNA cloning vehicles derived from the P15A cryptic miniplasmid. *J Bacteriol* **134**, 1141–1156.

Clavel, T., Lazzaroni, J. C., Vianney, A. & Portalier, R. (1996). Expression of the *tolQRA* genes of *Escherichia coli* K-12 is controlled by the RcsC sensor protein involved in capsule synthesis. *Mol Microbiol* **19**, 19–25.

Creasey, E. A., Delahay, R. M., Daniell, S. J. & Frankel, G. (2003). Yeast two-hybrid system survey of interactions between LEE-encoded proteins of enteropathogenic *Escherichia coli*. *Microbiology* **149**, 2093–2106.

Datsenko, K. A. & Wanner, B. L. (2000). One-step inactivation of chromosomal genes in *Escherichia coli* K-12 using PCR products. *Proc Natl Acad Sci U S A* **97**, 6640–6645.

Deng, W., Puente, J. L., Gruenheid, S., Li, Y., Vallance, B. A., Vázquez, A., Barba, J., Ibarra, J. A., O'Donnell, P. & other authors (2004). Dissecting virulence: systematic and functional analyses of a pathogenicity island. *Proc Natl Acad Sci U S A* **101**, 3597–3602.

Elliott, S. J., Wainwright, L. A., McDaniel, T. K., Jarvis, K. G., Deng, Y. K., Lai, L. C., McNamara, B. P., Donnenberg, M. S. & Kaper, J. B. (1998). The complete sequence of the locus of enterocyte effacement (LEE) from enteropathogenic *Escherichia coli* E2348/69. *Mol Microbiol* **28**, 1–4.

Feldman, M. (1983). Gastric bicarbonate secretion in humans. Effect of pentagastrin, bethanechol, and 11,16,16-trimethyl prostaglandin E2. *J Clin Invest* **72**, 295–303.

Francez-Charlot, A., Laugel, B., Van Gemert, A., Dubarry, N., Wiorowski, F., Castanié-Cornet, M. P., Gutierrez, C. & Cam, K. (2003). RcsCDB His-Asp phosphorelay system negatively regulates the *flhDC* operon in *Escherichia coli*. *Mol Microbiol* **49**, 823–832.

Friedberg, D., Umanski, T., Fang, Y. & Rosenshine, I. (1999). Hierarchy in the expression of the locus of enterocyte effacement genes of enteropathogenic *Escherichia coli*. *Mol Microbiol* **34**, 941–952.

Gauger, E. J., Leatham, M. P., Mercado-Lubo, R., Laux, D. C., Conway, T. & Cohen, P. S. (2007). Role of motility and the *flhDC* operon in *Escherichia coli* MG1655 colonization of the mouse intestine. *Infect Immun* **75**, 3315–3324.

Grant, A. J., Farris, M., Alefounder, P., Williams, P. H., Woodward, M. J. & O'Connor, C. D. (2003). Co-ordination of pathogenicity island expression by the BipA GTPase in enteropathogenic *Escherichia coli* (EPEC). *Mol Microbiol* **48**, 507–521.

Guzman, L. M., Belin, D., Carson, M. J. & Beckwith, J. (1995). Tight regulation, modulation, and high-level expression by vectors containing the arabinose PBAD promoter. *J Bacteriol* **177**, 4121–4130.

Huang, L. H. & Syu, W. J. (2008). GrlA of enterohemorrhagic *Escherichia coli* O157:H7 activates *LEE1* by binding to the promoter region. *J Microbiol Immunol Infect* **41**, 9–16.

Iyoda, S. & Watanabe, H. (2004). Positive effects of multiple *pch* genes on expression of the locus of enterocyte effacement genes and adherence of enterohaemorrhagic *Escherichia coli* O157:H7 to HEp-2 cells. *Microbiology* **150**, 2357–2371.

Iyoda, S., Koizumi, N., Satou, H., Lu, Y., Saitoh, T., Ohnishi, M. & Watanabe, H. (2006). The GrlR-GrlA regulatory system coordinately controls the expression of flagellar and LEE-encoded type III protein secretion systems in enterohemorrhagic *Escherichia coli*. *J Bacteriol* **188**, 5682–5692.

Kenny, B., Abe, A., Stein, M. & Finlay, B. B. (1997). Enteropathogenic *Escherichia coli* protein secretion is induced in response to conditions similar to those in the gastrointestinal tract. *Infect Immun* **65**, 2606–2612.

Krin, E., Danchin, A. & Soutourina, O. (2010). RcsB plays a central role in H-NS-dependent regulation of motility and acid stress resistance in *Escherichia coli*. *Res Microbiol* **161**, 363–371.

Kulasekara, B. R., Jacobs, M., Zhou, Y., Wu, Z., Sims, E., Saenphimmachak, C., Rohmer, L., Ritchie, J. M., Radey, M. & other authors (2009). Analysis of the genome of the *Escherichia coli* O157:H7 2006 spinach-associated outbreak isolate indicates candidate genes that may enhance virulence. *Infect Immun* **77**, 3713–3721.

Laaberki, M. H., Janabi, N., Oswald, E. & Repoila, F. (2006). Concert of regulators to switch on LEE expression in enterohemorrhagic *Escherichia coli* O157:H7: interplay between Ler, GrlA, HNS and RpoS. *Int J Med Microbiol* **296**, 197–210.

Leatham, M. P., Stevenson, S. J., Gauger, E. J., Krogfelt, K. A., Lins, J. J., Haddock, T. L., Autieri, S. M., Conway, T. & Cohen, P. S. (2005). Mouse intestine selects nonmotile *flhDC* mutants of *Escherichia coli* MG1655 with increased colonizing ability and better utilization of carbon sources. *Infect Immun* **73**, 8039–8049.

Lio, J. C. & Syu, W. J. (2004). Identification of a negative regulator for the pathogenicity island of enterohemorrhagic *Escherichia coli* O157:H7. *J Biomed Sci* **11**, 855–863.

Livak, K. J. & Schmittgen, T. D. (2001). Analysis of relative gene expression data using real-time quantitative PCR and the $2^{-\Delta\Delta CT}$ method. *Methods* **25**, 402–408.

Manning, S. D., Motiwala, A. S., Springman, A. C., Qi, W., Lacher, D. W., Ouellette, L. M., Mladonicky, J. M., Somsel, P., Rudrik, J. T. & other authors (2008). Variation in virulence among clades of *Escherichia coli* O157:H7 associated with disease outbreaks. *Proc Natl Acad Sci U S A* **105**, 4868–4873.

McDaniel, T. K. & Kaper, J. B. (1997). A cloned pathogenicity island from enteropathogenic *Escherichia coli* confers the attaching and effacing phenotype on *E. coli* K-12. *Mol Microbiol* **23**, 399–407.

McKee, M. L. & O'Brien, A. D. (1995). Investigation of enterohemorrhagic *Escherichia coli* O157:H7 adherence characteristics and invasion potential reveals a new attachment pattern shared by intestinal *E. coli*. *Infect Immun* **63**, 2070–2074.

Mellies, J. L., Barron, A. M. & Carmona, A. M. (2007). Enteropathogenic and enterohemorrhagic *Escherichia coli* virulence gene regulation. *Infect Immun* **75**, 4199–4210.

Michino, H., Araki, K., Minami, S., Takaya, S., Sakai, N., Miyazaki, M., Ono, A. & Yanagawa, H. (1999). Massive outbreak of *Escherichia coli* O157:H7 infection in schoolchildren in Sakai City, Japan, associated with consumption of white radish sprouts. *Am J Epidemiol* **150**, 787–796.

Miller, J. (1972). Assay of β-galactosidase. In *Experiments in Molecular Genetics*, pp. 352–355. Cold Spring Harbor, NY: Cold Spring Harbor Laboratory.

Mitra, A., Fay, P. A., Morgan, J. K., Vendura, K. W., Versaggi, S. L. & Riordan, J. T. (2012). Sigma factor N, liaison to an *ntrC* and *rpoS* dependent regulatory pathway controlling acid resistance and the LEE in enterohemorrhagic *Escherichia coli*. *PLoS ONE* **7**, e46288.

Murphy, K. C. & Campellone, K. G. (2003). Lambda Red-mediated recombinogenic engineering of enterohemorrhagic and enteropathogenic *E. coli*. *BMC Mol Biol* **4**, 11.

Nataro, J. P. & Kaper, J. B. (1998). Diarrheagenic *Escherichia coli*. *Clin Microbiol Rev* **11**, 142–201.

Neupane, M., Abu-Ali, G. S., Mitra, A., Lacher, D. W., Manning, S. D. & Riordan, J. T. (2011). Shiga toxin 2 overexpression in *Escherichia coli* O157:H7 strains associated with severe human disease. *Microb Pathog* **51**, 466–470.

Perna, N. T., Mayhew, G. F., Pósfai, G., Elliott, S., Donnenberg, M. S., Kaper, J. B. & Blattner, F. R. (1998). Molecular evolution of a pathogenicity island from enterohemorrhagic *Escherichia coli* O157:H7. *Infect Immun* **66**, 3810–3817.

Pescaretti, M. L., Morero, R. & Delgado, M. A. (2009). Identification of a new promoter for the response regulator *rcsB* expression in *Salmonella enterica* serovar *Typhimurium*. *FEMS Microbiol Lett* **300**, 165–173.

Rangel, J. M., Sparling, P. H., Crowe, C., Griffin, P. M. & Swerdlow, D. L. (2005). Epidemiology of *Escherichia coli* O157:H7 outbreaks, United States, 1982–2002. *Emerg Infect Dis* **11**, 603–609.

Riley, L. W., Remis, R. S., Helgerson, S. D., McGee, H. B., Wells, J. G., Davis, B. R., Hebert, R. J., Olcott, E. S., Johnson, L. M. & other authors (1983). Hemorrhagic colitis associated with a rare *Escherichia coli* serotype. *N Engl J Med* **308**, 681–685.

Riordan, J. T., Tietjen, J. A., Walsh, C. W., Gustafson, J. E. & Whittam, T. S. (2010). Inactivation of alternative sigma factor 54 (RpoN) leads to increased acid resistance, and alters locus of enterocyte effacement (LEE) expression in *Escherichia coli* O157:H7. *Microbiology* **156**, 719–730.

Rivera, F. E., Miller, H. K., Kolar, S. L., Stevens, S. M., Jr & Shaw, L. N. (2012). The impact of CodY on virulence determinant production in community-associated methicillin-resistant *Staphylococcus aureus*. *Proteomics* **12**, 263–268.

Schauer, D. B. & Falkow, S. (1993). Attaching and effacing locus of a *Citrobacter freundii* biotype that causes transmissible murine colonic hyperplasia. *Infect Immun* **61**, 2486–2492.

Shin, S., Castanie-Cornet, M. P., Foster, J. W., Crawford, J. A., Brinkley, C. & Kaper, J. B. (2001). An activator of glutamate decarboxylase genes regulates the expression of enteropathogenic *Escherichia coli* virulence genes through control of the plasmid-encoded regulator, Per. *Mol Microbiol* **41**, 1133–1150.

Simons, R. W., Houman, F. & Kleckner, N. (1987). Improved single and multicopy *lac*-based cloning vectors for protein and operon fusions. *Gene* **53**, 85–96.

Sperandio, V., Mellies, J. L., Nguyen, W., Shin, S. & Kaper, J. B. (1999). Quorum sensing controls expression of the type III secretion gene transcription and protein secretion in enterohemorrhagic and enteropathogenic *Escherichia coli*. *Proc Natl Acad Sci U S A* **96**, 15196–15201.

Stout, V., Torres-Cabassa, A., Maurizi, M. R., Gutnick, D. & Gottesman, S. (1991). RcsA, an unstable positive regulator of capsular polysaccharide synthesis. *J Bacteriol* **173**, 1738–1747.

Sturny, R., Cam, K., Gutierrez, C. & Conter, A. (2003). NhaR and RcsB independently regulate the *osmCp1* promoter of *Escherichia coli* at overlapping regulatory sites. *J Bacteriol* **185**, 4298–4304.

Tauschek, M., Yang, J., Hocking, D., Azzopardi, K., Tan, A., Hart, E., Praszkier, J. & Robins-Browne, R. M. (2010). Transcriptional analysis of the *grlRA* virulence operon from *Citrobacter rodentium*. *J Bacteriol* **192**, 3722–3734.

Tobe, T., Ando, H., Ishikawa, H., Abe, H., Tashiro, K., Hayashi, T., Kuhara, S. & Sugimoto, N. (2005). Dual regulatory pathways integrating the RcsC-RcsD-RcsB signalling system control enterohaemorrhagic *Escherichia coli* pathogenicity. *Mol Microbiol* **58**, 320–333.

Tree, J. J., Wolfson, E. B., Wang, D., Roe, A. J. & Gally, D. L. (2009). Controlling injection: regulation of type III secretion in enterohaemorrhagic *Escherichia coli*. *Trends Microbiol* **17**, 361–370.

Umanski, T., Rosenshine, I. & Friedberg, D. (2002). Thermoregulated expression of virulence genes in enteropathogenic *Escherichia coli*. *Microbiology* **148**, 2735–2744.

Uzzau, S., Figueroa-Bossi, N., Rubino, S. & Bossi, L. (2001). Epitope tagging of chromosomal genes in *Salmonella*. *Proc Natl Acad Sci U S A* **98**, 15264–15269.

Venkatesh, G. R., Kembou Koungni, F. C., Paukner, A., Stratmann, T., Blissenbach, B. & Schnetz, K. (2010). BglJ-RcsB heterodimers relieve repression of the *Escherichia coli bgl* operon by H-NS. *J Bacteriol* **192**, 6456–6464.

Vizcaíno, J. A., Côté, R., Reisinger, F., Foster, J. M., Mueller, M., Rameseder, J., Hermjakob, H. & Martens, L. (2009). A guide to the Proteomics Identifications Database proteomics data repository. *Proteomics* **9**, 4276–4283.

Wehland, M. & Bernhard, F. (2000). The RcsAB box. Characterization of a new operator essential for the regulation of exopolysaccharide biosynthesis in enteric bacteria. *J Biol Chem* **275**, 7013–7020.

Edited by: D. Gally

OPEN ACCESS Freely available online

PLOS ONE

Sigma Factor N, Liaison to an *ntrC* and *rpoS* Dependent Regulatory Pathway Controlling Acid Resistance and the LEE in Enterohemorrhagic *Escherichia coli*

Avishek Mitra, Pamela A. Fay, Jason K. Morgan, Khoury W. Vendura, Salvatore L. Versaggi, James T. Riordan*

Department of Cell Biology, Microbiology, and Molecular Biology (CMMB), University of South Florida, Tampa, Florida, United States of America

Abstract

Enterohemorrhagic *Escherichia coli* (EHEC) is dependent on acid resistance for gastric passage and low oral infectious dose, and the locus of enterocyte effacement (LEE) for intestinal colonization. Mutation of *rpoN*, encoding sigma factor N (σ^N), dramatically alters the growth-phase dependent regulation of both acid resistance and the LEE. This study reports on the determinants of σ^N-directed acid resistance and LEE expression, and the underlying mechanism attributable to this phenotype. Glutamate-dependent acid resistance (GDAR) in TW14359Δ*rpoN* correlated with increased expression of the *gadX-gadW* regulatory circuit during exponential growth, whereas upregulation of arginine-dependent acid resistance (ADAR) genes *adiA* and *adiC* in TW14359Δ*rpoN* did not confer acid resistance by the ADAR mechanism. LEE regulatory (*ler*), structural (*espA* and *cesT*) and effector (*tir*) genes were downregulated in TW14359Δ*rpoN*, and mutation of *rpoS* encoding sigma factor 38 (σ^S) in TW14359Δ*rpoN* restored acid resistance and LEE genes to WT levels. Stability, but not the absolute level, of σ^S was increased in TW14359Δ*rpoN*; however, increased stability was not solely attributable to the GDAR and LEE expression phenotype. Complementation of TW14359Δ*rpoN* with a σ^N allele that binds RNA polymerase (RNAP) but not DNA, did not restore WT levels of σ^S stability, *gadE*, *ler* or GDAR, indicating a dependence on transcription from a σ^N promoter(s) and not RNAP competition for the phenotype. Among a library of σ^N enhancer binding protein mutants, only TW14359Δ*ntrC*, inactivated for nitrogen regulatory protein NtrC, phenocopied TW14359Δ*rpoN* for σ^S stability, GDAR and *ler* expression. The results of this study suggest that during exponential growth, NtrC-σ^N regulate GDAR and LEE expression through downregulation of σ^S at the post-translational level; likely by altering σ^S stability or activity. The regulatory interplay between NtrC, other EBPs, and σ^N–σ^S, represents a mechanism by which EHEC can coordinate GDAR, LEE expression and other cellular functions, with nitrogen availability and physiologic stimuli.

Citation: Mitra A, Fay PA, Morgan JK, Vendura KW, Versaggi SL, et al. (2012) Sigma Factor N, Liaison to an *ntrC* and *rpoS* Dependent Regulatory Pathway Controlling Acid Resistance and the LEE in Enterohemorrhagic *Escherichia coli*. PLoS ONE 7(9): e46288. doi:10.1371/journal.pone.0046288

Editor: Eric Cascales, Centre National de la Recherche Scientifique, Aix-Marseille Université, France

Received May 30, 2012; **Accepted** August 28, 2012; **Published** September 27, 2012

Funding: This research was supported by intramural start-up funds from the University of South Florida. The funders had no role in study design, data collection and analysis, decision to publish, or preparation of the manuscript.

Competing Interests: The authors have declared that no competing interests exist.

* E-mail: jtriordan@usf.edu

Introduction

Enterohemorrhagic *Escherichia coli* (EHEC) is an enteric pathogen commonly implicated in food-borne outbreaks of hemorrhagic colitis, and in the life-threatening illness hemolytic uremic syndrome [1–3]. To cause disease in humans, EHEC must overcome two formidable innate barriers to infection: the acidity of the stomach, and competition for intestinal colonization sites. For the former, EHEC (and other *E. coli*) has evolved multiple discrete acid resistance mechanisms [4], which allow for survival in highly acidic environments such as the stomach, and which determine a low oral infectious dose [5,6]. For competitive gut colonization, EHEC utilize a type III secretion system (T3SS) encoded on the locus of enterocyte effacement (LEE) pathogenicity island [7–10]. This T3SS translocates EHEC effector proteins into host intestinal cells that mediate intimate attachment to the gut and subvert host cellular processes [11].

The expression of acid resistance and the LEE is influenced by various environmental and intracellular signals, including nutrient availability, stress, and growth phase [12–21]. During exponential growth acid resistance is largely repressed, but is activated as cultures transition into stationary phase [13]; for the LEE, the inverse is true [18]. This pattern of expression may reflect the importance of colonization and replication when resources are abundant, and that of stress durability when they are scarce. Many auxiliary regulators communicate these changes in growth conditions to regulatory components of both acid resistance and the LEE [12,22–28]. Alternative sigma factor 38 (σ^S) is a global regulator that plays an important role in coordinating acid resistance and LEE expression with growth phase. σ^S is a protein of low abundance during exponential growth, but accumulates during transition into stationary phase [29]. The acid resistance phenotype of stationary phase cultures is largely attributed to σ^S and expectedly, strains mutated for *rpoS* (encoding σ^S) are sensitive to acid [13,14], whereas LEE expression is both decreased and increased in response to *rpoS* mutation, depending on growth conditions [28,30–32]. Not surprisingly, *rpoS* mutants are impaired in their ability to survive passage in both murine and bovine

models of infection [33]. σ^S is tightly regulated at multiple levels of control [34], and the factors that dictate *rpoS*/σ^S expression indirectly influence acid resistance, the LEE, and EHEC pathogenesis.

Recently, another alternative sigma factor, sigma N (σ^N), has been shown to control structural and regulatory genes of both acid resistance and the LEE in EHEC serotype O157:H7 [35]. When bound to RNA polymerase (RNAP), the RNAP-σ^N holoenzyme ($E\sigma^N$) directs transcription from an estimated twenty-one promoters in *E. coli* which specify the transcription of over sixty genes involved in nitrogen and carbon metabolism, and stress resistance [36–39]. EHEC strains null for *rpoN* (encoding σ^N) express elevated levels of acid resistance genes belonging to the glutamate-dependent acid resistance (GDAR) system, and reduced levels of expression for genes encoded on all five operons of the LEE [35]. This altered expression of GDAR and LEE genes is restricted to exponential phase cultures. Furthermore, GDAR upregulation in *rpoN* mutants is correlated with increased survival in acidic environments, and is dependent on an intact *rpoS* gene, suggesting that GDAR is controlled by an as yet uncharacterized σ^N–σ^S regulatory pathway in *E. coli* [35].

There is precedent for such a pathway in *Borrelia burgdorferi*, in which a σ^N–σ^S regulatory pathway controls the expression of membrane lipoproteins essential for transmission and pathogenesis [40–42]. In the *B. burgdorferi* model, σ^N has been shown to directly activate *rpoS* transcription, which is contrary to *E. coli* in which *rpoS* inactivation abrogates the GDAR phenotype of an *rpoN* null mutant, suggesting that σ^N downregulates *rpoS*/σ^S by some unknown mechanism. There is evidence that this negative regulation is at the post-transcriptional level, as *rpoN* mutation does not alter *rpoS* mRNA levels [35]. In addition, a recent study reported increased levels and stability of σ^S in an *rpoN* mutant of the nonpathogenic *E. coli* strain K-12 MG1655 [43]. This study further explores the regulatory interplay of σ^N and σ^S, and uncovers mechanistic details about σ^N–σ^S directed control of acid resistance and the LEE, and other genetic factors which contribute to the expression of this regulatory pathway.

Results

σ^N–σ^S Directed Regulation of Glutamate-dependent Acid Resistance and the Locus of Enterocyte Effacement

Independent regulatory pathways control glutamate-dependent acid resistance (GDAR) genes in response to discrete environmental stimuli through transcriptional modulation of the central regulator *gadE*. These include pathways that stimulate *gadE* during exponential growth in minimal, acidified media (EvgAB-YdeO) [16,44], or during stationary phase growth in rich media (σ^S-GadX-GadW) [12], or rich media containing glucose (TrmE) [15]. The growth conditions under which *rpoN*-dependent acid resistance is expressed do not conform precisely to any of these stimulating environments. And yet, mutation of *rpoS* in an *rpoN* null background suppresses GDAR, suggesting that in the WT background σ^N negatively regulates GDAR through a σ^S-dependent pathway; namely, σ^S-GadX-GadW. To explore this further, transcript levels of GDAR regulatory genes from these activating circuits were measured in WT and mutant backgrounds of TW14359 during exponential growth.

As anticipated, *gadE* transcript levels were significantly higher in TW14359Δ*rpoN* compared to TW14359 ($p = 0.001$), as well as TW14359Δ*rpoS* ($p = 0.007$), and TW14359Δ*rpoN*Δ*rpoS* ($p = 0.005$) (Fig. 1A). Adding to this, both *gadX* and *gadW* transcripts were upregulated in TW14359Δ*rpoN* ($p<0.05$), but not in TW14359Δ*rpoS* for *gadX*, or TW14359Δ*rpoN*Δ*rpoS* for either *gadX* or *gadW*. Transcript levels for *trmE* and *ydeO*, key regulators of alternative pathways for *gadE* activation, were in low abundance, and did not differ significantly between strains (Fig. 1A); the presence of amplicons for *trmE* and *ydeO* was validated by gel electrophoresis. Thus, a *rpoN* null mutation leads to increased expression of the GDAR-activating GadX-GadW pathway, agreeing with the *rpoS*-dependency of the phenotype.

In addition to GDAR, σ^S regulates at least two more acid resistance systems in *E. coli*: the arginine-dependent acid resistance (ADAR) system [45], and the oxidative-dependent acid resistance (ODAR) system [33]. Both GDAR and ADAR systems protect the cell from acid by a proton scavenging mechanism that is facilitated by the conversion of glutamate to γ-aminobutyric acid (GDAR) or arginine to agmatine (ADAR), and catalyzed by amino acid decarboxylases. ODAR on the other hand does not require glutamate or arginine, and is repressed by glucose [4]. Except for *rpoS*, the regulatory and structural determinants of ODAR are not well understood, and thus were not investigated in this study. For ADAR, the structural genes *adiA* (arginine decarboxylase) and *adiC* (arginine-agmatine exchanger) were slightly but significantly upregulated in TW14359Δ*rpoN* relative to TW14359 and TW14359Δ*rpoN*Δ*rpoS* ($p<0.05$) (Fig. 1B). However, *adiY*, encoding a putative regulator of *adiA* and *adiC* [46], was not altered in expression in either of the mutant backgrounds. Despite the

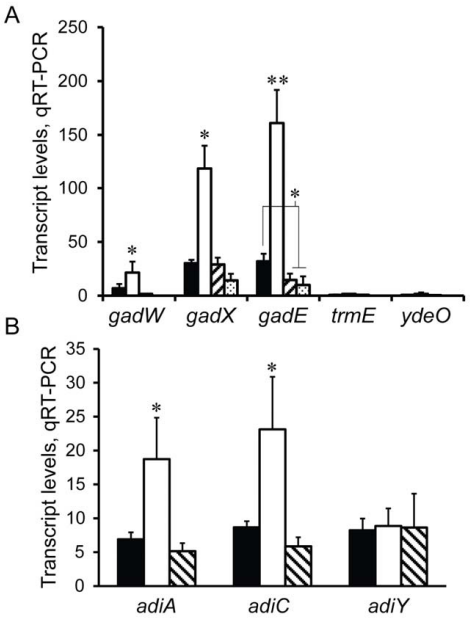

Figure 1. Transcript levels for acid resistance genes. Gene transcript levels as determined by qRT-PCR are plotted for genes of the GDAR system (panel A) and genes of the ADAR system (panel B). Mean transcript levels are normalized to the 16S rRNA gene *rrsH*. Transcript levels are plotted against WT TW14359 (filled), TW14359Δ*rpoN* (empty), TW14359Δ*rpoN* Δ*rpoS* (hatched), and TW14359Δ*rpoS* (stippled, *gadX* and *gadE* only) for panel A. Asterisks denote significant differences by Tukey's HSD following a significant F-test ($n\geq3$, $p<0.05$ [*]; $p<0.01$ [**]). Error bars indicate standard error of the mean.
doi:10.1371/journal.pone.0046288.g001

increase in *adiA* and *adiC* expression in TW14359Δ*rpoN*, there was no corresponding increase in acid resistance by the ADAR mechanism (Table 1), and exclusion of either glutamate or arginine from acidified EG media resulted in no growth for any strains (data not shown). Therefore the only known requirements for *rpoN*-dependent acid resistance are *rpoS*, *gadE*, and glutamate.

σ^S has also been shown to upregulate and downregulate transcription of LEE genes in EHEC. For upregulation, σ^S is hypothesized to enhance expression of the central regulator of the LEE, *ler* (encoded on operon *LEE1*), in a manner dependent on the non-coding RNA DsrA [28]. It has also been reported that both the *LEE3* and *LEE5* operons possess σ^S-responsive promoters [30]. For downregulation, σ^S is proposed to stimulate an unknown repressor of PchA, which is a positive regulator of *ler* [31,32,47]. The mutation of *rpoN* leads to the downregulation of LEE genes during exponential growth [35]. Since σ^N controls GDAR through a σ^S-dependent pathway, it was predicted that σ^N-directed regulation of the LEE may be similarly dependent on *rpoS*. As expected, transcript levels for LEE genes encoding the T3SS translocon component *espA* (encoded on *LEE4*), the effector chaperone *cesT* (on *LEE5*), and the translocated intimin receptor *tir* (on *LEE5*) were downregulated during exponential growth of TW14359Δ*rpoN* relative to TW14359 ($p<0.05$) (Fig. 2A). In addition, transcript levels of *ler* (on *LEE1*) were reduced in TW14359Δ*rpoN* compared to TW14359 ($p = 0.015$) and TW14359Δ*rpoS* ($p = 0.011$) (Fig. 2B). Importantly, mutation of *rpoS* in TW14359Δ*rpoN* restored *ler* expression to levels consistent with TW14359Δ*rpoS*; *ler* expression was increased in *rpoS* null backgrounds relative to WT, but not significantly increased. These results indicate that σ^N positively regulates the LEE during exponential growth in an *rpoS*-dependent manner, and is consistent with the role of σ^S as a negative regulator of LEE expression via the PchA-Ler pathway [31,32,47].

Effect of *rpoN* Mutation on *rpoS* mRNA and σ^S Stability in EHEC

There is evidence that the mutation of *rpoN* in EHEC does not alter *rpoS* mRNA levels, but instead leads to post-transcriptional alternations in *rpoS*/σ^S [35]. The mutation of *rpoN* in *E. coli* strain K-12 MG1655 was recently shown to lead to increased σ^S levels and stability [43]. However, there are substantial differences at the genomic level between K-12 and EHEC O157:H7 strains [48]. As an important example, the TW14359 genome (and the genomes of many other EHEC strains), does not contain two of the thirteen σ^N enhancer-binding proteins found in K-12 and most other *E. coli*. This study thus aimed to validate the effect of *rpoN* mutation on σ^S levels and stability in the EHEC background and under the growth conditions that promote σ^N-dependent control of GDAR and the LEE.

As anticipated, no difference was observed in the stability of *rpoS* mRNA between TW14359 and TW14359Δ*rpoN* (Fig. 3A). After 12 min of rifampin addition, *rpoS* transcript was barely detectable in both backgrounds and the mean half-life for *rpoS* transcript was estimated at 2.43 min (TW14359) and 2.51 min (TW14359Δ*rpoN*), which agrees with previous estimates [49,50]. Before addition of rifampin, however, levels of *rpoS* transcript were higher (1.5-fold) in TW14359Δ*rpoN* compared to TW14359, but not significantly higher. In agreement with experiments using strain MG1655, σ^S was more stable in TW14359Δ*rpoN* compared to TW14359, however absolute levels were not observed to be higher in TW14359Δ*rpoN* (Fig. 3B) as described for MG1655 [43].

Table 1. Acid resistance by the GDAR and ADAR mechanisms.

		Percent survival (SD)[a]	
Growth condition	**Strain/genotype**	**GDAR**	**ADAR**
DMEM	TW14359	<0.01[b]	<0.01
	TW14359Δ*rpoN*	24.2 (0.24)	<0.01
	TW14359Δ*fhlA*	21.2 (0.31)	ND[c]
	TW14359Δ*glnG*	15.7 (1.88)	ND
	TW14359Δ*rpoN*Δ*rpoS*	<0.01	<0.01
	TW14359Δ*rpoN* pRAM-1	0.141 (0.11)	0.125 (0.79)
	TW14359Δ*rpoN* pRAM-2	10.61 (1.22)	ND
DMEM +3, 4-DCI[d]	TW14359	<0.01	ND
	TW14359Δ*rpoN*	29.1 (9.3)	ND

[a]Percent survival by the glutamate-dependent (GDAR) and arginine-dependent (ADAR) acid resistance system; standard deviation (SD).
[b]Less than 10 CFU/ml remains following 1 h exposure to acidified GDAR or ADAR test environment.
[c]Not determined (ND).
[d]DMEM growth media with addition of 5 μM 3,4-dichloroisocoumarin (3,4-DCI).
doi:10.1371/journal.pone.0046288.t001

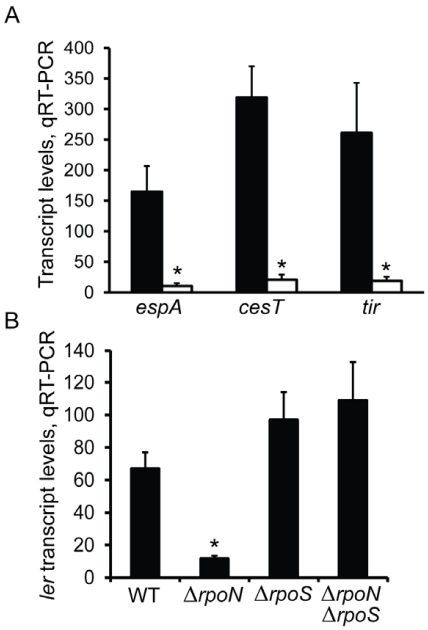

Figure 2. Transcript levels for LEE genes. (Panel A): gene transcript levels as determined by qRT-PCR are plotted for representative LEE genes in WT TW14359 (filled) and TW14359Δ*rpoN* (empty). (Panel B): *ler* transcript levels by qRT-PCR are plotted against TW14359 and various mutant derivative strains of TW14359. Mean transcript levels are normalized to the 16S rRNA gene *rrsH*. For panel A, an asterisk denotes a significant difference between TW14359 and TW14359Δ*rpoN* for each gene by Welch's t-test ($n\geq3$, $p<0.05$). For panel B, the asterisk denotes a significant difference between TW14359Δ*rpoN* and the remaining strains by Tukey's HSD following a significant F-test ($n\geq3$, $p<0.05$). Error bars indicate standard error of the mean.
doi:10.1371/journal.pone.0046288.g002

In TW14359, σ^S was barely detectable after 4 min of tetracycline addition, but was detected for up to 12 min in TW14359Δ*rpaN*. The mean half-life for σ^S was estimated at 2.4 min for TW14359 and 5.5 min for TW14359Δ*rpaN*, increasing by 2.3-fold in the *rpaN* null background. The half-life for σ^S has been estimated at 1.4–6.5 min in exponential cultures of *E. coli* [29,51,52], and 10.5–30 min in stationary phase cultures [29,51]. These results reveal that in TW14359Δ*rpaN*, *rpoS*-dependency and control of GDAR and the LEE is correlated with an increase in exponential phase stability, but not absolute levels, of σ^S.

Role for Core RNA Polymerase and σ^N–dependent Transcription in the σ^S Stability, GDAR and LEE Expression Phenotype of TW14359Δ*rpoN*

The ability of *E. coli* sigma factors to successfully compete for core RNA polymerase (RNAP) differs substantially. For example, the RNAP binding affinity of σ^N is second only to the primary sigma factor, σ^{70}, whereas σ^S binding affinity lies at the bottom of this rank order [53,54]. In addition, the relative cellular abundance of each sigma factor influences gene expression through competition for RNAP [55]. During exponential growth,

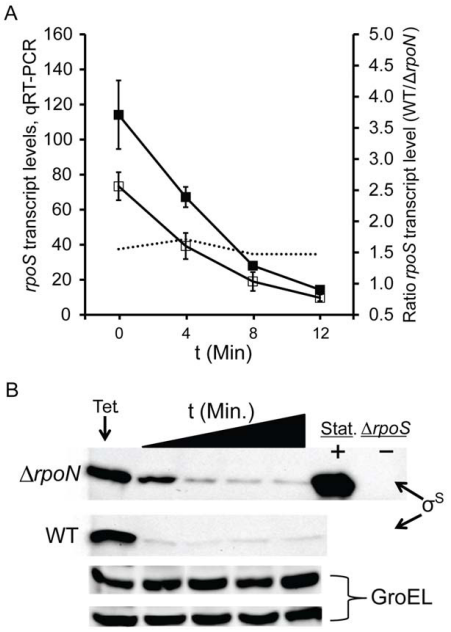

Figure 3. Stability of *rpoS* mRNA and σ^S. (Panel A): Mean *rpoS* transcript levels (1st ordinate) and ratio of *rpoS* transcript (2nd ordinate) plotted against time following addition of rifampin at t = 0 min for WT TW14359 (filled) and TW14359Δ*rpoN* (empty); ratio is indicated by the dotted line. Error bars denote standard error of the mean (n≥3). (Panel B): Representative western immunoblot for σ^S as a function to time following addition of tetracycline at t = 0 min for TW14359 (WT) and TW14359Δ*rpoN* (Δ*rpoN*); blots are in increments of 4 min. Stationary phase (Stat.) protein extracts were used as a positive control for σ^S, and TW14359Δ*rpoS* (Δ*rpoS*) as a negative control. Equal loading was controlled for by westerns for GroEL (top row is Δ*rpoN*, bottom row is WT).

doi:10.1371/journal.pone.0046288.g003

σ^N levels have been estimated at 10–16% those of σ^{70}, whereas σ^S is barely detectable [56–58]. Together, this suggests that σ^S is at a substantial disadvantage for competitive RNAP binding during exponential growth. However, in an *rpaN* null background, the absence of competing σ^N may allow for an increase in σ^S RNAP binding sufficient enough to protect σ^S from ClpXP degradation, leading to increased transcription from σ^S promoters. This hypothesis might explain the σ^S stability, GDAR and LEE expression phenotype of TW14359Δ*rpaN*. To examine this possibility, a mutant version of the *rpaN* gene (*rpaN*^{R456A}) was constructed, the product of which can efficiently form Eσ^N holoenzyme but cannot bind DNA to direct transcription from σ^N promoters [91,92]. If the increased stability of σ^S in TW14359Δ*rpaN* is solely the result of increased RNAP binding by σ^S, the expression of *rpaN*^{R456A} in TW14359Δ*rpaN* should reproduce WT levels of σ^S stability. This was not determined to be the case however, as the stability of σ^S in TW14359Δ*rpaN*pRAM-2 did not differ from that of TW14359Δ*rpaN*, and both were increased in comparison to TW14359 and TW14359Δ*rpaN*-pRAM-1 (Fig. 4A). The effect of *rpaN*^{R456A} expression on the GDAR and LEE expression phenotype of TW14359Δ*rpaN* was also examined. Transcript levels for the GDAR regulator *gadE*, and the LEE regulator *ler* in TW14359Δ*rpaN* and TW14359Δ*rpaN*pRAM-2 did not differ, and were significantly higher or lower than TW14359 and TW14359Δ*rpaN*pRAM-1, respectively ($p<0.05$) (Fig. 4B). Interestingly, survival by GDAR for TW14359Δ*rpaN*pRAM-2 was partially reduced compared to TW14359Δ*rpaN*, but remained substantially higher than TW14359 and TW14359Δ*rpaN*pRAM-1 (Table 1).

Sensitivity of σ^N-dependent GDAR and LEE Expression to Protease Inhibition

The low abundance of σ^S during exponential growth is due to rapid proteolytic turnover by the serine protease complex ClpXP [29,51]. In strains mutated for *clpP* (the protease of ClpXP), σ^S is completely stable in exponential phase [51], however in exponential phase cultures of TW14359Δ*rpaN*, σ^S is still largely unstable (Fig. 3B), suggesting that there remains a sufficient amount of σ^S proteolysis. To reproduce the level of increased σ^S stability characteristic of TW14359Δ*rpaN* in the WT background, sub-inhibitory concentrations of the serine protease inhibitor 3, 4-dichloroisocoumarin (3, 4-DCI) [97] were titrated into growing exponential cultures and σ^S stability was measured.

The addition of 5 μM 3, 4-DCI (or 1/12X MIC) increased σ^S stability levels in TW14359 similar to σ^S stability levels observed in TW14359Δ*rpaN* without the addition of 3, 4-DCI (Fig. 5A). Addition of 3, 4-DCI further increased σ^S levels in TW14359Δ*rpaN* as well, revealing that σ^S stability is sensitive to serine protease inhibition in both backgrounds. It was predicted that if the GDAR and LEE expression phenotype of TW14359Δ*rpaN* was simply a result of decreased σ^S proteolysis, then experimentally increasing σ^S stability with 3,4-DCI should reconstitute a similar phenotype in TW14359. For GDAR this was not shown to be true, as 3, 4-DCI had no impact on survival of TW14359 in acid, and only marginally increased percent survival in TW14359Δ*rpaN* (Table 1). Thus increased stability of σ^S alone cannot account for GDAR in TW14359Δ*rpaN*. The expression of LEE genes is known to be positively influenced by ClpP through its proteolytic effect on σ^S [31,32]. Consistent with this, 3, 4-DCI addition reduced expression from ler_{P430}-*lacZ* in TW14359 as indicated by a decrease in percent β-galactosidase activity relative to untreated controls (Fig. 5B). Since addition of 3,4-DCI further increased σ^S stability in TW14359Δ*rpaN*, it was expected that this increase would correspond with a further decrease in *ler*

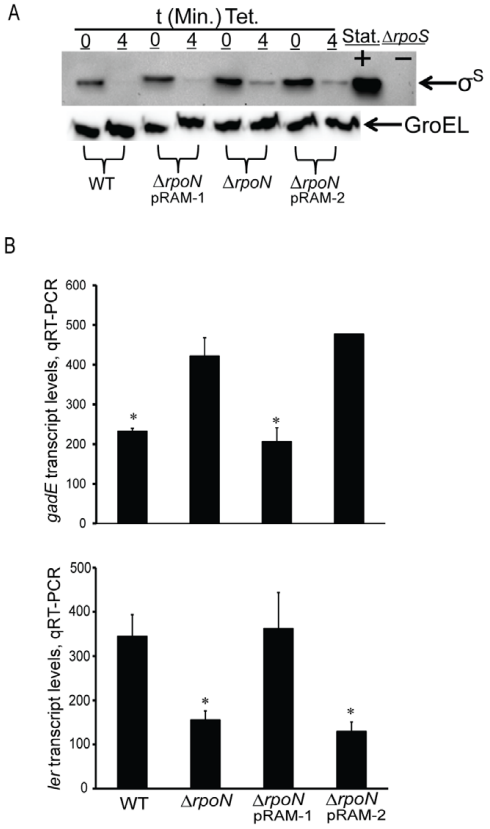

Figure 4. Effect of *rpoN*^{R456A} expression in TW14359Δ*rpoN* on σ^S stability, *gadE* and *ler* transcription. (Panel A): Representative western immunoblots for σ^S in TW14359 (WT), TW14359Δ*rpoN* complemented with *rpoN*$^+$ (TW14359Δ*rpoN*pRAM-1), TW14359Δ*rpoN* (Δ*rpoN*), TW14359Δ*rpoN* complemented with *rpoN*^{R456A} (TW14359Δ*rpoN*pRAM-2) before (t = 0 min) and 4 min after addition of tetracycline (Tet.). Stationary phase (Stat.) protein extracts were used as a positive control for σ^S, and TW14359Δ*rpoS* (Δ*rpoS*) as a negative control. Equal gel loading was controlled for by westerns for GroEL. (Panel B): Mean *gadE* and *ler* transcript levels by qRT-PCR are plotted against TW14359 (WT) and derivative strains from Panel A. Transcript levels are normalized to the 16S rRNA gene *rrsH*. Asterisks denote significant differences between WT and TW14359Δ*rpoN*pRAM-1 when compared to TW14359Δ*rpoN* and TW14359Δ*rpoN*pRAM-2 by Tukey's HSD following a significant F-test ($n \geq 3$, $p < 0.05$). Error bars indicate standard error of the mean.
doi:10.1371/journal.pone.0046288.g004

expression. On the contrary, ler_{P430}-*lacZ* expression did not differ in 3,4-DCI-treated TW14359Δ*rpaN* cultures compared to untreated controls, and β-galactosidase activity was unchanged throughout growth compared to significantly reduced activity in TW14359 ($p < 0.05$) (Fig. 5B). These results reveal that although σ^S stability is sensitive to protease inhibition using 3, 4-DCI in TW14359Δ*rpaN*, GDAR and *ler* expression is not and indicates that the underlying mechanism responsible for these phenotypes

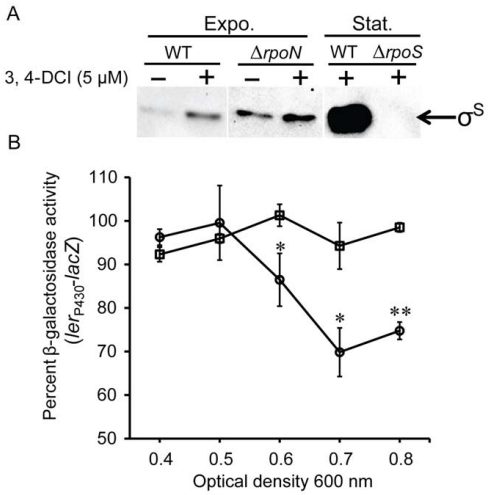

Figure 5. Effect of the serine protease inhibitor 3,4-DCI on σ^S stability and *ler* expression. (Panel A): Representative western immunoblot for σ^S stability in TW14359 (WT) and TW14359Δ*rpoN* (Δ*rpoN*) during exponential phase (Expo.) 4 min after the addition of tetracycline, and with or without 3,4-DCI, as well as in WT and TW14359Δ*rpoS* (Δ*rpoS*) during stationary phase (Stat.) with 3,4-DCI. Equal gel loading was controlled for by westerns for GroEL. (Panel B): Expression from ler_{P430}-*lacZ* as measured by mean percent β-galactosidase activity following addition of 3,4-DCI and relative to untreated controls during exponential growth for TW14359 (circles) and TW14359Δ*rpoN* (squares). Asterisks denote significant differences between TW14359 and TW14359Δ*rpoN* at each OD_{600} by Welch's t-test ($n \geq 3$, $p < 0.05$ [*]; $p < 0.01$ [**]).
doi:10.1371/journal.pone.0046288.g005

are at least partially distinct. The addition of 1/2X MIC of 3, 4-DCI did not significantly alter the outcome for GDAR or *ler* expression in either strain (data not shown).

Identification of the Enhancer-binding Protein Required for σ^N-directed Regulation of GDAR and the LEE

σ^N is a unique sigma factor in its requirement for enhancer-binding proteins (EBP) to initiate transcription [59]. If σ^S stability, GDAR and LEE expression in TW14359Δ*rpaN* is dependent on σ^N-directed transcription, at least one of these EBPs is required for this control. To examine this, a library of EBP isogenic deletion mutants in TW14359 was constructed and screened for GDAR during exponential growth. Of the eleven mutants, only TW14359Δ*glnG* and TW14359Δ*fhlA* expressed GDAR comparable to levels observed for TW14359Δ*rpaN* (Table 1). *fhlA* encodes a regulator of formate metabolism [60], and *ntrC* (also *glnG*) encodes NtrC, a major regulator of nitrogen assimilation [61,62]. The impact of *fhlA* or *ntrC* mutation on LEE expression was then determined by transforming pRJM-1 containing ler_{P430}-*lacZ* into both EBP isogenic backgrounds, TW14359Δ*rpaN* and TW14359, and β-galactosidase activity was measured during exponential growth. Expression from ler_{P430}-*lacZ* increased in TW14359 to mid-exponential phase ($OD_{600} = 0.5$), then tapered off as cells entered late exponential phase ($OD_{600} = 1.0$) (Fig. 6). For TW14359Δ*rpaN*, ler_{P430}-*lacZ* expression only slightly increased during growth, and was significantly reduced to 56% of WT levels

at $OD_{600} = 0.5$, concordant with qRT-PCR data ($p = 0.008$) (Figs. 2 and 6). Mutation of *fhlA* had no apparent effect on ler_{P430}-*lacZ* expression, yet *ntrC* mutation reduced ler_{P430}-*lacZ* expression to 50% of WT at $OD_{600} = 0.5$ ($p = 0.006$) to levels comparable with TW14359Δ*rpoN* (Fig. 6). Thus the mutation of *ntrC* faithfully reproduces the GDAR and LEE expression phenotype of TW14359Δ*rpoN*. Interestingly, σ^S stability was increased in both EBP mutant backgrounds to the level of stability observed in TW14359Δ*rpoN* (Fig. 7). These results reveal that mutation of *fhlA* and *ntrC* similarly influence σ^S stability, yet only *ntrC* mutation phenocopies GDAR and LEE expression observed in TW14359Δ*rpoN*. A strain deleted for both *rpoN* and *ntrC* was constructed to validate the dependence on *rpoN* for NtrC-directed GDAR and LEE expression, but the mutant was too growth-impaired in DMEM to be phenotypically informative.

Discussion

The importance of σ^N in *E. coli* metabolism, particularly nitrogen metabolism, is undisputed. Strains mutated for *rpoN* are growth-impaired under nitrogen-limiting conditions due to an inability to activate nitrogen regulatory response promoters. Mutation of *rpoN* also clearly affects many genes in *E. coli* that are not directly tied to metabolism, but which are perhaps cued to the metabolic status of the cell through σ^N, such as those involved in the regulation of motility [63,64], NO detoxification [65], and biofilm formation [66]. In the present study, the phenotype of acid resistance and LEE expression previously described for *rpoN* mutants in EHEC [35], represents a case in which σ^N-dependent regulation is indirectly communicated through the downregulation of another sigma factor, σ^S. The antagonistic interplay of σ^N and σ^S in the control of these discrete systems resembles that described on a genomic scale by Dong et al. [43], in which it was estimated that as many as 60% of σ^N regulated genes are counter-regulated by σ^S.

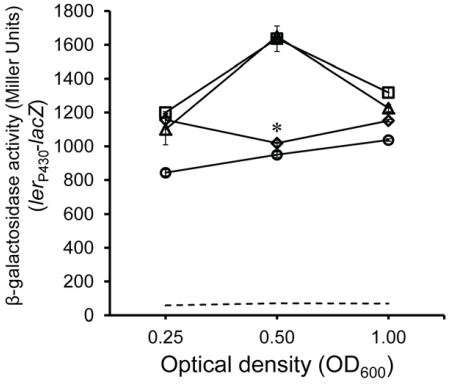

Figure 6. Expression from ler_{P430}-*lacZ* in σ^N enhancer binding protein mutants. Mean expression from ler_{P430}-*lacZ* represented as β-galactosidase activity during exponential growth for TW14359 (triangles), TW14359Δ*rpoN* (circles), TW14359Δ*fhlA* (squares), TW14359Δ*ntrC* (diamonds) and empty vector pRS551 (hatched line). The asterisk denotes a significant difference for TW14359Δ*rpoN* and TW14359Δ*ntrC* when compared to the remaining strains by Tukey's HSD following a significant F-test ($n \geq 3$, $p < 0.05$).
doi:10.1371/journal.pone.0046288.g006

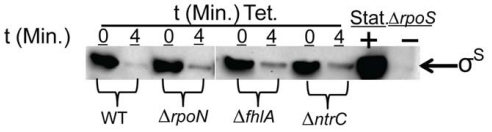

Figure 7. Stability of σ^S in σ^N enhancer binding protein mutants. Representative western immunoblots for σ^S in TW14359 (WT), TW14359Δ*rpoN* (Δ*rpoN*), TW14359Δ*fhlA* (Δ*fhlA*), and TW14359Δ*ntrC* (Δ*ntrC*) before (t = 0 min) and 4 min after addition of tetracycline (Tet.). Stationary phase (Stat.) protein extracts were used as a positive control for σ^S, and TW14359Δ*rpoS* (Δ*rpoS*) as a negative control. Equal loading was controlled for by westerns for GroEL.
doi:10.1371/journal.pone.0046288.g007

For control of acid resistance, σ^N negatively regulates the σ^S-directed GadX-GadW pathway of glutamate-dependent acid resistance (GDAR) activation. This agrees with the dependence on *rpoS* and *gadE* for acid resistance formerly described for *rpoN* mutants [35], and with research showing that *rpoS* expression in a Δ*gadXW* background cannot induce the GDAR central regulator *gadE* [67]. In this regulatory circuit, σ^S drives the transcription of *gadX*, the product of which then activates *gadE* transcription. GadX also downregulates GadW, which is a negative regulator of σ^S [12]. As observed for GDAR, σ^N is clearly dependent on *rpoS* for upregulation of the LEE, conforming to the role of σ^S as a negative regulator of LEE expression [31,32]. This σ^N–σ^S regulatory pathway is predicted to converge on the LEE central regulator, *ler*. The fact that *ler* expression was not observed to be significantly decreased in previous microarray studies of *rpoN* mutated EHEC [35] but is in the current study, may be explained by the increased sensitivity of qRT-PCR.

The GDAR and LEE expression phenotype of TW14359Δ*rpoN* correlates with an increase in σ^S stability similar to that described for K-12 [43], however no increase in σ^S levels was observed as was for K-12. This disparity in results could reflect genetic differences between K-12 and TW14359, or differences in experimental growth conditions. For the latter, the M9 glucose media used by Dong et al. [43] should be strongly growth restrictive for *rpoN* mutants, which are auxotrophic for glutamine in minimal media containing glucose [61]. As the production of σ^S is sensitive to reduced growth [29], increased σ^S levels during growth of *rpoN* mutants in M9 glucose may be attributed to metabolic stress, and not specific to σ^N. The growth of *rpoN* mutants is impaired in DMEM (Fig. S1), but not prohibitively, as it contains glutamine.

This study further scrutinized the genetic basis for and significance of increased σ^S stability in the GDAR and LEE expression phenotype of *rpoN*. The expression of a transcriptionally silent allele of σ^N ($rpoN^{R456A}$) in TW14359Δ*rpoN* did not reconstitute WT levels of σ^S stability, *gadE* or *ler* expression, suggesting that competition for core RNAP is unlikely to be the primary underlying mechanism for this phenotype, and that transcription from a σ^N promoter(s) is a requirement. The RNAP competition hypothesis implies that the simple removal of a competing sigma factor may allow for increased competition of the remaining sigma factors for RNAP core. However, due to the low intrinsic affinity of σ^S for RNAP [53], all else being equal, it is more likely that σ^{70}, or other sigma factors present during exponential phase (ex. σ^F) will out-compete σ^S for extant core. Naturally, this competition dynamic changes in stationary phase cultures, as small molecules and proteins modulate the ability of specific sigma subunits to interact with RNAP.

Addition of the serine protease inhibitor 3,4-DCI was shown to result in increased σ^S stability in TW14359, and further increased σ^S stability in TW14359Δ*rpoN*. This cumulative increase in σ^S stability in TW14359Δ*rpoN* could reflect the sum of effects of 3,4-DCI and *rpoN* mutation on a common pathway (i.e. ClpP), or independent pathways. There is no direct evidence however, that 3, 4-DCI is increasing σ^S stability by inhibiting ClpP. Regardless of which is true, increasing σ^S stability alone by interfering with proteolysis did not alter GDAR and LEE expression in TW14359Δ*rpoN*, suggesting that the mechanistic basis of these phenotypes is distinct. Mutation of *rpoN* could lead to increased σ^S activity at promoters, or modulate its affinity for RNAP. For the former, both FliZ and 6S RNA have been reported to reduce σ^S activity at selective promoters [68,69]. Interestingly, transcript levels of *fliZ* were markedly upregulated in *rpoN* null K-12 [43], but not in EHEC [35]. For the latter, various proteins and small molecules are known to facilitate Eσ^S holoenzyme formation, including Crl [70], Rsd [71], and ppGpp [72]. Currently, the involvement of any of these regulators in σ^N–σ^S control of GDAR and the LEE is unknown.

This study revealed that a strain mutated for *ntrC*, encoding nitrogen regulatory protein NtrC, is phenotypically similar to an *rpoN* mutant in regards to σ^S stability, GDAR and LEE expression. NtrC is a canonical σ^N EBP, activating transcription from at least 16 promoters in *E. coli* by binding as a hexameric ring to an upstream activator sequence (UAS) distal to the σ^N−24/−12 binding site [62,73,74]. The transcription of *ntrC* dramatically increases when *E. coli* is grown in media that does not contain ammonia (i.e. DMEM), and plays an integral role in controlling nitrogen utilization pathways. This finding suggests that the product(s) of an NtrC/σ^N driven promoter directly or indirectly downregulates σ^S, which in-turn affects GDAR and LEE expression. Currently however, there is no experimental evidence to support a role for any of the known NtrC/σ^N regulated genes in this. Alternatively, NtrC could activate σ^N promoters independent of DNA binding, which may relax the site selectivity of NtrC/σ^N dependent transcription initiation. Examples of this have been described for Rrp2 of *B. burgdorferi*, and FlgR of *Campylobacter jejuni*, that activate σ^N promoters in the absence of known UAS sites for these EBPs by some unknown mechanism [75–77]. There is also a precedent for NtrC regulating transcription independent of σ^N. NtrC binds to the core promoters of $glnA_{P1}$ and $glnA_{P3}$, repressing *glnLG*/*glnALG* (glutamine synthetase operon) transcription by interfering with σ^{70}-dependent initiation [61]. Other *E. coli* promoters that are directly downregulated by NtrC have not however been described.

This study further identified FhlA as a putative EBP involved in the control of σ^S and GDAR, but not the LEE. FhlA activates transcription from multiple operons involved in formate metabolism, including structural components of the formate hydrogen lysase hydrogenase-3 (Hyd-3) complex. Interestingly, the Hyd-3 complex has been reported to confer acid resistance by a unique mechanism that involves the consumption of protons during the conversion of formic acid to CO_2 and H_2 [78]. However, the fact that *fhlA* mutation leads to acid resistance is inconsistent with its role as a positive regulator of the Hyd-3 acid resistance mechanism. Adding to this, Hyd-3 has only been shown to be protective under anaerobic growth conditions [78], together suggesting that the acid resistance conferred by *fhlA* mutation is independent of this mechanism. Alternatively, mutation of *fhlA* may lead to the accumulation of formic acid during growth on glucose (DMEM contains 4 g/l glucose) leading to acid-adaptation. Volatile fatty acid (VFAs, including acetic, formic and butyric acid) production during growth on glucose has been attributed to inorganic acid resistance in *Salmonella* and *E. coli* [79,80]. The broader significance of this finding is that multiple σ^N EBPs regulate GDAR and the LEE by discrete pathways, some of which may be independent of *rpoS*. In further support of this hypothesis, the EBP QseF has been independently shown to be important for attaching and effacing lesion formation, and for the control of T3SS effectors in response to autoinducer 3 (AI-3) and norepinephrine/epinephrine [81–83]. The mutation of *qseF* did not however affect GDAR in this study (data not shown).

Given the essential roles of NtrC and σ^N in nitrogen metabolism, the results of this study infer that these proteins coordinate the expression of GDAR and the LEE with nitrogen (i.e. NH_3) availability through σ^S. This proposed regulatory pathway shares many similarities with that described for *rfaH* expression and O-antigen production in *Salmonella enterica*. Specifically, σ^N has been observed to activate *rfaH* transcription in an *rpoS*-dependent manner [84]. However, the mutation of *rpoN* was epistatic for *rfaH* control by σ^S, indicating a regulatory relationship in which σ^S is positively controlling σ^N; there is no evidence that σ^S influences *rpoN*/σ^N expression or activity in *E. coli* [35,43]. Remarkably however, *rfaH* transcription was further determined to be stimulated under nitrogen-limiting conditions [85], which suggests the potential for involvement of NtrC in σ^N–σ^S dependent control of O-antigen production in *S. enterica*.

This study concludes that σ^N exerts its regulatory influence on GDAR and the LEE through negative post-translational control of σ^S. Thus the inactivation of *rpoN* relaxes the requirement for stationary phase-induced mechanisms of σ^S accumulation during exponential growth. Furthermore, the results suggest that σ^N–σ^S dependent GDAR and LEE expression is at least partially controlled by NtrC, an EBP that activates transcription from σ^N promoters specifying genes for nitrogen utilization. The regulatory interplay of NtrC and other EBPs with σ^N and σ^S is likely to play a significant role in coordinating transcription with the various nutritional and physiological stimuli EHEC is exposed to during transmission, and in the course of infection.

Materials and Methods

Bacterial Strains and Culture Conditions

The strains and plasmids used in this study are listed in Table 2. Strains were stocked at −80°C in glycerol (15% v/v final) diluted in Lysogeny Broth (LB) and were maintained in LB or on LB with 1.5% agar (LBA). Unless otherwise noted, overnight (18–20 h) cultures grown in MOPS (50 mM)-buffered Dulbecco's Modified Eagle's Medium (DMEM) (Sigma-Aldrich, cat. #D2902, St. Louis, MO) [86] containing 4 g/l glucose and 4 mM glutamine (pH 7.4) were used to inoculate fresh DMEM to a final $OD_{600} = 0.05$ and cultured at 37°C on a rotary shaker (200 RPM) using a 1:10 ratio of media-to-flask volume as described [35]. The growth of strains in DMEM was monitored by taking OD_{600} readings at 1 h intervals over 12 h (Fig. S1). Antibiotics (Sigma-Aldrich) were added to cultures when required. The *rpoS*$^+$ status of strains was confirmed by catalase activity and glycogen storage following previous protocols [87,88].

Directed Gene Deletion and Site-specific Mutation

Gene deletion mutants were constructed using the λ Red recombinase-assisted approach [89,90] and as described [35]. Primers used for the deletion of σ^N EBPs, as well as *rpoN* and *rpoS* are provided in Table S1. For site-specific mutation, a 1,518 bp *Cla*I/*Hind*III-digested PCR fragment containing the *rpoN* gene from strain TW14359 nucleotide positions 4,144,833–4,146,311 was generated using primers rpoN-45/*Cla*I and rpoN+1455/

Table 2. Strains and plasmids used in this study.

Strain/plasmid	Relevant characteristics	Source/reference
Strain name:		
DH5α	Vector propagation, *recA1 endA1*	
XL10-Gold®	Competent cells	Agilent, Santa Clara, CA
TW14359	WT 2006 outbreak, western U.S.	[98]
EcRPF-6	TW14359Δ*rpoN*	This study
EcRPF-9	TW14359Δ*rpoN*Δ*rpoS*	This study
EcRPF-7	TW14359Δ*rpoS*	This study
EcRAM-26	TW14359Δ*glnG*	This study
EcRAM-25	TW14359Δ*fhlA*	This study
EcRAM-28	TW14359Δ*qseF*	This study
EcRAM-27	TW14359Δ*pspF*	This study
EcRAM-29	TW14359Δ*ygeV*	This study
EcRAM-4	TW14359*norR*::*kan* Kan^R	This study
EcRAM-7	TW14359*rtcR*::*kan* Kan^R	This study
EcRAM-3	TW14359*hyfR*::*kan* Kan^R	This study
EcRAM-11	TW14359*zraR*::*kan* Kan^R	This study
EcRAM-8	TW14359*tyrR*::*kan* Kan^R	This study
EcRAM-5	TW14359*prpR*::*kan* Kan^R	This study
Plasmid name:		
pACYC177	Low copy cloning vector, Amp^R Kan^R P15A	[99]
pRAM1	*rpoN*::pACYC177, Amp^R Kan^S	This study
pRAM2	$rpoN^{R456A}$::pACYC177 Amp^R Kan^S	This study
pRS551	*lac* fusion vector, Amp^R Kan^R *lacZ*$^+$ ColE1	[95]
pRJM-1	pRS551 containing ler_{P430}-*lacZ*fusion	This study

doi:10.1371/journal.pone.0046288.t002

*Hin*dIII (Table S1). This fragment was ligated into *Cla*I/*Hin*dIII-digested pACYC177 to produce pRAM-1 (Table 2). Point mutations C1366G and G1367C were introduced into the *rpoN* gene present on the pRAM-1 template plasmid by PCR using mutagenic primers rpoNR456A-F and rpoNR456A-R (Table S1) and *Pfu Ultra*™ high fidelity DNA polymerase (Agilent, Santa Clara, CA) to produce pRAM-2 (Table 2). The resultant σ^N allele has a R456A mutation ($rpaN^{R456A}$) in the DNA binding domain which interferes with the ability of the protein to bind DNA, but does not affect its capacity for RNAP association and holoenzyme formation [91,92]. pRAM-1, in addition to pRAM-2 purified from *E. coli* XL10-Gold® (Agilent) transformants, were transformed into strain TW14359Δ*rpaN* as described [35]. Genetic constructs were validated by PCR, and restriction mapping, or by DNA sequencing and qRT-PCR.

Tests for Acid Resistance

Acid resistance by the glutamate- and arginine-dependent systems was measured as described [35] with slight adaptations. For the glutamate-dependent acid resistance mechanism, mid-exponential ($OD_{600} = 0.5$) DMEM cultures were inoculated to 10^6 CFU/ml final cell density into E minimal glucose (EG) media with or without 5.7 mM L-glutamate at pH 7 (control) or acidified with HCl (pH 2). To test for arginine-dependent acid resistance, exponential phase DMEM cultures were inoculated into EG media as above but with or without 0.6 mM L-arginine at pH 7 and pH 2.5. EG media acid resistance test environments were incubated at 37°C (200 RPM) for 1 h before sampling. For cell counts (CFU/ml) and percent survival determinations, samples were serially-diluted in PBS (pH 7), plated to LBA and incubated overnight at 37°C.

Quantitative Real-time PCR (qRT-PCR)

Primers for qRT-PCR are provided in Table S1. RNA purification, cDNA synthesis, qRT-PCR cycling conditions and data analysis followed previously described protocols [35,93].

Protein Extraction, SDS-PAGE and Western Immunoblots

To extract total cellular protein, 10 ml culture samples were centrifuged at 10,000×*g* for 2 min and the cell pellet was washed twice with sterile water with centrifugation as above. Washed cell pellets were resuspended in 0.7 ml 0.5 M triethyl ammonium bicarbonate buffer (TEAB) (Sigma-Aldrich) and sonicated with a Sonic Dismembrator 120 (Fisher, Waltham, MA) at 50% amplitude for 30 sec intervals totaling 5 min, followed by incubation at 95°C in 4X Laemmli Buffer for 5 min. Total cell protein was collected from lysed cells by centrifugation at 10,000×*g* for 5 min, and supernatant was removed by aspiration. For western immunoblots, 10–30 μg extracted protein was resolved using 10% SDS-PAGE at 13 V/cm for 80 min before transfer at 15 V for 20 min to polyvinylidene fluoride (PVDF) membranes using a Trans-Blot semi-dry transfer cell (Bio-Rad, Hercules, CA). For detection of σ^S, PVDF membranes were blocked in Tris-buffered saline (1X Tris, pH 7.4) with 0.1% (v/v) Tween-20 (TBST) containing 5% skim milk for 2 h at room temperature before incubation with anti-σ^S mAbs (Neoclone,

Madison, WI) diluted 1:5000 in TBST containing 2% skim milk overnight on a Veri Mix platform rocker (Fisher) at 4°C. Membranes were then incubated for 1 h at room temperature with HRP-conjugated goat anti-mouse pAbs (Bio-Rad) diluted 1:10,000 in TBST with 2% skim milk. Protein was detected using an enhanced chemiluminescence (ECL) Plus detection system (Amersham-Pharmacia, Piscataway, NJ) following the manufacturer's instructions. Protein levels were measured and analyzed using a ChemiDoc XRS and Image Lab Software (Bio-Rad). The amount of protein loaded was measured using a Bradford protein assay standard curve. Equal loading was validated by western blots for GroEL using anti-GroEL mAbs (Bio-Rad) diluted 1:40,000 in TBST with 2% skim milk. Western blots were repeated a minimum of three times in independent trials.

σ^S and *rpoS* mRNA Stability

Cultures were grown to mid-exponential phase ($OD_{600} = 0.5$) before the addition of a subinhibitory concentration of the transcription inhibitor rifampin (300 μg/ml final) or the translation inhibitor tetracycline (60 μg/ml final). Sampling was performed immediately before addition of antibiotics, and at 4 min intervals thereafter for 12 min (*rpoS* mRNA stability) or 16 min (σ^S protein stability). RNA was purified and validated as described [93]. For *rpoS* mRNA stability, gene transcript levels were measured using qRT-PCR and primers rpoS+356 and rpoS+466 (Table S1). Protein was extracted, and σ^S levels measured by western immunoblots. The half-life in minutes for *rpoS* mRNA and σ^S was extrapolated from gene transcript or protein levels, respectively, using linear regression analysis and as described [94]. The strength of linearity was estimated by the correlation coefficient (r^2), and exceeded 0.85 (85%) for all analyses.

lacZ Transcriptional Fusions and β-galactosidase Assay

A 429-bp *Bam*HI/*Eco*RI digested PCR fragment generated using primers ler-1/BamHI and ler-430/EcoRI (Table S1) and corresponding to nucleotide positions 4,679,303-4,679,731 in strain TW14359 was cloned into the similarly digested vector pRS551 [95] using T4-DNA ligase (Fisher) to create pRJM-1 (Table 2). This cloned fragment included 429-bp upstream of the translation initiation codon for *ler* (ECSP_4703) and both *ler* P1 and P2 promoters transcriptionally fused to *lacZ* (ler_{P430}-*lacZ*). pRJM-1 purified from DH5α transformants was used for transformation into various WT and mutant backgrounds. The ler_{P430}-*lacZ* fusion was confirmed by PCR and sequencing. To measure β-galactosidase activity from ler_{P430}-*lacZ*, 50 μl culture samples taken at $OD_{600} = 0.25$ (early exponential), $OD_{600} = 0.5$ (mid-exponential) and $OD_{600} = 1.0$ (late exponential) were immediately added to 950 μl Z-buffer (1 M KCl, 1 mM MgSO4, 0.05 M β-mercaptoethanol, 0.06 M Na_2HPO_4, 0.04 M $NaH_2PO_4{\cdot}H_2O$, pH 7) with 0.1 ml chloroform and 50 μl 0.1% (v/v) SDS) and mixed vigorously for 30 sec. Samples were then incubated static at 28°C for 5 min before addition of 0.2 ml ortho-nitrophenyl β-D-galactopyranoside (ONPG, 4 mg/ml in 0.1 M phosphate buffer, pH 7) at 28°C for 20 min. Following development of the yellow cleavage product orthonitrophenol, the reaction was terminated by the addition of 0.5 ml Stop Solution (1 M Na_2CO_3) and samples were mixed and then centrifuged at 21,000×*g* for 5 min before measuring β-galactosidase activity. β-galactosidase activity was converted to Miller Units as described [96].

Serine Protease Inhibition

Selective inhibition of serine protease activity was performed using subinhibitory concentrations (i.e. 1/12X minimum inhibitory concentration (MIC) or 5 μM) of 3, 4-dichloroisocoumarin (3,4-DCI) (Sigma-Aldrich) [97]. The MIC for 3,4-DCI was at 60 μM for both WT and *rpaN* null backgrounds. The effect of 3,4-DCI addition to growing cultures on σ^S stability, GDAR and LEE expression was determined as described above. For σ^S stability, 3, 4-DCI was added to cultures at mid-exponential phase ($OD_{600} = 0.4$) and incubated to $OD_{600} = 0.5$ before addition of 60 μg/ml tetracycline. Sampling was performed immediately before tetracycline addition and 4 min after addition. For GDAR and LEE expression, 3,4-DCI was added at $OD_{600} = 0.4$ as for σ^S stability, and then GDAR tested, or β-galactosidase activity measured from ler_{P430}-*lacZ* as described above. Control cultures did not contain 3, 4-DCI for all experiments.

Supporting Information

Figure S1 Growth of strains in Dulbecco's Modified Eagle's Medium (DMEM). Mean (n = 2) optical density 600 nm (OD_{600}) plotted for TW14359 (empty squares), TW14359Δ*rpaN* (filled squares), TW14359Δ*rpoS* (circles), TW14359Δ*fhlA* (plus signs), TW14359Δ*ntrC* (triangles), and TW14359Δ*rpaN*Δ*rpoS* (diamonds). Individual OD_{600} measurements for each strain varied by less than 5%. For ler_{P430}-*lacZ* expression (Fig. 6), sampling was done for all strains except for TW14359Δ*rpoS* and TW14359Δ*rpaN*Δ*rpoS* at $OD_{600} = 0.25$, $OD_{600} = 0.5$, and $OD_{600} = 1.0$ approximately corresponding to early-, mid- and late-exponential phase, respectively. For all remaining experiments, sampling was done at $OD_{600} = 0.5$.
(TIF)

Table S1 Primers used in this study.
(PDF)

Acknowledgments

We thank Edward G. Dudley (Pennsylvania State University) for kindly providing vector pRS551 for *lacZ* reporter fusion construction, and Galeb Abu-Ali (U.S. Food and Drug Administration) for critical review of previous versions of the manuscript.

Author Contributions

Conceived and designed the experiments: JTR AM. Performed the experiments: AM PAF JKM KWV SLV. Analyzed the data: JTR AM. Wrote the paper: JTR AM PAF.

References

1. Mead PS, Slutsker L, Dietz V, McCaig LF, Bresee JS, et al. (1999) Food-related illness and death in the United States. Emerg Infect Dis 5(5): 607 25.
2. Mead P, Bender I, Dembek Z, et al. (1998) Active surveillance for hemolytic uremic syndrome at selected sites, United States, In Abstracts of the International Conference on Emerging Infectious Diseases (Atlanta), Abstract P-3.12.
3. Banatvala N, Griffin PM, Greene KD, Barrett TJ, Bibb WF, et al. (2001) The United States National Prospective Hemolytic Uremic Syndrome Study: microbiologic, serologic, clinical, and epidemiologic findings. J Infect Dis 183(7): 1063 70.
4. Foster JW (2004) *Escherichia coli* acid resistance: tales of an amateur acidophile. Nat Rev Microbiol 2(11): 898 907.
5. Teunis P, Takumi K, Shinagawa K (2004) Dose response for infection by *Escherichia coli* O157:H7 from outbreak data. Risk Anal 24(2): 401 7.
6. Chart H (2000) VTEC enteropathogenicity. Symp Ser Soc Appl Microbiol (29): 12S 23S.

7. Perna NT, Mayhew GF, Posfai G, Elliott S, Donnenberg MS, et al. (1998) Molecular evolution of a pathogenicity island from enterohemorrhagic *Escherichia coli* O157:H7. Infect Immun 66(8): 3810 7.
8. McDaniel TK, Kaper JB (1997) A cloned pathogenicity island from enteropathogenic *Escherichia coli* confers the attaching and effacing phenotype on *E. coli* K-12. Mol Microbiol 23(2): 399 407.
9. Hartland EL, Batchelor M, Delahay RM, Hale C, Matthews S, et al. (1999) Binding of intimin from enteropathogenic *Escherichia coli* to Tir and to host cells. Mol Microbiol 32(1): 151 8.
10. Elliott SJ, Wainwright LA, McDaniel TK, Jarvis KG, Deng YK, et al. (1998) The complete sequence of the locus of enterocyte effacement (LEE) from enteropathogenic *Escherichia coli* E2348/69. Mol Microbiol 28(1): 1 4.
11. Wong AR, Pearson JS, Bright MD, Munera D, Robinson KS, et al. (2011) Enteropathogenic and enterohaemorrhagic *Escherichia coli*: even more subversive elements. Mol Microbiol 80(6): 1420 38.
12. Ma Z, Richard H, Foster JW (2003) pH-Dependent modulation of cyclic AMP levels and GadW-dependent repression of RpoS affect synthesis of the GadX regulator and *Escherichia coli* acid resistance. J Bacteriol 185(23): 6852 9.
13. Castanie-Cornet MP, Penfound TA, Smith D, Elliott JF, Foster JW (1999) Control of acid resistance in *Escherichia coli*. J Bacteriol 181(11): 3525 35.
14. Small P, Blankenhorn D, Welty D, Zinser E, Slonczewski JL (1994) Acid and base resistance in *Escherichia coli* and *Shigella flexneri*: role of *rpoS* and growth pH. J Bacteriol 176(6): 1729 37.
15. Gong S, Ma Z, Foster JW (2004) The Era-like GTPase TrmE conditionally activates *gadE* and glutamate-dependent acid resistance in *Escherichia coli*. Mol Microbiol 54(4): 948 61.
16. Ma Z, Masuda N, Foster JW (2004) Characterization of EvgAS-YdeO-GadE branched regulatory circuit governing glutamate-dependent acid resistance in *Escherichia coli*. J Bacteriol 186(21): 7378 89.
17. Yona-Nadler C, Umanski T, Aizawa S, Friedberg D, Rosenshine I (2003) Integration host factor (IHF) mediates repression of flagella in enteropathogenic and enterohaemorrhagic *Escherichia coli*. Microbiology 149(Pt 4): 877 84.
18. Bergholz TM, Wick LM, Qi W, Riordan JT, Ouellette LM, et al. (2007) Global transcriptional response of *Escherichia coli* O157:H7 to growth transitions in glucose minimal medium. BMC Microbiol 7(1): 97.
19. Abe H, Tatsuno I, Tobe T, Okutani A, Sasakawa C (2002) Bicarbonate ion stimulates the expression of locus of enterocyte effacement-encoded genes in enterohemorrhagic *Escherichia coli* O157:H7. Infect Immun 70(7): 3500 9.
20. Abe A, Kenny B, Stein M, Finlay BB (1997) Characterization of two virulence proteins secreted by rabbit enteropathogenic *Escherichia coli*, EspA and EspB, whose maximal expression is sensitive to host body temperature. Infect Immun 65(9): 3547 55.
21. Kenny B, Abe A, Stein M, Finlay BB (1997) Enteropathogenic *Escherichia coli* protein secretion is induced in response to conditions similar to those in the gastrointestinal tract. Infect Immun 65(7): 2606 12.
22. Krin E, Danchin A, Soutourina O (2010) RcsB plays a central role in H-NS-dependent regulation of motility and acid stress resistance in *Escherichia coli*. Res Microbiol 161(5): 363 71.
23. Tobe T, Ando H, Ishikawa H, Abe H, Tashiro K, et al. (2005) Dual regulatory pathways integrating the RcsC-RcsD-RcsB signalling system control enterohaemorrhagic *Escherichia coli* pathogenicity. Mol Microbiol 58(1): 320 33.
24. Shin S, Castanie-Cornet MP, Foster JW, Crawford JA, Brinkley C, et al. (2001) An activator of glutamate decarboxylase genes regulates the expression of enteropathogenic *Escherichia coli* virulence genes through control of the plasmid-encoded regulator, Per. Mol Microbiol 41(5): 1133 50.
25. Sanchez-SanMartin C, Bustamante VH, Calva E, Puente JL (2001) Transcriptional regulation of the *orf19* gene and the *tir-cesT-eae* operon of enteropathogenic *Escherichia coli*. J Bacteriol 183(9): 2823 33.
26. De Biase D, Tramonti A, Bossa F, Visca P (1999) The response to stationary-phase stress conditions in *Escherichia coli*: role and regulation of the glutamic acid decarboxylase system. Mol Microbiol 32(6): 1198 211.
27. Lease RA, Smith D, McDonough K, Belfort M (2004) The small noncoding DsrA RNA is an acid resistance regulator in *Escherichia coli*. J Bacteriol 186(18): 6179 85.
28. Laaberki MH, Janabi N, Oswald E, Repoila F (2006) Concert of regulators to switch on LEE expression in enterohemorrhagic *Escherichia coli* O157:H7: interplay between Ler, GrlA, HNS and RpoS. Int J Med Microbiol 296(4 5): 197 210.
29. Lange R, Hengge-Aronis R (1994) The cellular concentration of the sigma S subunit of RNA polymerase in *Escherichia coli* is controlled at the levels of transcription, translation, and protein stability. Genes Dev 8(13): 1600 12.
30. Sperandio V, Mellies JL, Nguyen W, Shin S, Kaper JB (1999) Quorum sensing controls expression of the type III secretion gene transcription and protein secretion in enterohemorrhagic and enteropathogenic *Escherichia coli*. Proc Natl Acad Sci U S A 96(26): 15196 201.
31. Iyoda S, Watanabe H (2005) ClpXP protease controls expression of the type III protein secretion system through regulation of RpoS and GrlR levels in enterohemorrhagic *Escherichia coli*. J Bacteriol 187(12): 4086 94.
32. Tomoyasu T, Takaya A, Handa Y, Karata K, Yamamoto T (2005) ClpXP controls the expression of LEE genes in enterohaemorrhagic *Escherichia coli*. FEMS Microbiol Lett 253(1): 59 66.
33. Price SB, Cheng CM, Kaspar CW, Wright JC, DeGraves FJ, et al. (2000) Role of *rpoS* in acid resistance and fecal shedding of *Escherichia coli* O157:H7. Appl Environ Microbiol 66(2): 632 7.
34. Hengge-Aronis R (2002) Signal transduction and regulatory mechanisms involved in control of the sigma(S) (RpoS) subunit of RNA polymerase. Microbiol Mol Biol Rev 66(3): 373 95.
35. Riordan JT, Tietjen JA, Walsh CW, Gustafson JE, Whittam TS (2010) Inactivation of alternative sigma factor 54 (RpoN) leads to increased acid resistance, and alters locus of enterocyte effacement (LEE) expression in *Escherichia coli* O157 : H7. Microbiology 156(Pt 3): 719 30.
36. Powell BS, Court DL, Inada T, Nakamura Y, Michotey V, et al. (1995) Novel proteins of the phosphotransferase system encoded within the *rpoN* operon of *Escherichia coli*. Enzyme IIANtr affects growth on organic nitrogen and the conditional lethality of an *ersA* mutant. J Biol Chem 270(9): 4822 39.
37. Bueno R, Pahel G, Magasanik B (1985) Role of *glnB* and *glnD* gene products in regulation of the *glnALG* operon of *Escherichia coli*. J Bacteriol 164(2): 816 22.
38. Weiner L, Brissette JL, Model P (1991) Stress-induced expression of the *Escherichia coli* phage shock protein operon is dependent on sigma 54 and modulated by positive and negative feedback mechanisms. Genes Dev 5(10): 1912 23.
39. Reitzer L, Schneider BL (2001) Metabolic context and possible physiological themes of sigma(54)-dependent genes in *Escherichia coli*. Microbiol Mol Biol Rev 65(3): 422 44.
40. Boardman BK, He M, Ouyang Z, Xu H, Pang X, et al. (2008) Essential role of the response regulator Rrp2 in the infectious cycle of *Borrelia burgdorferi*. Infect Immun 76(9): 3844 53.
41. Yang XF, Lybecker MC, Pal U, Alani SM, Blevins J, et al. (2005) Analysis of the *ospC* regulatory element controlled by the RpoN-RpoS regulatory pathway in *Borrelia burgdorferi*. J Bacteriol 187(14): 4822 9.
42. Hubner A, Yang X, Nolen DM, Popova TG, Cabello FC, et al. (2001) Expression of *Borrelia burgdorferi* OspC and DbpA is controlled by a RpoN-RpoS regulatory pathway. Proc Natl Acad Sci U S A 98(22): 12724 9.
43. Dong T, Yu R, Schellhorn H (2011) Antagonistic regulation of motility and transcriptome expression by RpoN and RpoS in *Escherichia coli*. Mol Microbiol 79(2): 375 86.
44. Masuda N, Church GM (2002) *Escherichia coli* gene expression responsive to levels of the response regulator EvgA. J Bacteriol 184(22): 6225 34.
45. Lin J, Smith MP, Chapin KC, Baik HS, Bennett GN, et al. (1996) Mechanisms of acid resistance in enterohemorrhagic *Escherichia coli*. Appl Environ Microbiol 62(9): 3094 100.
46. Stim-Herndon KP, Flores TM, Bennett GN (1996) Molecular characterization of *adiY*, a regulatory gene which affects expression of the biodegradative acid-induced arginine decarboxylase gene (*adiA*) of *Escherichia coli*. Microbiology 142 (Pt 5): 1311 20.
47. Iyoda S, Watanabe H (2004) Positive effects of multiple pch genes on expression of the locus of enterocyte effacement genes and adherence of enterohaemorrhagic *Escherichia coli* O157 : H7 to HEp-2 cells. Microbiology 150(Pt 7): 2357 571.
48. Hayashi T, Makino K, Ohnishi M, Kurokawa K, Ishii K, et al. (2001) Complete genome sequence of enterohemorrhagic *Escherichia coli* O157:H7 and genomic comparison with a laboratory strain K-12. DNA Res 8(1): 11 22.
49. Paesold G, Krause M (1999) Analysis of *rpoS* mRNA in *Salmonella dublin*: identification of multiple transcripts with growth-phase-dependent variation in transcript stability. J Bacteriol 181(4): 1264 8.
50. Zgurskaya HI, Keyhan M, Matin A (1997) The sigma S level in starving *Escherichia coli* cells increases solely as a result of its increased stability, despite decreased synthesis. Mol Microbiol 24(3): 643 51.
51. Schweder T, Lee KH, Lomovskaya O, Matin A (1996) Regulation of *Escherichia coli* starvation sigma factor (sigma S) by ClpXP protease. J Bacteriol 178(2): 470 6.
52. Muffler A, Traulsen DD, Lange R, Hengge-Aronis R (1996) Posttranscriptional osmotic regulation of the sigma(s) subunit of RNA polymerase in *Escherichia coli*. J Bacteriol 178(6): 1607 13.
53. Maeda H, Fujita N, Ishihama A (2000) Competition among seven *Escherichia coli* sigma subunits: relative binding affinities to the core RNA polymerase. Nucleic Acids Res 28(18): 3497 503.
54. Colland F, Fujita N, Ishihama A, Kolb A (2002) The interaction between sigmaS, the stationary phase sigma factor, and the core enzyme of *Escherichia coli* RNA polymerase. Genes Cells 7(3): 233 47.
55. Farewell A, Kvint K, Nystrom T (1998) Negative regulation by RpoS: a case of sigma factor competition. Mol Microbiol 29(4): 1039 51.
56. Ishihama A (1990) Molecular assembly and functional modulation of *Escherichia coli* RNA polymerase. Adv Biophys 26: 19 31.
57. Jishage M, Iwata A, Ueda S, Ishihama A (1996) Regulation of RNA polymerase sigma subunit synthesis in *Escherichia coli*: intracellular levels of four species of sigma subunit under various growth conditions. J Bacteriol 178(18): 5447 51.
58. Jishage M, Ishihama A (1995) Regulation of RNA polymerase sigma subunit synthesis in *Escherichia coli*: intracellular levels of sigma 70 and sigma 38. J Bacteriol 177(23): 6832 5.
59. Shingler V (1996) Signal sensing by sigma 54-dependent regulators: derepression as a control mechanism. Mol Microbiol 19(3): 409 16.
60. Sankar P, Shanmugam KT (1988) Biochemical and genetic analysis of hydrogen metabolism in *Escherichia coli*: the *hydB* gene. J Bacteriol 170(12): 5433 9.
61. Reitzer LJ, Magasanik B (1986) Transcription of *glnA* in *E. coli* is stimulated by activator bound to sites far from the promoter. Cell 45(6): 785 92.

62. Zimmer DP, Soupene E, Lee HL, Wendisch VF, Khodursky AB, et al. (2000) Nitrogen regulatory protein C-controlled genes of *Escherichia coli*: scavenging as a defense against nitrogen limitation. Proc Natl Acad Sci U S A 97(26): 14674 9.
63. Claret L, Hughes C (2002) Interaction of the atypical prokaryotic transcription activator FlhD2C2 with early promoters of the flagellar gene hierarchy. J Mol Biol 321(2): 185 99.
64. Zhao K, Liu M, Burgess RR (2010) Promoter and regulon analysis of nitrogen assimilation factor, sigma54, reveal alternative strategy for *E. coli* MG1655 flagellar biosynthesis. Nucleic Acids Res 38(4): 1273 83.
65. Gardner AM, Gessner CR, Gardner PR (2003) Regulation of the nitric oxide reduction operon (*norRVW*) in *Escherichia coli*. Role of NorR and sigma54 in the nitric oxide stress response. J Biol Chem 278(12): 10081 6.
66. Belik AS, Tarasova NN, Khmel IA (2008) Regulation of biofilm formation in *Escherichia coli* K12: effect of mutations in *hns*, *stpA*, *lon*, and *rpoN* genes. Mol Gen Mikrobiol Virusol (4): 3 5.
67. Sayed AK, Odom C, Foster JW (2007) The Escherichia coli AraC-family regulators GadX and GadW activate gadE, the central activator of glutamate-dependent acid resistance. Microbiology 153(Pt 8): 2584 92.
68. Pesavento C, Becker G, Sommerfeldt N, Possling A, Tschowri N, et al. (2008) Inverse regulatory coordination of motility and curli-mediated adhesion in *Escherichia coli*. Genes Dev 22(17): 2434 46.
69. Trotochaud AE, Wassarman KM (2004) 6S RNA function enhances long-term cell survival. J Bacteriol 186(15): 4978 85.
70. Dong T, Kirchhof MG, Schellhorn HE (2007) RpoS regulation of gene expression during exponential growth of *Escherichia coli* K12. Mol Genet Genomics 279(3): 267 277.
71. Jishage M, Ishihama A (1999) Transcriptional organization and in vivo role of the *Escherichia coli rsd* gene, encoding the regulator of RNA polymerase sigma D. J Bacteriol 181(12): 3768 76.
72. Jishage M, Kvint K, Shingler V, Nystrom T (2002) Regulation of sigma factor competition by the alarmone ppGpp. Genes Dev 16(10): 1260 70.
73. Dixon R, Kahn D (2004) Genetic regulation of biological nitrogen fixation. Nat Rev Microbiol 2(8): 621 31.
74. Weiss V, Claverie-Martin F, Magasanik B (1992) Phosphorylation of nitrogen regulator I of *Escherichia coli* induces strong cooperative binding to DNA essential for activation of transcription. Proc Natl Acad Sci U S A 89(11): 5088 92.
75. Burtnick MN, Downey JS, Brett PJ, Boylan JA, Frye JG, et al. (2007) Insights into the complex regulation of *rpoS* in *Borrelia burgdorferi*. Mol Microbiol 65(2): 277 93.
76. Blevins JS, Xu H, He M, Norgard MV, Reitzer L, et al. (2009) Rrp2, a {sigma}54-dependent transcriptional activator of *Borrelia burgdorferi*, activates *rpoS* in an enhancer-independent manner. J Bacteriol 191(8): 2902 2905.
77. Joslin SN, Hendrixson DR (2008) Analysis of the *Campylobacter jejuni* FlgR response regulator suggests integration of diverse mechanisms to activate an NtrC-like protein. J Bacteriol 190(7): 2422 33.
78. Noguchi K, Riggins DP, Eldahan KC, Kitko RD, Slonczewski JL (2010) Hydrogenase-3 contributes to anaerobic acid resistance of *Escherichia coli*. PLoS One, 2010. 5(4): e10132.
79. Baik HS, Bearson S, Dunbar S, Foster JW (1996) The acid tolerance response of *Salmonella typhimurium* provides protection against organic acids. Microbiology 142 (Pt 11): 3195 200.
80. Kwon YM, Ricke SC (1998) Induction of acid resistance of *Salmonella typhimurium* by exposure to short-chain fatty acids. Appl Environ Microbiol 64(9): 3458 63.
81. Reading NC, Rasko DA, Torres AG, Sperandio V (2010) A transcriptome study of the QseEF two-component system and the QseG membrane protein in enterohaemorrhagic *Escherichia coli* O157 : H7. Microbiology 156(Pt 4): 1167 75.
82. Reading NC, Rasko DA, Torres AG, Sperandio V, et al. (2009) The two-component system QseEF and the membrane protein QseG link adrenergic and stress sensing to bacterial pathogenesis. Proc Natl Acad Sci U S A 106(14): 5889 94.
83. Reading NC, Torres AG, Kendall MM, Hughes DT, Yamamoto K, et al. (2007) A novel two-component signaling system that activates transcription of an enterohemorrhagic *Escherichia coli* effector involved in remodeling of host actin. J Bacteriol 189(6): 2468 76.
84. Bittner M, Saldias S, Altamirano F, Valvano M A, Contreras I (2004) RpoS and RpoN are involved in the growth-dependent regulation of rfaH transcription and O antigen expression in *Salmonella enterica* serovar Typhi. Microb Pathog 36(1): 19 24.
85. Bittner M, Saldias S, Estevez C, Zaldivar M, Marolda C L, et al. (2002) O-antigen expression in *Salmonella enterica* serovar Typhi is regulated by nitrogen availability through RpoN-mediated transcriptional control of the *rfaH* gene. Microbiology 148(Pt 12): 3789 99.
86. Morton HJ (1970) A survey of commercially available tissue culture media. In Vitro 6(2): 89 108.
87. Hengge-Aronis R, Fischer D (1992) Identification and molecular analysis of *glgS*, a novel growth-phase-regulated and *rpoS*-dependent gene involved in glycogen synthesis in *Escherichia coli*. Mol Microbiol 6(14): 1877 86.
88. Bohannon DE, Connell N, Keener J, Tormo A, Espinosa-Urgel M, et al. (1991) Stationary-phase-inducible "gearbox" promoters: differential effects of *katF* mutations and role of sigma 70. J Bacteriol 173(14): 4482 92.
89. Murphy KC, Campellone KG (2003) Lambda Red-mediated recombinogenic engineering of enterohemorrhagic and enteropathogenic *E. coli*. BMC Mol Biol, 4: 11.
90. Datsenko KA, Wanner BL (2000) One-step inactivation of chromosomal genes in *Escherichia coli* K-12 using PCR products. Proc Natl Acad Sci U S A 97(12): 6640 5.
91. Taylor M, Butler R, Chambers S, Casimiro M, Badii F, et al. (1996) The RpoN-box motif of the RNA polymerase sigma factor sigma N plays a role in promoter recognition. Mol Microbiol 22(5): 1045 54.
92. Wang L, Gralla JD (2001) Roles for the C-terminal region of sigma 54 in transcriptional silencing and DNA binding. J Biol Chem 276(12): 8979 86.
93. Neupane M, Abu-Ali GS, Mitra A, Lacher DW, Manning SD, et al. (2011) Shiga toxin 2 overexpression in *Escherichia coli* O157:H7 strains associated with severe human disease. Microb Pathog 51(6): 466 70.
94. Bernstein JA, Khodursky AB, Lin PH, Lin-Chao S, Cohen SN (2002) Global analysis of mRNA decay and abundance in *Escherichia coli* at single-gene resolution using two-color fluorescent DNA microarrays. Proc Natl Acad Sci U S A 99(15): 9697 702.
95. Simons RW, Houman F, Kleckner N, (1987) Improved single and multicopy lac-based cloning vectors for protein and operon fusions. Gene, 53(1): p. 85 96.
96. Miller J (1972) Assay of B-galactosidase *In:* Experiments in molecular genetics. Cold Spring Harbor, NY. Cold Spring Harbor Laboratory, 352 255.
97. Powers JC, Kam CM, Narasimhan L, Oleksyszyn J, Hernandez MA, et al. (1989), Mechanism-based isocoumarin inhibitors for serine proteases: use of active site structure and substrate specificity in inhibitor design. J Cell Biochem 39(1): 33 46.
98. Manning SD, Motiwala AS, Springman AC, Qi W, Lacher DW, et al. (2008) Variation in virulence among clades of *Escherichia coli O157:H7* associated with disease outbreaks. Proc Natl Acad Sci U S A 105(12): 4868 73.
99. Chang AC, SN Cohen (1978) Construction and characterization of amplifiable multicopy DNA cloning vehicles derived from the P15A cryptic miniplasmid. J Bacteriol 134(3): 1141 56.